ÇUKUROVA UNIVERSITY
INSTITUTE OF NATURAL AND APPLIED SCIENCES

PhD THESIS

Mehmet Azmi AKTACİR

INFLUENCE OF OUTDOOR AIR CONDITIONS ON OPERATING CAPACITY OF AIR CONDITIONING SYSTEMS

DEPARTMENT OF MECHANICAL ENGINEERING

ADANA 2005

ÇUKUROVA ÜNİVERSİTESİ
FEN BİLİMLERİ ENSTİTÜSÜ

INFLUENCE OF OUTDOOR AIR CONDITIONS ON OPERATING CAPACITY OF AIR CONDITIONING SYSTEMS

Mehmet Azmi AKTACİR

DOKTORA TEZİ

MAKİNA MÜHENDİSLİĞİ ANABİLİM DALI

Bu Tez 11 / 05 / 2005 Tarihinde Aşağıdaki Jüri Üyeleri Tarafından Oybirliği ile Kabul Edilmiştir.

İmza:……………………..	İmza:…………………	İmza:…………………
Prof. Dr. Tuncay YILMAZ	Prof. Dr. Beşir ŞAHİN	Prof. Dr. Orhan BÜYÜKALACA
DANIŞMAN	ÜYE	ÜYE
İmza:…………………….	İmza:…………………	
Prof. Dr. Ertuğrul BALTACIOĞLU	Prof. Dr. Tuğrul OĞULATA	
ÜYE	ÜYE	

Bu Tez Enstitümüz Makina Mühendisliği Anabilim Dalında Hazırlanmıştır.

Kod No:

Prof. Dr. Aziz ERTUNÇ
Enstitü Müdürü

**Bu çalışma Çukurova Üniversitesi Bilimsel Araştırma Projeleri Birimi tarafından desteklenmiştir.
Proje No: MMF.2003.D9**

ABSTRACT

PhD THESIS

INFLUENCE OF OUTDOOR AIR CONDITIONS ON OPERATING CAPACITY OF AIR CONDITIONING SYSTEMS

Mehmet Azmi AKTACİR

DEPARTMENT OF MECHANICAL ENGINEERING
INSTITUTE OF NATURAL AND APPLIED SCIENCES
UNIVERSITY OF ÇUKUROVA

Supervisor : Prof. Dr. Tuncay YILMAZ
Year: 2005, Pages: 189
Jury : Prof. Dr. Tuncay YILMAZ
Prof. Dr. Orhan BÜYÜKALACA
Prof. Dr. Ertuğrul BALTACIOĞLU
Prof. Dr. Tuğrul OĞULATA
Prof. Dr. Beşir ŞAHİN

The performance of HVAC equipment changes with the variation of outside weather conditions. This thesis presents psychometric analysis of an air-conditioning system at variable outdoor air conditions for a sample building located in Adana. In this study, computer programs were developed in order to simulate the hourly operating of air conditioning systems under real operating conditions. The results obtained by the programs show that the air conditioning systems are affected by both supply air temperature and variable outdoor air conditions. In addition, this study presents a life-cycle cost (LCC) analysis using detailed load profiles and initial and operating costs to evaluate economic feasibility of constant-air-volume (CAV) and variable-air-volume (VAV) air-conditioning systems. In the analysis, two different use of the building (as a school or as an office center), two different operating scenarios for the air-conditioning system (scenario 1 and scenario 2) were considered. It was found for all the cases considered that although initial cost of the VAV system is higher than that of the CAV system, the present worth cost of the VAV system is lower than that of the CAV system at the end of the lifetime (15 years) due to lower fan operating costs.

Keywords: RTS Method, cooling load, cooling coil capacity, CAV and VAV systems, variable outdoor air conditions.

ÖZ

DOKTORA TEZİ

DIŞ İKLİM VERİLERİNİN İKLİMLENDİRME SİSTEMİ CİHAZ KAPASİTESİNE ETKİSİ

Mehmet Azmi AKTACİR

ÇUKUROVA ÜNİVERSİTESİ
FEN BİLİMLERİ ENSTİTÜSÜ
MAKİNA MÜHENDİSLİĞİ ANABİLİM DALI

Danışman : Prof. Dr. Tuncay YILMAZ
Yıl: 2005, Sayfa: 189
Jüri : Prof. Dr. Tuncay YILMAZ
Prof. Dr. Orhan BÜYÜKALACA
Prof. Dr. Ertuğrul BALTACIOĞLU
Prof. Dr. Tuğrul OĞULATA
Prof. Dr. Beşir ŞAHİN

HVAC elemanlarının performansı dış iklim şartlarıyla değişir. Bu tezde, Adana'da bulunan örnek bir binanın iklimlendirme sisteminin değişken dış hava koşullarındaki psikrometrik analizi gerçekleştirilmiştir. Bu çalışmada, iklimlendirme sistemlerinin gerçek çalışma koşularında saatlik olarak simülasyonlarını yapan bilgisayar programları hazırlanmıştır. Bu programlardan elde edilen sonuçlar iklimlendirme sistemlerinin hem üfleme havası sıcaklığından hem de değişken dış hava koşullarından etkilendiğini göstermiştir. Ayrıca, bu çalışmada sabit (CAV) ve değişken debili (VAV) iklimlendirme sistemlerinin ekonomik fizibilitelerini değerlendirmek için detaylı yük profilleri ve ilk yatırım ve işletme giderleri kullanılarak ömür boyu maliyet analizi (LCC) çıkartılmıştır. Analizde, iki farklı bina (iş merkezi ve okul), iklimlendirme sistemlerinin iki farklı çalışma senaryosu (senaryo 1 ve senaryo 2) dikkate alınmıştır. VAV sisteminin ilk yatırım maliyetinin CAV sistemin ilk yatırım maliyetinden fazla olmasına rağmen, dikkate alınan tüm durumlarda fanların çalışma maliyetlerindeki azalmadan dolayı, sistem ömrü sonunda (15 yıl) VAV sisteminin şimdiki değer maliyetinin CAV sisteminkinden düşük olduğu bulunmuştur.

Anahtar Kelimeler: RTS metodu, soğutma yükü, soğutma serpantini kapasitesi, CAV ve VAV sistemleri, değişken dış hava şartları.

ACKNOWLEDGEMENTS

I am truly grateful to my research supervisor, Prof. Dr.-Ing Tuncay YILMAZ, for his encouragement, advice, invaluable guidance, understanding and endless support during my PhD thesis.

Thanks are extended to Prof. Dr. Orhan BÜYÜKALACA for providing valuable research advice, his understanding, continuous support and motivation during my PhD thesis.

I would like to express my special thanks to Advisory Committee Member Prof. Dr. Tuğrul OĞULATA for his devotion of invaluable time throughout my research activities.

I would also like to express my grate thanks to head of the Mechanical Engineering Department of Çukurova University Prof. Dr. Beşir ŞAHİN, for his continuous help and advise on my PhD thesis.

In addition, I want to express my sincere appreciation to all research assistants, lecturers and all staff of the Mechanical Engineering Department of Çukurova University and Harran University for their continuous help, support and motivation, especially research assistants Hasan SERİN, Ahmet FERTELLİ, Arif ÖZBEK, Ertaç HÜRDOĞAN, D.Ali BİRCAN, Asst. Prof. Dr. Hüseyin AKILLI, Asst. Prof. Dr. Hüsamettin BULUT and Assoc. Prof. Dr. Bülent YEŞİLATA.

Finally, I want to express my gratitude to my wife, my lovely son and other family members, each of whom gave support, help and love in my life and made this thesis possible.

TABLE OF CONTENTS **PAGE**

LIST OF TABLES **PAGE**

LIST OF FIGURES **PAGE**

NOMENCLATURE

Latin letters

a	:	Constant, given in Equation (3.79) [dimensionless]
A	:	Coefficient in Equation 4.1 [dimensionless]
A	:	Surface area [m^2]
A_P	:	Apparent solar constant
AST	:	Apparent solar time [decimal hours]
B	:	Atmospheric extinction coefficient
b	:	Constant, given in Equation (3.85) [dimensionless]
C	:	Sky diffuse factor
c_0, c_1, c_2, etc.	:	Conduction time series (factors)
C_8, …, C_{13}	:	Constants used in Equation (3.101)
CN	:	Clearness number multiplier for clear/dry or hazy/humid locations
c_p	:	Specific heat capacity of the air [J/kg °C]
DR	:	Daily temperature range [°C]
E	:	Surface irradiance [W/m^2]
ET	:	Equation of time [decimal minutes]
F	:	Diversity factor (equipment, lighting and occupant)
H	:	Hour angle [°]
h	:	Specific enthalpy, [J/kg]
IAC	:	Inside shading attenuation coefficient.
k	:	Number of values (Equation 3.35)
k_p	:	Number of parameters (Equation 3.35)
L	:	Local latitude
LON	:	Local longitude [decimal ° of arc]
LSM	:	Local standard time meridian [decimal ° of arc]
LST	:	Local solar time [decimal hours]
m	:	Coefficient in Equation (3.49)
M	:	Mass flow rate [kg/s]
n	:	Rotational speed (1/min)
n	:	The number of days from January 1
N	:	Number of people expected to occupy the space
n_o	:	The coefficient in Equation (3.49)
P	:	Pressure [Pa]
P_t	:	Percentage of daily temperature range for the current (t) hour

q	:	Heat gain due to people [W/person]
Q	:	Total heat gain (from people or lighting or equipment) [W]
$Q_{c, t}$	:	Convective cooling load for the exterior surfaces at current hour [W]
$Q_{i,t-n}$	:	Conductive heat input for the surface n hours ago [W]
$Q_{lat,room}$	:	Total latent cooling load of the space [W]
$Q_{r,t}$	:	Radiant heat gain for the current hour [W]
$Q_{r,t-n}$	:	Radiant heat gain n hours ago [W]
$Q_{rc,t}$	:	Radiant cooling load for the exterior surfaces at the current hour [W]
$Q_{sen,outdoor}$	:	Sensible cooling load form fresh air, [W]
$Q_{sen,room}$	:	Sensible cooling load of the space [W]
Q_t	:	Hourly conductive heat gain for the surface [W]
$Q_{tot,outdoor}$	:	Total cooling load form fresh air, [W]
$Q_{tot,room}$	:	Total cooling load of the space [W]
Q_{tot_ES}	:	Total cooling load for the exterior surfaces [W]
Q_{tot_F}	:	Total fenestration heat gain [W]
R	:	Correlation Coefficient
r_0, r_1, r_2,etc.	:	Radiant time series (factors)
R_A	:	The convective heat transfer resistance of air (m^2°C/W)
R_T	:	thermal resistant (m^2°C /W) between air and water flows
ΔR	:	Difference between long-wave radiation incident on surface from sky and surroundings and radiation emitted by blackbody at outdoor air temperature [W/m^2]
SHGC	:	Solar heat gain coefficient
T	:	Temperature
t	:	Time [hour]
T_1,……., T_4	:	The coefficient used in Equations (3.43) and (3.44)
U	:	Overall heat transfer coefficient [W/(m^2K)]
V	:	Total installed light wattage [W]
W	:	Air absolute humidity [kg/kg dry air]
W_1, W_2, W_3	:	The coefficient in Equation (3.49)
X	:	Heat output of equipment [W]
Y	:	Ratio of sky diffuse on vertical surface to sky diffuse on horizontal surface

Greek Letter

α	:	Absorptance of surface for solar radiation
ε	:	Hemispherical emittance of surface
$\hbar$	:	Coefficient of heat transfer by long-wave radiation and convection at outer surface, [W/m^2K]
β	:	Solar altitude [°]
γ	:	Surface solar azimuth [°]
δ	:	Solar declination [°]
θ	:	Incident angle [°]
ρ_g	:	Ground reflectivity
Σ	:	Surface tilt from horizontal [°]
Φ	:	The ratio of the fresh air mass flow rate to total mass flow rate
Φ_S	:	Solar azimuth [°]
Ψ	:	Surface azimuth [°]

Subscripts

A	:	Air
C	:	Apparatus dew point
D	:	Direct
DT	:	Design
e	:	Solar air
I	:	Room air (indoor air)
lat	:	Latent
max	:	Maximum
min	:	Minimum
M	:	Mixed air
outdoor	:	Fresh air
O	:	Outdoor air
sen	:	Sensible
sr	:	Surface
S	:	Supply air
r	:	Reflected
d	:	Diffuse
tot	:	Total

LIST OF ABBREVIATIONS AND ACRONYMS

ACS	Air Conditioning System
AE	Absolute Error
ASHRAE	American Society Of Heating, Refrigeration And Air-Conditioning Engineers Inc.
BRI	Building Related Illness
CAV	Constant Air Volume
CLTD/SCL/CLF	Cooling Load Temperature Difference/Solar Cooling Load /Cooling Load Factor
CSHF	Coil Sensible Heat Factor
CTS	Conduction Time Series
CV	The Calculated Value
EIA	Energy Information Administration
EREE	Office Of Energy Efficiency And Renewable Energy
HB	Heat Balance Cooling Load Calculation Method
HVAC	Heating Ventilation Air Conditioning
IAQ	Indoor Air Quality
LCC	Life Cost Cycle
MMV	Average of Measured Values
MV	The Measured Value
RE	Relative Error
RMSE	Root Mean Square Error
RSHF	The Room Sensible Heat Factor
RTS	Radiant Time Series
RTSM	Radiant Time Series Cooling Load Calculation Method
SBS	Sick Building Syndrome
TETD/TA	Total Equivalent Temperature Difference/Time Average
TFM	Transfer Function Cooling Load Calculation Method
VAV	Variable Air Volume

1. INTRODUCTION

In the periods 1970-2001 and 2001-2025, the world energy consumption, shown in Figures 1.1 and 1.2, has been increasing considerably, however various energy resources such as hard coal, lignite, oil and natural gas have limited storage. This is a very big problem for all countries. It is necessary that all countries should energy sources correctly and productively with new technologies. There is an urgent need to develop efficient information management and access systems for promoting energy efficient technologies and applications in the built environment. For example in Japan, energy-saving technology has been showing many good results as an important measure not only to reduce the emission of air pollutants but also to reduce the emission of gases that cause global warming since the oil shocks of the 1973 (Hui, 1999).

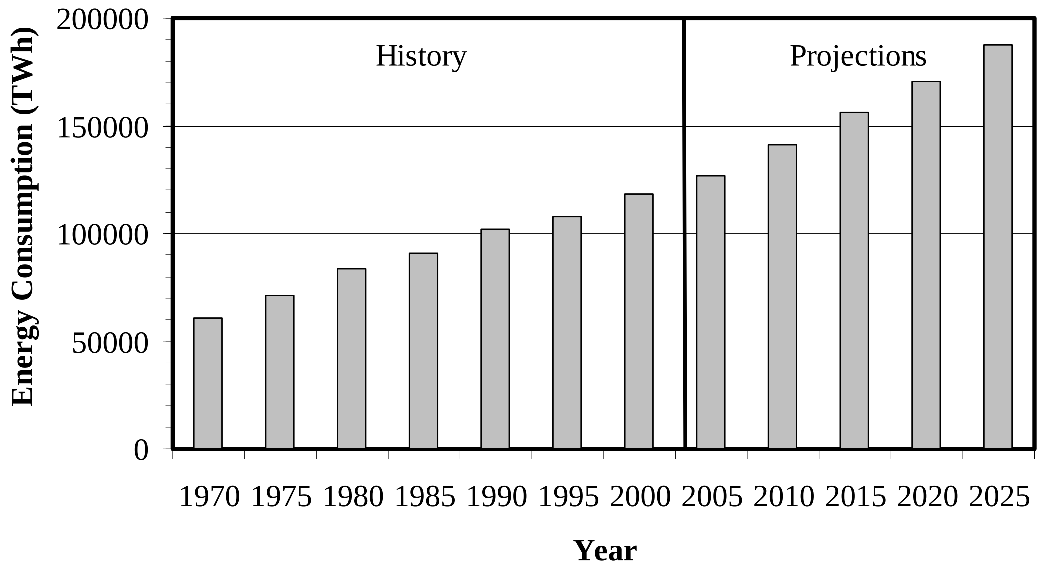

Figure 1.1. World energy consumption, 1970-2025 [EIA, 2003]

Today, a significant part of the energy is used in commercial and residential buildings. More than one third of world primary energy is consumed by commercial and residential buildings, and the building sector accounts for 25-30% of total energy-related carbon dioxide emissions [Wiel et al., 1998]. Buildings are, consequently, a primary contributor to global warming and ozone depletion. From oil embargo in 1973, building energy efficiency has become one of world's major concerns. Nowadays, important trend is global concern of sustainable human settlement, which calls for green buildings that create healthy and comfortable built environment with less energy consumption and negative impact on the ambient. The design of green buildings makes the application of building simulation a must rather than a need. As lighting, heating, ventilating and air conditioning of spaces consume most of the building energy, it is vital that thermal performance of buildings and mechanical systems is well understood and optimized in order to achieve energy efficient buildings. The operating costs of a building could be improved upon if the HVAC system of the building is made more energy efficient [Mathews et al., 2002]. This will not only result in a monetary saving for the building owner, but also less greenhouse gases will be released into the atmosphere. This clearly shows that HVAC system of a building has a large potential for energy saving.

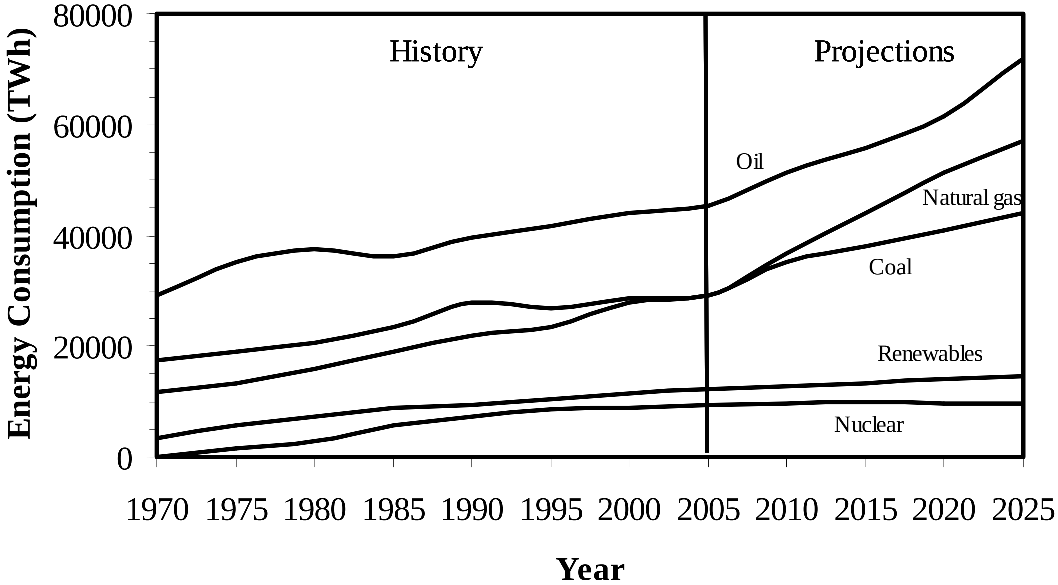

Figure 1.2. Projection of world energy sources, 1970-2025 [EIA, 2003]

On the other hand, Turkey's energy consumption has risen dramatically over the past 20 years due to the combined demands of industrialization and urbanization. Domestic energy production has not exceeded half of energy demand. Turkey is importing over 70% of energy consumption [WECTNC, 2000; WECTNC, 2003]. Turkey is heavily dependant on imported oil and natural gas because of its limited energy resources. Consequently, there is an increasing trend in energy consumption in Turkey like world energy consumption. This trend will eventually lead to an energy deficit and energy crisis in future. Turkey and developing countries must use their energy sources efficiently. In Turkey, the amount of annual energy consumption in the buildings was estimated to be 35-45 % of the total energy consumption, and 85-90% of this amount is consumed for heating and cooling [Dağsöz and Yüksel, 2000; Kılkış, 1991]. Due to wide spread use of air conditioning systems energy consumption in buildings is at a significant level.

The purpose of the HVAC systems is to provide conditions for thermal comfort and indoor air quality (IAQ) in a building. Thermal comfort can be achieved by controlling the temperature, humidity, air movement, air contaminations and level of noise. Current comfort standards stated by The American Society for Heating, Refrigerating, and Air Conditioning Engineers Inc. (ASHRAE-Standard 55) and the International Organization for Standardization (ISO-Standard 7730) describe a comfort zone as a combination of optimal thermal and personal conditions where at least 80% of building occupants are satisfied. Thermal comfort refers to air temperature, velocity and humidity while personal comfort refers to the amount of clothing being worn and the level of individual activity within the workspace. In order to provide optimal comfort to building occupants, a general recommendation is that the temperature be held constant in the range of 23-26°C and relative humidity 40-60% during heating season. During cooling season, indoor temperature is 20-23 °C and relative humidity 40-60%.

A healthy and safe environment can be attained by achieving good IAQ, which entails introducing minimum outside air to every space of the building, cleaning the air through filtration and other cleaning devices, removing airborne contaminants as close as possible to the source, and providing adequate air movement for contamination control. Sick Building Syndrome (SBS) is a term used to describe a situation in which occupants become ill due to time spent in a building, but no specific illness can be directly linked to the building conditions. In contrast, Building Related Illness (BRI) is when the illness is diagnosed and can be directly linked to the building. Causes of SBS include indoor, outdoor, and biochemical contaminants, all of which are compounded by inadequate ventilation [EPA, 1991]. IAQ has become increasingly important in facility design. It is only one part of the overall environmental quality of a facility. It is closely related to the psychometric analysis leading to system design because air quality depends largely on the amount of outdoor air brought into the conditioned space. For a typical occupied space, the amount of fresh air (clean outdoor air) is proportional to the number of the people in the space. ASHRAE standard 62, Ventilation for Acceptable Indoor Air Quality, covers this subject and is the recognized source of data for purpose of system design. IAQ has a direct effect on the productivity of the building occupants. A cost penalty is experienced if poor IAQ is traded for reduced energy consumption [Mathews, 2002].

The aim of the HVAC design is to provide systems that control the indoor environment and ensure a comfortable, healthy, and safe environment for the building occupants at a minimum cost. A minimum cost can be accomplished by reducing each of the cost elements: investment cost, annually recurring operation costs, such as energy and maintenance; future nonrecurring costs, such as spare parts and replacements; future nonrecurring costs due to occupancy changes [Dragan, 2000].

Correct HVAC system sizing requires consideration of a many factors; the local climate, size, shape, and orientation of the house, insulation levels, window area, location, and type, air infiltration rates, the number and ages of occupants, occupant comfort preferences, the types and efficiencies of lights and major home appliances [EREE, 2004] because total cooling load of the building is strongly affected by these factors. Local climate is one of the important parameters for building energy efficiency. The performance of HVAC equipment strongly changes with outdoor climatic conditions. The better design in building heating and cooling applications taken account of right climatic conditions, the more energy efficiently buildings and comfort. Outdoor design conditions are weather data information for design purposes, which show the characteristic features of the climate at a particular location. Outdoor design conditions directly affect building cooling loads. The effect of incorrect selection of outdoor design conditions can be dramatic. If some very conservative, extreme conditions are taken, uneconomic design and oversizing may result. If design loads are underestimated, equipment and system operation will be affected.

In Turkey, HVAC systems are designed using the peak outdoor design conditions [Önen, 1985 and Özkul, 1985]. The peak load occurs only a few hours each year and the peak load on one side of the building occurs at a different time of day and often in a different month of the year, than on another side of the building [Elovitz, 2002]. This may lead to an uneconomic design and oversizing may result in HVAC applications. Actually, the space requires only part of the designed capacity of the equipment most of the time. These design conditions may indicate performance of the mechanical equipment on peak, but they do not inform the designer on the cost of operating the mechanical system over the entire year. To understand the operating energy costs of systems and system alternatives, the designer is strongly encouraged to use simulation tools. Simulation tools can be used to perform the important evaluation of system part load operation [Koldrup et al, 2003].

The main goal of this study is to investigate the influence of variable outdoor air conditions on the air conditioning system. The first step in this study was to calculate cooling loads of a sample building. For this purpose, a computer program called C*oolingLoadRTS* based on the Radiant Time Series (RTS) method proposed by ASHRAE for calculating the hourly cooling loads of a building was written.

As a second step in this study, three computer programs were developed in order to determine the design capacity of an all-air central station air handling system and simulate hourly operating of this system.

Using the computer programs, design capacities of the air-conditioning system (ACS) were determined. Then, ACS under real outdoor air conditions during cooling season was simulated according to air distribution systems: constant-air-volume (CAV) and variable-air-volume (VAV).

The operating capacities of the cooling coil and return fan and supply fan in the ACS for part load operation during cooling season were obtained. Part load performances of the ACS were obtained for different conditions such as different outdoor design conditions and different operating hours.

At the final step of the study, life-cycle cost analysis using detailed load profiles and initial and operating costs to evaluate economic feasibility of CAV and VAV air-conditioning systems was performed.

2. LITERATURE REVIEW

2.1. Literature Review for Cooling Load Calculation Methods

ASHRAE has developed a number of cooling load calculation methods over the last twenty years. Three methods were included in the previous edition of ASHRAE Handbook-Fundamental (ASHRAE 1993 and 1997) and Cooling and Heating load Calculation Manual (McQuiston and Spitler 1992): the Transfer Function Method (TFM), the Cooling Load Temperature Difference/Solar Cooling Load/Cooling Load Factor (CLTD/SCL/CLF) method and the Total Equivalent Temperature Difference/Time Averaging (TETD/TA) method. More recently, Chapter 29 of 2001 ASHRAE Handbook-Fundamental (ASHRAE 2001), nonresidential cooling and heating load calculation procedures, presents two cooling load calculation methods namely Heat Balance (HB) and Radiant Time Series (RTS) methods. Chapter 28 of 2001 ASHRAE Handbook-Fundamental (ASHRAE 2001) covers residential cooling and heating load calculation procedures.

HB and RTS methods were developed by ASHRAE which has funded a research project entitled Advanced Methods for Calculating Peak Cooling Loads (RP-875). HB method was completely described by Pederson et al. in 1997. In addition, McClellan and Pederson (1997) presented a brief overview of the HB method.

Spitler et al. (1997) first described RTS methodology and explained the procedures for generating the wall/roof response factors and the radiant time factors. They gave a brief comparison with the HB method.

Chapter 27 of 2001 ASHRAE Handbook-Fundamental, Climatic Design Information, presents outdoor design conditions for many countries. Calculations of fenestration and energy estimation method were also outlined in Chapters 30 and 31 of 2001 ASHRAE Handbook-Fundamental, respectively.

Some selected papers on cooling load and its applications are given in the following part.

Shariah et al. (1997) calculated cooling and heating loads for three different cities in Jordan, representing three climatic regions; namely, Irbid, Amman and

Aqaba. To analyze the insulation effect of buildings, for each region four combinations of wall and ceiling insulation were considered: no insulation; only wall insulated; only ceiling insulated; and both ceiling and wall insulated.

Balaras (1996) investigated the role of thermal mass on the cooling load of buildings. He identified and classified 16 simplified design tools for calculating the cooling load and indoor air temperatures of a building. The models were categorized in term of their inputs, outputs and restrictions on their level of accuracy in treating thermal mass effect, type of loads or other design limitations.

Liesen and Pederson (1997) developed many radiant exchange models. These models range from the exact solutions using uniform radiosity networks and exact view factors to mean radiant temperature and area-weighed view factors. These radiant exchange models were directly compared to each other for a simple zone with varying aspect ratios. The radiant exchange models were then compared to determine their effect on the cooling load. Finally, other parameters that affect the inside surface heat balance were investigated to determine their sensitivity to the cooling load.

Al-Rabghi and Al-Johani (1997) programmed TFM cooling load calculation method to predict the hourly cooling load due to different types of wall, roof and fenestration. The developed computer code was tested against hand calculations and was found to be accurate. The outputs of the program were also compared with the well-known Carrier program, and the agreement was satisfactory. Various runs were made, and the results of these runs were discussed. Authors investigated effect of changing the wall color on cooling load and on sol-air temperature.

Hosni et al. (1998) evaluated the total heat gain and the split between radiant and convective heat gains for typical office and laboratory equipment such as desk computer, monitor, a copier, a laser printer, and a biological incubator. Results show that the radiant portion of the total heat gain ranged from a minimum of 11 % for the laser printer to a maximum of 57% for the incubator. The radiant portion of the heat gain from the heated surfaces was higher, at about 60%.

Spitler and Rees (1998) described the methodology used in a quantitative comparison between the current North American and United Kingdom cooling load calculation methods. Three calculation methods were tested as part of a joint ASHRAE and its U.K sister organization, the Chartered Institution of Building Services Engineers (CIBSE). These methods are the ASHRAE heat balance and radiant time series methods and the admittance method used in U.K. This project entitled Comparison of load Calculation Procedures (ASHRAE RP 942). The methodology presented and tools described could also be used to make comparisons between other calculation methods.

Rees et al. (1998) compared three design cooling calculation methods, the ASHRAE heat balance and radiant time series methods and the admittance method used in U.K. Methodology of this study was described by Spitler et al. (1998). The results show the general trends in over/under prediction of peak load in the simplified methods compared to the heat balance method. The performance of the simplified methods was explained in term of some of the underlying assumptions in the methods and by reference to specific examples.

Moujaes and Brickman (1998) described the results of a computer study that simulated the thermal behavior of radiant barriers placed on the underside of the roof sheathing. The results showed the reduction of the cooling load for a design-day condition in Las Vegas, Nevada. The reductions were due to (1) a decrease in the sensible heat gain through the ceiling of a typical residence, and (2) to the reduction in the heat gains incurred by the duct system (and eventually by the supply air) placed in the attic. In addition, they described the results of some field verifications of the magnitude of these reductions and the comparative results of the total instantaneous cooling using the model versus other established techniques.

Liesen et al. (1998) presented an investigation of the influence of the radiative/convective split on cooling loads obtained using the heat balance procedure. They started with an overview of the model used for a heat balance procedure and then presented an exhaustive case study of the effects of changing the mode split on load calculations for wedge 1 of the Pentagon building.

Spitler and Fisher (1999) discussed the steady periodic nature of the cooling load calculation and developed the steady periodic conduction and thermal zone response factors used in the new Radiant Time Series Method. The periodic response factors used in the RTS method were compared to the periodic response factors used in the Transfer Function Method described by McQuiston and Spitler (1992). Periodic response factors simplify the computational procedure and provide a means of comparing zone and surface types.

Rees and Spitler (1999) proposed a set of the tests that are designed to exercise the principal features of any implementation of a design cooling load calculation methods. The purpose of the tests was qualification to a certain standard of accuracy and not diagnosis of particular faults. They used the heat balance method as a reference model. They gave some example of how the tests were used in the project “Comparison of Cooling Load Calculation Methods”.

Hosni et al. (1999) investigated the heat gain and split ratio between the radiant and convective heat load from the equipment in buildings. Results of the experimental study were obtained total heat gain and radiant/convective split for equipment in offices, hospitals and laboratories. The nameplate vs. measured values, peak vs. average values, operational vs. idle values, and radiant vs. convective values were compared and discussed. Furthermore, a brief guideline for use of the experimental results by practicing engineers for estimating equipment cooling load was presented.

Tianzhen et al. (1999) described how a design day for building energy performance simulation can be selected from a typical meteorological year (TMY) of a location. The selection criterion addresses the balance between the need to minimize the part-load performance of the air conditioning systems and plants. To validate the versatility of the design day weather file, authors compared simulation results of the peak load and load profile of a building obtained from the DOE-2.1E code and a specially developed load estimation program, PEAKLOAD. PEAKLOAD was developed using the transfer function method and ASHRAE databases. Comparative results were in good agreement, indicating that a design day thus selected can be used when quick answers were required and simulations using a TMY file cannot be easily done or justified.

Davies (1999) reviewed methods of handling wall conduction and room internal heat exchange adopted by ASHRAE, CIBSE and the CEN/TC89/WG6 proposals to calculate heating and cooling loads and related topics. Author sought to trace the historical background to work in the area, which is concerned with handling the transfer of heat in walls by conduction and transfer within an enclosure by convection and radiation.

Joudi and Salah (2000) investigated the application of the indirect evaporative cooling in fulfillment of the variable cooling load of a typical Iraqi dwelling. A two story house located in Baghdad was the object of the study. The application was evaluated through a systematic simulation, along with a comparison between two arrangements of an indirect-direct evaporative cooling system. The simulation involved the operation of the cooling system under four operating modes for variable ambient temperature and cooling load conditions during the summer season. The concept of variable air volume (VAV) was employed as a control strategy over the day by changing the supply air flow rate through a variable speed fan according to the variation in the cooling load. Hourly computerized calculations were programmed for the variable cooling load using the transfer function method (TFM) over 24 hour daily cycles.

Joudi and Dhaidan (2001) evaluated performance of solar assisted heating and desiccant cooling systems for a domestic two story residence located in Baghdad. A computer simulation was developed to assess the effects of various designs and operating conditions on the performance of the system and its components. The transfer function method was used to evaluate the hourly variation of the cooling load.

Papadopoulos (2001) investigated the impact of microclimatic conditions in urban areas on the thermal loads of buildings. The modulation of street canyons led to temperature conditions that depart from the climatic data monitored at meteorological stations, affecting the heating balance of buildings, while the building operation affects the present conditions. The installation of air conditioning units leads to heat emission, which, at a microscale level, strengthens this phenomenon. The author outlined a computational approach to the street canyon phenomenon, with the determination of flow and temperature fields which were developed, and discussed their influence on the dynamic thermal balance of the building.

Yik et al. (2001) described a method used in estimations of the simultaneous cooling demand of a large group of buildings on a district scale and the energy use for air conditioning such buildings. Comparisons of the results estimated by this method with the results obtained by detailed simulation, and with the building energy use data obtained from surveys and audits were presented.

Kossecka and Kosny (2002) focused on the energy performance of buildings containing massive exterior building envelope components. The effect of mass and insulation location on heating and cooling loads was analyzed for six characteristic wall configurations. Correlations between structural and dynamic thermal characteristics of walls were discussed. A simple one-room model of a building exposed to periodic temperature changes was analyzed to illustrate the effect of material configuration on the ability of a wall to dampen interior temperature swings. Whole-building dynamic modeling using DOE-2.1E was employed for the energy analysis of a one-story residential building with various exterior wall configurations for six different US climates. The best thermal performance was obtained when massive material layers are located at the inner side and directly exposed to the interior space.

Eskin and Türkmen (2003) developed a computer program based on the TFM proposed by ASHRAE for calculating the cooling loads of nonresidential buildings. Yearly heating and cooling loads of an office building with different dimensions and located in different province of Turkey were investigated.

Atmaca (2003) developed a computer program based on the CLTD/SCL/CLF method proposed by ASHRAE for calculating the cooling loads of a building. Author described the method and the procedure used for the computer program written.

2.2. Literature Review for Climatic Effect on Cooling Load/Coil Load

Al-Homoud (1997) presented the results of applying an optimization model to the design of energy conserving office buildings in different climatic regions to test the impact of mainly envelope related parameters on the thermal performance of offices. Optimum sets of building design variables for three different sized office buildings in four U.S. and two Saudi Arabian cities were presented with the objective of minimizing annual energy consumption for those buildings.

Al-Rabghi et al. (1999) presented the experimental and theoretical variations of electric power consumed by an air conditioning system. The study consists of two parts. For the experimental part, a building was chose, and different sensors were installed to measure and record electric consumption for different indoor and outdoor conditions. In the theoretical part, the Visual DOE simulation program, which is based on the well known DOE-2E program, was used. Actual building data was fed to the program to generate the instantaneous electric consumption due to air conditioning cooling load. Comparison between measured and predicted electric consumptions was presented.

Sawhney et al. (1999) studied the thermal performance of the underground airpipe air conditioning system constructed at the Non-Conventional Energy Research Institute, Ghosi in India. The heat exchanger was used in recirculation mode to air condition eight rooms in a guest house at the Institute. The temperature and relative humidity of a conditioned and non-conditioned room were measured every two hours. Authors estimated the cooling potential of the system. Results showed that reasonably good thermal comfort conditions can be created in the building with such a system.

Bellia et al. (2000) presented a work involving the processing of climatic data relating to some Italian cities, taken from a set of data known as European test reference year (TRY). They aimed to make a critical comparison of the thermohygrometric conditions of outdoor air in the summer season thus obtained with those design conditions as laid down by Italian regulations (UNI 10339) and with those recently suggested by ASHRAE. Subsequently, and with reference to some traditional and recent applications in the field of air-conditioning, authors reported how performance differs according to outdoor summer thermohygrometric design conditions, such as those indicated by UNI 10339, by ASHRAE and by the processing of TRY data. Finally, they discussed the optimal choice of design conditions according to the type of application.

Hassid et al. (2000) investigated the effect of the summer heat island of the western part of the Greater Athens area on cooling energy and peak power using the building energy estimating software DOE2.1.E and measured values of temperature and other meteorological data at selected sites. Heat island occurs when the air temperatures in densely built urban area are higher than the temperatures of the surrounding countryside. The calculations were shown to underestimate both energy consumption and peak power.

Ealiwa et al. (2001) reviewed the results from a field survey of thermal comfort within two types of buildings; old (traditional) and new (contemporary), in Ghadames oasis in Libya. The survey was undertaken in the summer seasons 1997 and 1998, which were typical of the hot-dry climate of North Africa. The survey showed how the 237 residents responded to the environmental conditions. Questionnaires were collected from the residents of 51 buildings: 24 old buildings that employ natural ventilation systems and 27 new buildings that employ air-conditioning systems. The field study also investigated occupants' overall impression of the indoor condition. The results suggested that people have an overall impression of higher standard of thermal comfort in old buildings than in new buildings.

Li and Lam (2001) developed an approach for calculating solar heat gain factors (SHGFs) for the horizontal and vertical surfaces at the peak and other significant levels based on solar angles and clearness index (K_t). An analysis of the SHGF data show that the proposed model performs better than the ASHRAE clear sky approach, particularly at high significant levels. The findings provided information for the determination of total air conditioning plant capacity at both the peak load operation and the multiple equipment sizing under part load condition.

Li et al. (2003) presented a work on the determination of outdoor design conditions for cooling load calculation. The computer package DOE-2.1E was used to simulate the hourly cooling load of a generic commercial office building in Hong Kong. Totally, 22 weather data sets, from 1979 to 2000, were used for the analysis. The findings indicate that the outdoor climatic conditions developed for cooling load estimation via the simulations are less stringent than the current outdoor design data and approaches adopted by local architectural and engineering practices.

3. MATERIAL AND METHOD

3.1. Calculation of Space Cooling Loads

In commercial, residential, industrial, and institutional HVAC design, it is critical for design contractors and engineers to perform a load calculation. Not only it is important for occupant comfort, it is also needed in order to avoid air quality problems, which can lead to costly, even ruinous litigations [Checket, 2002]. Detailed calculation of space cooling loads is a complex process, which involves the determination of each type of heat gain entering the space (e.g., solar, conduction through exterior surfaces, or that from people, lights, and equipment), the radiative and convective interaction between each type of heat gain, and storage and release of energy in thermal mass. Many cooling load components vary in magnitude over a wide range during a 24 hours period. Because these cyclic changes in load components often are not in phase with each other, each must be analyzed to establish the maximum cooling load for a building or zone. The rate at which heat enters or is generated within a space at a given moment is called heat gain. Heat gain is classified by the mode in which it enters the space, and whether it is sensible or latent gain. Modes of heat gain that are present in a building include [McQuiston and Spitler, 1992; ASHRAE, 2001]:

1) Solar radiation through transparent surfaces,
2) Heat conduction through exterior walls and roofs,
3) Heat conduction through interior partitions, ceilings, and floors.
4) Heat generated within the space by occupants, lights, and equipment.
5) Heat transfer as a result of infiltration of outdoor air,
6) Miscellaneous heat gains.

The space-cooling load is the rate at which heat must be removed from the space to maintain a constant air temperature. The space-cooling load is equal to the instantaneous rate of heat convected into the space air, which includes the convective portion of heat gain plus the rate of heat released by thermal mass in the zone. This amount may be more or less than the hourly heat gain. The cooling load is greater than the hourly heat gain for situations in which heat is given up by thermal mass in the zone.

Radiant energy must first be absorbed by the surfaces that enclose the space and the objects in the space. When these surfaces and objects become warmer than the surrounding air, some of their heat is transferred to the air by convection. The composite heat storage capacity of these surfaces and objects determines the rate at which their respective surface temperatures increase for a given radiant input and thus governs the relationship between the radiant portion of heat gain and its corresponding part of the space-cooling load. Heat transfer mechanics of a space is shown in Figure 3.1 [McQuiston and Spitler, 1992; ASHRAE, 2001].

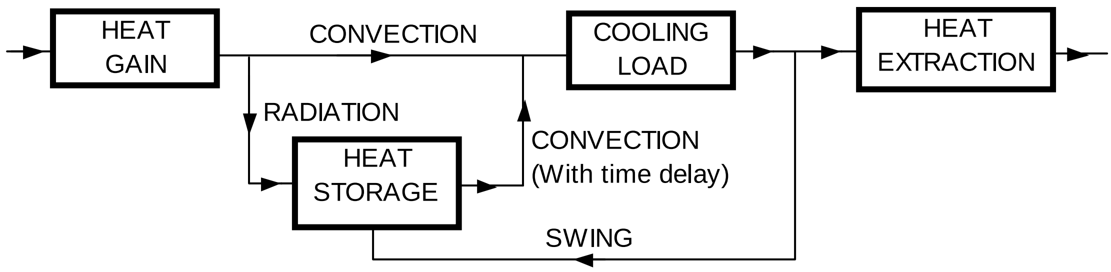

Figure 3.1. Schematic of heat transfer for the space

The first step in this study is to calculate cooling loads of a sample building that depend on the building characteristics, the indoor conditions to be maintained and the outdoor air conditions. In Turkey, the calculations of cooling loads are based on Technical Publications No 9, Turkish Ministry of Reconstruction and Settlement. In this study, cooling load of the selected building is determined according to the Radiant Time Series method, which was presented in 2001 ASHRAE Fundamentals Handbook.

3.1.1. Description of Different Cooling Load Calculation Methods

ASHRAE has developed a number of cooling load calculation procedures over the last twenty years. The evolution of the current load calculation methodology as a continuing process that started in 1967 is described [Checket, 2002]. It began with Total Equivalent Temperature Difference/Time Average (TETD/TA) methods, which is presented in the 1967 ASHRAE Fundamentals Handbook. Then came (in 1972) the Transfer Function Method (TFM), which factors together heat gain by conduction through exterior walls and roof; conversion of the cooling load from heat gain and use room transfer function. In 1977, the Cooling Load Temperature Difference/Cooling Load Factor (CLTD/CLF) method was devised, offering greater simplicity due to its single step calculation, tabular data and manual method. The latest step in evolution has resulted in the Radiant Time Series method (RTSM) and Heat Balance (HB) method. Radiant Time Series method, which is a simplified method directly related to and derived from the HB calculation procedure. HB method was introduced by Pedersen (1997) and presented in the 2001 ASHRAE Handbook of Fundamentals.

In comparing the HB and RTS methods against other methods, the primary difference is the directness of approach as opposed to the simplifying techniques necessitated by computer capability available in earlier years. The TFM, for example, required many calculation steps. Also, this method was originally designed for energy analysis with emphasis on daily, monthly, and annual energy use and, thus, was more oriented to average hourly cooling loads than peak design loads.

TETD/TA has been a highly reliable method. Originally conceived as a manual method of calculation, it proved suitable only as a computer application because of need to calculate an extended profile of hourly heat gain values from which the radiant components had to be averaged over a time perceived to represent the general mass of building involved. Because this perception of thermal storage characteristics of a given building was almost entirely subjective, with little specific information for the user to judge variation, the TETD/TA method’s primary usefulness has always been to the experienced engineer.

The CLTD/CLF was an attempt to simplify the two-step TFM and TETD/TA methods into a single step technique that allowed proceeding directly from raw data to cooling load without the intermediate conversion of radiant heat gain to cooling load. A series of factors were taken from cooling load calculation results as equivalent temperature differences for use in traditional conduction equations. The results, however, are approximate cooling load values rather than simple heat gain values. The simplifications required for this process limit the applicability of this method.

3.1.2. Radiant Time Series Method

The RTS method introduced by Spitler et al. (1997) and 2001 ASHRAE Fundamentals Handbook is a new simplified method for performing design cooling load calculations that is derived from the HB method. It effectively replaces all other simplified methods.

This method was developed in response to the desire to offer a method that is rigorous, yet does not require iterative calculations, and that quantifies each component contribution to the total cooling load. In addition, it is desirable for user to be able to inspect and compare the coefficients for different construction and zone types in a form illustrating their relative impact on the result. These characteristics of the RTS method make it easier to apply engineering judgment during the cooling load calculation process.

Design cooling loads are based on assumption of steady periodic conditions. Thus, the heat gain for a particular component at a particular hour is the same as 24 hours prior, which is the same as 48 hours prior, etc. This assumption is the basis for the RTS method derivation from the HB method.

Cooling load calculations must address two time-delay effects inherent in building heat transfer processes,

1) Delay of conductive heat gain through opaque massive exterior surfaces,
2) Delay of radiative heat gain conversion to cooling loads.

Exterior walls and roofs conduct heat due to temperature differences between outdoor and indoor air. In addition, solar energy on exterior surfaces is absorbed, and then transferred by conduction to the building interior. Due to the mass and thermal capacity of the wall or roof construction materials, there is a substantial time delay in heat input at the exterior surface becoming heat gain at the interior surface.

3.1.3. Overview of the RTS Method

Figure 3.2 gives an overview of radiant time series methods. In the calculation of solar radiation, transmitted solar heat gain through windows, sol-air temperature, and infiltration, the RTS method is exactly the same as previous methods. Important areas that are different include the computation of conductive heat gain, the splitting of all heat gains into radiant and convective portions, and the conversion of radiant heat gains into cooling loads.

The RTS method accounts for both conduction time delay and radiant time delay effects by multiplying hourly heat gains by 24 hours time series. The time series multiplication, in effect, distributes heat gains over time. Series coefficients, which are called radiant time factors (RTS) and conduction time factors (CTS), are derived using the heat balance method. Radiant time factors reflect the percentage of an earlier radiant heat gain that becomes cooling load during the current hour. Likewise, conduction time factors reflect the percentage of an earlier heat gain at the exterior of a wall or roof that becomes heat gain at the inside during the current hour.

3.1.4. RTS Method Procedure

The general procedure for calculating cooling load for each load component is as follows:

1) Calculate 24 hours profile of component heat gain for design day (for conduction, first account for conduction time delay by applying CTS)
2) Split heat gains into radiant and convective parts (see Table 3.1.).
3) Apply appropriate RTS to radiant part of heat gains to account for time delay in conversion to cooling load.
4) Sum convective part of heat gain and delayed radiant part of heat gain to determine cooling load for each hour for each cooling load component.

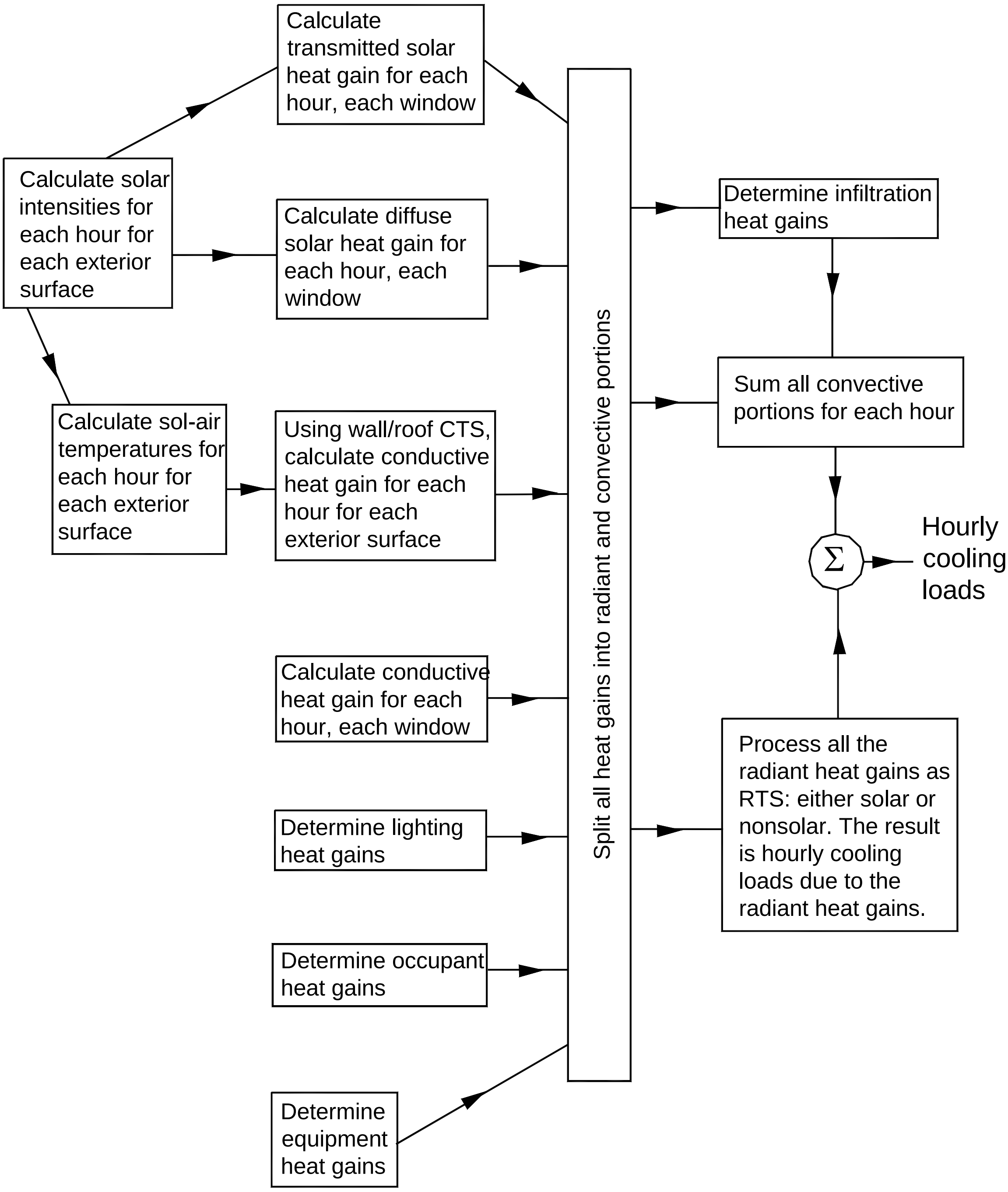

Figure 3.2. Overview of Radiant Time Series Method [Spitler et al., 1997]

According to the radiant time series procedure, once each heat gain is split into radiative and convective portions, the heat gains can be converted to cooling loads. Table 3.1 contains provisional recommendations for splitting each of the heat gain components.

In this method, conduction through exterior walls and roofs is calculated using CTS. Wall and roof conductive heat input at the exterior is defined by the familiar conduction equation as:

$$Q_{i,t-n} = UA\left(T_{e,t-n} - T_R\right) \tag{3.1}$$

where $Q_{i,t-n}$ is conductive heat input [W] for the surface n hours ago, U is overall heat transfer coefficient for the surface[W/(m^2.K)], A is surface area [m^2], $T_{e,t-n}$ is solar-air temperature n hours ago [°C] and T_R is presumed constant room air temperature [°C].

Conductive heat gain through walls or roofs can be calculated using conductive heat inputs for the current hours and past 23 hours and CTS:

$$Q_t = c_0 Q_{i,t} + c_1 Q_{i,t-1} + c_2 Q_{i,t-2} + c_3 Q_{i,t-3} + \ldots\ldots\ldots + c_{23} Q_{i,t-23} \tag{3.2}$$

where Q_t is hourly conductive heat gain [W] for the surface, $Q_{i,t}$ is heat input [W] for the current hour, $Q_{i,t-n}$ is heat input [W] n hours ago, and c_0, c_1, etc. are CTS. CTS for representative wall and roof types are given as tabular in chapter 29 of the 2001 ASHRAE Fundamentals Handbook.

Conductive heat gain through walls or roofs is divided according to split rate from Table 3.1. Convective portions immediately become cooling load. Radiant heat gains become cooling load over a delayed period of time. The radiant time series is used to convert the radiant portion of hourly heat gains to hourly cooling loads with Equation 3.3.

$$Q_{rc,t} = r_0 Q_{r,t} + r_1 Q_{r,t-1} + r_2 Q_{r,t-2} + r_3 Q_{r,t-3} + \ldots\ldots\ldots + r_{23} Q_{r,t-23} \tag{3.3}$$

Table 3.1. Radiative and convective split for heat gain [Spitler et al., 1997]

Heat Gain Type	Radiative Fraction	Convective Fraction	Comments
Occupants	0.7	0.3	Rudoy and Duran(1975)
Lighting • Suspended fluorescent-unvented • Recessed fluorescent-vented to return air • Recessed fluorescent-vented to supply and return air • Incandescent	 0.67 0.59 0.19 0.71	 0.33 0.41 0.81 0.29	York and Cappielo (1981)
Equipment	0.2-0.8	0.8-0.2	ASHRAE 4.1 has ongoing research. In the meantime, use higher values of radiation fractions for equipment with higher surface temperatures. See for detail Hosni et al., (1998, 1999)
Conductive heat gain through walls	0.63	0.37	
Conductive heat gain through roof	0.84	0.16	
Absorbed (by fenestration) solar	0.63	0.37	
Transmitted solar radiation	1.00	0	
Infiltration and ventilation	0	1.00	

where $Q_{rc,t}$ is radiant cooling load [W] for the current hour, $Q_{r,t}$ is radiant heat gain [W] for the current hour, $Q_{r,t-n}$ is radiant heat gain [W] n hours ago, and r_0, r_1, etc. are radiant time series (RTS). RTS for representative wall and roof types are given in two different tables in the 2001 ASHRAE Fundamentals Handbook. They are solar and nonsolar. Nonsolar RTS apply to radiant heat gains from people, lights, appliances, walls, roofs and floor. Also, for diffuse solar heat gain and direct solar heat gain from fenestration with inside shading, the nonsolar RTS should be used. Solar RTS apply to radiant heat gains from glass (direct transmitted solar heat gain).

Finally, total cooling load for the exterior surfaces (Q_{tot_ES}) is calculated by summing the parts of radiant ($Q_{rc,t}$) and convective ($Q_{c,t}$).

$$Q_{tot\_ES}=Q_{rc,t}+Q_{c,t} \tag{3.4}$$

For fenestration heat gain, the following equations is used [ASHRAE, 2001]. Fenestration heat gains consist of three portions; direct beam solar heat gain, diffuse solar heat gain and convective heat gain.

Direct beam solar heat gain is given by:

$$Q_b=AE_DSHGC(\theta) \tag{3.5}$$

Diffuse solar heat gain is given by:

$$Q_d=A(E_d+E_r)<SHGC>_DIAC \tag{3.6}$$

Conductive heat gain is given by:

$$Q_c=UA(T_O-T_R) \tag{3.7}$$

Total fenestration heat gain is given by:

$$Q_{tot\_F}=Q_b+Q_d+Q_c \tag{3.8}$$

where,

A	:	Window area [m^2]
E_D, E_d and E_r	:	Direct, diffuse and ground-reflected irradiance [W/m^2],
SHGC(θ)	:	Direct solar heat gain coefficient, a function of incident angle [θ]

$\langle SHGC \rangle_D$: Diffuse solar heat gain coefficient,
T_R : Inside temperature [°C],
T_O : Outside temperature [°C],
U : Overall U factor [W/m^{2}K],
IAC : Inside shading attenuation coefficient.

In the first step, direct beam solar heat gain through windows, which is calculated from Equation, (3.5) is divided according to split rate taken from Table 3.1. Convective portions immediately become cooling load. Radiant heat gains become cooling load over a delayed period of time. Radiant portion of direct beam solar heat gains is converted to direct solar radiant cooling loads using Equation (3.3) with solar RTS.

In the second step, the conductive heat gain calculated from equation (3.7) and the diffuse solar heat gain calculated from equation (3.6) are summed. Then, heat gain is split into radiant and convective parts. The appropriate nonsolar RTS is applied to radiant portions. Finally, all the parts of radiant cooling load and convective cooling load from windows are summed to determine total fenestration cooling load.

For others, to obtain heat gain to calculate cooling load, the following equations are used:

Interior Surfaces : $Q=AU(T_b-T_R)$ (3.9)

Infiltration&Ventilation : $Q=Mc_p(T_O-T_R)$ (3.10)

Internal Heat Gains

People Sensible : $Q_s=Nq_{sen}F_u$ (3.11)

People Latent : $Q_l=Nq_{lat}F_u$ (3.12)

Lighting : $Q=VF_uF_s$ (3.13)

Equipment : $Q=XF_uF_l$ (3.14)

where;

Q	:	Heat gain [W]
A	:	Area of separating section concerned [m^2]
T_b	:	Average air temperature in adjacent space [°C],
N	:	Maximum number of people expected to occupy the space
q_{lat}	:	Latent heat gain per people [W/person]
q_{sen}	:	Sensible heat gain per people [W/person]
V	:	Total installed light wattage [W]
X	:	Heat output of equipment [W]
M	:	Infiltration mass flow rate [kg/s]
c_p	:	Specific heat coefficient [J/kg °C]
F_u	:	Diversity (use) factor
F_l	:	Motor load factor
Fs	:	Special allowance factor

The heat gain, which can be calculated using Equations (3.9) to (3.14), is divided according to split rate taken from Table 3.1; the convective and radiant heat gains. The convective component of heat gain immediately becomes the cooling load. The radiant component of the heat gain is converted to radiant cooling load using Equation (3.3) with nonsolar RTS. Then, the radiant cooling load and the convective cooling load are summed to determine total cooling load due to miscellaneous heat gain, such as internal people, lighting, ventilation, etc.

3.1.5. Solar Equation

The primary weather-related variable influencing the cooling load for a building is solar radiation. The effect of solar radiation is more pronounced and immediate in its impact on exposed non-opaque surfaces. For fenestration heat gain, the following solar equation is used [ASHRAE, 2001].

$$AST = LST + \frac{ET}{60} + (LSM - LON)15 \tag{3.15}$$

where AST is apparent solar time (decimal hours), LST is local solar time (decimal hours), ET is equation of time (decimal minutes), LSM is local standard time meridian (decimal ° of arc), and LON is local longitude (decimal ° of arc).

The sun's position in the sky is conveniently expressed in terms of solar altitude β above the horizontal and the solar azimuth Φ_S measured from the south. This angle, in turn, depends on the local latitude L, the solar declination δ, and the apparent solar time, expressed as the hour angle H, where

$$H=15(AST-12) \tag{3.16}$$

The equations relate β and Φ to the three angles mentioned are:

$$\sin\beta=\cos L\cos\delta\cos H+\sin L\sin\delta \tag{3.17}$$

$$\cos\Phi_S=(\sin\beta\sin L-\sin\delta)/(\cos\beta\cos L) \tag{3.18}$$

γ is surface solar azimuth, defined as

$$\gamma=\Phi_S-\Psi \tag{3.19}$$

The solar azimuth is positive for afternoon hours and negative for morning hours. Ψ is surface azimuth. Table 3.2 gives values in degrees for the surface azimuth, applicable to the orientations of interest.

Table 3.2. Surfaces orientations and surface azimuth

Orientation	**N**	**NE**	**E**	**SE**
Ψ	180	-135	-90	-45
Orientation	**S**	**SW**	**W**	**NW**
Ψ	0	45	90	135

For any surface, the incident angle θ is related to β, γ, and the tilt angle of the surface Σ by,

$$\cos\theta=\cos\beta\cos\gamma\sin\Sigma+\sin\beta\cos\Sigma \tag{3.20}$$

Direct normal irradiance E_{DN};

If $\beta>0$

$$E_{DN} = \left(\frac{A_p}{e^{\left(\frac{B}{\sin\beta}\right)}} \right) CN \qquad (3.21)$$

Otherwise;

$$E_{DN}=0 \qquad (3.22)$$

Surface direct irradiance E_D,

If cosθ>0

$$E_D=E_{DN}\cos\theta \qquad (3.23)$$

Otherwise,

$$E_D=0 \qquad (3.24)$$

Ratio Y of sky diffuse on vertical surface to sky diffuse on horizontal surface,

If cosθ>-0.2

$$Y=0.55+0.437\cos\theta+0.313\cos^2\theta \qquad (3.25)$$

Otherwise,

$$Y=0.45 \qquad (3.26)$$

Diffuse irradiance E_d,

For vertical surfaces,

$$E_d=CYE_{DN} \qquad (3.27)$$

Surfaces other than vertical

$$E_d=CE_{DN}(1+\cos\Sigma)/2 \qquad (3.28)$$

Ground-reflected irradiation E_r,

$$E_r=E_{DN}(C+\sin\beta)\rho_g(1-\cos\Sigma)/2 \qquad (3.29)$$

Total surface irradiance E_t,

$$E_t=E_D+E_d+E_r \tag{3.30}$$

where A_p is apparent solar constant, B is atmospheric extinction coefficient, C is sky diffuse factor, CN is clearness number multiplier for clear/dry or hazy/humid locations, and ρ_g is ground reflectivity.

The heat balance at a sunlit surface gives the heat flux into the surface Q/A as

$$\frac{Q}{A} = \alpha E_t + \hbar\left(T_O - T_{sr}\right) - \varepsilon\Delta R \tag{3.31}$$

where;

α	:	Absorptance of surface for solar radiation,
$\hbar$	:	Coefficient of heat transfer by long-wave radiation and convection at outer surface, [W/m^2K]
T_{sr}	:	Surface temperature, [°C]
ε	:	Hemispherical emittance of surface
ΔR	:	Difference between long-wave radiation incident on surface from sky and surroundings and radiation emitted by blackbody at outdoor air temperature, [W/m^2]

The rate of heat transfer can be expressed in term of the sol-air temperature T_e,

$$\frac{Q}{A} = \hbar\left(T_e - T_{sr}\right) \tag{3.32}$$

and from Equations (3.31) and (3.32), the solar-air temperature can be written as:

$$T_e = T_O + \frac{\alpha E_t}{\hbar} - \frac{\varepsilon\Delta R}{\hbar} \tag{3.33}$$

For horizontal surfaces that receive long-wave radiation from sky only, an appropriate value of ΔR is about 63 W/m^2. It is common practice to assume $\varepsilon\Delta R$ equal to 0 for vertical surfaces. Sol-air temperature values are given for two values of parameter $\alpha/\hbar$, the value of 0.026 is appropriate for a light-colored surface, while 0.052 represents the usual maximum value for this parameter [McQuiston and Spitler, 1992; ASHRAE, 2001].

Outdoor air temperature is calculated from outdoor design temperature (T_{DT}). Hourly outdoor air temperature ($T_{O,t}$) is calculated using Equation (3.34.)

$$T_{O,t}=T_{DT}-(DR*P_t) \tag{3.34}$$

where P_t is percentage of daily temperature range for the current (t) hour (Table 3.3) and DR is daily temperature range [ASHRAE, 2001].

Table 3.3. Percentage of daily temperature range for Equation (3.34)

Time	P_t [%]	Time	P_t [%]	Time	P_t [%]
1^{00}	87	9^{00}	71	17^{00}	10
2^{00}	92	10^{00}	56	18^{00}	21
3^{00}	96	11^{00}	39	19^{00}	34
4^{00}	99	12^{00}	23	20^{00}	47
5^{00}	100	13^{00}	11	21^{00}	58
6^{00}	98	14^{00}	3	22^{00}	68
7^{00}	93	15^{00}	0	23^{00}	76
8^{00}	84	16^{00}	3	24^{00}	82

3.1.6. Computer Program CALL_*CoolingLoadRTS*

In this study, a computer program calculating the hourly cooling loads of a sample building was written according to RTS method, for which the details are given in Appendix A1. The program is called *CoolingLoadRTS*, and is written on MS-EXCEL environment.

3.2. Equations for Weather Data

As a second step in this study, outdoor air conditions were determined on an hourly basis during whole day (24 hours). Hourly dry-bulb temperature and humidity ratio were taken as outdoor air conditions. Hourly absolute humidity, and hourly dry-bulb temperature were modeled with trigonometric functions using suitable equations given in literature [Oğulata and Yılmaz, 1989; Yılmaz et al., 1995; Bulut et al., 1999; Bulut, 2001].

The weather data on which this study is based on were taken from The State Meteorological Affairs General Directorate (DMİ). The meteorological parameters obtained from DMİ are hourly dry-bulb temperature, absolute humidity records at 07^{00}, 14^{00} and 21^{00} o'clock, and daily minimum and maximum dry-bulb temperatures. Weather data set contains the period between 1981and 1998.

The parameters of the recommended equations for hourly absolute humidity, and dry-bulb temperature were determined by means of statistical analysis. The following statistical indicators were used (Johnson and Bhattacharya, 1996; Daniel et al. 1971).

Root Mean Square Error (RMSE),

$$RMSE = \left(\frac{\sum_{i=1}^{k} \left(CV_i - MV_i \right)^2}{k - k_p} \right)^{1/2} \tag{3.35}$$

where CV denotes the value calculated from the equation, MV denotes the measured value, k is the number of values, and k_p is the number of parameters in the particular model (k_p=2 for model used in this study).

Absolute Error (AE),

$$AE = \left| CV - MV \right| \tag{3.36}$$

Relative Error (RE),

$$RE = \frac{\left| CV - MV \right|}{MV} \tag{3.37}$$

Correlation Coefficient (R),

$$R \equiv \sqrt{\frac{S_t - S_r}{S_t}} \tag{3.38}$$

where S_t and S_r are defined as follow:

$$S_t = \sum_{i=1}^{k} (MMV - MV_i)^2 \tag{3.39}$$

where MMV is the average of measured values:

$$MMV = \frac{\sum_{i=1}^{k} MV_i}{k} \tag{3.40}$$

$$S_r = \sum_{i=1}^{k} (MV_i - CV_i)^2 \tag{3.41}$$

For better data modeling, the RMSE, AE and RE must be minimal and the correlation coefficient r must approach unity as close as possible. In this study, the coefficients of the equations obtained were determined by considering the mean of RMSE, AE and RE by using long-term measured data.

3.2.1. Hourly Dry-Bulb Temperature

Hourly variation of outdoor dry-bulb temperature can be expressed with mathematical formulations using the daily minimum and maximum temperatures. The day is divided into two parts for modeling. These parts are determined according to the time at which the daily minimum or maximum temperature occurs. The first part covers the time period between occurrence of daily minimum temperature and maximum temperature. The second part covers the remaining period. The equations for hourly outdoor dry-bulb temperature (T) are determined for two periods of the day separately [Oğulata and Yılmaz, 1989; Yılmaz and Bulut, 1996; Bulut, 2001]:

For the 1st period ($t_{max} \geq t \geq t_{min}$):

$$T = T_{min} + (T_{max} - T_{min}) \left\{ \operatorname{Sin}\left[\frac{\pi}{2} \left(\frac{t - t_{min}}{t_{max} - t_{min}} \right) \right] \right\}^{1.4} \tag{3.42.a}$$

For the 2nd period ($t_{min} \geq t \geq t_{max}$):

$$T = T_{max} - (T_{max} - T_{min})\left\{ Sin\left[\frac{\pi}{2}\left(\frac{t - t_{max}}{24 + t_{min} - t_{max}} \right) \right] \right\}^{1.2} \quad (3.42.b)$$

in which T_{max} and T_{min} are respectively the daily maximum and minimum temperature. They can be calculated from Equations (3.43) and (3.44),

$$T_{max} = T_1 - (T_1 - T_2)Cos\left[\frac{2\pi}{365}(n - 25) \right] \quad (3.43)$$

$$T_{min} = T_3 - (T_3 - T_4)Cos\left[\frac{2\pi}{365}(n - 25) \right] \quad (3.44)$$

where n is the number of days from January 1 and T_1, T_2, T_3 and T_4 are coefficients given in Tables 3.4 and 3.5. They were determined for each province by means of statistical error tests. t_{min} is the time for the occurrence of daily minimum temperature and t_{max} is the time for the occurrence of daily maximum temperature. They can be calculated as follows:

$$t_{min} = 12 - \frac{t_d}{2} \quad (3.45)$$

$$t_{max} = 12 + \frac{t_{min}(12 - t_{min})}{13.5} \quad (3.46)$$

where t_d is the day length and can be calculated from Equation (3.47).

$$t_d = \frac{2}{15} ArcCos[-\tan L \tan \delta] \quad (3.47)$$

where L is the local latitude; δ is the solar declination angle. The solar declination angle can be calculated from Equation (3.48)

$$\delta = 23.45 Sin\left[\frac{2\pi}{365}(n + 284) \right] \quad (3.48)$$

Table. 3.4. Coefficients and statistical errors for daily maximum temperature equation of some province [Bulut, 2001]

Province	T_1	T_2	$\pm$MAE [^oC]	MRE [%]	RMSE [^oC]	R
Adana	25.27	15.28	2.66	12	3.42	0.90
Ankara	17.57	4.72	3.75	33	4.65	0.89
Antalya	24.01	13.88	2.72	12	3.38	0.90
Diyarbakır	22.16	6.25	2.97	21	3.79	0.95
Gaziantep	21.61	7.51	2.97	19	3.72	0.94
İstanbul	18.29	8.08	3.01	21	3.79	0.89
İzmir	22.56	11.84	2.73	14	3.43	0.91
Konya	17.54	4.54	3.87	36	4.82	0.89
Samsun	17.72	9.55	3.07	22	4.04	0.82
Şanlıurfa	23.95	9.37	2.83	16	3.58	0.95
Trabzon	17.70	9.65	2.95	20	3.86	0.83
Van	14.58	1.08	2.49	48	3.19	0.95
Erzurum	11.94	-4.19	3.60	175	4.58	0.93
Elazığ	18.68	2.17	3.61	48	4.52	0.92
Balıkesir	20.10	8.66	3.70	24	4.62	0.87

Table 3.5. Coefficients and statistical errors for daily minimum temperature equation of some provinces [Bulut, 2001]

Province	T_3	T_4	$\pm$MAE [^oC]	MRE [%]	RMSE [^oC]	R
Adana	14.27	5.04	2.08	21	2.65	0.93
Ankara	6.14	-3.28	2.81	2368	3.62	0.88
Antalya	12.51	3.95	2.05	24	2.60	0.92
Diyarbakır	8.60	-3.00	2.72	187	3.51	0.92
Gaziantep	9.21	-1.60	2.41	1647	3.02	0.93
İstanbul	10.71	2.46	2.34	38	2.95	0.89
İzmir	13.40	4.74	2.43	27	3.09	0.89
Konya	5.26	-4.96	2.86	206	3.72	0.89
Samsun	10.67	2.77	2.30	36	2.97	0.88
Şanlıurfa	12.59	1.22	2.32	44	2.88	0.94
Trabzon	11.47	3.49	2.21	30	2.84	0.89
Van	3.73	-7.53	2.57	108	3.41	0.92
Erzurum	-1.91	-14.39	4.51	145	5.87	0.83
Elazığ	7.23	-4.00	2.72	161	3.46	0.92
Balıkesir	9.17	0.50	2.83	110	3.60	0.86

3.2.2. Hourly Absolute Humidity

The following equation is proposed [Yılmaz et al., 1995] for hourly humidity ratio in gr/kg-dry air. The day was divided into two parts for modeling. These parts were determined according to the time for sunrise and sunset.

For the 1st period ($t_{gd} \leq t \leq t_{gb}$)

$$W = W_1 + W_2 \left\{ Sin\left[\frac{\pi}{365}(n - n_o) \right] \right\}^m \tag{3.49.a}$$

For the 2nd period ($t_{gb} > t > t_{gb}$):

$$W = W_1 + (W_3 - W_1) \left\{ Sin\left[\frac{\pi}{365}(n - n_o) \right] \right\}^m \tag{3.49.b}$$

where W_1, W_3, m and n_o are coefficients. The values of these coefficients were determined by Yılmaz et al. (1995) for Adana by means of statistical errors. It was found that W_1, W_3, m and n_o are 4.5, 17, 4 and 25 respectively.

W_2 can be calculated from the following equation;

$$W_2 = W_3 - W_1 - 2\sin\left[\frac{\pi}{t_{gi}}(t - t_{gd}) \right] \tag{3.50}$$

where t is the hour of the day. t_{gd} and t_{gb} are time for sunrise and sunset, respectively, and can be calculated from Equations (3.51) and (3.52).

$$t_{gb} = 12 + \frac{\left(12 - \frac{t_d}{2}\right) t_d}{27} + \frac{t_{gi}}{2} \tag{3.51}$$

$$t_{gd} = 12 + \frac{\left(12 - \frac{t_d}{2}\right) t_d}{27} - \frac{t_{gi}}{2} \tag{3.52}$$

where t_{gi} is the imaginary day length and can be calculated as follows:

$$t_{gi} = 1.25 t_d^{0.875} \tag{3.53}$$

where t_d is the day length and can be calculated from equation (3.47).

In this study, equation (3.49) was used for hourly humidity ratio for some provinces of Turkey, which are located different climate regions. Table 3.6 gives W_1 and W_3 coefficients, statistical errors and coefficient of correlations for the selected provinces. Other coefficients, m and n_o are 3 and 25, respectively.

It can be seen from Table 3.6 that the correlation coefficient is in the range of 0.84 and 0.93. The mean absolute errors are between 0.93 and 1.70, whilst RMSEs are in the range of 1.23 and 2.47 for analyses. Figure 3.3 shows variation of the measured hourly humidity ratio and the data obtained from equation (3.49) for Adana.

Table 3.6. W_1 and W_3 coefficients and statistical errors for hourly humidity ratio equation for some provinces

Province	**W_1**	**W_3**	**$\pm$MAE [^{o}C]**	**MRE [%]**	**RMSE [^{o}C]**	**R**
Adana	4.2	16.4	1.70	25	2.19	0.84
Ankara	2.7	8.1	0.97	22	1.19	0.92
Antalya	4.0	15.0	1.95	29	2.47	0.84
Diyarbakır	3.2	7.9	1.56	28	2.00	0.93
Gaziantep	3.4	9.0	1.49	26	1.92	0.91
İstanbul	4.1	12.8	1.26	18	1.59	0.92
İzmir	4.4	12.2	1.40	19	1.72	0.92
Konya	3.2	7.8	1.19	24	1.51	0.90
Samsun	3.4	13.5	1.19	17	1.5	0.87
Şanlıurfa	3.6	8.8	1.49	26	1.89	0.92
Trabzon	3.5	13.0	1.21	17	1.57	0.87
Van	2.0	6.7	0.93	24	1.23	0.90

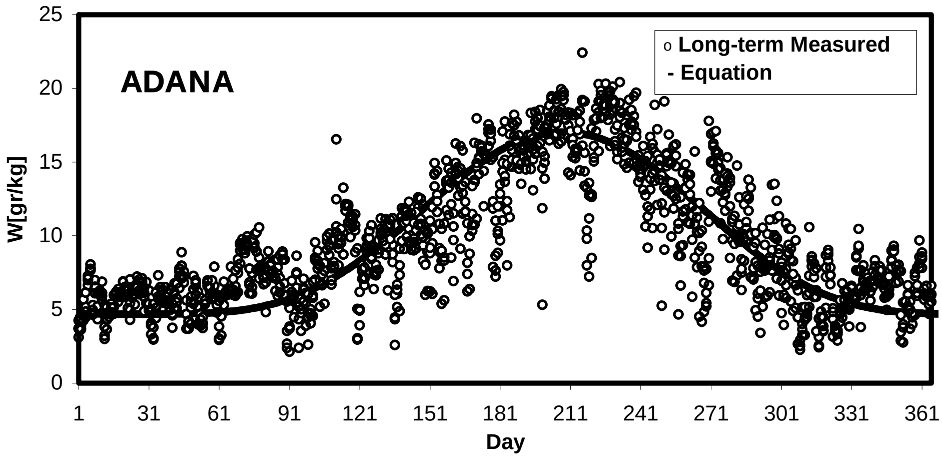

Figure 3.3 Variation of the measured hourly humidity ratio and data obtained from Equation 3.49 for Adana

3.3. Description of Air Conditioning System

3.3.1. General Cooling Process

All-air air conditioning systems commonly consist of air handling unit (AHU), air-cooled chiller system, supply and return fans, duct, and control units. Figure 3.4 is a schematic of an air conditioning system showing typical operating conditions.

The returned room air (state R) is mixed with the required outdoor air (state O) at the air handling unit. The mixed air (state M) passes through the cooling coil. In the conventional or typical case, the outdoor air condition is always warmer and more humid than the return air. Therefore, the cooling process generally involves both cooling and dehumidification, with the conditioned air leaving the cooling coil at state (S). The cooled and dehumidified air leaving the coil at state (S) is then supplied into the conditioned space which is at state (R) to complete the cycle.

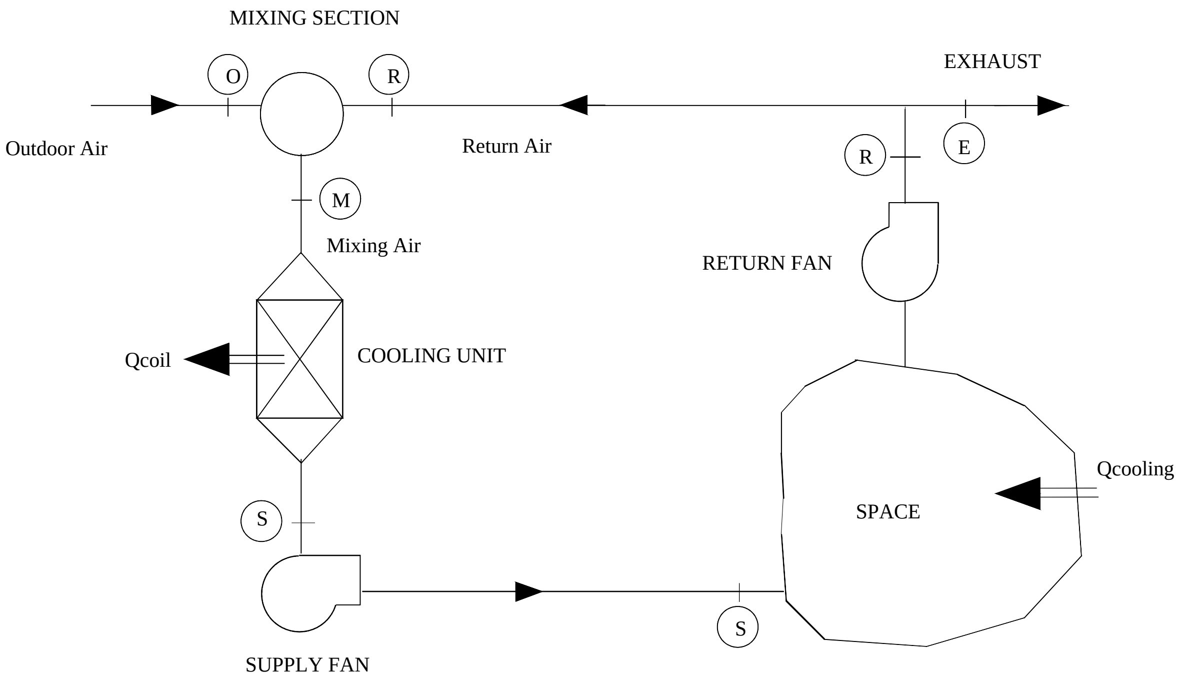

Figure 3.4. Schematic of an Air-conditioning system

3.3.2. Air Distribution System

All air systems have been widely used in air-conditioning system applications. Air movement is one of the biggest areas of energy use in these systems. Two main air distribution systems associated with all-air air-conditioning systems are constant-air-volume (CAV) and variable-air-volume (VAV) systems.

In CAV system; mass flow rate of supply air is constant while supply air temperature is variable during operating time to achieve thermal comfort. The basic principle of VAV system is to vary the amount of constant temperature air to a space to satisfy the building cooling load. Different types of these two approaches are available; such as single duct, dual duct, reheat and multi zone systems.

CAV systems have been used since the introduction of air-conditioning while VAV systems have only been utilized since the 1960s. Energy saving is one of primary reasons that VAV systems are very popular design choices today for some commercial buildings and many industrial applications [Mumma, S.A. and Bolin R.J., 1997; Reddy et al., 1998; Pan et al., 2003]. With these systems, the volume of the air delivered is reduced whenever operating loads are less than design loads. A VAV system operates identically to a CAV system under peak cooling conditions, with AHU operating at maximum supply flow rate. The CAV systems have significant inefficiencies and energy waste at part load. The VAV system is a commonly used design that significantly reduces energy consumption as the load is decreased. It uses variable speed supply fans to distribute air at a constant temperature.

For example, VAV system is compared to the CAV system that is used in existing Biopharmacology Laboratory in Canada. Using VAV and applying the concept of system diversity, the selected equipment capacity totaled 7000 cfm (11844 kg/m^3) for both supply and exhaust airflows. In contrast, a conventional CAV design would have required approximately 13000 cfm (21996 kg/m^3) of supply and exhaust airflows with commensurate heating, cooling and humidification capacity. Comparing the installation cost of VAV system ($155000) and with CAV system ($107000), applying diversity reduced the first cost of the HVAC mechanical system by $48,000. Under actual operating conditions the annual energy costs for the HVAC system were $155000 or a saving of $30320 [Harrison, 2004].

Other example, in 1997, a Bank of Montreal building in Vancouver, British Columbia, retrofitted its HVAC systems as part of a building upgrade. The building's previous main air system consisted of a 75-hp supply fan and a 40-hp return fan, which provided air for variable and constant volume mixing, and heating boxes that provided heating and cooling to various zones. The fan was fitted with variable inlet vanes (VIV), which modulated to maintain the pressure in the system. The retrofit consisted of replacing the fan motors with a 50-hp supply and a 25-hp return, and installing a variable frequency drive (VSD) in place of the inlet vanes. Based on the 24-hour duty cycle of operation shown in Table 3.7 the new system saves an estimated $6294 per year based on 1997 rates, with a simple payback period of three years [OEE, 2004].

Table 3.7. Savings Estimate for Bank of Montreal VSD

Installation			
Input Data		**Duty Cycle**	
		Percent Flow	**Hours/Day**
Energy Rate	$0.05/kWh	0%	8
Capital Cost	$18750	60%	4
Rated Power	75+50 hp (VIV)	80%	6
Operation	365 days/year	100%	6
Payback Summary			
		VSD	**VIV**
Monthly Cost		$1096	$1422
Yearly Cost		$10472	$16766
Monthly Savings			$517
Yearly Savings			$6294
Payback Period (Years)			3.0
Return on Investment			34%

The lower initial cost and lower operating cost of the VAV systems have made them attractive, especially for the design of speculative office space. Unfortunately, in reducing the volume of air that is conditioned, VAV systems can compromise indoor air quality. In a VAV system, if the room temperature varies too slowly, the ventilation system may not run long enough to maintain adequate air circulation. For this reason, it is important that a VAV system be set to provide a minimum flow of fresh air, sufficient to ensure occupant health [Aronoff and Kaplan, 1997].

CAV systems constantly supply air to building, making them less energy-efficient than VAV systems. However, the building air conditioned with a CAV system is provided the concentration of air contaminants at an acceptably low level. CAV system is recommended for clean rooms; operation theatres and laboratories applications. It is important parameter both constant air flow rate and IAQ at these applications.

3.3.3. Working Principle of the Variable Air Volume System

VAV systems have some kind of system to control the air volume. The simplest control is On-Off control of fans but the damper control is more common and variable speed drive control of fans is the most economic method to control the air volume. The system is usually designed to maintain constant static pressure in the supply duct. The positive building static pressure is kept by regulating the airflow of both the supply and return fans. Terminal devices or VAV boxes supply the conditioned space with a variable flow of constant temperature airflow.

Working principle of the VAV system with variable speed control fans is given in Figure 3.5.

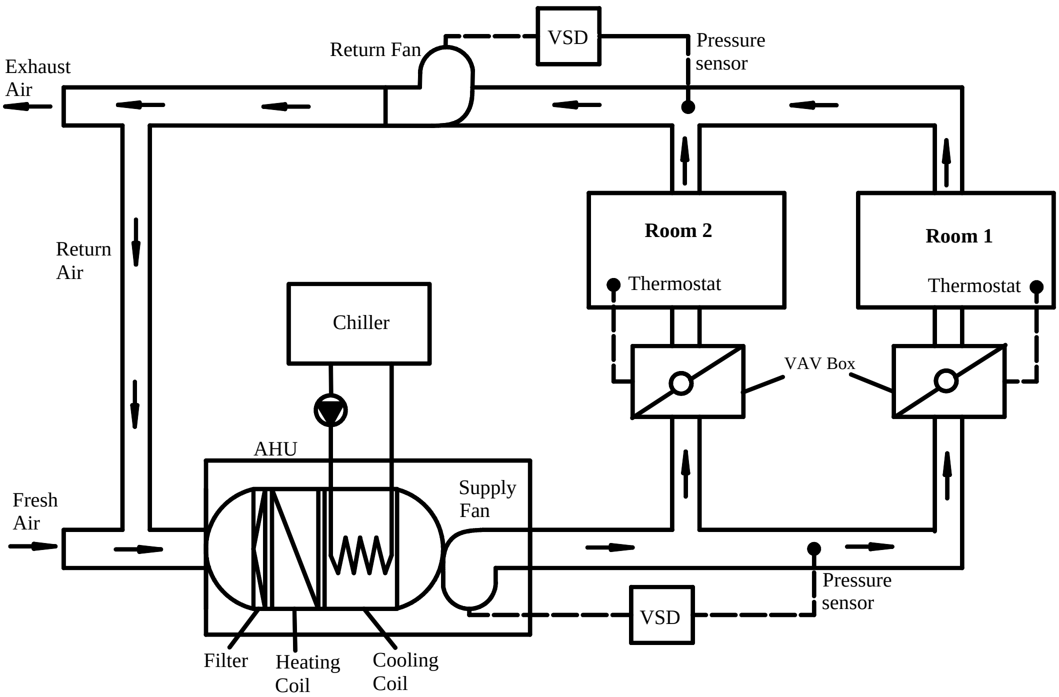

Figure 3.5. Variable air volume system with variable speed control fans

This VAV system brings fresh air and return air to the Air Handling Unit (AHU) where the incoming air temperature and humidity can be controlled. The main AHU components are supply fan, heating coil, cooling coil and filter. The air flow to each zone is controlled by the thermostat’s control of the damper position. The supply air fan is speed controlled by a VSD and it delivers the air to individual rooms throughout the building by supply air ducts. The VSD controls the air volume by keeping the air pressure constant. The pressure is measured by the sensor. The return air fan delivers the exhaust air out of the building or part of the air is returned back to the AHU. The fan is controlled by a VSD which keeps the room pressure measured by sensor constant [CSE, 2005].

3.3.4. Comparison of the VSD Control and Other Control Methods

The implementation of variable volume control has been done with dampers or other mechanical control methods. Other control methods that reduce delivered air flow include discharge dampers, inlet vanes, fan cycling or diverting air. Options to reduce air flow that do not change the fan speed will not result in as much energy reduction [Powell, 2002]. Discharge dampers and inlet vanes trade pressure drop for the reduction in air flow. Although there are some savings they are not as great as with fan speed control. With fan cycling there is no change in fan power, the air flow and fan energy are reduced in proportion to the amount of time that the fan is cycled off. With bypassing there is no savings at all because the fan delivers the same flow at the same pressure, and the by-passed air is essentially wasted.

Figure 3.6 shows the difference in power consumption of a typical VSD compared to the common retrofit applications, including variable inlet vane control (VIV), outlet damper control (OD) and constant speed (CAV)[Kreider and Rabl, 1994; Küçükçalı R., 2003; OEE, 2004]. It is clear that the variable speed approach has the largest saving over a wider operating range.

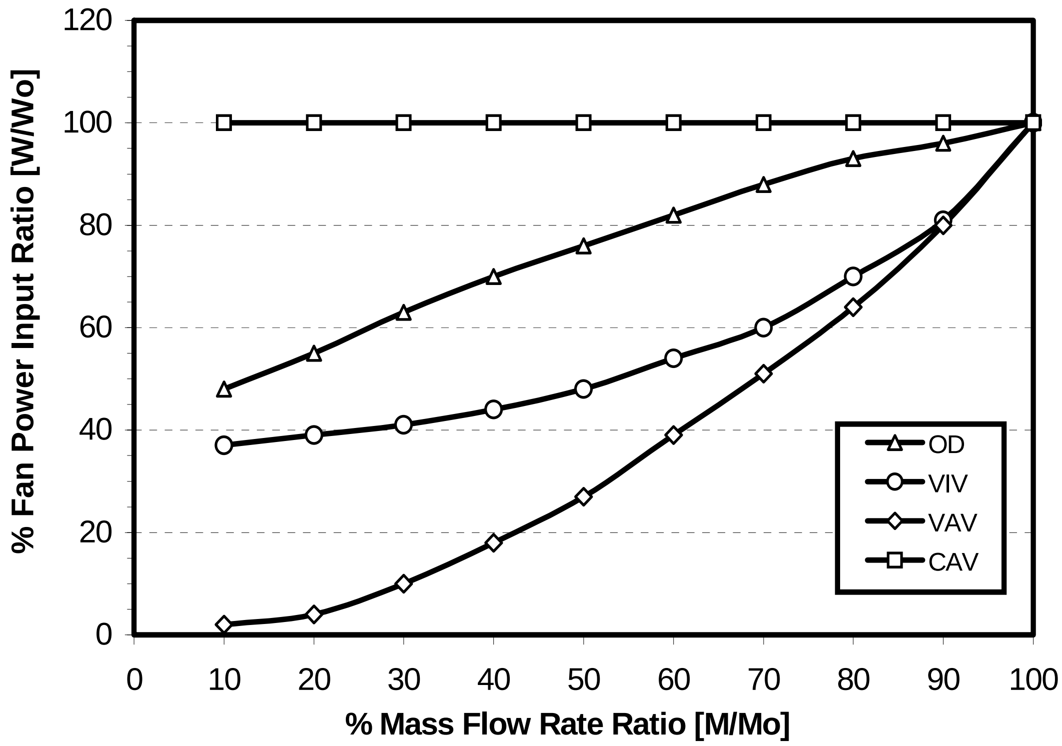

Figure 3.6. Part load fan characteristics for different control methods

The advantages of variable air volume system implemented with variable speed control are [ARCH, 2005 and CSE, 2005]:

- Fast control to keep the comfort zone limits
- Simpler to keep noise level down
- When combined with a perimeter heating system, it offers inexpensive temperature control for multiple zoning and a high degree of simultaneous heating-cooling flexibility.
- Capital cost is lower since diversities of loads from lights, occupancy, solar and equipment of as much as 30% are permitted.
- Virtually self-balancing.
- It is easy and inexpensive to subdivide into new zones and to handle increased loads with new usage if load does not exceed the original design peak.
- No zoning is required in central equipment.

- Lower operating cost, because;
  - Fans run long hours at reduced speed
  - Refrigeration, heating and pumping matches diversity of loads.
  - Lower consumption of heating and cooling energy than in constant air volume systems
  - Unoccupied areas may be fully cut-off
- Reduced noise level when the system is running at off-peak loads.
- Allows simultaneous heating and cooling without seasonal changeover.

3.3.5. Saving Energy with VSD

One of the primary measures to save energy is to reduce the volume of air that is delivered to heat and cool. A variable speed drive regulates the speed of the motor, and in turn the speed of the fan, by controlling the energy that goes into the motor, rather than restricting the flow of a process running constantly at full speed.

The real energy savings from variable frequency drives come from the basic laws of fan and pump operation. For variable volume systems, fan input power should be adjusted as a function of fan flow.

Theoretically, the air-flow load (V/V_o) in (m^3/h) is directly proportional to rotational speed of the fan (n/n_o) according to fan laws.

$$\frac{V}{V_o} = \frac{n}{n_o} \tag{3.54}$$

where V is the air volume flow rate under the real operating conditions (m^3/h), V_o is the maximum air volume flow rate (m^3/h), n is rotational speed of the fan under the real operating conditions and n_o is the maximum rotational speed of the fan.

Fan power (W_o) is given by;

$$W_o = V_o \Delta P_o \tag{3.55}$$

where ΔP is total pressure difference (Pa). Assuming that the duct load characteristic can be described by Equation (3.56),

$$\frac{\Delta P}{\Delta P_o} = \left(\frac{V}{V_o}\right)^2 \tag{3.56}$$

The relationship between air mass flow rate (M) and air volume flow rate (V) is given by;

$$V = \frac{M}{\rho} \tag{3.57}$$

where ρ is air density (kg/m^3). Combining Equations (3.55), (3.56) and (3.57), the fan power used (W) is obtained;

$$W = W_o \left(\frac{M}{M_o}\right)^3 \tag{3.58}$$

where, M is the air mass flow rate under the real operating conditions (kg/h), and W_o and M_o are the maximum fan power (kW) and the maximum air mass flow rate (kg/h) respectively. Air density is assumed as constant.

The fan power difference between the fan power at the full load (W_o) and at the reduced air flow fan power (W) is found with the following equation;

$$\Delta W = W - W_o \tag{3.59}$$

The annual cost savings resulting from the reduction of fan energy (ES) is given by,

$$ES = \Delta W . T_{year} . C \tag{3.60}$$

where T_{year} is fan operating hours per year [h] and C is a typical average cost per kilowatt hour [\$/kWh].

3.4. Load Calculation of Air Conditioning System

In this study, three computer programs were developed in order to determine design capacity of the air conditioning system (ACS) and simulate hourly operating of the ACS, as the next step. These programs are written in FORTRAN programming language.

The first computer program was written to determine design conditions of the all-air air-conditioning system under the condition of constant coil wall temperature (T_C).

The second program was written to calculate hourly apparatus dew-point temperature (coil wall temperature) and amount of variable air volume. The apparatus dew-point temperature is shown on the Psychometric chart in Figure 3.4 as state C, under the condition of constant supply air temperature (T_S).

The third computer program was written to determine the condition of the supply air (the air conditions leaving the coil, state S) and the apparatus dew-point temperature (state C), as shown on the Psychometric chart in Figure 3.7, under the conditions of constant air volume.

In the study, it is assumed that the ducts are insulated. The losses from connecting ducts and heat gain from the fan were neglected.

3.4.1. Psychrometric Equations

The room sensible heat factor (RSHF), which is influenced by the amount of latent load in the conditioned space, is determined by:

$$RSHF = \frac{Q_{sen,room}}{Q_{tot,room}} \tag{3.61}$$

Total cooling load for conditioned space ($Q_{tot,room}$) is the sum of latent cooling load ($Q_{lat,room}$) and sensible cooling load ($Q_{sen,room}$). They are defined with the following equations:

$$Q_{tot,room} = Q_{lat,room} + Q_{sen,room} \tag{3.62}$$

$$Q_{lat,room} = M_{tot} h_g (W_R - W_S) \tag{3.63}$$

$$Q_{sen,room} = M_{tot} c_p (T_R - T_S) \tag{3.64}$$

where,

h_g : Specific enthalpy of the saturated water vapor, [J/kg]
T_R : Indoor air dry bulb temperature, [°C]
T_S : Supply air dry bulb temperature, [°C]
W_R : Indoor air absolute humidity, [kg/kg dry air]
W_S : Supply air absolute humidity, [kg/kg dry air]

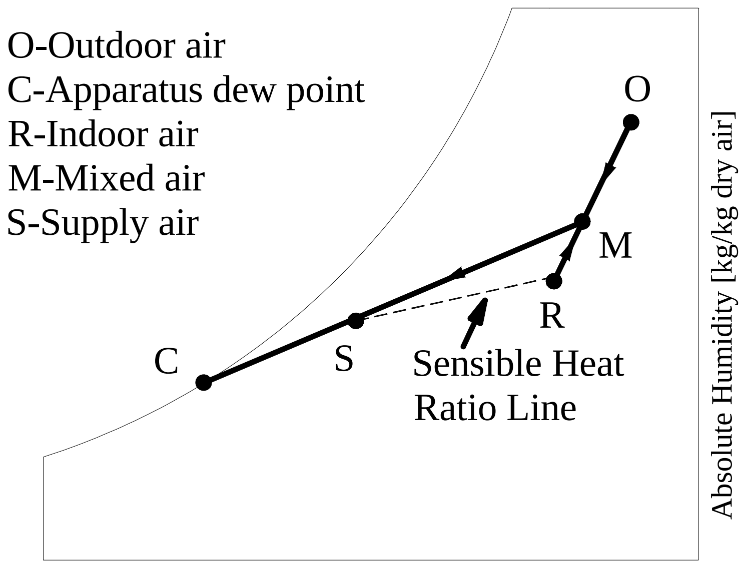

Figure 3.7. State points of air during psychometric processing for summer air conditioning systems

Using the Equations (3.62) to (3.64), Equation (3.61) can be rewritten as:

$$RSHF = \frac{c_p \Delta T}{c_p \Delta T + h_g \Delta W} = \frac{1}{1 + \frac{h_g}{c_p} \frac{\Delta W}{\Delta T}} \tag{3.65}$$

where $\frac{\Delta W}{\Delta T}$ is slope of the cooling process on psychometric chart and can be calculated as:

$$\frac{\Delta W}{\Delta T} = \frac{h_g}{c_p}\left(\frac{1}{RSHF} - 1\right) \tag{3.66}$$

The slope of the line C-M (Figure 3.7) is determined by the coil sensible heat factor (CSHF), which is influenced by the amount of outdoor air and RSHF. CSHF is given by,

$$CSHF = \frac{Q_{sen,room} + Q_{sen,outdoor}}{Q_{tot,room} + Q_{tot,outdoor}} \tag{3.67}$$

where;

$Q_{sen,outdoor}$: Sensible cooling load form fresh air, [W]
$Q_{tot,outdoor}$: Total cooling load form fresh air, [W]

In term of enthalpy, CSHF can be expressed as:

$$\begin{aligned} CSHF &= \frac{h_{MS} - h_S}{h_M - h_S} \\ &= \frac{(h_{RS} - h_S) + (h_{MS} - h_{RS})}{(h_M - h_{MR}) + (h_{MR} - h_{MS}) + (h_{MS} - h_{RS}) + (h_{RS} - h_S)} \end{aligned} \tag{3.68}$$

It can be seen from Figure 3.8 that the enthalpy difference between state (MR) and state (R) on the psychometric chart can be expressed as:

$$h_{MR}-h_R=h_{MS}-h_{RS} \tag{3.69}$$

The enthalpy difference between state (R) and state (RS) on the psychometric chart is given by,

$$h_R-h_{RS}=h_{MR}-h_{MS} \tag{3.70}$$

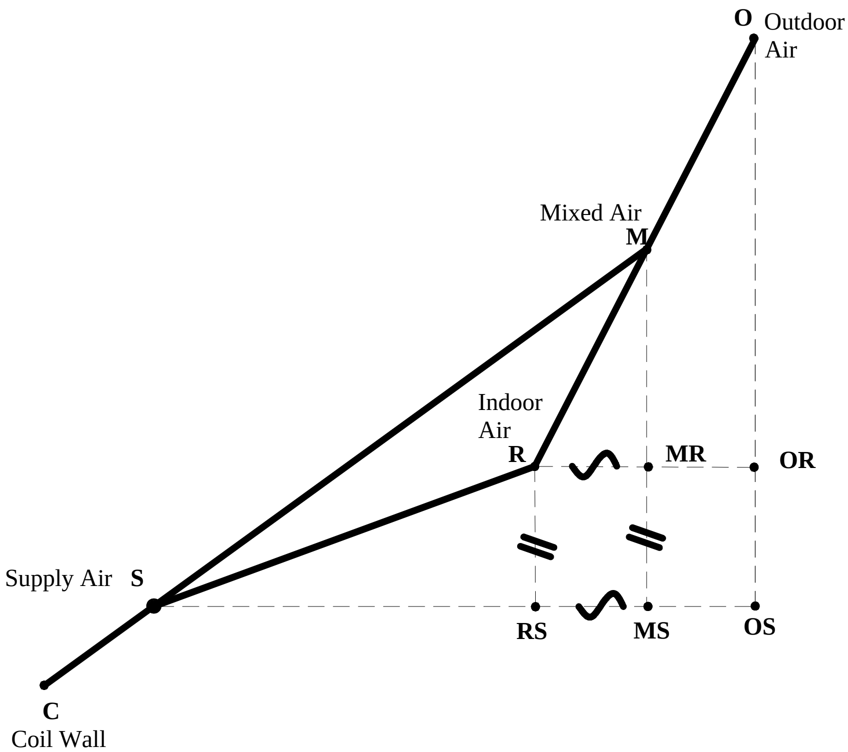

Figure 3.8. Schematic of cooling process of the air conditioning systems on the psychometric chart

Inserting equations (3.69) and (3.70) in equation (3.68) the following equation is obtained.

$$CSHF = \frac{(h_{RS} - h_S) + (h_{MR} - h_R)}{(h_M - h_{MR}) + (h_R - h_{RS}) + (h_{MR} - h_R) + (h_{RS} - h_S)} \quad (3.71)$$

Specific enthalpy of the mixed air (h_M) and specific enthalpy of the air at state (MR) in Figure 3.8 (h_{MR}) can be calculated using the equations (3.72) and (3.73), respectively.

$$h_M = \frac{M_{outdoor} h_O + (M_{tot} - M_{outdoor}) h_R}{M_{tot}} \quad (3.72)$$

$$h_{MR} = \frac{M_{outdoor} h_{OR} + (M_{tot} - M_{outdoor}) h_R}{M_{tot}} \quad (3.73)$$

Inserting equations (3.72) and (3.73) in equation (3.71) the following equation is obtained.

$$CSHF = \frac{M_{tot}\left(h_{RS} - h_S\right) + M_{outdoor}\left(h_{OR} - h_R\right)}{M_{tot}\left(h_R - h_S\right) + M_{outdoor}\left(h_O - h_R\right)} \tag{3.74}$$

CSHF is finally obtained in the following form;

$$CSHF = \frac{Q_{sen,room} + M_{outdoor}(h_{OR} - h_R)}{Q_{tot,room} + M_{outdoor}(h_O - h_R)} \tag{3.75}$$

where;

h_{OR} : Specific enthalpy of the state (OR), [J/kg]
h_O : Specific enthalpy of the outdoor air, [J/kg]
h_R : Specific enthalpy of the indoor air, [J/kg]
h_S : Specific enthalpy of the supply air, [J/kg]

In addition, an equation for the apparatus dew-point temperature (coil wall temperature) which is represented by state (C) in Figure 3.7 should be derived for the calculations. The procedure to obtain such an equation is explained in the following section.

3.4.2. Temperature of Cooling Coil Wall

Air-side surface temperature of cooling coil (T_C) can be calculated from the heat transfer between air and cooling water (Figure 3.9):

$$T_C = T_A - \dot{Q} R_A \tag{3.76}$$

where T_A is air temperature (°C) and R_A is convective heat transfer resistance of air (m^2°C/W).

Heat flux ($\dot{Q}$) in this equation is given by:

$$\dot{Q} = \frac{(T_A - T_W)}{R_T} \tag{3.77}$$

where T_W is mean temperature of water (°C) and R_T is thermal resistant (m^2°C /W) between air and water flows.

Inserting equation (3.77) in equation (3.76) the following equation is obtained:

$$T_C = T_A(1 - \frac{R_A}{R_T}) + \frac{T_W R_A}{R_T} \tag{3.78}$$

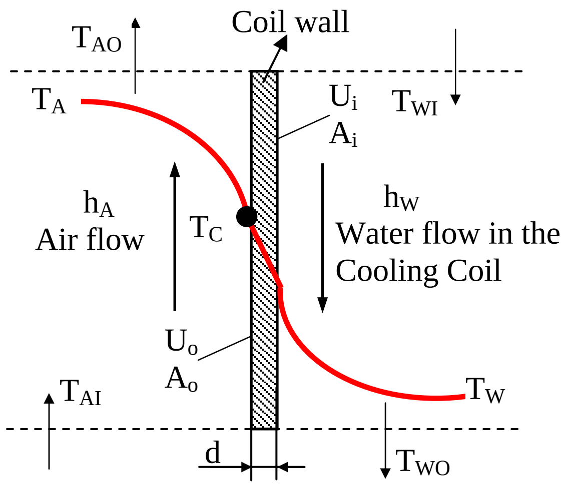

Figure 3.9. Distribution of temperature of cooling coil systems

With the definition of;

$$a = \frac{R_A}{R_T} \tag{3.79}$$

equation (3.78) can be written in the following form:

$$T_C = (1 - a)T_A + aT_W \tag{3.80}$$

The air temperature (T_A) is the average of inlet (T_{AI}) and outlet (T_{AO}) air temperatures;

$$T_A = \frac{T_{AI} + T_{AO}}{2} \tag{3.81}$$

Temperature difference between inlet and outlet air temperature is calculated as;

$$\Delta T_A = T_{AI} - T_{AO} \tag{3.82}$$

Replacing equations (3.81) and (3.82) into equation (3.80) the following equation is obtained;

$$T_C = (1-a)T_{AO} + aT_W + (\frac{1-a}{2})\Delta T_A \tag{3.83}$$

By arranging this equation one gets;

$$T_C = (1-a)T_{AO} + aT_W + b \tag{3.84}$$

where b is defined as

$$b = (\frac{1-a}{2})\Delta T_A \tag{3.85}$$

Constants a, and b can be determined statistically from the chart given in literature [Baumgarth et al, 2000]. From the chart was found that constants a, and b is 0.66 and 1.5 respectively. Finally, a general equation for surface temperature of cooling coil (T_C) depended on outlet air temperature and water mean temperature can be written as follows:

$$T_C = T_W + \frac{T_{AO} - T_W}{3} + 1.5 \tag{3.86}$$

From this equation, it is seen that the value of a is approximately 2/3, which is in accordance with industrial experience.

3.4.3. Computer Program P_CCWT

A computer program named P_CCWT was written to calculated design capacities of the air conditioning system (Appendix A2). The program uses the outdoor design conditions (T_O, W_O), amount of fresh air ($M_{outdoor}$), apparatus dew-point (coil wall) temperature (T_C), sensible heat load of the conditioned space ($Q_{sen,room}$) and RSHF as input data.

3.4.4. Algorithm of Program P_CCWT

Psychometric properties of outdoor air, indoor air, and apparatus dew-point temperature can be calculated using psychometric equations [ASHRAE, 2001]. Psychometric properties of mixed air and total mass flow rate (M_{tot}) are estimated by assuming that the ratio of outdoor air mass flow rate to the mixed air mass flow rate is 100 % (Φ=1).

$$\Phi = \frac{M_{outdoor}}{M_{tot1}} \tag{3.87}$$

Total mass flow rate as named M_{tot1} is calculated using equation (3.88).

$$M_{tot1} = \frac{M_{outdoor}}{\Phi} \tag{3.88}$$

As can be seen from Figure 3.10, the slope of Line1 between mixing point (M) and the apparatus dew-point (C) ($Slope_1$) can be obtained using equation (3.89).

$$Slope_1 = \frac{(W_M - W_C)}{(T_M - T_C)} \tag{3.89}$$

Similarly, slope of Line2 between the room condition (R) and the condition of the supply air (S) ($Slope_2$) can be obtained using Equation (3.90). Furthermore, $Slope_2$ is also equal to equation (3.66):

$$\text{Slope}_2 = \frac{(W_R - W_S)}{(T_R - T_S)} = \frac{h_g}{c_p}\left(\frac{1}{\text{RSHF}} - 1\right) \tag{3.90}$$

Intersection of Line1 and Line2 gives the condition of the supply air (S):

$$T_S = \frac{(W_M - W_R + \text{Slope}_2 T_R - \text{Slope}_1 T_M)}{(\text{Slope}_2 - \text{Slope}_1)} \tag{3.91}$$

$$W_S = W_R - \text{Slope}_2 (T_R - T_S) \tag{3.92}$$

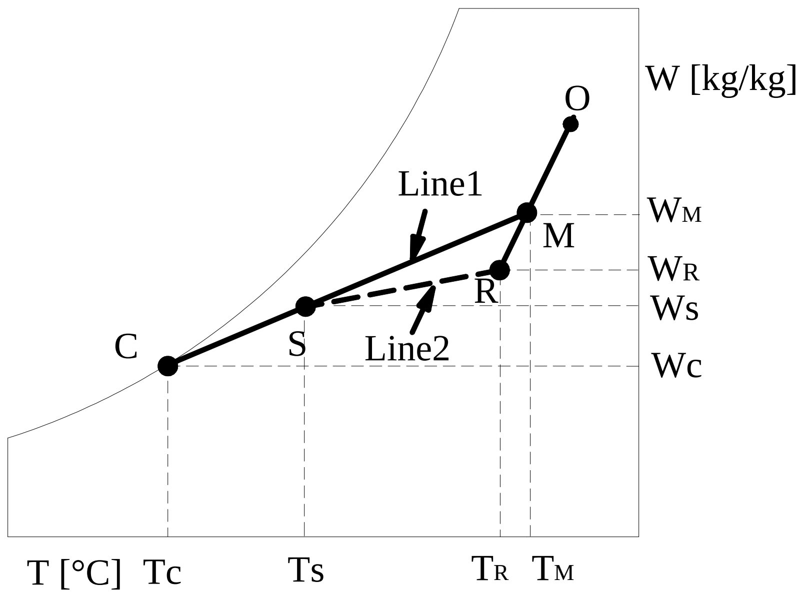

Figure 3.10. Line1 and line2 on the psychometric chart

Other psychometric properties of the mixed air and the total mass flow rate as named M_{tot2} can also be computed from the condition of the supply air:

$$M_{tot2} = \frac{Q_{tot,room}}{(h_R - h_S)} \tag{3.93}$$

where $Q_{tot,room}$ is the total cooling load of conditioned space (W) and h is specific enthalpy (J/kg).

After calculation of the total mass flow rates calculated with equations (3.88) and (3.93) (M_{tot2} and M_{tot1}), they are compared. If the mass flow rates are not equal to each other ($M_{tot2} \neq M_{tot1}$), the ratio of outdoor air mass flow rate to the mixed air mass flow rate (Φ) is decreased until they are equal to each other ($\Phi_{new}=\Phi_{old}-\Delta\Phi$). Consequently, a new value for the temperature of the mixed air can be calculated according to Φ_{new}. Iteration continues until the following limit is satisfied:

$$\varepsilon < \left|(1-\frac{M_{tot2}}{M_{tot1}})\right| = 0.0001 \tag{3.94}$$

The algorithm of computer program P_CCWT is shown in Figure 3.11.

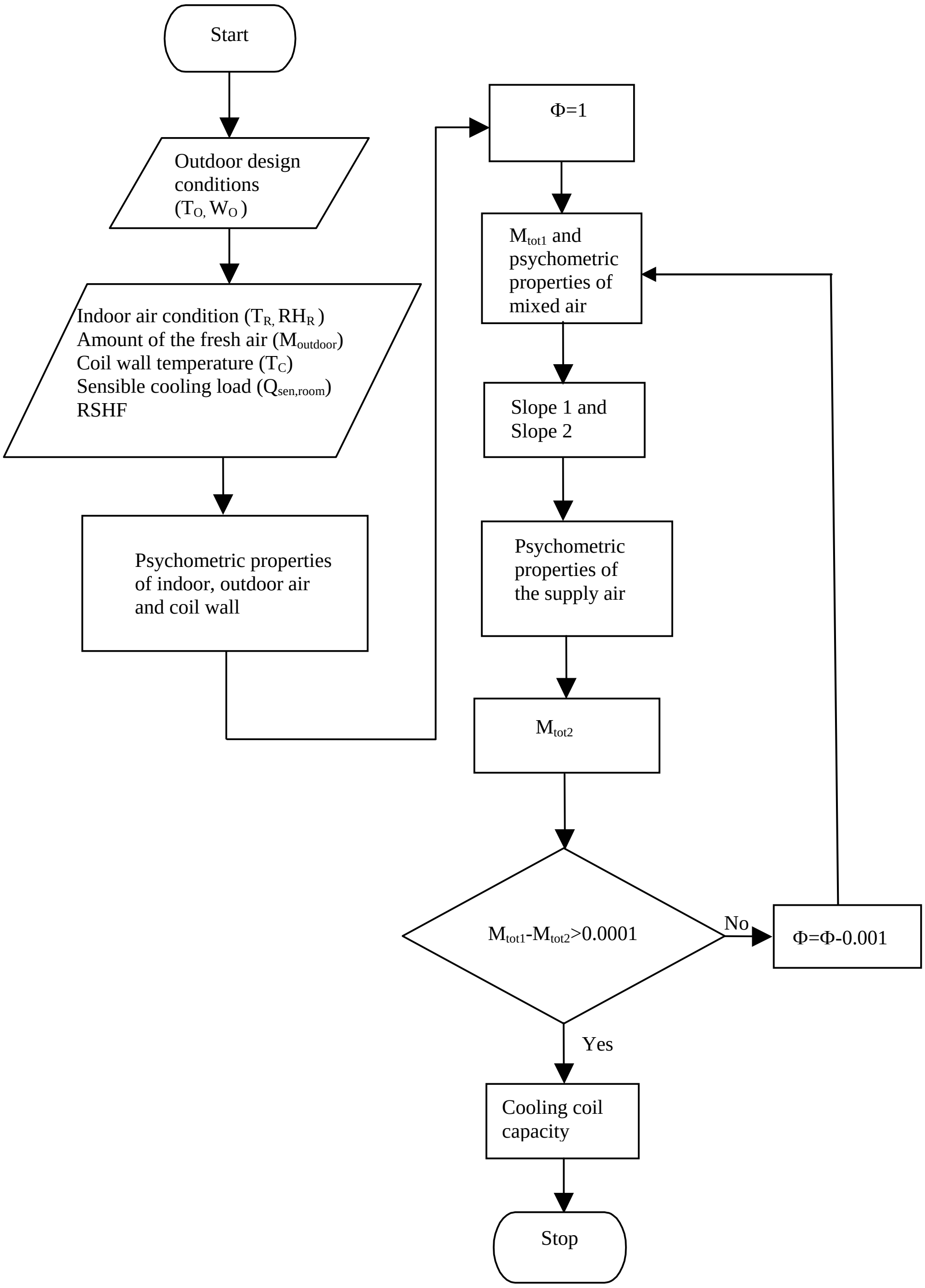

Figure 3.11. Algorithm of the Program P_CCWT

3.4.5. Computer Program P_VAV

The computer program called P_VAV was developed in order to simulate hourly operating of the air conditioning system and to determine the design cooling coil load (Appendix A3).

The outdoor air conditions (T_O, W_O) which can be calculated using equations (3.42) and (3.49), indoor design conditions (T_R, RH_R), amount of the fresh air ($M_{outdoor}$), dry bulb temperature of the supply air (T_S), simulation time (operating date) or design day, sensible cooling load of the conditioned space ($Q_{sen,room}$) and RSHF can be used as input data in the program.

3.4.6. Algorithm of Program P_VAV

The first step is calculation of the psychometric properties of outdoor air and indoor air using psychometric equations [ASHRAE, 2001].

In the second step of the program, total mass flow rate is computed using equation (3.95) to find psychometric properties of the mixed air. In equation (3.95) enthalpy of the supply air (h_S) is not known. Therefore, absolute humidity of the supply air (W_S) is computed firstly using Equation (3.92), and then, supply air enthalpy (h_S) is found using the psychometric equation for enthalpy (Equation 3.96). Inserting (h_S) in equation (3.95), total mass flow rate is computed.

$$M_{tot} = \frac{Q_{tot,room}}{(h_R - h_S)} \tag{3.95}$$

$$h_S = 1.006T_S + W_S(2501 + 1.085T_S) \tag{3.96}$$

Schematic diagram of adiabatic mixing is shown in Figure 3.12. Temperature of the mixed air can be calculated using equation (3.97).

$$T_M = \frac{(M_{outdoor}T_O + (M_{tot} - M_{outdoor})T_R)}{M_{tot}} \tag{3.97}$$

Ratio of the mass flow rate of the fresh air to the total mass flow rate is calculated for determining the psychometric properties of the mixed air.

After completing the steps explained above, the slope of the Line1 and the conditions of the supply air (S), can be calculated using equation (3.98).

$$Slope_1 = \frac{(W_M - W_S)}{(T_M - T_S)} \tag{3.98}$$

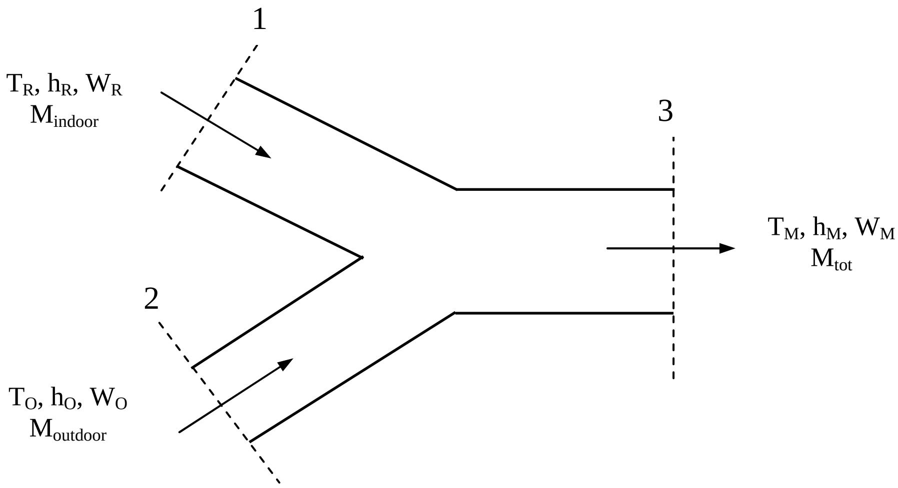

Figure 3.12. Schematic of adiabatic mixing of two moist airstreams

As can be seen from Figure 3.13., the line drawn between M and C intersects the saturation curve at state C. State C gives the condition of the coil wall temperature. Thus, absolute humidity at point C named as W_{C1} is calculated using Equation (3.99) by assuming 0˚C as the initial value for temperature of supply air.

$$W_{C1}=W_M-Slope_1(T_M-T_C) \tag{3.99}$$

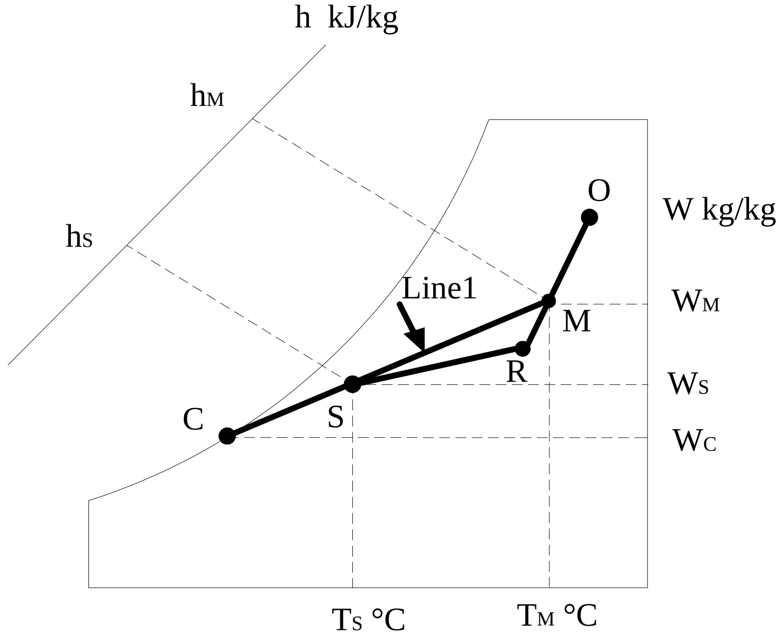

Figure 3.13. Line1 and other points on the psychometric chart.

In addition to W_{C1}, absolute humidity at state C can also be estimated according to saturation curve, using Equation (3.100). This absolute humidity is named as W_{C2}.

$$W_{C2} = \frac{(0.62198P_w)}{(P_{AT} - P_W)} \tag{3.100}$$

where P_{AT} is atmospheric pressure, and P_{WS} is saturation pressure of water vapor, which is given as a function of temperature T [K].

The saturation pressure over liquid water for the temperature range of 0 to 200 °C is given by [ASHRAE, 2001]:

$$\ln(P_{WS}) = \frac{C_8}{T} + C_9 + C_{10}T + C_{11}T^2 + C_{12}T^3 + C_{13}\ln(T) \tag{3.101}$$

where C_8, C_9, C_{10}, C_{11}, C_{12}, and C_{13} are coefficients. C_8: -5.8002206 10^3,

C_9:-5.5162560, C_{10}:-4.8640239 10^{-2}, C_{11}:4.1764768 10^{-5}, C_{12}:-1.4452093 10^{-8} C_{13}:6.5459673.

After calculation of the absolute humidities of the apparatus dew point (W_{C1} and W_{C2}), which are obtained with Equations (3.99) and (3.100), they are compared. If absolute humidities of the apparatus dew point (W_{C1} and W_{C2}) are not equal to each other ($W_{C2} \neq W_{C1}$), apparatus dew-point temperature is increased until they are equal to each other ($T_{Cnew}=T_{Cold} + \Delta T$). Consequently, the value of W_C that provides the equality, gives the apparatus dew-point temperature. Iteration continues until the following limit is satisfied (Equation 3.102).

$$\varepsilon < \left|(1-\frac{W_{C1}}{W_{C2}})\right| = 0.0001 \qquad (3.102)$$

Finally, during simulation date or design day hourly cooling coil load and others parameters can be determined using the program. The algorithm of Program P_VAV is shown in Figure 3.14.

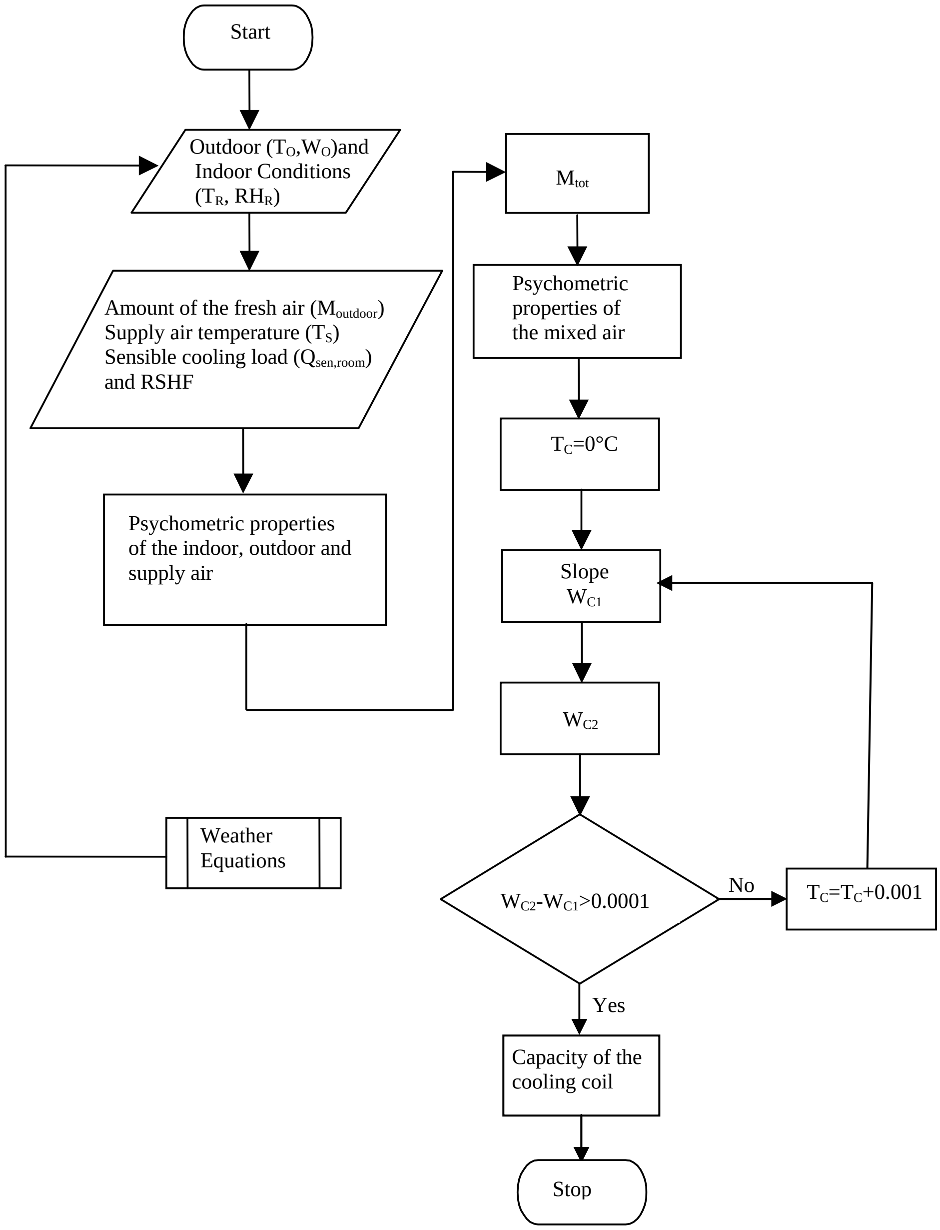

Figure 3.14. Algorithm of Program P_VAV

3.4.7. Computer Program P_CAV

A computer program called P_CAV was written to calculate Psychometric properties of all-air constant air volume (CAV) air conditioning system (Appendix A4).

The outdoor air conditions, which can be calculated using Equations (3.42) and (3.49), indoor design conditions (dry bulb temperature (T_R) and relative humidity RH_R), amount of the fresh air ($M_{outdoor}$) and total mass flow rate (M_{tot}), simulation time (operating time) or design day, sensible cooling load of conditioned space ($Q_{sen,room}$) and RSHR are used as input data in the program.

3.4.8. Algorithm of Program P_CAV

Psychometric properties of outdoor air and indoor air are calculated using psychometric equations. The ratio of the outdoor air mass flow rate to the mixed air mass flow rate is computed using Equation (3.87) and then the psychometric properties of mixed air are computed using adiabatic mixing equation. CSHF is calculated using Equation (3.75). Furthermore, a relationship between slope of Line1 (Figure 3.13) and CSHR can be obtained using Equation (3.103):

$$\text{Slope} = \frac{h_g}{c_p}\left(\frac{1}{\text{CSHF}} - 1\right) \tag{3.103}$$

Humidity ratio at state S named W_{S1} is calculated firstly using Equation (3.104) by assuming mixed air temperature as the initial value for temperature of supply air.

$$W_{S1} = W_M - \text{Slope}(T_M - T_S) \tag{3.104}$$

Humidity ratio state S named W_{S2} is calculated secondly using Equation (3.105).

$$W_{S2} = \frac{(h_M - 1.006T_S)}{(2501 + 1.805T_S)} \tag{3.105}$$

After calculation of the absolute humidities of the supply air (W_{S1} and W_{S2}), which are obtained with Equations (3.104) and (3.105), they are compared. If they are not equal to each other ($W_{S2} \neq W_{S1}$), supply air temperature is decreased until they are equal to each other ($T_{Snew} = T_{Sold} - \Delta T$). Consequently, the value of W_S that provides the equality, gives the supply air temperature. Iteration continues until the following limit is satisfied:

$$\varepsilon < \left|(1 - \frac{W_{S1}}{W_{S2}})\right| = 0.0001 \tag{3.106}$$

The algorithm of Program P_CAV is shown in Figure 3.15.

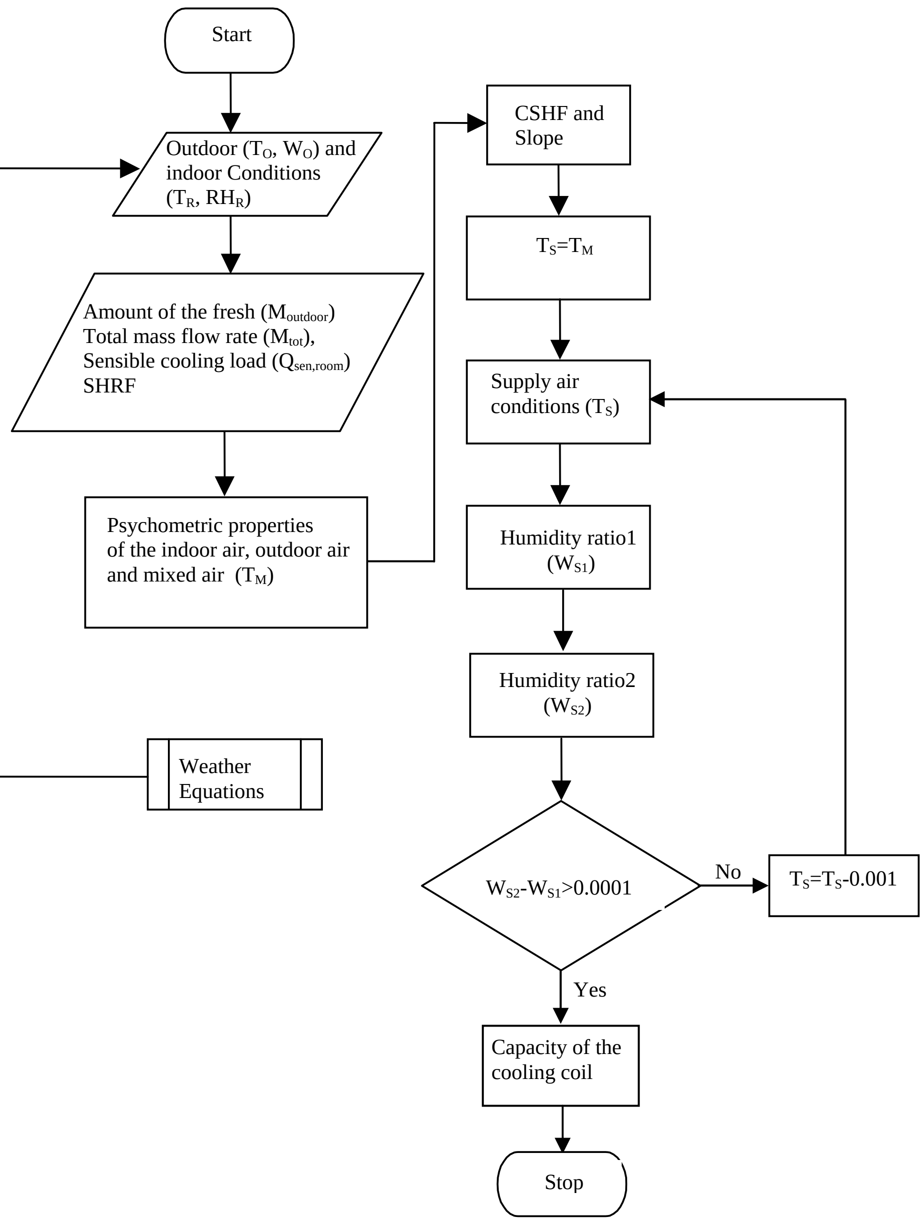

Figure 3.15. Algorithm of Program P_CAV

3.5. Economic Analyses for Air Conditioning System

An initial estimate of the costs must be computed in order to determine the economic feasibility of any project. There are two main methods to compare the cost of any two or more systems. The first one is the First Cost Comparison. It reflects only the initial price, installed and ready to operate, and ignores such factors as expected life, ease of maintenance and even, to some extent, efficiency. Typically, first cost is used in buildings built for speculation or short-term investment [Elsafty and Al-Daini, 2002].

The seconds is the Life-Cycle Cost (LCC). LCC analysis method has traditionally been considered an appropriate means of combining initial and operating costs into a single economic factor for use in effective decision-making. LCC is a measure of the total cost of producing, operating and disposing a design option. The technique is based on discounting, or reducing, all costs to current values or representing them as an annual cost [Lee et al., 2003].

Selecting the most suitable and economic air-conditioning system among the available alternatives is one of the important problems that engineers usually face. An air-conditioning system that saves operating costs usually requires a higher initial investment. In this case engineers should decide whether it is worth paying the extra first cost for a system that has lower operating cost [Kreider and Rabl, 1994].

This study presents a life-cycle cost analysis using detailed load profiles and initial and operating costs to evaluate the economic feasibility of systems (all-air variable air-volume system and all-air constant air volume system). The costs presented in this study produce a very good estimate of the initial costs and operating costs.

3.5.1. Economic Comparison Criteria

The selection of an HVAC system requires a specific criterion that can be applied in describing and evaluating the different alternatives. Analysis of overall initial and operating costs and comparisons of alternatives require an understanding of the cost, the comfort demands and the environmental impacts of the system. The present worth method is normally used to evaluate and compare the life-cycle costs of HVAC systems [Economic Analysis Handbook, 1993; Elsafty and Al-Daini, 2002]. In this study the present worth cost (PWC) in addition to the equivalent annual cost (EAC) methods were used to evaluate the cost of the two air-conditioning systems.

3.5.2. The Present Worth Cost (PWC)

The present worth value of a cash flow over time is its value today. Figure 3.16 graphically represents the cash flow diagrams of the decision data of the two HVAC systems to facilitate understanding of the selection problem. The least common multiple is 15 years for CAV and VAV systems [Economic Analysis Handbook, 1993; Elsafty and Al-Daini, 2002].

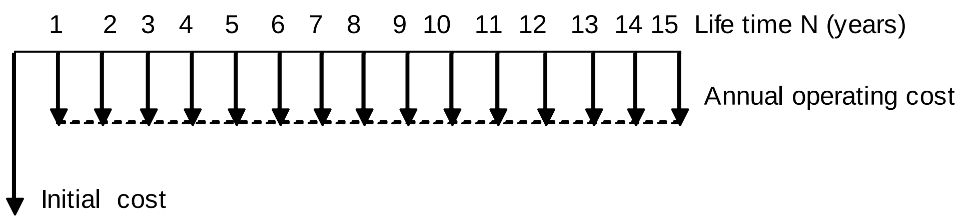

Figure 3.16. Cash flow of the CAV and VAV systems

The total present worth value for any analysis is determined by summing the present worth values of all individual items under consideration. The cost or the value of money is a function of the available interest rate and inflation rate. The uniform series present worth factor can be expressed as in Equation (3.107).

$$PWC = (\text{ Initial Cost} + P_o) \tag{3.107}$$

The present value P_o of a series of uniform end-of-period payments Ao (the annual operating cost) is calculated using Equation (3.108) [Economic Analysis

Handbook, 1993; Elsafty and Al-Daini, 2002].

$$P_o = A_o PWF \tag{3.108}$$

The PWF, called discount factor, can be expressed as in equation (3.110) or (3.113). It depends upon the inflation rate (g) and the interest rate (I) and is adjusted for inflation as shown below [Hasan, 1999]. The interest rate adjusted for inflation rate, which is indicated as i, is given by the following equations:
If g<I then

$$i = \frac{(I - g)}{(1 + g)} \tag{3.109}$$

$$PWF = \left[\frac{(i + 1)^N - 1}{i(i + 1)^N} \right] \tag{3.110}$$

If g>I then

$$i = \frac{(g - I)}{(1 + I)} \tag{3.111}$$

PWF is calculated using Equation (3.110)
If g=I then

$$i = \frac{(I - g)}{(I + g)} \tag{3.112}$$

$$PWF = \left[\frac{1}{(i + 1)} \right] \tag{3.113}$$

where N is lifetime year.

The payback period describes how quickly the savings accrue. Discounted payback occurs when the present value of accumulated savings equal the present value of the investment [Economic Analysis Handbook, 1993]. Discounting is the process of converting future values to present values. Computation of the discount saving is given by:

$$DS = S.PWF \tag{3.114}$$

where S is the annual savings. The discounted payback period (n) can be determined using Equation (3.115) [Economic Analysis Handbook, 1993].

$$n = \frac{-\ln\left(1 - i\,\dfrac{IN}{S}\right)}{\ln(1+i)} \tag{3.115}$$

where IN is the investment of the system.

3.5.3. Equivalent (Uniform) Annual Cost (EAC)

With the equivalent annual method, all the costs occurring over a period are converted to an equivalent uniform yearly amount. The EAC comparison method is one of the most convenient methods, particularly for systems that are composed of several subsystems with unequal life spans. The EAC for the two systems is the summation of the EAC values for the system and subsystems and the annual operating cost; Equation (3.116) [Economic Analysis Handbook, 1993; Elsafty and Al-Daini, 2002]. EA_I value expressed with Equation (3.117) is used to determine the amount of each future annuity payment required to dissipate a given present value (initial cost of the system or the subsystem) when the interest rate and life year are known.

$$EAC = (EA_I + \text{Annual operating cost}) \tag{3.116}$$

$$EA_I = P_I\left[\frac{i(i+1)^N}{(i+1)^N - 1}\right] \tag{3.117}$$

where P_I is initial cost of the system.

3.6. Application of the Theory to A Sample Building

For this purpose, a nonresidential building was chosen as the sample building for cooling load calculations. In the study, the sample building is located in different climatic regions of Turkey described by Turkish Standard 825, (Thermal Insulation in Buildings TS825, 1999). The provinces selected for this purpose are given in Table 3.8.

Table 3.8. Selected provinces of Turkey for analysis

Region	Province
I	İzmir, Adana, Antalya
II	İstanbul, Diyarbakır, Gaziantep, Samsun, Şanlıurfa, Trabzon
III	Ankara, Konya
IV	Van, Erzurum

3.6.1. Characteristics of the Sample Building

The sample building is a 3-story building with a gross area of 1628 m^2. The outside walls of the building are light colored. Figure 3.17 shows the architectural plan of the sample building. All the components such as the walls, windows, doors and roof are made of typical composite construction. Details of the building construction materials are presented in Table 3.9. Long sides of the building face to the North and the South.

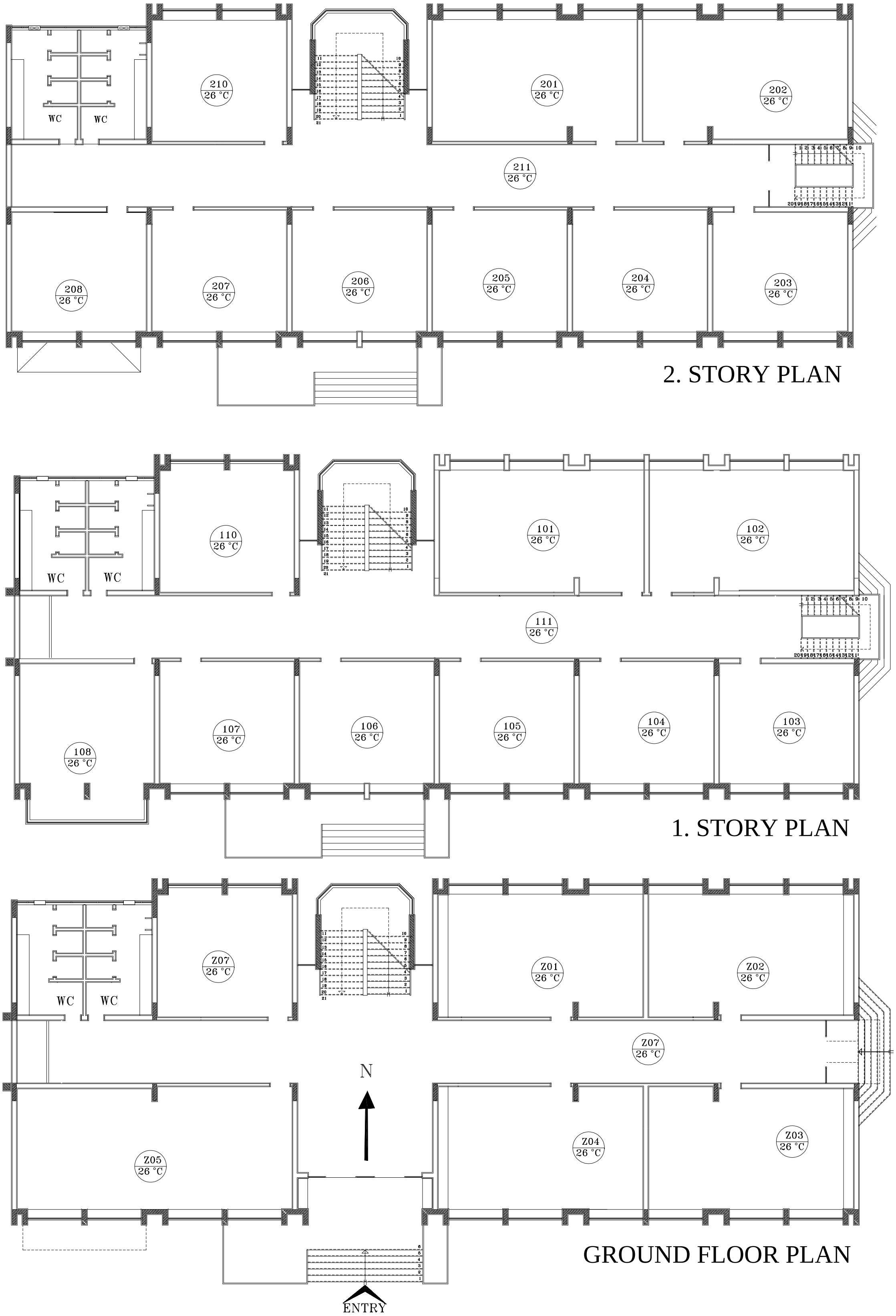

Figure 3.17. Architectural plan of the sample building

Table 3.9. Details of building construction materials

Building Component	Details
Exterior wall	Internal plaster, brick, thermal insulation, external plaster
Interior wall	Internal plaster, brick, internal plaster
Floor	Mosaic tile, lightweight concrete, heavyweight concrete, lightweight concrete, Blockage
Ceiling	Mosaic tile, lightweight concrete, heavyweight concrete, Internal plaster
Windows	Single glassing, wood frame
Roof	Slate, wood sheathing, attic, thermal insulation, heavyweight concrete, Internal plaster
Door	Steel door
Interior door	Wood door

It was assumed that the sample building can be used as an office center or a school building. If it is used as a school, the building has 14 classrooms, 3 laboratories, 4 offices, 1 library, 1 teacher's room, 1 computer room and 3 corridors. In the case of office center, all the rooms are used as offices (totally 24 offices) and additionally there are 3 corridors. Table 3.10 lists the rooms in the sample building.

Table 3.11 shows floor area, outside wall area and window area of the sample building.

Table 3.10. Education building and office center zones

Room Code	Type of the building	
	Education Building	**Office Center**
Z01	Director Office	Office
Z02	Science Lab	Office
Z03	Biology Lab	Office
Z04	Chemistry Lab	Office
Z05	Computer Room	Office
Z06	WC	WC
Z07	Office	Office
Z08	Corridor	Corridor
101	Picture Class.	Office
102	Library	Office
103	Classroom	Office
104	Classroom	Office
105	Classroom	Office
106	Classroom	Office
107	Classroom	Office
108	Teachers Room	Office
109	WC	WC
110	Office	Office
111	Corridor	Corridor
201	Classroom	Office
202	Classroom	Office
203	Classroom	Office
204	Classroom	Office
205	Classroom	Office
206	Classroom	Office
207	Classroom	Office
208	Classroom	Office
209	WC	WC
210	Office	Office
211	Corridor	Corridor

Table 3.11. Details for area of sample building [m^2]

Room Code	Floor Area	Outside Wall Area				Window Area			
		North	East	South	West	North	East	South	West
Ground Floor									
Z01	54.90	16.5	0	0	12	12	0	0	0
Z02	54.90	16.5	18.3	0	0	12	0	0	0
Z03	54.90	0	18.3	16.5	0	0	0	12	0
Z04	54.90	0	0	16.5	6	0	0	12	0
Z05	71.96	0	6	22.9	18.3	0	0	16	0
Z06	32.20	7.8	0	0	8.4	0.4	0	0	0
Z07	37.80	10.8	0	0	3	8	0	0	0
Z08	174.17	9.5	10.7	3	19.4	10.9	7.7	12.1	1.3
1. Story									
101	54.90	16.5	0	0	12	12	0	0	0
102	54.90	16.5	18.3	0	0	12	0	0	0
103	35.28	0	18.3	10.9	0	0	0	8	0
104	36.54	0	0	10.9	0	0	0	8	0
105	36.54	0	0	10.9	0	0	0	8	0
106	36.54	0	0	10.9	0	0	0	8	0
107	36.54	0	0	10.9	0	0	0	8	0
108	41.16	0	0	10.9	18.3	0	0	8	0
109	32.20	7.8	0	0	8.4	0.4	0	0	0
110	37.80	10.8	0	0	3	8	0	0	0
111	146.87	9.5	13.7	0	19.4	10.9	5.3	0	1.3
2. Story									
201	54.90	16.5	0	0	12	12	0	0	0
202	54.90	16.5	18.3	0	0	12	0	0	0
203	35.28	0	18.3	10.9	0	0	0	8	0
204	36.54	0	0	10.9	0	0	0	8	0
205	36.54	0	0	10.9	0	0	0	8	0
206	36.54	0	0	10.9	0	0	0	8	0
207	36.54	0	0	10.9	0	0	0	8	0
208	35.28	0	0	10.9	18.3	0	0	8	0
209	32.20	7.8	0	0	8.4	0.4	0	0	0
210	37.80	10.8	0	0	3	8	0	0	0
211	146.87	9.5	13.7	0	19.4	10.9	5.3	0	1.3
Total Area	1628.39	183.3	153.9	189.7	189.3	129.9	18.3	148.1	3.9

Thermal Insulation Regulation (8 May 2000-24043 numbered official gazette) in buildings is in force in Turkey and it is prepared according to Turkish standard for thermal insulation in buildings called TS 825. In the regulation, the buildings are classified as “A type”, “B type” or “C type” according to the ratio of the calculated annual energy requirement of building (Q) to the maximum allowed annual energy requirement of building (Q_I). Table 3.12 presents classification of the energy efficiency index of buildings according to the regulation. If Q/Q_I is higher than 0.99, insulation should be applied to reduce annual energy demand of the building.

In this study, the sample building was assumed to be insulated and it is a “B type” building according to Thermal Insulation Regulation. Table 3.13 shows overall heat transfer coefficients of the building envelope for different climatic regions in Turkey.

Table 3.12. Classification of buildings according to the Thermal Insulation Regulation

Type	**Q/Q_I**	**Energy Efficiency**
A	≤ 0.80	Very Good
B	≤ 0.90	Good
C	≤ 0.99	Normal

Table 3.13. Overall heat transfer coefficients of the sample building envelope for different climatic regions of Turkey

Region	**Q [kWh/m^3]**	**Q_I [kWh/m^3]**	**Q/Q_I**	**Type**	**U [W/m^{2}K]**			
					Wall	**Roof**	**Floor**	**Window**
I	10.55	11.85	0.89	B	0.783	0.508	0.757	2.8
II	17.44	19.59	0.89	B	0.525	0.375	0.549	2.6
III	22.59	25.38	0.89	B	0.464	0.326	0.482	2.6
IV	35.13	39.47	0.89	B	0.395	0.246	0.388	2.4

3.6.2. Internal Heat Gains for Sample Building

Internal heat gains in buildings include heat gained from people, lights and equipments. The most serious problem in making accurate estimates of internal heat gain is lack of information on the exact schedule of occupants, lights usage and equipment operation. It is probable that any particular room will be fully loaded but the complete building will never experience a full internal load. Every building must be examined using available information, experience and judgment to determine the internal load diversity and schedule. Some typical diversity factors for large buildings are given in Table 3.14 [McQuiston and Spitler, 1992].

Table 3.14. Typical use factors for large buildings

Type of Application	Use (Diversity) Factor	
	People	Lights
Office	0.75-0.90	0.70-0.85
Apartment, Hotel	0.40-0.60	0.30-0.50
Department store	0.80-0.90	0.90-1.00
Industrial*	0.85-0.95	0.80-0.90

3.6.2.1. Internal Heat Gain in Education Building

Education building has 224 students, 15 teachers, 4 officers and 3 laborers. The internal loads owing to people were selected 75 W sensible and 55 W latent heat per person following the recommendation of ASHRAE Fundamentals. The rooms of the education building include miscellaneous computers, printers, television, etc.

In this study, internal heat gains in the building were determined considering the actual conditions. Lessons are 50 minutes and the use (diversity) factor for calculation of heat gain from people in classrooms is 0.8. Use factor for equipment in the education building was estimated to be 1.0. For other zones, the use factors for lighting and people were taken from Table 3.14. Table 3.15 lists internal heat gains parameters for the education building.

Table 3.15. Description of the internal heat gain parameters for education building

Room Code	People		Lighting		Equipment	
	No	Use Factor	Heat Gain (W)	Use Factor	Heat Gain (W)	Use Factor
Z01	1	0.90	480	0.50	2000	1.0
Z02	16	0.20	480	0.30	1366	1.0
Z03	16	0.20	480	0.30	2000	1.0
Z04	16	0.20	480	0.30	2000	1.0
Z05	16	0.50	640	0.30	6040	1.0
Z07	2	0.90	320	0.50	1766	1.0
Z08	60	0.15	1120	0.50	-	-
101	16	0.30	480	0.30	-	-
102	20	0.30	480	0.50	1366	1.0
103	16	0.80	480	0.30	500	1.0
104	16	0.80	320	0.30	500	1.0
105	16	0.80	320	0.30	500	1.0
106	16	0.80	320	0.30	500	1.0
107	16	0.80	320	0.30	500	1.0
108	15	0.50	480	0.30	1000	1.0
110	2	0.90	320	0.50	1766	1.0
111	110	0.15	1120	0.50	-	-
201	24	0.80	480	0.30	500	1.0
202	24	0.80	480	0.30	500	1.0
203	16	0.80	480	0.30	500	1.0
204	16	0.80	320	0.30	500	1.0
205	16	0.80	320	0.30	500	1.0
206	16	0.80	320	0.30	500	1.0
207	16	0.80	320	0.30	500	1.0
208	16	0.80	320	0.30	500	1.0
210	2	0.90	320	0.50	1766	1.0
211	140	0.15	1120	0.50	-	-

3.6.2.2. Internal Heat Gain in Office Center

Office center has 78 people. It was assumed that number of the additional people in an office, who are clients or visitors, are 3 between 9^{00}-12^{00} and 14^{00}-17^{00} hours. The internal loads owing to people were selected 75 W sensible and 55 W latent heat per person following the recommendation of ASHRAE Fundamentals. Offices include computer terminals at most desks and some other equipment such as personal computers, printers and copiers. Use factor for equipment in the office center is 0.8. For others rooms, use factors for lighting and people were taken from Table 3.14. Description of the internal heat gain parameters for office center are given in Table 3.16.

3.6.3. Operating (Working) Hours

In the study two different operating scenarios, namely scenario 1 and scenario 2 were considered. For scenario 1, operating time of the air-conditioning systems is between 8^{00}-17^{00} hours during the day. Other scenario is that operating time of the systems is between 8^{00}-24^{00} hours.

3.6.4. Indoor and Outdoor Design Conditions

The primary purpose of the air conditioning system is to maintain the space in a comfortable and healthy condition. Therefore, the system must generally maintain the dry bulb temperature and the relative humidity within an acceptable range. Experience has shown that, except in critical cases, the indoor design condition should be selected on the high side of the comfort envelope to avoid overdesigning the system.

In this study, indoor design conditions of building were selected as 50% relative humidity and 26 °C dry bulb temperature. Dry-bulb temperature (T) and wet-bulb temperature (WT) were taken as outdoor air conditions. Outdoor design conditions of the provinces selected are given in Table 3.17.

Table 3.16. Description of the internal heat gain parameters for office center

Room Code	People		Lighting		Equipment	
	No	Use Factor	Heat Gain (W)	Use Factor	Heat Gain (W)	Use Factor
Z01	5	0.85	480	0.50	1766	0.8
Z02	5	0.85	480	0.30	1766	0.8
Z03	5	0.85	480	0.30	1766	0.8
Z04	5	0.85	480	0.30	1766	0.8
Z05	5	0.85	640	0.30	1766	0.8
Z07	5	0.85	320	0.50	1766	0.8
Z08	10	0.50	1120	0.50	-	-
101	5	0.85	480	0.30	1766	0.8
102	5	0.85	480	0.50	1766	0.8
103	5	0.85	480	0.30	1766	0.8
104	5	0.85	320	0.30	1766	0.8
105	5	0.85	320	0.30	1766	0.8
106	5	0.85	320	0.30	1766	0.8
107	5	0.85	320	0.30	1766	0.8
108	5	0.85	480	0.30	1766	0.8
110	5	0.85	320	0.50	1766	0.8
111	10	0.50	1120	0.50	-	-
201	5	0.85	480	0.30	1766	0.8
202	5	0.85	480	0.30	1766	0.8
203	5	0.85	480	0.30	1766	0.8
204	5	0.85	320	0.30	1766	0.8
205	5	0.85	320	0.30	1766	0.8
206	5	0.85	320	0.30	1766	0.8
207	5	0.85	320	0.30	1766	0.8
208	5	0.85	320	0.30	1766	0.8
210	5	0.85	320	0.50	1766	0.8
211	10	0.50	1120	0.50	-	-

Table 3.17. Outdoor design conditions, latitude and longitude

Province	Latitude [^{o}N]	Longitude [^{o}E]	T [^{o}C]	WT [^{o}C]	Daily Range [^{o}C]
Adana	36.59	35.18	38	26	12.4
Ankara	39.57	32.53	34	20	15.0
Antalya	36.53	30.42	39	28	11.4
Diyarbakır	37.55	40.12	43	23	17.7
Erzurum	39.55	41.16	30	19	14.7
Gaziantep	37.05	37.22	39	23	13.5
İstanbul	40.58	29.05	33	24	10.5
İzmir	38.24	27.10	37	24	12.8
Konya	37.52	32.30	34	21	15.4
Samsun	41.17	36.20	32	25	7.8
Şanlıurfa	37.08	38.46	43	24	15.2
Trabzon	41.00	39.43	31	25	5.8
Van	38.28	43.21	33	20	15.5

3.6.5. Fresh Air Requirement

Indoor Air Quality (IAQ) is closely related to the psychometric analysis leading to system design because air quality depends largely on the amount of outdoor air brought into the conditioned space. For a typical occupied space, the amount of fresh air (outdoor air) is proportional to the number of the people in the space. ASHRAE standard 62, Ventilation for Acceptable Indoor Air Quality, covers this subject and is the recognized source of data for the purpose of system design.

According to the ASHRAE Standard 62 ventilation rate procedure, offices and classrooms should be ventilated at 28 m^3/h per person. Outdoor air requirement is 36 m^3/h per person for laboratories and 1.8 m^3/h per square meter for corridors. These values resulted in a minimum ventilation level of 7001 m^3/h and 3359 m^3/h for education building and office center ventilation, respectively. Outdoor air requirements for the rooms are given in Table 3.18. The right most column of Table 3.18 shows the required minimum fresh air. It was calculated by the number of people, use factor and fresh air requirement for one person for offices and classroom. In the one of corridors, it was obtained by multiplying the floor area, use factor and outdoor air requirement for square meter.

Table 3.18. Outdoor air requirements for the occupied spaces

Room Code	Education Building					Office Center				
	People		Outdoor Air Requirement		Total Fresh Air	People		Outdoor Air Requirement		Total Fresh Air
	NO	Use Factor	m^3/h person	m^3/h per m^2	m^3/h	NO	Use Factor	m^3/h person	m^3/h per m^2	m^3/h
Z01	1	0.9	28.8	-	25.92	5	0.85	28.8	-	122.40
Z02	16	0.3	36.0	-	172.80	5	0.85	28.8	-	122.40
Z03	16	0.3	36.0	-	172.80	5	0.85	28.8	-	122.40
Z04	16	0.3	36.0	-	172.80	5	0.85	28.8	-	122.40
Z05	16	0.5	28.8	-	230.40	5	0.85	28.8	-	122.40
Z07	2	0.9	28.8	-	51.84	5	0.85	28.8	-	122.40
Z08	60	0.4	-	1.8	125.40	10	0.5	-	1.8	156.75
101	16	0.3	28.8	-	138.24	5	0.85	28.8	-	122.40
102	20	0.3	28.8	-	172.80	5	0.85	28.8	-	122.40
103	16	0.8	28.8	-	368.64	5	0.85	28.8	-	122.40
104	16	0.8	28.8	-	368.64	5	0.85	28.8	-	122.40
105	16	0.8	28.8	-	368.64	5	0.85	28.8	-	122.40
106	16	0.8	28.8	-	368.64	5	0.85	28.8	-	122.40
107	16	0.8	28.8	-	368.64	5	0.85	28.8	-	122.40
108	15	0.5	28.8	-	216.00	5	0.85	28.8	-	122.40
110	2	0.9	28.8	-	51.84	5	0.85	28.8	-	122.40
111	110	0.5	-	1.8	132.18	10	0.5	-	1.8	132.18
201	24	0.8	28.8	-	552.96	5	0.85	28.8	-	122.40
202	24	0.8	28.8	-	552.96	5	0.85	28.8	-	122.40
203	16	0.8	28.8	-	368.64	5	0.85	28.8	-	122.40
204	16	0.8	28.8	-	368.64	5	0.85	28.8	-	122.40
205	16	0.8	28.8	-	368.64	5	0.85	28.8	-	122.40
206	16	0.8	28.8	-	368.64	5	0.85	28.8	-	122.40
207	16	0.8	28.8	-	368.64	5	0.85	28.8	-	122.40
208	16	0.8	28.8	-	368.64	5	0.85	28.8	-	122.40
210	2	0.9	28.8	-	51.84	5	0.85	28.8	-	122.40
211	140	0.5	-	1.8	132.18	10	05	-	1.8	132.18
Total outdoor air requirement=					7001	Total outdoor air requirement =				3359

4. RESULTS AND DISCUSSION

4.1. Calculation of the Cooling Load with RTS Method

Cooling load of a building consists of external loads through the building envelope and internal loads from people, lights, appliances and other heat sources. In this study, cooling load of the sample building was calculated according to RTS method [Spitler et al., 1997; ASHRAE 2001]. A computer program called CoolingLoadRTS was written and used for the calculation of cooling load. Detailed information about program CoolingLoadRTS is given in Appendix1.

4.1.1 Exterior Surfaces of a Room

Exterior surfaces involved exterior walls and roofs conduct heat due to temperature differences between outdoor air and indoor air. In addition, solar energy on exterior surfaces is absorbed, and then transferred by conduction to the building interior. Due to the mass and thermal capacity of the wall or roof construction materials, there is a substantial time delay in heat input at the exterior surface becoming heat gain at the interior surface.

As an example to the cooling load calculation procedure with RTS method for exterior walls of a room, Table 4.1 is given that shows the calculation steps for room 101. The results are for education building located in Adana. Heat input, which is given in column 4 of Table 4.1, can be calculated using Equation 3.1. Conductive heat gain can be calculated using conductive heat inputs for the current hours and past 23 hours and CTS (Equation 3.2). Conductive heat gain due to exterior surfaces includes convective and radiant portions. Convective and radiant portions can be determined by multiplying the total heat gains and split rates given in Table 3.1. Convective portion, which is given in column 6 of Table 4.1, immediately become cooling load. Radiant heat gain becomes cooling load over a delayed period of time. The radiant time series (RTS), which is given in eighth column of Table 4.1, can be used to convert the radiant portion of hourly heat gains to hourly cooling loads with

Equation 3.3. Finally, total cooling load for the exterior surface, which is given in right most column of Table 4.1, can be calculated by summing the parts of radiant and convective cooling loads.

Hourly profiles of the heat input, heat gain and total cooling load are shown in Figure 4.1.

Table 4.1. Hourly heat input heat gain and cooling load profiles for exterior walls of room 101

Time	North Solar Air [°C]	CTS	Heat Input [W]	Heat Gain [W]	Split Heat Gain		RTS	Radiant CL [W]	Total CL [W]
					Conv. 0.37% [W]	Radiant 0.63% [W]			
1^{00}	27.21	0	15.7	103.7	38.4	65.3	0.33	83.4	121.7
2^{00}	26.59	0.05	7.6	85.5	31.6	53.9	0.16	75.2	106.8
3^{00}	26.10	0.14	1.2	69.7	25.8	43.9	0.10	67.3	93.1
4^{00}	25.72	0.17	-3.6	55.5	20.5	35.0	0.07	59.9	80.4
5^{00}	26.61	0.15	7.9	43.2	16.0	27.2	0.05	53.0	69.0
6^{00}	35.40	0.12	121.5	33.2	12.3	20.9	0.04	46.7	59.0
7^{00}	35.17	0.09	118.4	31.6	11.7	19.9	0.03	42.5	54.2
8^{00}	33.15	0.07	92.4	42.9	15.9	27.0	0.03	41.8	57.6
9^{00}	35.77	0.05	126.2	57.1	21.1	36.0	0.02	43.6	64.7
10^{00}	38.34	0.04	159.4	68.8	25.5	43.4	0.02	46.4	71.8
11^{00}	40.85	0.03	191.8	81.1	30.0	51.1	0.02	50.0	80.0
12^{00}	42.91	0.02	218.5	97.0	35.9	61.1	0.02	55.0	90.9
13^{00}	44.16	0.02	234.7	117.3	43.4	73.9	0.01	61.6	105.0
14^{00}	44.60	0.01	240.3	138.9	51.4	87.5	0.01	69.5	120.9
15^{00}	44.12	0.01	234.1	160.0	59.2	100.8	0.01	78.0	137.2
16^{00}	44.55	0.01	239.6	178.1	65.9	112.2	0.01	86.5	152.4
17^{00}	46.51	0.01	265.0	192.0	71.1	121.0	0.01	94.1	165.2
18^{00}	42.41	0.01	212.0	204.8	75.8	129.0	0.01	101.3	177.0
19^{00}	33.78	0	100.6	214.1	79.2	134.9	0.01	107.6	186.8
20^{00}	32.17	0	79.7	212.1	78.5	133.6	0.01	111.1	189.6
21^{00}	30.81	0	62.1	195.8	72.5	123.4	0.01	110.4	182.8
22^{00}	29.57	0	46.1	172.6	63.9	108.7	0.01	106.1	169.9
23^{00}	28.58	0	33.3	148.5	54.9	93.5	0.01	99.5	154.5
24^{00}	27.83	0	23.7	124.8	46.2	78.6	0.00	91.7	137.9

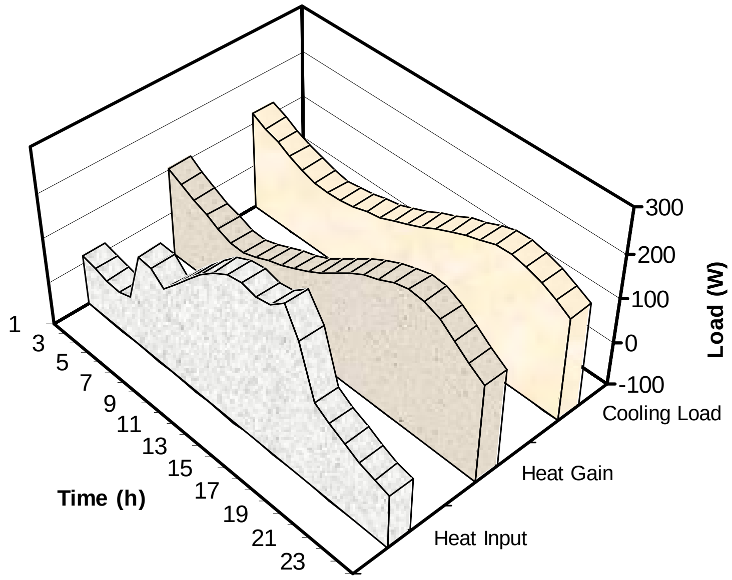

Figure 4.1. Heat input, heat gain and total cooling load profiles for exterior wall of room 101

4.1.2. Fenestration of a Room

Window heat gain consists of three portions; direct, diffuse and conductive heat gain. For calculation of fenestration cooling load, direct and diffuse heat gain should be determined. Solar equations and other properties, such as, local standard time, declination angel, etc., can be calculated using Equations (3.15) through (3.30). Direct and diffuse heat gains can be obtained using Equations (3.5) and (3.6). Conductive heat gain (Equation 3.7) can be determined by multiplying the temperature difference between outdoor and indoor air temperatures, the overall heat transfer coefficient of the component and the fenestration area. Results obtained the direct, the diffuse and the conductive heat gains are summed in order to compute the fenestration total heat gain. Total heat gain from a window, which involved radiant and convective portions, is split. Then, the appropriate RTS to the radiant portion is applied. Finally, total cooling load can be determined by summing up the convective and the radiant cooling load components.

This procedure was applied to room 101 of the education building located in Adana. Results are presented in Tables 4.2 and 4.3 as an example for calculation of fenestration cooling load.

Table 4.2. Solar heat gain due to fenestration of room 101

Solar Equation				Direct Beam Solar Heat Gain						Diffuse Beam Solar Heat Gain						Conduction		Total
Time	H	β	Φ	E_{DN}	γ	E_D	θ	SGHC	Direct Sol. HG	Er	Y	Ed	Total E	(SGHC)D	Diffuse Sol. HG	Tout-air	Conduc. HG	Total HG
1^{00}	-161.4	-30.2	-159.8	0	-339.8	0	35.8	0.842	0	0	1.11	0	0	0.78	0	27.21	41	41
2^{00}	-146.4	-24.6	-145.2	0	-325.2	0	41.7	0.837	0	0	1.05	0	0	0.78	0	26.59	20	20
3^{00}	-131.4	-16.7	-132.8	0	-312.8	0	49.4	0.821	0	0	0.97	0	0	0.78	0	26.10	3	3
4^{00}	-116.4	-7.1	-122.3	0	-302.3	0	58.0	0.788	0	0	0.87	0	0	0.78	0	25.72	-9	-9
5^{00}	-101.4	3.5	-113.2	38	-293.2	15	66.9	0.704	125	1	0.77	4	5	0.78	44	25.60	-13	155
6^{00}	-86.37	14.9	-104.8	485	-284.8	120	75.7	0.528	760	19	0.68	45	64	0.78	597	25.85	-5	1352
7^{00}	-71.37	26.7	-96.7	685	-276.7	71	84.0	0.251	215	40	0.60	56	96	0.78	898	26.47	16	1129
8^{00}	-56.37	38.8	-88.1	779	-268.1	0	91.5	0.000	0	59	0.45	48	107	0.78	1002	27.58	53	1056
9^{00}	-41.37	50.7	-77.6	830	-257.6	0	97.8	0.000	0	76	0.45	51	126	0.78	1183	29.20	107	1290
10^{00}	-26.37	62.0	-62.4	858	-242.4	0	102.6	0.000	0	87	0.45	53	140	0.78	1310	31.06	170	1480
11^{00}	-11.37	71.2	-34.9	872	-214.9	0	105.3	0.000	0	94	0.45	53	148	0.78	1383	33.16	241	1624
12^{00}	3.63	73.7	12.2	875	-167.8	0	105.9	0.000	0	96	0.45	54	149	0.78	1398	35.15	307	1705
13^{00}	18.63	67.2	50.5	867	-129.5	0	104.3	0.000	0	92	0.45	53	145	0.78	1355	36.64	357	1712
14^{00}	33.63	56.7	70.6	847	-109.4	0	100.5	0.000	0	82	0.45	52	134	0.78	1255	37.63	391	1646
15^{00}	48.63	44.9	83.0	809	-97.0	0	94.9	0.000	0	68	0.45	50	118	0.78	1102	38.00	403	1505
16^{00}	63.63	32.9	92.4	741	-87.6	26	88.0	0.083	26	50	0.57	57	107	0.78	1005	37.63	391	1422
17^{00}	78.63	21.0	100.6	608	-79.4	105	80.1	0.417	525	30	0.63	53	83	0.78	773	36.76	362	1660
18^{00}	93.63	9.3	108.8	303	-71.2	96	71.5	0.633	731	9	0.72	30	39	0.78	362	35.40	316	1409
19^{00}	108.6	-1.7	117.4	0	-62.6	0	62.6	0.752	0	0	0.82	0	0	0.78	0	33.78	262	262
20^{00}	123.6	-11.9	127.2	0	-52.8	0	53.7	0.805	0	0	0.92	0	0	0.78	0	32.17	207	207
21^{00}	138.6	-20.8	138.6	0	-41.4	0	45.5	0.829	0	0	1.01	0	0	0.78	0	30.81	162	162
22^{00}	153.6	-27.6	152.0	0	-28.0	0	38.5	0.841	0	0	1.08	0	0	0.78	0	29.57	120	120
23^{00}	168.6	-31.8	167.5	0	-12.5	0	34.0	0.843	0	0	1.13	0	0	0.78	0	28.58	87	87
24^{00}	183.6	-32.7	176.0	0	-4.0	0	32.9	0.844	0	0	1.14	0	0	0.78	0	27.83	62	62

Table 4.3. Solar cooling load converted to solar heat gain of room 101

	Direct Beam Solar Cooling Load							Diffuse Solar and Conduction Cooling Load								Total Cooling Load
Time	Window Total HG	Direct Solar HG	Conv. 0%	Rad. 100%	Solar RTS	Direct Solar Rad. CL	Direct Solar Total CL	Diffuse Solar HG	Cond. HG	Tot. Diff. & Cond. HG	Conv.. 37%	Rad. 63%	Non solar RTS	Diff.& Cond. Radiant CL	Diff.& Cond. Total CL	Total Window CL
1^{00}	41	0	0	0	0.29	49	49	0	41	41	15	26	0.33	191	206	255
2^{00}	20	0	0	0	0.15	48	48	0	20	20	7	13	0.16	168	175	223
3^{00}	3	0	0	0	0.10	35	35	0	3	3	1	2	0.10	150	151	186
4^{00}	-9	0	0	0	0.07	26	26	0	-9	-9	-3	-6	0.07	134	130	156
5^{00}	155	125	0	125	0.06	62	62	44	-13	30	11	19	0.05	127	138	200
6^{00}	1352	760	0	760	0.05	264	264	597	-5	592	219	373	0.04	236	455	719
7^{00}	1129	215	0	215	0.04	209	209	898	16	913	338	575	0.03	352	690	899
8^{00}	1056	0	0	0	0.03	130	130	1002	53	1056	391	665	0.03	441	831	961
9^{00}	1290	0	0	0	0.03	95	95	1183	107	1290	477	813	0.02	539	1016	1111
10^{00}	1480	0	0	0	0.03	80	80	1310	170	1480	548	933	0.02	633	1181	1260
11^{00}	1624	0	0	0	0.02	69	69	1383	241	1624	601	1023	0.02	716	1317	1386
12^{00}	1705	0	0	0	0.02	58	58	1398	307	1705	631	1074	0.02	783	1414	1471
13^{00}	1712	0	0	0	0.02	48	48	1355	357	1712	634	1079	0.01	827	1461	1509
14^{00}	1646	0	0	0	0.02	40	40	1255	391	1646	609	1037	0.01	844	1453	1493
15^{00}	1505	0	0	0	0.01	32	32	1102	403	1505	557	948	0.01	831	1388	1420
16^{00}	1422	26	0	26	0.01	32	32	1005	391	1396	517	879	0.01	811	1328	1359
17^{00}	1660	525	0	525	0.01	178	178	773	362	1134	420	715	0.01	754	1174	1352
18^{00}	1409	731	0	731	0.01	315	315	362	316	678	251	427	0.01	635	886	1202
19^{00}	262	0	0	0	0.01	185	185	0	262	262	97	165	0.01	491	587	772
20^{00}	207	0	0	0	0.01	125	125	0	207	207	77	131	0.01	403	480	604
21^{00}	162	0	0	0	0.01	95	95	0	162	162	60	102	0.01	339	399	494
22^{00}	120	0	0	0	0.00	82	82	0	120	120	44	76	0.01	289	334	416
23^{00}	87	0	0	0	0.00	69	69	0	87	87	32	55	0.01	250	282	351
24^{00}	62	0	0	0	0.00	57	57	0	62	62	23	39	0.00	217	240	297

Figure 4.2 shows hourly profiles of heat gain and total cooling load due to window for room 101. As seen from this figure, the major percentage of the heat gain due to fenestration comes from diffuse heat gain. Direct heat gain of this room is very small because the outside walls of the room face to the North.

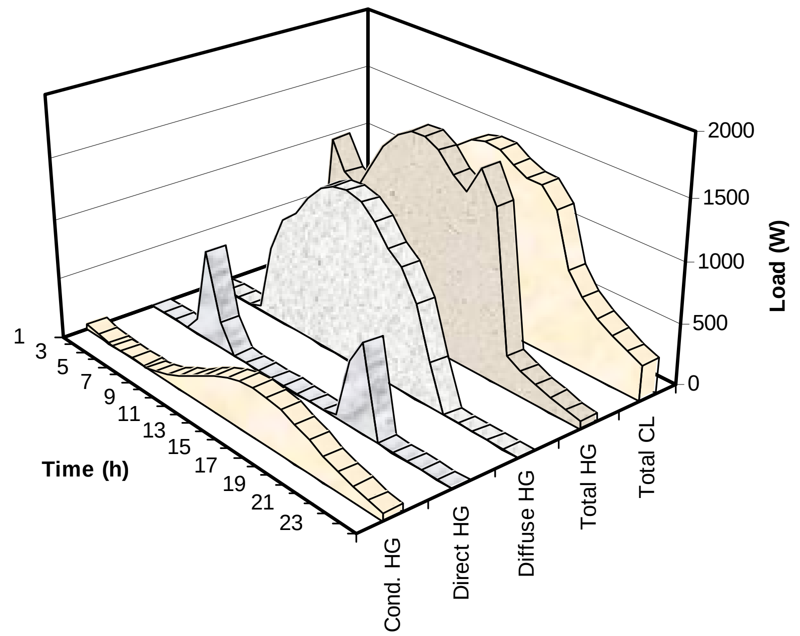

Figure 4.2. Heat gains and cooling load due to fenestration of room 101

4.1.3. Internal Heat Gain of a Room

Internal heat gain consists of people, lighting and miscellaneous equipment heat gains. It is independent of the outdoor condition and is a function of occupancy and operating schedules. In order to determine the internal cooling load, the hourly heat gain profile for the internal load such as lighting load is calculated firstly, then heat gains are split into radiant and convective portions, and finally the appropriate RTS values to the radiant portion are applied. Summing the convective and radiant cooling load components, the total cooling load is determined.

Figure 4.3 shows heat gain and cooling load due to people for room 101 of education building in Adana. The room is designed for 16 people. Sensible and latent heat gains per occupant are 75 and 55 W respectively. It is assumed that diversity factor is 0.3 considering the laboratory conditions. The latent heat gain due to people is converted immediately to latent cooling load. Sensible heat gain due to people involves radiant and convective heat gain. Convective portion of the sensible heat gain is converted to cooling load as latent heat gain immediately. RTS is applied to radiant portion to obtain radiant cooling load. Total sensible cooling load is calculated by summing up the radiant cooling load and the convective cooling load. It can be seen Figure 4.3 that the sharp increase in the cooling load at 8^{00} o'clock and the sharp decrease at 17^{00} o'clock is due to change in the number of people at the beginning and at the end of working hours, respectively. The cooling load due to people during 8^{00} to 17^{00} hours is less than the hourly total heat gain because of thermal storage. At these hours the hourly cooling load increases slightly because of reducing of thermal storage. Cooling load is approximately 500 W.

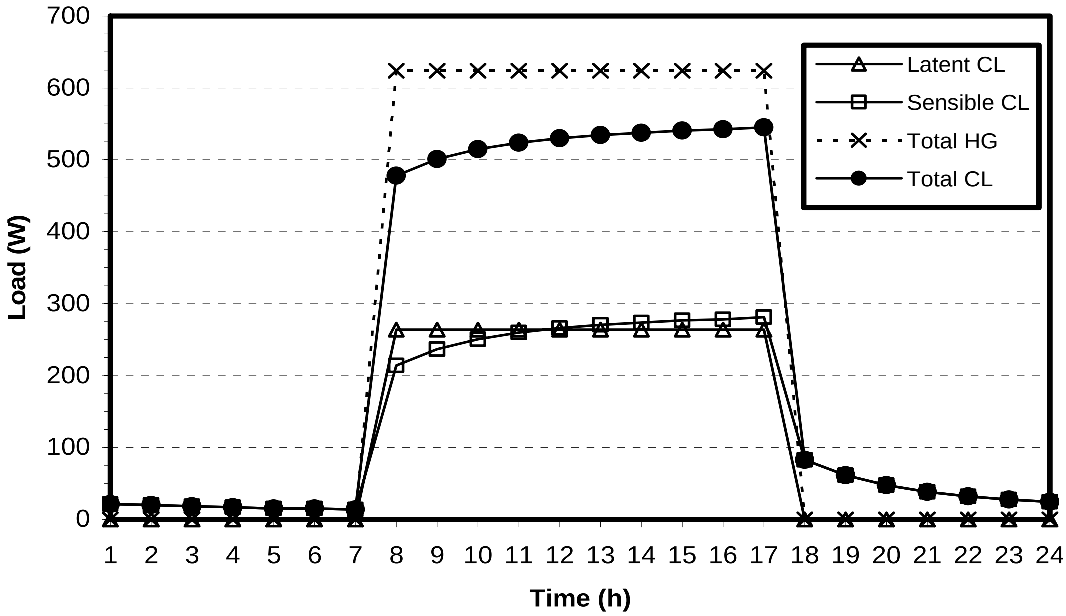

Figure 4.3. Heat gain and cooling load due to people for room 101

Figure 4.4 shows heat gain and cooling load due to lighting for room 101. The room is lightened with 480 W fluorescent lighting. The cooling load consist of radiant and convective cooling loads. It is assumed that diversity factor is 0.3 because of daytime. As can be seen from this figure that the sharp increase in the cooling load at 8^{00} o'clock, and the sharp decrease at 17^{00} are observed, because lighting is turned on and off at these hours, respectively. The cooling load due to lighting during operating time is less than the hourly heat gain because of thermal storage. The cooling load increases slightly because of reducing of thermal storage. Cooling load involves radiant and convective portions. Hourly profiles of the radiant and convective cooling loads are also clearly shown in Figure 4.4 for room 101.

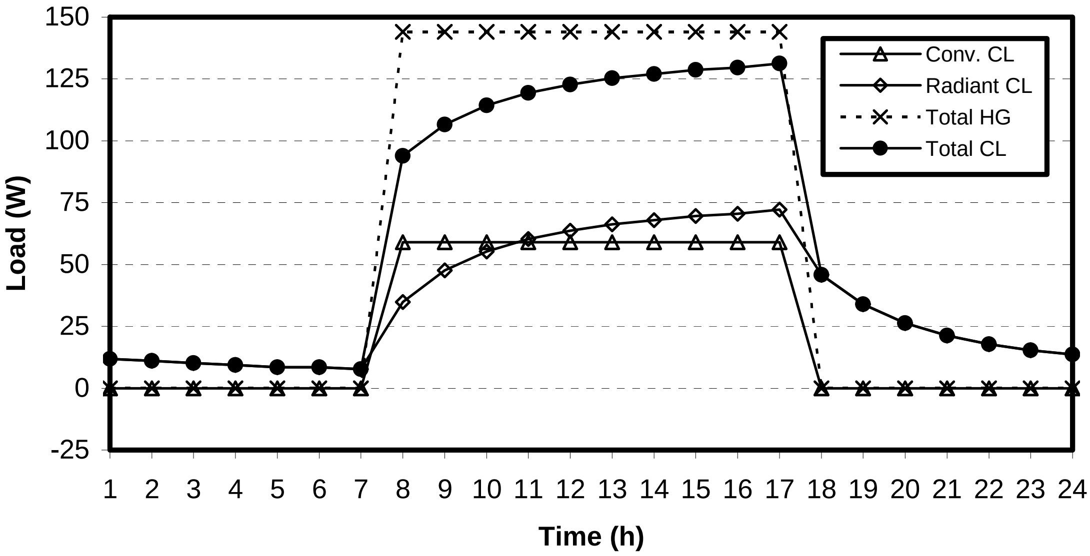

Figure 4.4. Heat gain and cooling load due to lighting for room 101

Figure 4.5 shows the heat gain and cooling load due to equipments for room 102. Sensible heat gain of the equipment used in the room is 1366 W. It's diversity factor is assumed to be 1.0 during the working hours. As can be seen from this figure that the sharp increase in the cooling load at 8^{00} o'clock, and the sharp decrease at 17^{00} are observed, because equipment used in the building is switched on and off at these hours, respectively. The difference between hourly heat gain and hourly cooling load at early operating time is greater than at the other hours because of reducing of thermal storage. At peak hour, cooling load due to equipment is obtained to be approximately 1250 W.

Analysis of the building cooling load shows that building cooling load strongly depends on the outdoor environment, occupant and operating schedules of internal heat gains and thermal capacity of the building construction materials and the objects in the space (furniture, etc.).

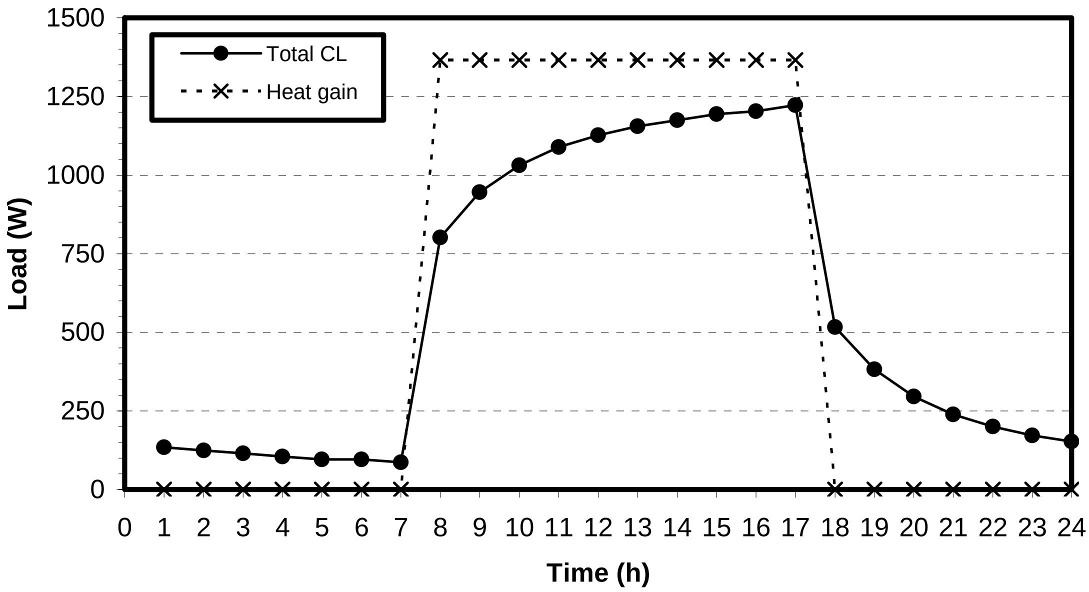

Figure 4.5. The heat gain due to equipment and total cooling load for room 102

4.1.4. Hourly Total Cooling Load of a Room

Total cooling load can be determined by summing up the cooling load for each load components which is explained above. Total cooling load and components of this load for room 101 in education building located in Adana are given in Table 4.4. External wall and fenestration areas of this room are 16.5 m^2 and 12 m^2, respectively. The outer walls of the room face to the North. No equipment is used in this room. There is no heat gain from internal walls because all the neighbour rooms are maintained at an indoor air temperature of 26 °C. The building is maintained at positive pressure by AHU for mechanical ventilation; therefore infiltration cooling load is not computed in calculation of the building cooling load.

Table 4.4. Total cooling load, components of it, and RSHF for room 101

TIME	Total cooling load components [W]									Total Cooling Load [W]			RSHF
						People		Equipment					
	Wall&Roof	Window	Int. Surfaces	Infiltration	Lighting	Latent	Sensible	Latent	Sensible	Sensible	Latent	Total	
1^{00}	274	255	0	0	12	0	21	0	0	563	0	563	1.00
2^{00}	238	223	0	0	11	0	20	0	0	492	0	492	1.00
3^{00}	205	186	0	0	10	0	18	0	0	420	0	420	1.00
4^{00}	176	156	0	0	9	0	17	0	0	358	0	358	1.00
5^{00}	151	200	0	0	8	0	15	0	0	375	0	375	1.00
6^{00}	129	719	0	0	8	0	15	0	0	872	0	872	1.00
7^{00}	115	899	0	0	8	0	14	0	0	1035	0	1035	1.00
8^{00}	113	961	0	0	94	264	214	0	0	1382	264	1646	0.84
9^{00}	118	1111	0	0	107	264	237	0	0	1573	264	1837	0.86
10^{00}	126	1260	0	0	114	264	251	0	0	1751	264	2015	0.87
11^{00}	138	1386	0	0	119	264	260	0	0	1903	264	2167	0.88
12^{00}	157	1471	0	0	123	264	266	0	0	2017	264	2281	0.88
13^{00}	183	1509	0	0	125	264	271	0	0	2088	264	2352	0.89
14^{00}	218	1493	0	0	127	264	274	0	0	2112	264	2376	0.89
15^{00}	262	1420	0	0	129	264	277	0	0	2088	264	2352	0.89
16^{00}	315	1359	0	0	130	264	278	0	0	2082	264	2346	0.89
17^{00}	370	1352	0	0	131	264	281	0	0	2135	264	2399	0.89
18^{00}	422	1202	0	0	46	0	83	0	0	1752	0	1752	1.00
19^{00}	459	772	0	0	34	0	61	0	0	1326	0	1326	1.00
20^{00}	466	604	0	0	26	0	47	0	0	1144	0	1144	1.00
21^{00}	443	494	0	0	21	0	38	0	0	996	0	996	1.00
22^{00}	403	416	0	0	18	0	32	0	0	869	0	869	1.00
23^{00}	359	351	0	0	15	0	28	0	0	753	0	753	1.00
24^{00}	315	297	0	0	14	0	24	0	0	650	0	650	1.00

Figure 4.6 shows, sensible, latent and total cooling loads and Sensible heat factor (RSHF) for room 101. RSHF of the room varies between 0.82 and 1. RSHF is less than 1 during working period and it is equal to 1 for the remaining period. RSHF is a function of latent heat gain which occurs when humidity is added to the room from vapor emitted by occupants and equipment. The maximum total cooling load of this room is obtained at 14^{00} o'clock and it is approximately 2500 W. At this hour RSHF is 0.89.

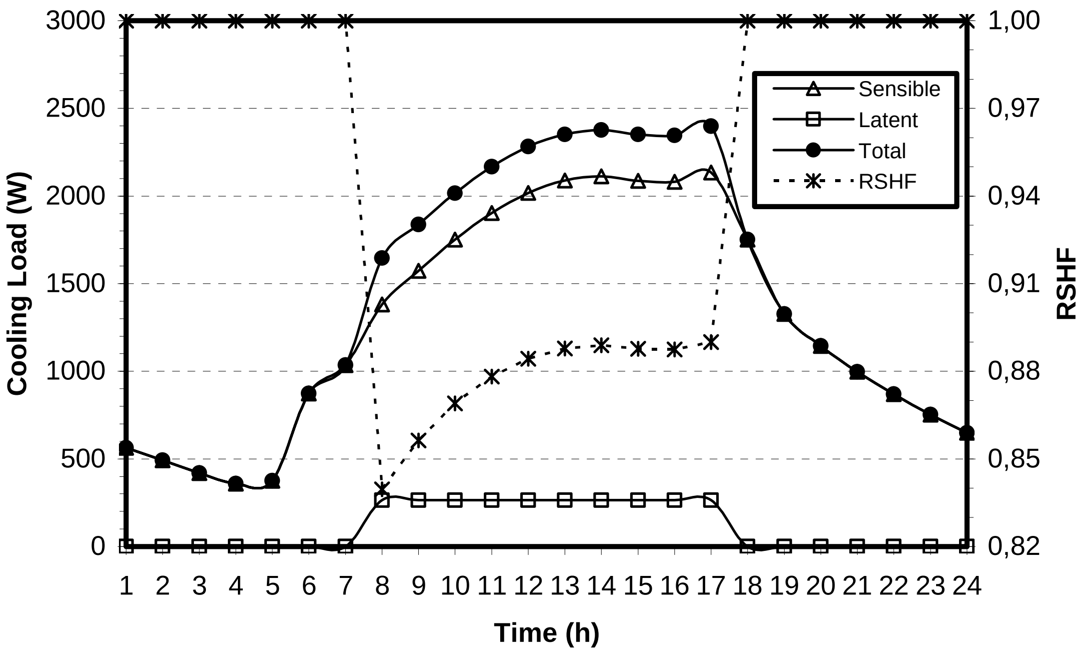

Figure 4.6. Sensible, latent and total cooling loads and RSHF for room 101

Cooling loads of all components for room 101 given in Table 4.4 are graphically shown in Figure 4.7. As can be seen from this figure that total cooling load of the room consist of heat gains due to window, wall-roof, lighting and people. It is not affected by other components such as infiltration and equipment. The major percentage of total cooling load comes from the fenestration cooling load.

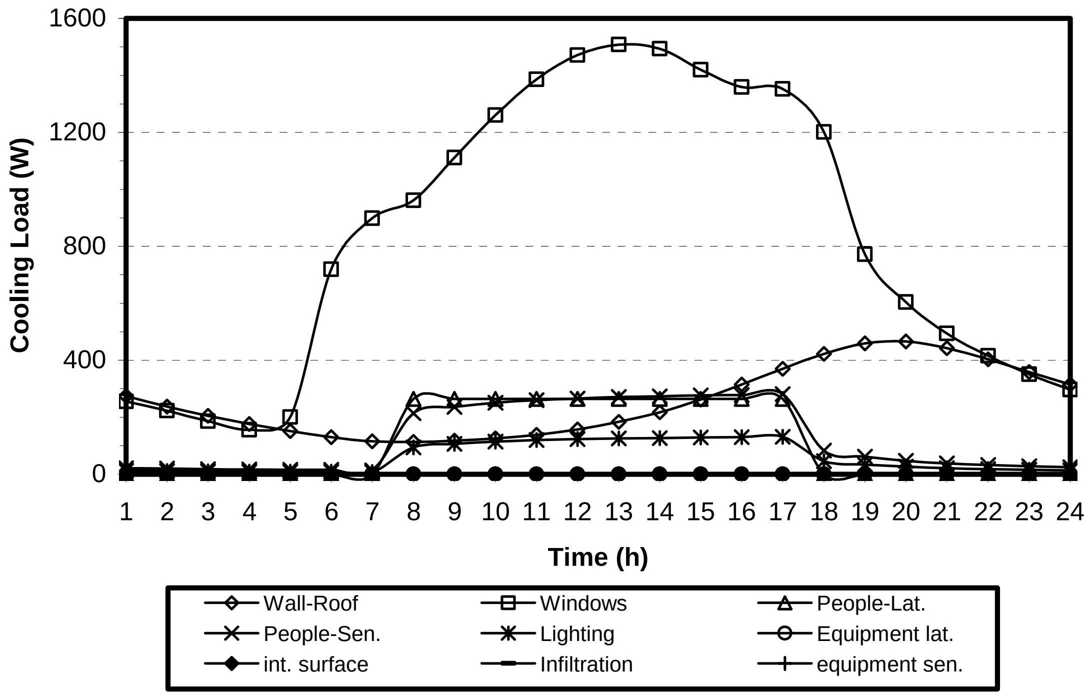

Figure 4.7. Parts of the cooling load for 101 room

4.1.5. Hourly Total Cooling Load of the Sample Building

Hourly total cooling loads of all the rooms of the sample building were summed in order to determine hourly total cooling load. Table 4.5 presents separately hourly total cooling load of some selected rooms (room 210, room 108 and room Z01) and total cooling load of the education building in Adana. Total cooling load of the education building for Adana was calculated for July 21 because design day for cooling system design is selected July 21 in Turkey. It should be noted that the sample building is thermally insulated and it is a “B type building” according to Thermal Insulation Regulation.

In this study, hourly total design cooling load of the education building located in different provinces of Turkey were also performed for July 21 and given in Table 4.6. The provinces considered are Adana, Antalya, Ankara, İstanbul, İzmir, Konya, Diyarbakır, Gaziantep, Samsun, Şanlıurfa, Trabzon and Van. Outdoor design conditions of these provinces are given in Table 3.12.

Table 4.5. Sensible and total cooling load of selected rooms and education building

Time	Total and Sensible Cooling Load for some Selected Rooms [W]						Total Cooling Load of the Education Building [W]	
	210		108		Z01			
	Sen.	Total	Sen.	Total	Sen.	Total	Sensible	Total
1^{00}	592	592	674	674	863	863	19151	19151
2^{00}	509	509	589	589	775	775	16753	16753
3^{00}	430	430	514	514	685	685	14487	14487
4^{00}	361	361	452	452	606	606	12541	12541
5^{00}	347	347	413	413	603	603	11973	11973
6^{00}	669	669	548	548	1092	1092	21645	21645
7^{00}	790	790	661	661	1233	1233	27524	27524
8^{00}	2017	2116	1747	2159	2514	2563	62354	77089
9^{00}	2476	2575	2131	2544	2895	2945	75634	90368
10^{00}	2882	2981	2531	2943	3186	3235	88208	102942
11^{00}	3242	3341	2900	3313	3412	3462	99086	113820
12^{00}	3540	3639	3175	3588	3576	3625	107241	121976
13^{00}	3768	3867	3309	3721	3685	3735	112003	126738
14^{00}	3908	4007	3296	3708	3738	3787	112778	127513
15^{00}	3958	4057	3176	3589	3747	3796	110173	124907
16^{00}	3847	3946	2931	3344	3619	3668	102871	117605
17^{00}	3804	3903	2818	3230	3686	3735	98902	113636
18^{00}	2599	2599	1816	1816	2515	2515	65894	65894
19^{00}	1969	1969	1522	1522	1926	1926	51231	51231
20^{00}	1555	1555	1340	1340	1642	1642	42309	42309
21^{00}	1240	1240	1174	1174	1426	1426	35347	35347
22^{00}	1012	1012	1025	1025	1255	1255	30013	30013
23^{00}	837	837	891	891	1103	1103	25674	25674
24^{00}	703	703	777	777	976	976	22170	22170

It is seen from Table 4.6 that among the provinces considered, the highest cooling load of sample building is obtained in Antalya and the lowest one is obtained in Van. The peak (maximum) cooling load of the building is obtained at 13^{00} in Diyarbakır, Gaziantep, Samsun, Şanlıurfa, Trabzon and Van, and for other provinces at 14^{00}. For all the provinces considered, the major cooling load demands occur from 11^{00} to 15^{00} hours in general. RSHF is obtained between 0.87 and 0.89 when the peak cooling load occurs. Results given in Table 4.6 are also shown graphically in Figure 4.8. As clearly shown from this figure that hourly profiles of total cooling load obtained for all the provinces considered have similar trends because the building is thermally insulated and it is a “B type building” as described in Thermal Insulation Regulation. Therefore, the sample building for different provinces considered has different thickness of thermal insulation material.

Table 4.6. Total design cooling load of sample building for some provinces of Turkey

	ADANA			ANKARA			ANTALYA		
Time	**Sen.**	**RSHF**	**Total**	**Sen.**	**RSHF**	**Total**	**Sen.**	**RSHF**	**Total**
1^{00}	19151	1.00	19151	8308	1.00	8308	22578	1.00	22578
2^{00}	16753	1.00	16753	6108	1.00	6108	20223	1.00	20223
3^{00}	14487	1.00	14487	4044	1.00	4044	18028	1.00	18028
4^{00}	12541	1.00	12541	2254	1.00	2254	16088	1.00	16088
5^{00}	11973	1.00	11973	1297	1.00	1297	14790	1.00	14790
6^{00}	21645	1.00	21645	10828	1.00	10828	22892	1.00	22892
7^{00}	27524	1.00	27524	16631	1.00	16631	29632	1.00	29632
8^{00}	62354	0.81	77089	50966	0.78	65701	63922	0.81	78657
9^{00}	75634	0.84	90368	63946	0.81	78681	76597	0.84	91332
10^{00}	88208	0.86	102942	76400	0.84	91134	89057	0.86	103792
11^{00}	99086	0.87	113820	87483	0.86	102218	100261	0.87	114996
12^{00}	107241	0.88	121976	95867	0.87	110602	108990	0.88	123724
13^{00}	112003	0.88	126738	100800	0.87	115534	114673	0.89	129407
14^{00}	112778	0.88	**127513**	101467	0.87	**116201**	116391	0.89	**131125**
15^{00}	110173	0.88	124907	98469	0.87	113203	114471	0.89	129206
16^{00}	102871	0.87	117605	90025	0.86	104760	107185	0.88	121920
17^{00}	98902	0.87	113636	85257	0.85	99992	102937	0.87	117671
18^{00}	65894	1.00	65894	53864	1.00	53864	71353	1.00	71353
19^{00}	51231	1.00	51231	38191	1.00	38191	55226	1.00	55226
20^{00}	42309	1.00	42309	29763	1.00	29763	46198	1.00	46198
21^{00}	35347	1.00	35347	23271	1.00	23271	38980	1.00	38980
22^{00}	30013	1.00	30013	18342	1.00	18342	33480	1.00	33480
23^{00}	25674	1.00	25674	14341	1.00	14341	29096	1.00	29096
24^{00}	22170	1.00	22170	11115	1.00	11115	25589	1.00	25589
	DİYARBAKIR			**GAZİANTEP**			**İSTANBUL**		
1^{00}	19092	1.00	19092	16948	1.00	16948	11839	1.00	11839
2^{00}	16661	1.00	16661	14820	1.00	14820	9756	1.00	9756
3^{00}	14413	1.00	14413	12842	1.00	12842	7839	1.00	7839
4^{00}	12524	1.00	12524	11177	1.00	11177	6160	1.00	6160
5^{00}	16743	1.00	16743	12957	1.00	12957	4816	1.00	4816
6^{00}	24850	1.00	24850	22820	1.00	22820	13320	1.00	13320
7^{00}	29721	1.00	29721	28241	1.00	28241	19656	1.00	19656
8^{00}	64877	0.81	79611	62804	0.81	77538	53662	0.78	68396
9^{00}	78424	0.84	93159	75512	0.84	90247	66269	0.82	81004
10^{00}	90530	0.86	105265	87001	0.86	101735	78834	0.84	93569
11^{00}	100573	0.87	115308	96567	0.87	111301	90351	0.86	105086
12^{00}	107725	0.88	122460	103561	0.88	118296	99274	0.87	114008
13^{00}	111225	0.88	**125959**	107286	0.88	**122021**	104900	0.88	119635
14^{00}	110801	0.88	125536	107182	0.88	121916	106146	0.88	**120880**
15^{00}	107422	0.88	122156	103931	0.88	118665	103535	0.88	118269
16^{00}	100235	0.87	114970	96498	0.87	111233	94714	0.87	109449
17^{00}	96133	0.87	110867	92604	0.86	107338	89088	0.86	103823
18^{00}	60976	1.00	60976	58944	1.00	58944	58245	1.00	58245
19^{00}	48787	1.00	48787	45359	1.00	45359	43149	1.00	43149
20^{00}	40581	1.00	40581	37211	1.00	37211	33547	1.00	33547
21^{00}	34328	1.00	34328	31084	1.00	31084	26754	1.00	26754
22^{00}	29428	1.00	29428	26443	1.00	26443	21689	1.00	21689
23^{00}	25321	1.00	25321	22647	1.00	22647	17720	1.00	17720
24^{00}	21992	1.00	21992	19603	1.00	19603	14569	1.00	14569

Table 4.6 (Continued) Total cooling load of sample building for some provinces

	İZMİR			KONYA			SAMSUN		
Time	Sen.	RSHF	Total	Sen.	RSHF	Total	Sen.	RSHF	Total
1^{00}	17665	1.00	17665	7517	1.00	7517	12623	1.00	12623
2^{00}	15047	1.00	15047	5353	1.00	5353	10771	1.00	10771
3^{00}	12674	1.00	12674	3304	1.00	3304	9066	1.00	9066
4^{00}	10550	1.00	10550	1522	1.00	1522	7617	1.00	7617
5^{00}	8837	1.00	8837	172	1.00	172	10476	1.00	10476
6^{00}	15306	1.00	15306	9586	1.00	9586	19111	1.00	19111
7^{00}	22641	1.00	22641	15861	1.00	15861	23984	1.00	23984
8^{00}	56844	0.79	71578	50070	0.77	64805	58896	0.80	73631
9^{00}	69344	0.82	84078	62503	0.81	77237	72499	0.83	87233
10^{00}	82241	0.85	96976	74448	0.83	89182	85046	0.85	99780
11^{00}	94404	0.86	109139	84994	0.85	99728	95639	0.87	110373
12^{00}	104234	0.88	118969	92992	0.86	107726	102978	0.87	117712
13^{00}	111133	0.88	125867	97804	0.87	112538	106504	0.88	**121239**
14^{00}	113890	0.89	**128625**	98663	0.87	**113397**	105541	0.88	120275
15^{00}	112727	0.88	127462	96037	0.87	110772	101038	0.87	115773
16^{00}	105157	0.88	119892	88132	0.86	102867	91708	0.86	106443
17^{00}	100179	0.87	114914	83960	0.85	98694	86884	0.86	101618
18^{00}	69404	1.00	69404	52452	1.00	52452	54635	1.00	54635
19^{00}	54087	1.00	54087	37066	1.00	37066	39990	1.00	39990
20^{00}	43427	1.00	43427	28727	1.00	28727	31878	1.00	31878
21^{00}	35622	1.00	35622	22303	1.00	22303	25831	1.00	25831
22^{00}	29593	1.00	29593	17426	1.00	17426	21388	1.00	21388
23^{00}	24820	1.00	24820	13467	1.00	13467	17832	1.00	17832
24^{00}	20988	1.00	20988	10282	1.00	10282	15025	1.00	15025
	ŞANLIURFA			TRABZON			VAN		
1^{00}	21596	1.00	21596	12824	1.00	12824	6010	1.00	6010
2^{00}	19359	1.00	19359	11124	1.00	11124	3963	1.00	3963
3^{00}	17265	1.00	17265	9579	1.00	9579	2092	1.00	2092
4^{00}	15500	1.00	15500	8291	1.00	8291	562	1.00	562
5^{00}	18147	1.00	18147	13837	1.00	13837	7410	1.00	7410
6^{00}	27013	1.00	27013	21546	1.00	21546	14500	1.00	14500
7^{00}	32182	1.00	32182	26137	1.00	26137	19006	1.00	19006
8^{00}	67017	0.82	81752	61537	0.81	76272	54259	0.79	68993
9^{00}	80166	0.84	94900	75245	0.84	89980	67350	0.82	82084
10^{00}	92039	0.86	106774	87469	0.86	102204	78598	0.84	93333
11^{00}	101935	0.87	116669	97267	0.87	112001	87540	0.86	102274
12^{00}	109020	0.88	123755	103709	0.88	118443	93414	0.86	108148
13^{00}	112599	0.88	**127334**	106058	0.88	**120792**	95539	0.87	**110273**
14^{00}	112308	0.88	127042	104083	0.88	118818	93848	0.86	108583
15^{00}	108985	0.88	123719	98890	0.87	113625	89692	0.86	104427
16^{00}	101672	0.87	116407	89821	0.86	104556	82392	0.85	97126
17^{00}	97644	0.87	112378	85133	0.85	99867	78029	0.84	92764
18^{00}	63351	1.00	63351	51528	1.00	51528	41818	1.00	41818
19^{00}	50530	1.00	50530	38383	1.00	38383	31529	1.00	31529
20^{00}	42366	1.00	42366	30632	1.00	30632	24290	1.00	24290
21^{00}	36186	1.00	36186	24990	1.00	24990	18922	1.00	18922
22^{00}	31432	1.00	31432	20873	1.00	20873	14731	1.00	14731
23^{00}	27501	1.00	27501	17577	1.00	17577	11227	1.00	11227
24^{00}	24337	1.00	24337	15004	1.00	15004	8435	1.00	8435

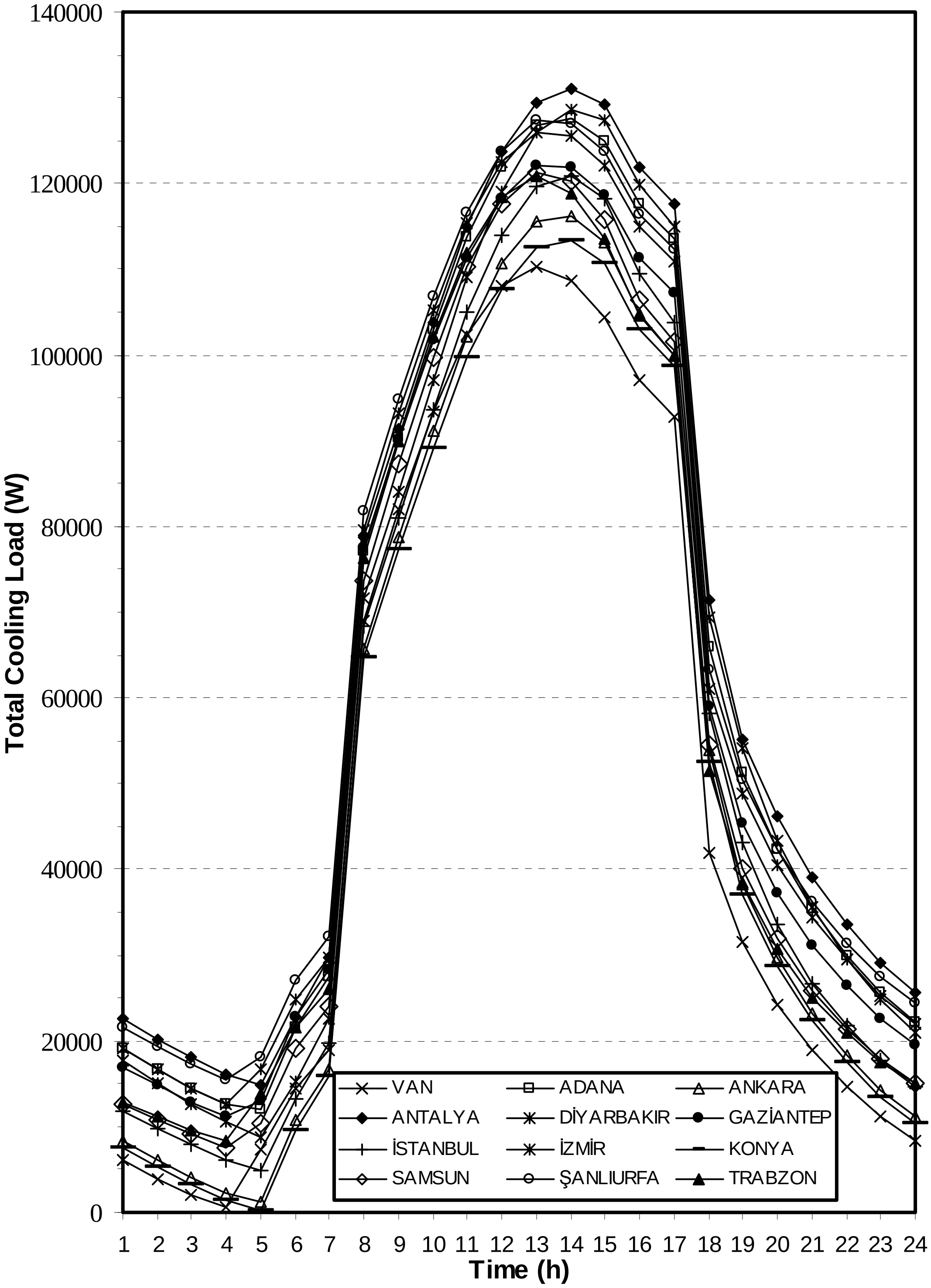

Figure 4.8. Hourly total design cooling load of education building for some provinces of Turkey

4.1.6. Hourly Total Cooling Load for Different Months of Cooling Season

When a HVAC system for cooling applications is designed, design cooling load can often be calculated using the outdoor design conditions at July 21. If the HVAC system is complex, such as variable air volume system, it may be necessary to provide calculations for two or more months. Furthermore, there is a need to calculate hourly total cooling load for different months of cooling season for economic analyses or energy analyses of HVAC systems.

In this section of the study, hourly total cooling load calculations for different months from April to October was performed for design day analysis. Hourly total cooling loads of education building in Adana for 21st day of each month from April to October are given in Table 4.7. Table 4.7 also presents RSHF and sensible design cooling loads. In the calculations, maximum dry bulb temperature of the outdoor air and daily range for 21st of each month are taken as outdoor design conditions. The distribution of hourly outdoor temperatures can be obtained using Equation (3.34). The loads were obtained for occupancy between 8^{00} and 24^{00} hours.

The results given in Table 4.7 are also shown graphically in Figure 4.9. It can be seen from Figure 4.9 that the peak cooling load is observed at 13^{00} and the major cooling load demands occur between 11^{00} and 16^{00} hours for all the months. The highest total cooling load of the education building is observed in August whilst the lowest hourly total cooling load is observed in April. Therefore, August 21 should be selected as the design day under these conditions.

Similar calculations were also performed for the office center. Figure 4.10 shows hourly total cooling load of the office building for 21st day of each month during cooling season. This graph is similar to previous graph. In this case, peak cooling load is obtained again at 13^{00} and the major cooling load demands occur between 11^{00} and 16^{00} hours for all the months. The highest hourly total cooling load of the office building is obtained in August and the lowest hourly total cooling load of office building is obtained in April. The peak total cooling load of the office building is approximately 125 kW at 13^{00} in August.

Table 4.7. Total cooling load of education building for 21st day of different months

	April			May		
Time	Total	Sen.	RSHF	Total	Sen.	RSHF
1^{00}	13212	13212	1.00	18622	18622	1.00
2^{00}	6978	6978	1.00	12327	12327	1.00
3^{00}	2739	2739	1.00	7988	7988	1.00
4^{00}	-343	-343	1.00	4839	4839	1.00
5^{00}	-2591	-2591	1.00	5087	5087	1.00
6^{00}	567	567	1.00	12336	12336	1.00
7^{00}	4258	4258	1.00	16284	16284	1.00
8^{00}	53537	38803	0.72	64270	49536	0.77
9^{00}	66189	51454	0.78	75834	61099	0.81
10^{00}	77482	62748	0.81	86147	71413	0.83
11^{00}	86669	71935	0.83	94677	79943	0.84
12^{00}	93378	78643	0.84	100713	85978	0.85
13^{00}	97473	82738	0.85	**103988**	89253	0.86
14^{00}	**97903**	83169	0.85	103827	89093	0.86
15^{00}	94998	80264	0.84	100901	86167	0.85
16^{00}	89541	74806	0.84	96990	82256	0.85
17^{00}	83892	69157	0.82	93778	79043	0.84
18^{00}	76445	61711	0.81	87016	72281	0.83
19^{00}	72450	57715	0.80	79750	65015	0.82
20^{00}	68616	53882	0.79	75154	60420	0.80
21^{00}	65405	50670	0.77	71462	56727	0.79
22^{00}	62647	47912	0.76	68430	53695	0.78
23^{00}	60231	45496	0.76	65813	51078	0.78
24^{00}	58410	43675	0.75	63864	49130	0.77
	June			July		
1^{00}	25127	25127	1.00	28168	28168	1.00
2^{00}	18751	18751	1.00	21750	21750	1.00
3^{00}	14327	14327	1.00	17262	17262	1.00
4^{00}	11072	11072	1.00	13969	13969	1.00
5^{00}	13253	13253	1.00	12986	12986	1.00
6^{00}	22025	22025	1.00	22914	22914	1.00
7^{00}	26648	26648	1.00	28594	28594	1.00
8^{00}	73820	59085	0.80	76668	62330	0.81
9^{00}	84377	69642	0.83	89054	74716	0.84
10^{00}	94064	79329	0.84	100572	86233	0.86
11^{00}	102068	87334	0.86	110282	95944	0.87
12^{00}	107741	93007	0.86	117245	102906	0.88
13^{00}	**110938**	96203	0.87	**121097**	106758	0.88
14^{00}	110766	96031	0.87	120972	106634	0.88
15^{00}	108371	93637	0.86	117495	103156	0.88
16^{00}	105639	90904	0.86	112662	98324	0.87
17^{00}	103447	88712	0.86	108798	94459	0.87
18^{00}	98030	83295	0.85	101607	87269	0.86
19^{00}	87902	73167	0.83	91534	77195	0.84
20^{00}	82707	67972	0.82	86053	71715	0.83
21^{00}	78605	63871	0.81	81691	67352	0.82
22^{00}	75319	60584	0.80	78196	63857	0.82
23^{00}	72524	57789	0.80	75232	60893	0.81
24^{00}	70448	55714	0.79	72996	58657	0.80

Table 4.7. (Continued) Total cooling load of education building for 21st day of different months

	August			September			October		
Time	**Total**	**Sen.**	**RSHF**	**Total**	**Sen.**	**RSHF**	**Total**	**Sen.**	**RSHF**
1^{00}	27538	27538	1.00	22171	22171	1.00	14830	14830	1.00
2^{00}	20993	20993	1.00	15607	15607	1.00	8264	8264	1.00
3^{00}	16467	16467	1.00	11171	11171	1.00	3874	3874	1.00
4^{00}	13158	13158	1.00	7814	7814	1.00	465	465	1.00
5^{00}	10725	10725	1.00	5277	5277	1.00	-2164	-2164	1.00
6^{00}	16227	16227	1.00	5302	5302	1.00	-4212	-4212	1.00
7^{00}	22646	22646	1.00	12560	12560	1.00	3792	3792	1.00
8^{00}	74771	60037	0.80	66399	51445	0.77	58435	43700	0.75
9^{00}	90795	76060	0.84	82716	67761	0.82	74989	60254	0.80
10^{00}	105648	90913	0.86	96622	81667	0.85	88704	73969	0.83
11^{00}	117675	102940	0.87	107705	92751	0.86	99597	84862	0.85
12^{00}	126258	111523	0.88	115709	100754	0.87	107471	92737	0.86
13^{00}	**131106**	116372	0.89	120392	105438	0.88	112049	97315	0.87
14^{00}	130775	116041	0.89	**120628**	105673	0.88	**112247**	97513	0.87
15^{00}	125744	111009	0.88	116356	101402	0.87	107915	93181	0.86
16^{00}	117262	102528	0.87	107695	92741	0.86	98177	83442	0.85
17^{00}	108571	93837	0.86	96628	81673	0.85	87139	72404	0.83
18^{00}	97176	82442	0.85	89352	74398	0.83	81193	66458	0.82
19^{00}	91143	76409	0.84	84475	69521	0.82	76489	61754	0.81
20^{00}	86036	71302	0.83	80101	65147	0.81	72337	57602	0.80
21^{00}	81885	67151	0.82	76383	61428	0.80	68692	53958	0.79
22^{00}	78426	63692	0.81	73117	58162	0.80	65440	50705	0.77
23^{00}	75441	60706	0.80	70262	55307	0.79	62599	47864	0.76
24^{00}	73137	58402	0.80	68055	53100	0.78	60406	45671	0.76

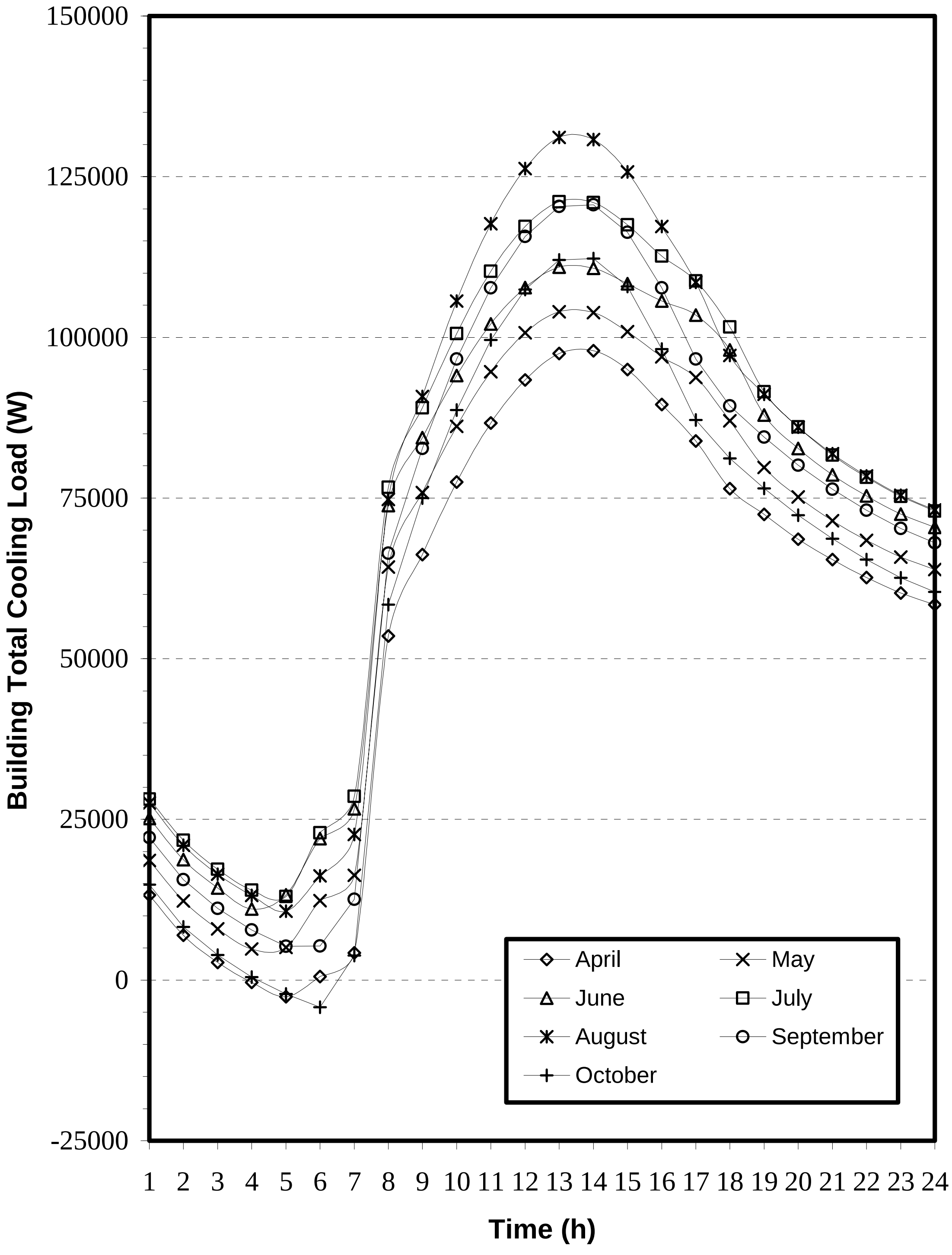

Figure 4.9. Hourly total cooling load of the education building for 21st day of each month during cooling season

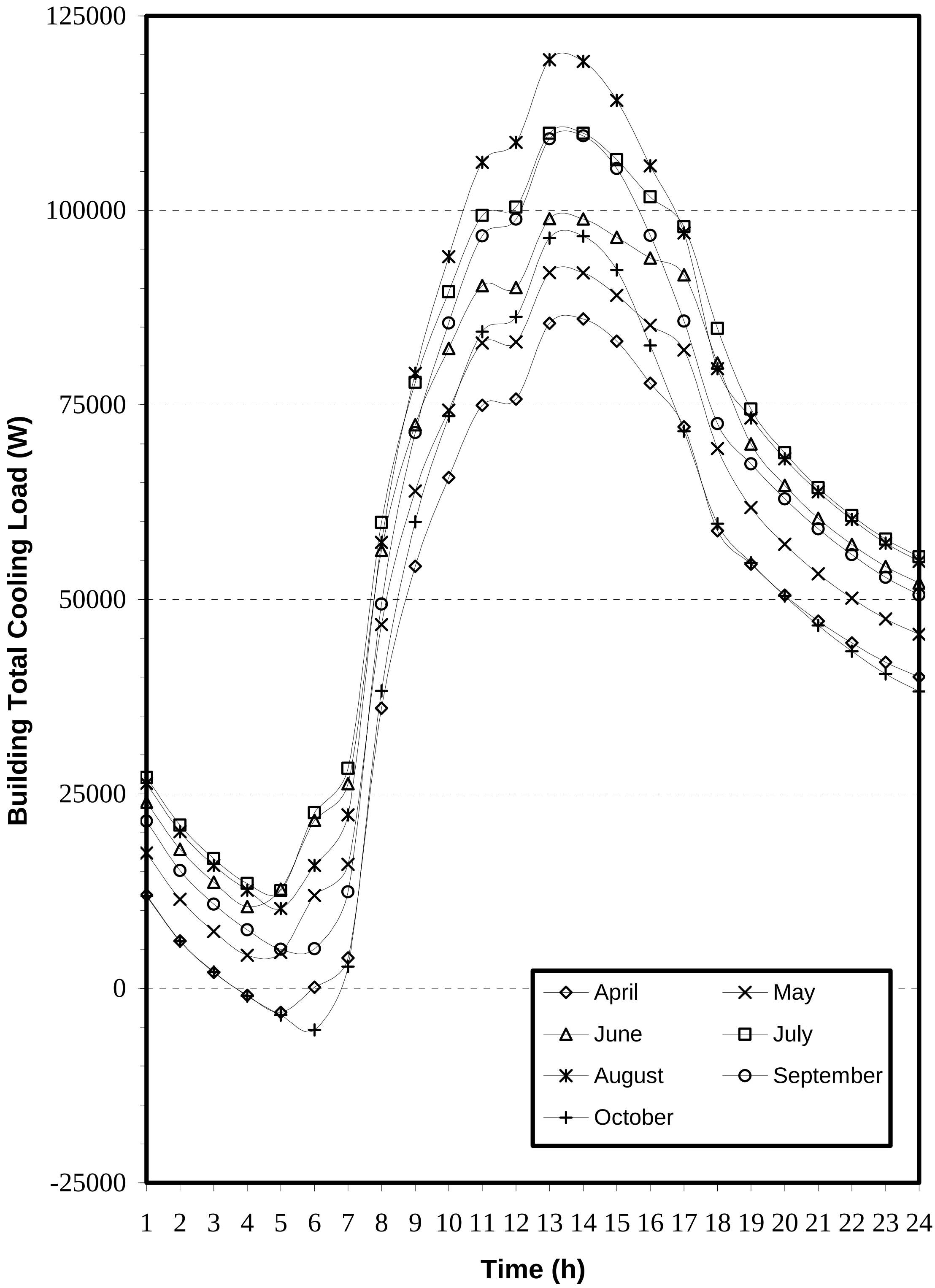

Figure 4.10. Hourly total cooling load of the office building for 21st day of each month during cooling season

4.2. Comparison of RTS Method and CLTD/SCL/CLF Method

In this section of the study, RTS and CLTD/SCL/CLF cooling load calculation methods, which directly affect the selection of the air conditioning system, were compared. For this purpose, cooling load of the education building located in Adana was calculated using the RTS method which is the latest load calculation method suggested by ASHRAE and the CLTD/SCL/CLF method which has been available for some time and known as a simple method. Calculation procedure of the CLTD/SCL/CLF method was explained in preceding Chapter. The results of the hourly building cooling load from different heat resource, which are obtained with the RTS and the CLTD/SCL/CLF methods for 21 July were evaluated and discussed in the following section.

4.2.1. Fenestration Cooling Load

Total Fenestration cooling load of the education building calculated using RTS and CLTD/SCL/CLF methods is shown in Figure 4.11. It is seen from this figure that the maximum total cooling load occurs at 13^{00} o’clock for both cases and the value calculated using the RTS method (61.3 kW) is approximately 17% higher than the one computed using the CLTD/SCL/CLF method (50.9 kW). The results obtained using RTS during 07^{00}-17^{00} period is higher than that is obtained using the CLTD/SCL/CLF method. However, the results obtained using CLTD/SCL/CLF method during remaining period are always higher than that were obtained using the RTS method.

4.2.2. External Surface Cooling Load

External surfaces of the building include roof and wall. Total external surface cooling load of the education building which were calculated using the RTS and the CLTD/SCL/CLF methods is presented in Figure 4.12. Total cooling load due to external surfaces of the education building obtained using the RTS and the CLTD/SCL/CLF methods have a similar profile, although there are some small differences.

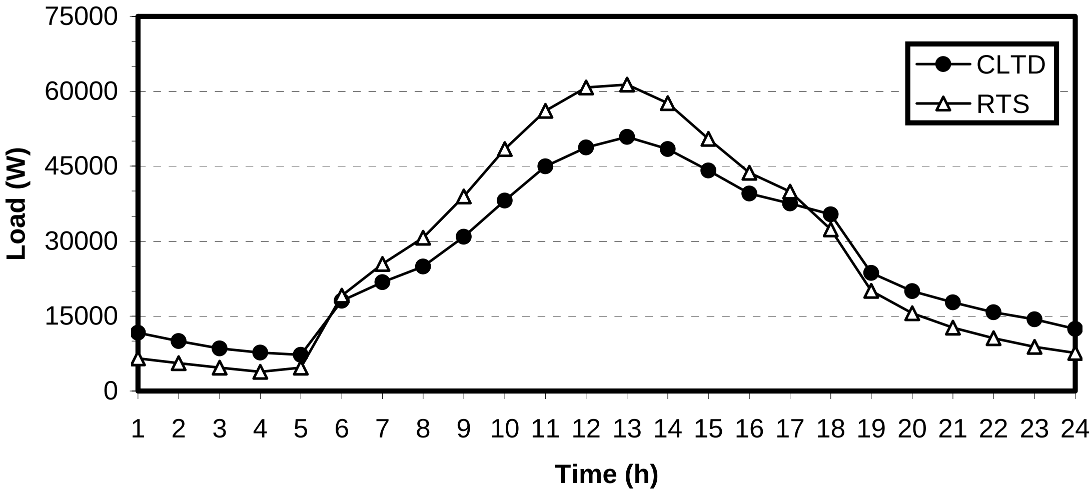

Figure 4.11. Fenestration total cooling load of the education building

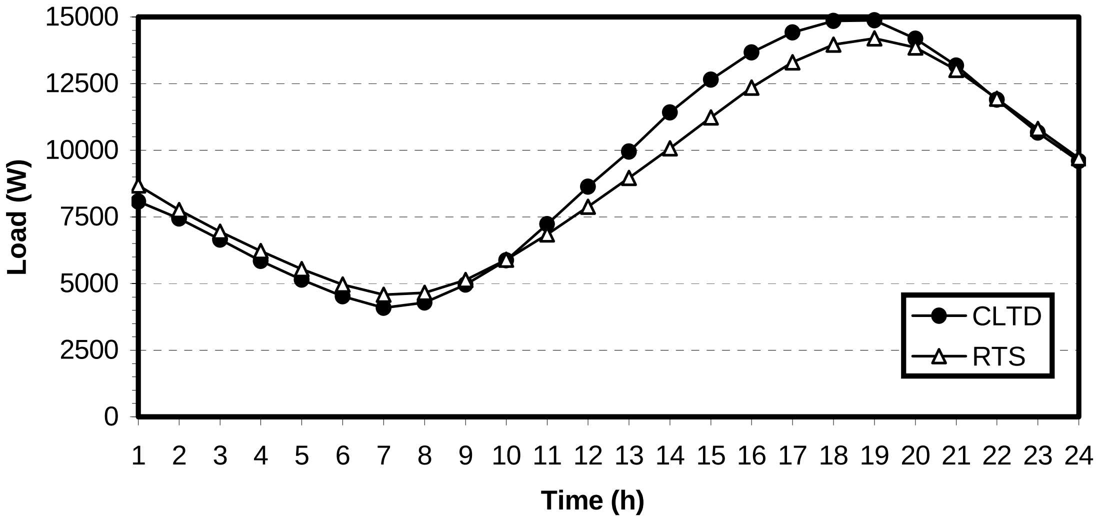

Figure 4.12. Total cooling load due to external surfaces of the education building

4.2.3. Cooling Load due to Equipment

Total equipment cooling load of the education building calculated using the RTS and the CLTD/SCL/CLF methods is shown in Figure 4.13. Total cooling load due to equipment, during the operating time period, calculated using RTS method is approximately 25% higher than that is obtained with CLTD/SCL/CLF method.

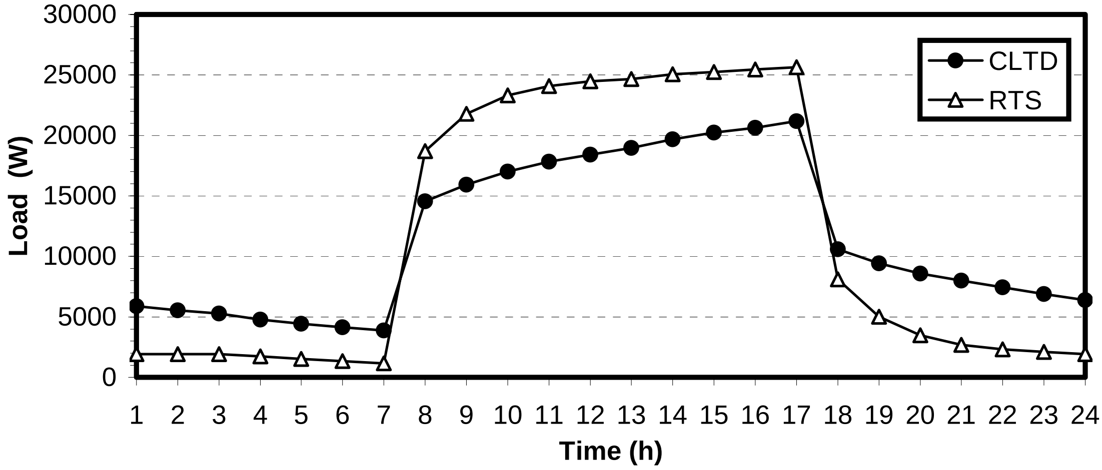

Figure 4.13. Total cooling load due to equipment in the education building

4.2.4. Cooling Load due to People

Total cooling load of the education building due to people calculated using the RTS and the CLTD/SCL/CLF methods is presented in Figure 4.14. Total cooling loads due to 250 people calculated using two methods have a similar profile, especially during the occupied time period.

4.2.5. Cooling Load due to Lighting

Total lighting cooling load of the education building calculated using the RTS and the CLTD/SCL/CLF methods is given in Figure 4.15. Total cooling load due to lighting, during the occupied time period, obtained using the RTS method is 20% higher than that is obtained with the CLTD/SCL/CLF method.

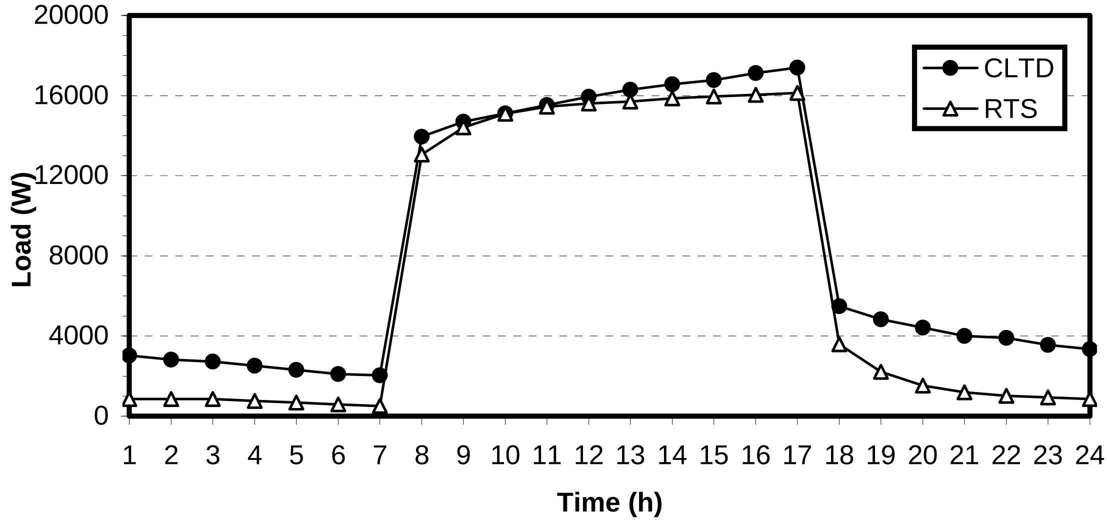

Figure 4.14. Total cooling load due to people in the education building

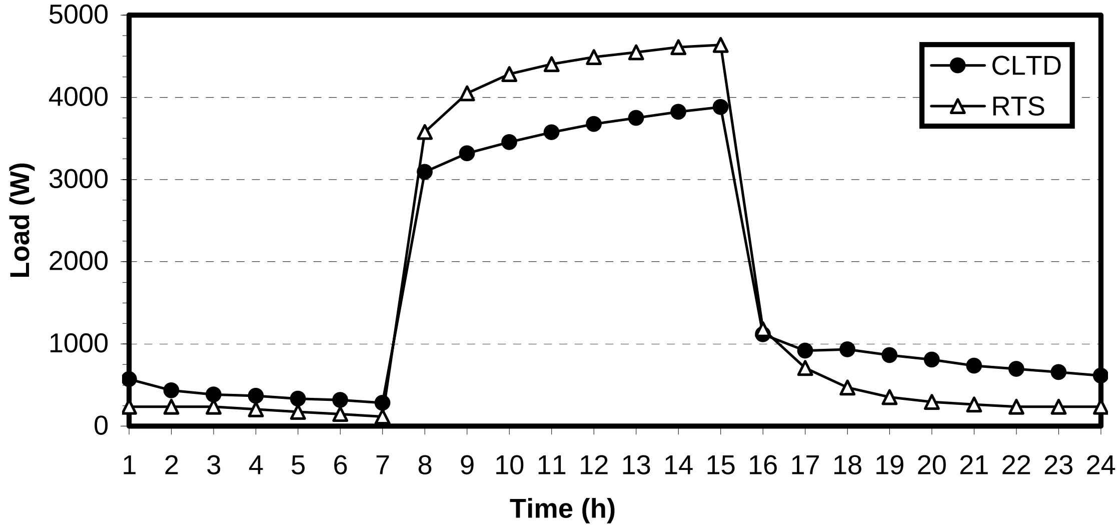

Figure 4.15. Total lighting cooling load of the education building

4.2.6. Total Cooling Load of the Building

Total cooling load of the education building calculated using RTS and CLTD/SCL/CLF methods is given in Figure 4.16. Total cooling loads are maximum at 13^{00} o'clock for both methods. It is also found that the maximum total cooling load calculated using the RTS (129.9 kW) is 12% higher at 13^{00} o'clock than that is obtained using the CLTD/SCL/CLF method (114.8 kW). The difference between total building cooling loads which are computed using two methods is explained by the difference between the cooling loads due to windows and equipments (Figures 4.11 and 4.13). However, there is a general agreement between results of the total cooling load obtained using both the RTS and the CLTD/SCL/CLF methods.

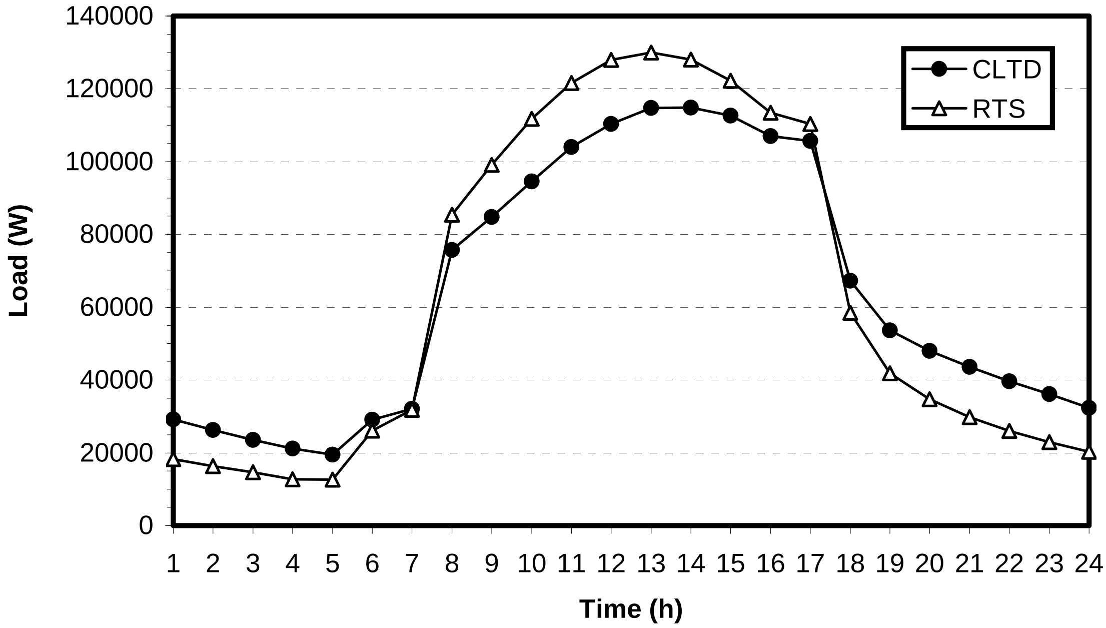

Figure 4.16. Total cooling load of the education building calculated using RTS and CLTD/SCL/CLF methods

Ratios of the miscellaneous cooling loads to the total cooling load which is calculated using two methods are given in Table 4.8. As can be seen from the table, the 44% of the hourly total cooling load calculated at 13^{00}using CLTD/SCL/CLF method originates from the windows, 9% of the total load is due to external surfaces and the remaining portion is from the internal heat resources. In the case of RTS method; 47% of the total cooling load originates from the windows, 7% from the external surfaces and remaining portion is from the internal heat resources.

Table 4.8. Ratio of the miscellaneous cooling loads to the total cooling load in education building

Cooling Load Calculation Method	Cooling Load of the Education Building					
	Windows [%]	External Surfaces [%]	Internal Heat Resources			
			Lighting [%]	People [%]	Equip. [%]	Total [%]
CLTD/CLF/SCL	44	9	3	27	17	47
RTS	47	7	4	23	19	46

The CLTD/SCL/CLF method use the data that are derived from TFM which is originally derived from HB method. Three inherent errors in the TFM are carried through the CLTD/SCL/CLF data. The CLTD/SCL/CLF method requires engineering judgment in its application. Accuracy of CLTD/SCL/CLF method depends on accuracy of CLF, SCL and CLTD. When the method is used in conjunction with customary tables generated by appropriate computer software and for buildings where external shading is not significant, it can be expected to produce results very close to those produced by the TFM. When the printed tables are used, some additional error is introduced. In many cases, the accuracy should be sufficient [ASHRAE, 1997].

The RTS is a proposed replacement method for the current simplified load calculation procedures, e.g. CLTD/SCL/CLF, TETD/TA. The RTS procedure requires more calculations than the CLTD/SCL/CLF procedure. However, it requires less determination of intermediate parameters. The RTS procedure is more accurate than the CLTD/SCL/CLF procedure. The accuracy of the RTS procedure is similar to that of the TFM if customary weighting factors and customary conduction transfer function coefficients were used [Spitler and et al, 1997]. RTS method can be simple and more accurate than current simplified methods.

4.3. Calculation of the Design Cooling Coil Load

Cooling coil capacity significantly depends on design cooling load of the conditioned space. Before the air conditioning system is designed, the design cooling load of the building must be calculated using outdoor design conditions for design day. Outdoor design conditions are weather data for design purposes showing the characteristic features of the climate at a particular location [Bulut et al., 2002]. Design day for cooling systems in Turkey is generally selected as July 21.

In this section of the study, design cooling coil load was calculated using the computer programs developed in this study for outdoor design condition currently used in Turkey and different outdoor design conditions in order to compare equipment capacity of HVAC.

The results obtained using currently used outdoor design data and different outdoor design conditions are evaluated in the following section.

4.3.1. Design Cooling Coil Load for Current Design Conditions

In this section of the study, maximum total cooling load of the sample building in Adana was calculated for July 21. In calculations, outdoor design conditions used in Turkey for Adana are taken as 38 °C dry bulb temperature and 26 °C wet bulb temperature. It is assumed that occupation occurs between 8^{00} and 17^{00} hours.

After building cooling load was calculated ($Q_{tot,room}$), design cooling coil load ($Q_{tot,coil}$) and other psychometric properties were determined under current design conditions. Table 4.9 gives design cooling coil capacity, total mass flow rate (M_{tot}) and some other parameters under current design conditions for different supply air temperatures between 14°C and 20°C.

It is seen from Table 4.9 that design cooling coil load is 186.05 kW for the building design cooling load of 127.55 kW and RSHF of 0.88. Cooling coil capacity

($Q_{tot,coil}$) does not change with supply air temperature between 14 °C to 20 °C. $Q_{tot,coil}$ is the sum of the total cooling load of the building ($Q_{tot,room}$) and load of the fresh air.

Table 4.9. Air conditioning system design capacity and total mass flow rate under current design conditions for different supply air temperatures

Supply Air Temperature [°C]	$Q_{tot.coil}$ [kW]	$Q_{tot.room}$ [kW]	RSHF [%]	M_{tot} [kg/h]	M_{out} [kg/h]	ϕ [%]
14	186.05	127.55	0.88	32943	7739	0.24
15				35935		0.22
16				39525		0.20
17				43913		0.18
18				49398		0.16
19				56451		0.14
20				65854		0.12

Total mass flow rate (M_{tot}) of the air conditioning system varies between 32943 kg/h and 65854 kg/h for different supply air temperatures. The total mass flow rate is greatly affected by the supply air temperature. 1°C increment in the supply air temperature increases mass flow rate considerably (Table 4.9). Consequently, the supply air temperature significantly affects capacities of the return and supply fans in AHU of the air-conditioning system. Therefore, optimum supply air temperature should be found by the designer when air conditioning system is designed. Variations of the total mass flow rate, fresh air rate ($M_{outdoor}$) and design cooling coil load with supply air temperature is shown in Figure 4.17.

Some psychometric properties, such as temperature, enthalpy and absolute humidity of supply air, mixed air and apparatus dew point for different supply air temperatures between 14°C and 20°C are given in Table 4.10.

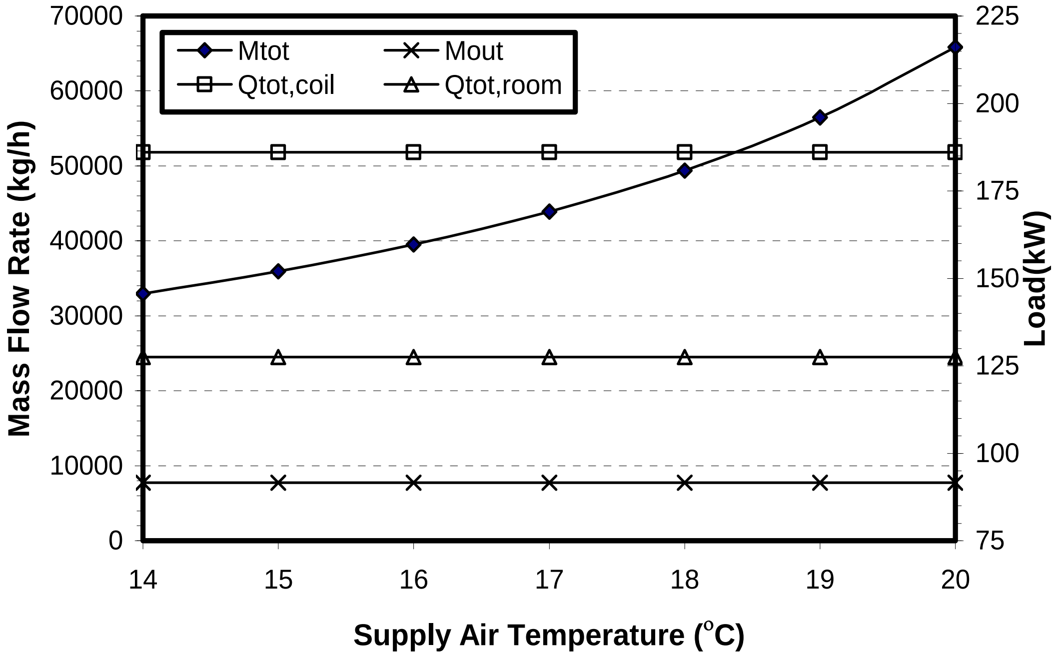

Figure 4.17. Variations of the mass flow rate, design cooling load and design cooling coil capacity with supply air temperature

Table 4 10. Some psychometric properties under current design conditions for supply air temperature between 14°C and 20°C

Supply Air			Mixed Air			Apparatus Dew Point			
T_S [°C]	W_S [kg/kg]	h_S [kJ/kg]	T_M [°C]	W_M [kg/kg]	h_M [kJ/kg]	T_C [°C]	W_C [kg/kg]	h_C [kJ/kg]	Tw [°C]
14.00	0.0098	38.96	28.82	0.0119	59.29	13.76	0.0098	38.63	11.39
15.00	0.0099	40.12	28.58	0.0117	58.76	13.60	0.0097	38.21	10.65
16.00	0.0100	41.28	28.35	0.0116	58.23	13.44	0.0096	37.78	9.91
17.00	0.0100	42.44	28.11	0.0115	57.70	13.27	0.0095	37.35	9.16
18.00	0.0101	43.60	27.88	0.0114	57.16	13.11	0.0094	36.92	8.41
19.00	0.0101	44.77	27.65	0.0113	56.63	12.94	0.0093	36.48	7.66
20.00	0.0102	45.93	27.41	0.0112	56.10	12.77	0.0092	36.04	6.90

It is seen from Table 4.10 that thermodynamic properties of the mixed air and coil state vary with supply air temperature. The increase of the supply air temperature decreases enthalpy and temperature of the mixed air and the apparatus dew point.

Enthalpy difference between the mixed air and the supply air decreases with supply air temperature. Similarly, enthalpy difference between the room air and the supply air also decreases. Ratio of the enthalpy difference between mixed air (h_M) and supply air (h_S) to the enthalpy difference between room air (h_R) and supply air (h_S) is defined as *A*;

$$A=(h_M-h_S)/(h_R-h_S) \tag{4.1}$$

The cooling coil capacity ($Q_{tot,coil}$) can be calculated as a function of the cooling load of the building using the following equation;

$$Q_{tot,coil}=Q_{tot,room}\,[(h_M-h_S)/(h_R-h_S)]= Q_{tot,room}\,A \tag{4.2}$$

As seen from this equation, the cooling coil capacity depends on coefficient *A*. Coefficient (*A*) is function of the amount of fresh air. Figure 4.18 presents the enthalpy distributions of the mixed air, supply air and indoor air and *A* at 14^{00} for different supply air temperatures. As seen the figure that *A* is constant for all the supply air temperatures. It should be noted that, the amount of fresh air was constant for all supply air temperatures.

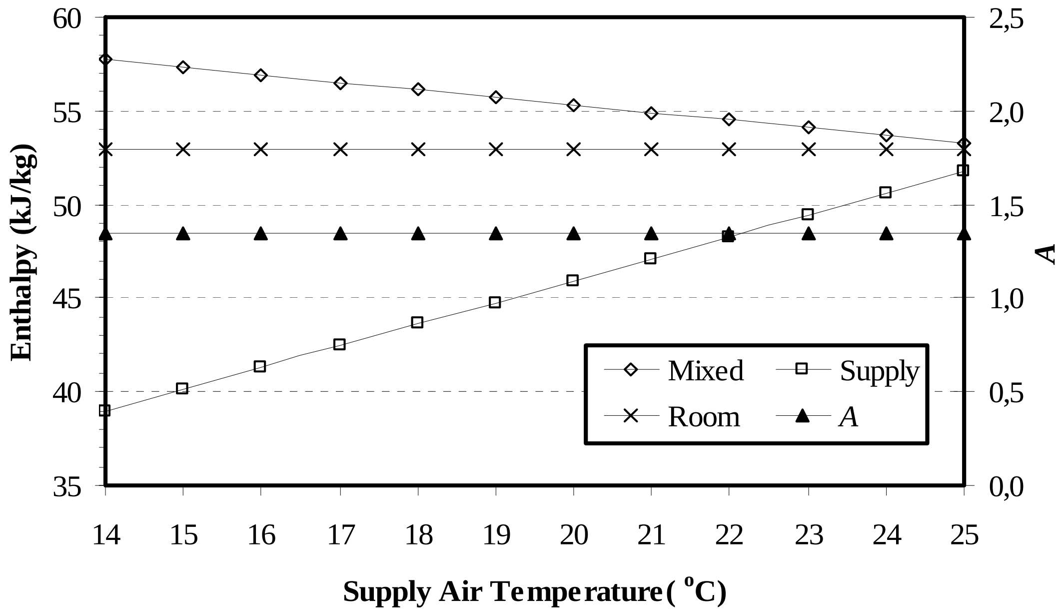

Figure 4.18. Distributions of the enthalpy and *A* at 14^{00} o'clock for different supply air temperature

4.3.2. Design Cooling Coil Load for Different Design Conditions

Design cooling coil load was calculated for different design conditions to compare with the design condition currently used in Turkey. Different design conditions for Adana are taken from ASHRAE and are obtained from local meteorological data. Weather data (outdoor design conditions) for cooling and evaporation systems outlined by ASHRAE for some provinces of Turkey are given in Table 4.11.

Weather data given in Table 4.11 include design values of dry bulb with mean coincident wet bulb temperature, design wet bulb with mean coincident dry-bulb temperature and design dew point bulb with mean coincident dry bulb temperature and corresponding humidity ratio. These data allow the designer to consider various operational peak conditions. The design conditions are provided for locations for which long term hourly observations (at least 12 years of data) are available.

Table 4.11. Cooling design conditions for some provinces of Turkey given by ASHRAE

Province	Cooling DB/MWB						Range of DB
	0.4%		1%		2%		
	DB	MWB	DB	MWB	DB	MWB	
Adana	36.1	21.6	34.6	21.8	33.2	22.3	11.0
Ankara	32.0	17.3	30.2	17.1	28.8	16.4	15.8
Erzurum	28.9	16.3	27.5	15.6	26.1	15.1	16.6
Eskişehir	32.2	19.8	30.8	19.4	29.2	18.9	14.4
İstanbul	30.2	21.0	29.1	20.8	28.1	20.3	8.5
İzmir	35.8	22.1	34.1	21.6	33.0	21.2	12.8
Malatya	36.3	20.0	35.1	19.6	33.9	19.1	15.2
Van	28.8	19.1	27.6	18.7	26.6	18.2	10.8
Province	**Evaporation WB/MDB**						**Range of DB**
	0.4%		**1%**		**2%**		
	WB	**MDB**	**WB**	**MDB**	**WB**	**MDB**	
Adana	26.0	31.7	25.4	30.5	24.9	29.9	11.0
Ankara	18.6	29.0	17.8	28.1	17.0	27.4	15.8
Erzurum	17.8	26.6	16.8	25.7	15.9	24.7	16.6
Eskişehir	21.4	29.2	20.4	28.5	19.7	28.1	14.4
İstanbul	23.2	27.6	22.5	26.7	21.8	25.8	8.5
İzmir	23.3	33.1	22.7	32.1	22.0	31.6	12.8
Malatya	21.1	34.6	20.2	33.7	19.5	33.0	15.2
Van	21.0	27.2	20.0	26.4	19.1	25.7	10.8

For cooling, temperature and humidity conditions correspond to annual percentile values of 0.4, 1.0 and 2.0. The 0.4%, 1.0% and 2.0% annual values of occurrence represent the value that occurs or is exceeded for a total of 35h, 88 h and 175 h, respectively, on average every year over the period of record. The selection of frequency as risk level in design conditions depends on applications. For example, hospitals or sensitive industrial process may prefer more stringent level of 0.4 or 1%.

In addition to these data given in Table 4.11, maximum dry bulb and wet bulb temperatures of ASHRAE design conditions were selected as outdoor design conditions for Adana. Daily maximum dry bulb and wet bulb temperatures which are obtained using Equations 4.49 and 4.42 were also taken as outdoor design conditions for Adana. Table 4.12 presents cooling design conditions data sets for Adana.

After cooling load of the sample building was computed, design cooling coil load and other psychometric properties were obtained using the computer program P_VAV for the outdoor design conditions sets given in 4.12.

Table 4.12. Alternative cooling design conditions for Adana

Outdoor Design Condition Set	**Outdoor Design Conditions**		
	Risk Level [%]	**T_O [°C]**	**WT_O [°C]**
DB-CWB (ASHRAE-Cooling)	0.4	36.1	21.6
	1	34.6	21.8
	2	33.2	22.3
WB-CDB (ASHRAE-Evaporation)	0.4	31.7	26.0
	1	30.5	25.4
	2	29.9	24.9
DBmax-WBmax (ASHRAE)	0.4	36.1	26
	1	34.6	25.4
	2	33.2	24.9
DBmax-WBmax (Equations)	-	35.2	24.1

Psychometric properties, which include temperature, enthalpy and absolute humidity, under current design condition for a supply air temperature of 16°C are given in Table 4.13. As clearly seen from Table 4.13 that mixed air, water and apparatus dew point temperatures for all outdoor design conditions are approximately 27°C, 10°C and 13°C respectively.

Table 4.14 gives design cooling coil capacity, total mass flow rate and some other parameter for different outdoor design conditions for supply air temperature of 16°C.

Table 4.13. Psychometric properties under different outdoor design conditions for supply air temperature 16°C

Design Conditions Set	Risk [%]	T_R [°C]	RH_R [%]	T_C [°C]	W_C [kg/kg]	T_W [°C]	T_M [°C]	W_M [kg/kg]
DB-CWB (ASHRAE-Cooling)	0.4	26	50	13.84	0.0099	10.52	28.05	0.0104
	1			13.78	0.0098	10.42	27.79	0.0106
	2			13.68	0.0098	10.28	27.54	0.0109
WB-CDB (ASHRAE-Evaporation)	0.4			12.78	0.0092	8.92	27.26	0.0124
	1			12.79	0.0092	8.93	27.02	0.0123
	2			12.85	0.0092	9.03	26.90	0.0122
DBmax-WBmax (ASHRAE)	0.4			13.33	0.0095	9.75	28.03	0.0118
	1			13.34	0.0095	9.75	27.78	0.0118
	2			13.32	0.0095	9.73	27.53	0.0118
DBmax-WBmax (Equations)	0			13.55	0.0097	10.07	27.89	0.0113

Table 4.14. Design cooling coil capacity, total mass flow rate for different outdoor design conditions for supply air temperature 16°C

Design Conditions Set	Risk [%]	$Q_{tot.room}$ [kW]	RSHF	$Q_{tot.coil}$ [kW]	M_{tot} [kg/h]	M_{out} [kg/h]	Φ [%]
DB-CWB (ASHRAE-Cooling)	0.4	124.95	0.88	145.9	38720	7863	20.3
	1	121.98	0.88	145.2	37798	7888	20.9
	2	119.20	0.88	146.1	36938	7909	21.4
WB-CDB (ASHRAE-Evaporation)	0.4	116.23	0.87	176.5	35615	7866	22.1
	1	113.85	0.87	168.9	34886	7903	22.7
	2	112.66	0.87	163.1	34521	7926	23.0
DBmax-WBmax (ASHRAE)	0.4	124.95	0.88	183.9	38720	7777	20.1
	1	121.98	0.88	175.7	37798	7820	20.7
	2	119.20	0.88	168.9	36938	7858	21.3
DBmax-WBmax (Equations)	0	122.51	0.88	164.7	37964	7834	20.6

It can be seen from Table 4.14 that the maximum design cooling coil load and mass flow rate among the outdoor design conditions sets given in 4.12 at DBmax-WBmax in 0.4% frequency level are obtained to be 183.9 kW and 38720 kg/h respectively.

4.3.3. Comparison of Design Cooling Coil Capacities

In the above section, design cooling coil load and other parameters were calculated for outdoor design conditions currently used in Turkey (38 °C and 26 °C) and outdoor design conditions given in Table 4.12.

In this section of this study, the results of cooling coil capacity obtained from the current design conditions (Table 4.9) and different design conditions (Table 4.14) are compared. Table 4.15 presents the ratio of design coil capacity ($Q_{tot,coil}$) obtained using different design conditions given in Table 4.12 to the design coil capacity obtained using current outdoor conditions used in Turkey for Adana.

It is seen from Table 4.15, the design cooling coil capacity ($Q_{tot,coil}$) obtained with current design conditions used in Turkey is 186.05 kW and it is approximately 22% higher than that obtained with all risk levels of the DB-CWB given by ASHRAE for cooling. For a set of design conditions, it is seen that the risk level has almost an influence on the $Q_{tot,coil}$. This can be explained with that Adana has the highest absolute humidity in Turkey, especially at nights.

Design cooling coil capacity ($Q_{tot,coil}$) obtained with current design conditions used in Turkey is 4%, 8% and 11% higher than that obtained with the WB-CDB in 0.4%, 1% and 2% risk levels given by ASHRAE for evaporation, respectively.

The design coil capacity ($Q_{tot,coil}$) obtained for daily maximum dry and wet bulb temperatures of July 21 is 11% lower than the one obtained using the current design conditions currently used in Turkey.

The design coil capacity obtained with current design conditions used in Turkey is equal to that obtained with maximum dry bulb and wet bulb temperatures given by ASHRAE for the frequency level of 0.4. It is proved that current design conditions used in Turkey are maximum dry bulb and wet bulb temperatures. Therefore, HVAC equipment designed in Turkey will be oversized and operate at part load conditions most of the time. This will result in higher initial and operating costs of the air conditioning system.

Table 4.15. Total design coil capacity and ratio of the design coil capacity obtained for different design conditions to the one obtained for current design condition

Design Conditions Set	Risk [%]	$Q_{tot.coil}$ [kW]	Ratio
DB-WB (Currently-used)	0	186.05	-
DB-CWB (ASHRAE-Cooling)	0.4	145.90	0.78
	1	145.20	0.78
	2	146.10	0.78
WB-CDB (ASHRAE-Evaporation)	0.4	176.50	0.95
	1	168.90	0.91
	2	163.10	0.88
DBmax-WBmax (ASHRAE)	0.4	183.90	0.99
	1	175.70	0.94
	2	168.90	0.91
DBmax-WBmax (Equations)	0	164.70	0.89

4.4. Operating Capacity of the Cooling Coil

Equipments of the HVAC are designed for peak cooling load. Most of the operating time, they are operated at partial load because of variable outdoor air condition depended on local climate and other parameters that affect the cooling coil load. The hourly operating capacity of the cooling coil in air conditioning system should be analyzed for real outside conditions. To do this, part load performance of the cooling coil should be found.

In this section of the study, cooling coil operating capacity for part load was calculated. Influence of outdoor air conditions on operating capacity of air conditioning systems was investigated. In addition, the hourly operating capacity of the air conditioning system was analyzed for 2 different air distribution systems and the results are given in the following section.

4.4.1. Operating Capacity of the Cooling Coil for Design Day

For this purpose, hourly total cooling load of education building in Adana was calculated for July 21. Indoor design conditions of building are 50% relative humidity and 26 °C dry bulb temperature. Distribution of the hourly outdoor temperatures can be obtained using Equation (3.34). Occupation time is between 8^{00} and 17^{00} hours and the sample building is insulated as B type building according to TS 825.

After the cooling load of the education building was calculated using the RTS method, hourly cooling coil load and other psychometric properties, such as, mixed air temperature, apparatus dew point temperature etc., were determined by the computer programs developed in this study.

4.4.1.1. Calculation of the Cooling Coil Load for VAV Air Distribution System

Hourly cooling coil load and other psychometric properties were determined by computer program P_VAV. The calculation of the cooling coil load was carried out for different supply air temperatures between 15°C to 20°C. Supply air temperature is constant during operating time while total mass flow rate is varied. This type of air conditioning system is called all-air Variable Air Volume (VAV) system.

Figure 4.19 shows cooling process on the psychometric chart at 10^{00} o'clock, 14^{00} o'clock and 17^{00} o'clock for July 21. Hourly outdoor air condition shown on the psychometric chart as (state O) is varied due to local climate. As seen from this figure, positions of the apparatus dew point (state C), supply air (sate S) and mixed air conditions (state M) in cooling process continually change on the psychometric chart with hour. Changing only one of these states affects other conditions because they are dependent on each other. Cooling process is variable in a day and it is a dynamic process.

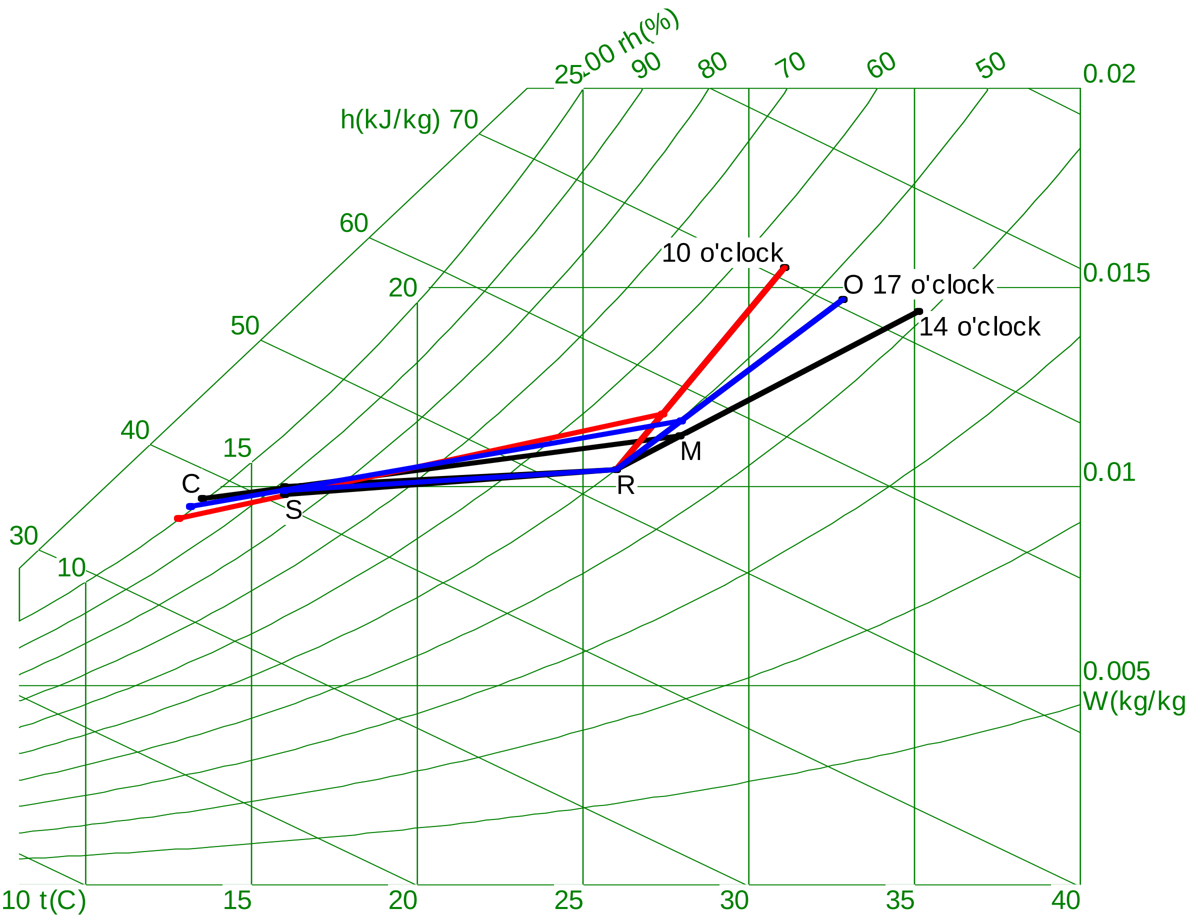

Figure 4.19. The cooling process on the psychometric chart for 10^{00}, 14^{00} and 17^{00} o'clock.

Table 4.16 gives hourly psychometric properties, which include temperature, enthalpy and absolute humidity, for different supply air temperatures between 15°C to 20°C. Table 4.17 presents hourly cooling coil load ($Q_{tot,coil}$), hourly total mass flow rate (M_{tot}) and some other parameters for different supply air temperatures between 15°C to 20°C.

It can be seen from these tables that hourly psychometric properties including temperature, absolute humidity, and enthalpy increase with increasing outdoor air temperature. Similarly, hourly psychometric properties considered also increase with increasing supply air temperature. To see this phenomena situation clearly, hourly distribution of the temperature and enthalpy at different state for a supply air temperature of 15 °C is presented in Figures 4.20 and 4.21, respectively.

Psychometric properties (temperature, absolute humidity, and enthalpy) are strongly affected by both the supply air temperature and the variable outdoor air conditions depended on local climate.

Table 4.16 Some psychometric properties of the air conditioning system under hourly outdoor condition of July 21 for supply air temperature of 15°C and 16 °C

Time	**Supply Air**			**Outdoor Air**			**Mixed Air**			**Apparatus Dew Point**			
	T_S [°C]	**W_S [kg/kg]**	**h_S [kJ/kg]**	**T_O [°C]**	**W_O [kg/kg]**	**h_O [kJ/kg]**	**T_M [°C]**	**W_M [kg/kg]**	**h_M [kJ/kg]**	**T_C [°C]**	**W_C [kg/kg]**	**h_C [kJ/kg]**	**Tw [°C]**
8^{00}	15	0.0094	38.87	27.66	0.0164	69.59	26.71	0.0130	60.07	11.03	0.0082	31.71	6.79
9^{00}		0.0096	39.37	29.41	0.0160	70.46	27.19	0.0124	59.02	12.50	0.0090	35.35	8.99
10^{00}		0.0097	39.68	31.10	0.0155	71.00	27.51	0.0120	58.26	13.07	0.0094	36.83	9.86
11^{00}		0.0098	39.83	32.60	0.0151	71.48	27.73	0.0117	57.78	13.32	0.0095	37.47	10.23
12^{00}		0.0098	39.98	33.82	0.0148	71.87	27.88	0.0115	57.47	13.50	0.0096	37.95	10.50
13^{00}		0.0099	40.12	34.69	0.0145	72.14	27.99	0.0114	57.30	13.65	0.0097	38.34	10.73
14^{00}		0.0099	40.12	35.16	0.0144	72.29	28.08	0.0114	57.30	13.66	0.0097	38.37	10.74
15^{00}		0.0099	40.12	34.94	0.0144	72.04	28.08	0.0114	57.35	13.66	0.0097	38.36	10.73
16^{00}		0.0098	39.98	33.98	0.0145	71.34	28.00	0.0115	57.53	13.51	0.0097	37.98	10.52
17^{00}		0.0098	39.83	32.88	0.0147	70.78	27.82	0.0116	57.62	13.35	0.0096	37.54	10.27
8^{00}	16	0.0095	40.14	27.66	0.0164	69.59	26.65	0.0128	59.42	10.10	0.0077	29.52	4.90
9^{00}		0.0097	40.60	29.41	0.0160	70.46	27.08	0.0122	58.47	12.08	0.0088	34.31	7.88
10^{00}		0.0098	40.88	31.10	0.0155	71.00	27.37	0.0119	57.77	12.82	0.0092	36.17	8.98
11^{00}		0.0099	41.02	32.60	0.0151	71.48	27.57	0.0116	57.33	13.14	0.0094	37.00	9.46
12^{00}		0.0099	41.15	33.82	0.0148	71.87	27.71	0.0114	57.05	13.36	0.0096	37.58	9.79
13^{00}		0.0100	41.28	34.69	0.0145	72.14	27.81	0.0113	56.90	13.53	0.0097	38.03	10.05
14^{00}		0.0100	41.28	35.16	0.0144	72.29	27.89	0.0113	56.90	13.55	0.0097	38.07	10.07
15^{00}		0.0100	41.28	34.94	0.0144	72.04	27.89	0.0113	56.94	13.54	0.0097	38.05	10.06
16^{00}		0.0099	41.15	33.98	0.0145	71.34	27.82	0.0114	57.11	13.38	0.0096	37.62	9.82
17^{00}		0.0095	40.14	27.66	0.0164	69.59	26.65	0.0128	59.42	10.10	0.0077	29.52	4.90

Table 4.16 (Continued) Some psychometric properties of the air conditioning system under hourly outdoor condition of July 21 for supply air temperature of 17°C and 18°C

Time	Supply Air			Outdoor Air			Mixed Air			Apparatus Dew Point			
	T_S [°C]	W_S [kg/kg]	h_S [kJ/kg]	T_O [°C]	W_O [kg/kg]	h_O [kJ/kg]	T_M [°C]	W_M [kg/kg]	h_M [kJ/kg]	T_C [°C]	W_C [kg/kg]	h_C [kJ/kg]	Tw [°C]
8^{00}	17	0.0096	41.42	27.66	0.0164	69.59	26.58	0.0126	58.77	9.03	0.0071	27.06	2.79
9^{00}		0.0098	41.83	29.41	0.0160	70.46	26.97	0.0121	57.91	11.65	0.0085	33.24	6.73
10^{00}		0.0099	42.08	31.10	0.0155	71.00	27.23	0.0117	57.28	12.56	0.0091	35.51	8.09
11^{00}		0.0099	42.20	32.60	0.0151	71.48	27.42	0.0115	56.89	12.95	0.0093	36.52	8.68
12^{00}		0.0100	42.33	33.82	0.0148	71.87	27.54	0.0113	56.64	13.22	0.0095	37.21	9.08
13^{00}		0.0100	42.44	34.69	0.0145	72.14	27.62	0.0113	56.50	13.41	0.0096	37.71	9.37
14^{00}		0.0100	42.44	35.16	0.0144	72.29	27.70	0.0112	56.50	13.44	0.0096	37.77	9.40
15^{00}		0.0100	42.44	34.94	0.0144	72.04	27.70	0.0112	56.54	13.43	0.0096	37.75	9.39
16^{00}		0.0100	42.33	33.98	0.0145	71.34	27.64	0.0113	56.69	13.24	0.0095	37.27	9.11
17^{00}		0.0099	42.20	32.88	0.0147	70.78	27.49	0.0114	56.76	13.03	0.0093	36.71	8.79
8^{00}	18	0.0097	42.69	27.66	0.0164	69.59	26.52	0.0123	58.12	7.71	0.0065	24.17	0.32
9^{00}		0.0098	43.05	29.41	0.0160	70.46	26.87	0.0119	57.36	11.21	0.0083	32.14	5.56
10^{00}		0.0099	43.28	31.10	0.0155	71.00	27.10	0.0116	56.80	12.30	0.0089	34.84	7.19
11^{00}		0.0100	43.39	32.60	0.0151	71.48	27.26	0.0114	56.45	12.77	0.0092	36.04	7.90
12^{00}		0.0100	43.50	33.82	0.0148	71.87	27.37	0.0112	56.22	13.07	0.0094	36.83	8.36
13^{00}		0.0101	43.60	34.69	0.0145	72.14	27.44	0.0112	56.10	13.29	0.0095	37.39	8.68
14^{00}		0.0101	43.60	35.16	0.0144	72.29	27.51	0.0111	56.10	13.32	0.0095	37.48	8.73
15^{00}		0.0101	43.60	34.94	0.0144	72.04	27.51	0.0112	56.13	13.31	0.0095	37.44	8.71
16^{00}		0.0100	43.50	33.98	0.0145	71.34	27.46	0.0112	56.27	13.11	0.0094	36.91	8.41
17^{00}		0.0100	43.39	32.88	0.0147	70.78	27.32	0.0113	56.33	12.86	0.0092	36.28	8.04

Table 4.16 (Continued) Some psychometric properties of the air conditioning system under hourly outdoor condition of July 21 for supply air temperature of 19°C and 20°C

Time	Supply Air			Outdoor Air			Mixed Air			Apparatus Dew Point			
	T_S [°C]	W_S [kg/kg]	h_S [kJ/kg]	T_O [°C]	W_O [kg/kg]	h_O [kJ/kg]	T_M [°C]	W_M [kg/kg]	h_M [kJ/kg]	T_C [°C]	W_C [kg/kg]	h_C [kJ/kg]	Tw [°C]
8^{00}	19	0.0098	43.97	27.66	0.0164	69.59	26.45	0.0121	57.47	5.92	0.0058	20.43	2.87
9^{00}		0.0099	44.28	29.41	0.0160	70.46	26.76	0.0117	56.80	10.73	0.0080	31.01	4.35
10^{00}		0.0100	44.48	31.10	0.0155	71.00	26.96	0.0114	56.31	12.03	0.0087	34.16	6.29
11^{00}		0.0100	44.58	32.60	0.0151	71.48	27.10	0.0113	56.01	12.58	0.0091	35.56	7.12
12^{00}		0.0101	44.67	33.82	0.0148	71.87	27.20	0.0112	55.81	12.93	0.0093	36.46	7.64
13^{00}		0.0101	44.77	34.69	0.0145	72.14	27.26	0.0111	55.70	13.17	0.0094	37.07	8.00
14^{00}		0.0101	44.77	35.16	0.0144	72.29	27.32	0.0111	55.70	13.21	0.0095	37.18	8.06
15^{00}		0.0101	44.77	34.94	0.0144	72.04	27.32	0.0111	55.73	13.19	0.0095	37.14	8.04
16^{00}		0.0101	44.67	33.98	0.0145	71.34	27.28	0.0111	55.85	12.97	0.0093	36.56	7.70
17^{00}		0.0100	44.58	32.88	0.0147	70.78	27.16	0.0112	55.91	12.70	0.0091	35.86	7.29
8^{00}	20	-	-	-	-	-	-	-	-	-	-	-	-
9^{00}		0.0100	45.51	29.41	0.0160	70.46	26.65	0.0115	56.24	10.24	0.0078	29.84	3.11
10^{00}		0.0101	45.69	31.10	0.0155	71.00	26.82	0.0113	55.82	11.75	0.0086	33.47	5.37
11^{00}		0.0101	45.77	32.60	0.0151	71.48	26.95	0.0112	55.56	12.39	0.0090	35.07	6.33
12^{00}		0.0101	45.85	33.82	0.0148	71.87	27.03	0.0111	55.39	12.78	0.0092	36.08	6.92
13^{00}		0.0102	45.93	34.69	0.0145	72.14	27.08	0.0110	55.30	13.04	0.0094	36.75	7.31
14^{00}		0.0102	45.93	35.16	0.0144	72.29	27.13	0.0110	55.30	13.09	0.0094	36.88	7.39
15^{00}		0.0102	45.93	34.94	0.0144	72.04	27.13	0.0110	55.33	13.07	0.0094	36.83	7.36
16^{00}		0.0101	45.85	33.98	0.0145	71.34	27.09	0.0110	55.42	12.83	0.0092	36.20	6.99
17^{00}		0.0101	45.77	32.88	0.0147	70.78	26.99	0.0111	55.48	12.53	0.0090	35.43	6.54

Table 4.17. Some properties of the air conditioning system under hourly outdoor condition of July 21 for supply air temperatures between 15°C and 20°C

Time	Supply Air Temperature				15°C		16°C		17°C	
	$Q_{tot.coil}$ [kW]	$Q_{tot.room}$ [kW]	RSHF [%]	M_{out} [kg/h]	M_{tot} [kg/h]	ϕ [%]	M_{tot} [kg/h]	ϕ [%]	M_{tot} [kg/h]	ϕ [%]
8^{00}	109.70	72.60	0.80	8005	18626	0.43	20486	0.39	22759	0.35
9^{00}	124.67	85.83	0.83	7963	22833	0.35	25114	0.32	27901	0.29
10^{00}	138.19	98.34	0.85	7925	26780	0.30	29454	0.27	32724	0.24
11^{00}	149.86	109.13	0.86	7891	30060	0.26	33063	0.24	36733	0.21
12^{00}	158.62	117.18	0.87	7864	32646	0.24	35907	0.22	39893	0.20
13^{00}	163.77	121.84	0.88	7844	34325	0.23	37755	0.21	41946	0.19
14^{00}	164.71	122.51	0.88	7834	34515	0.23	37964	0.21	42178	0.19
15^{00}	161.51	119.82	0.88	7840	33757	0.23	37130	0.21	41252	0.19
16^{00}	152.73	112.46	0.87	7863	31331	0.25	34461	0.23	38286	0.21
17^{00}	147.64	108.46	0.86	7888	29876	0.26	32861	0.24	36508	0.22
Time	**Supply Air Temperature**				**18°C**		**19°C**		**20°C**	
8^{00}	109.70	72.60	0.80	8005	25600	0.31	29253	0.27	-	-
9^{00}	124.67	85.83	0.83	7963	31385	0.25	35864	0.22	41836	0.19
10^{00}	138.19	98.34	0.85	7925	36810	0.22	42064	0.19	49070	0.16
11^{00}	149.86	109.13	0.86	7891	41321	0.19	47219	0.17	55083	0.14
12^{00}	158.62	117.18	0.87	7864	44876	0.18	51282	0.15	59823	0.13
13^{00}	163.77	121.84	0.88	7844	47185	0.17	53921	0.15	62903	0.12
14^{00}	164.71	122.51	0.88	7834	47447	0.17	54220	0.14	63251	0.12
15^{00}	161.51	119.82	0.88	7840	46405	0.17	53030	0.15	61863	0.13
16^{00}	152.73	112.46	0.87	7863	43068	0.18	49217	0.16	57414	0.14
17^{00}	147.64	108.46	0.86	7888	41068	0.19	46930	0.17	54746	0.14

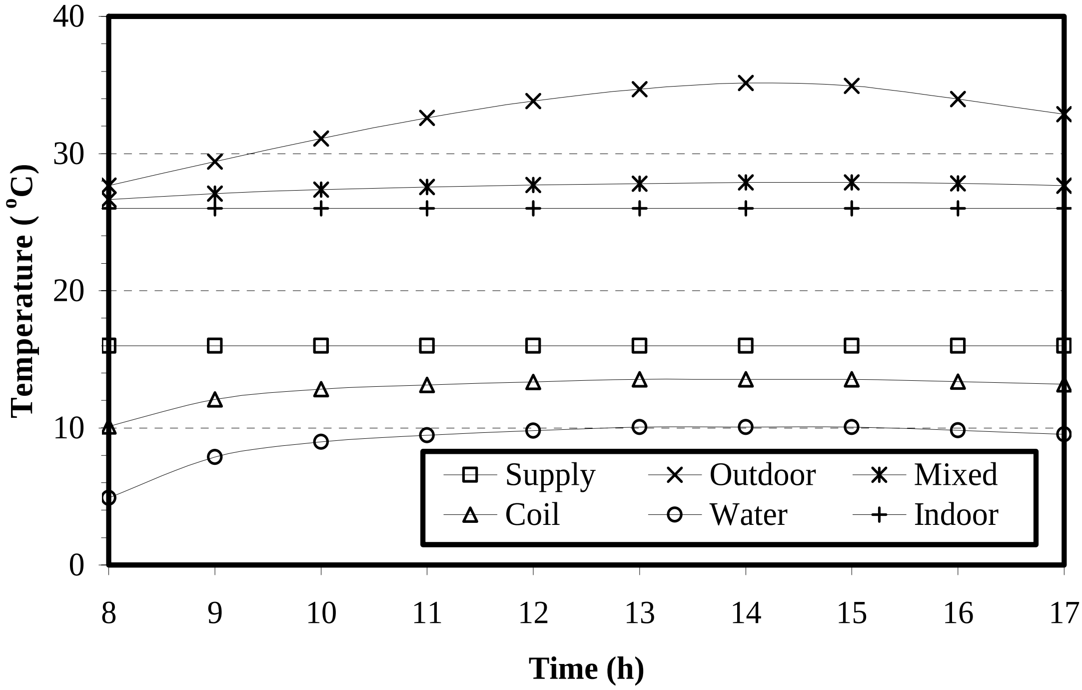

Figure 4.20. Distribution of the temperature at different states of the ACS for supply air temperature of 15 °C

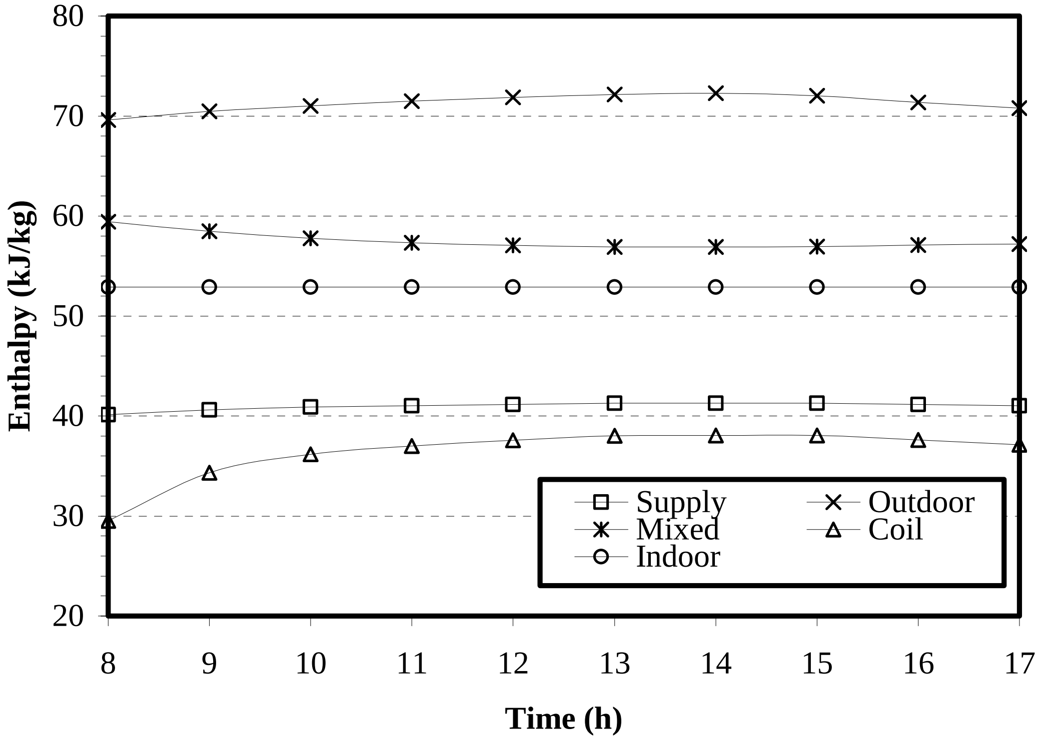

Figure 4.21. Distribution of the enthalpy at different states of ACS for supply air temperature of 15 °C

Variation of the hourly total mass flow rate requirement for different supply air temperatures between 15°C and 20°C (Table 4.16) is shown in Figure 4.22. Hourly cooling coil load demand and total cooling load of the building (Table 4.17) are also shown in Figure 4.22. As seen from the figure, the cooling load demand and the mass flow rate requirement increase from 8^{00} to 14^{00} o'clock. At 14^{00} o'clock they reach to the peak and then they decrease for all the supply air temperatures considered. The increase of the outdoor air temperature increases both the cooling load demand and the mass flow rate requirement. Similarly, the increase of the supply air temperature also increases the mass flow rate requirement although the cooling coil capacity is not changed. Hourly profiles of the mass flow rate obtained for different supply air temperatures exhibit similar trends.

It is clearly seen from Figure 4.22 that, the return and the supply fans which provide air for the air conditioning system and the chiller unit usually operate at part load under real operating conditions because of varying building cooling load.

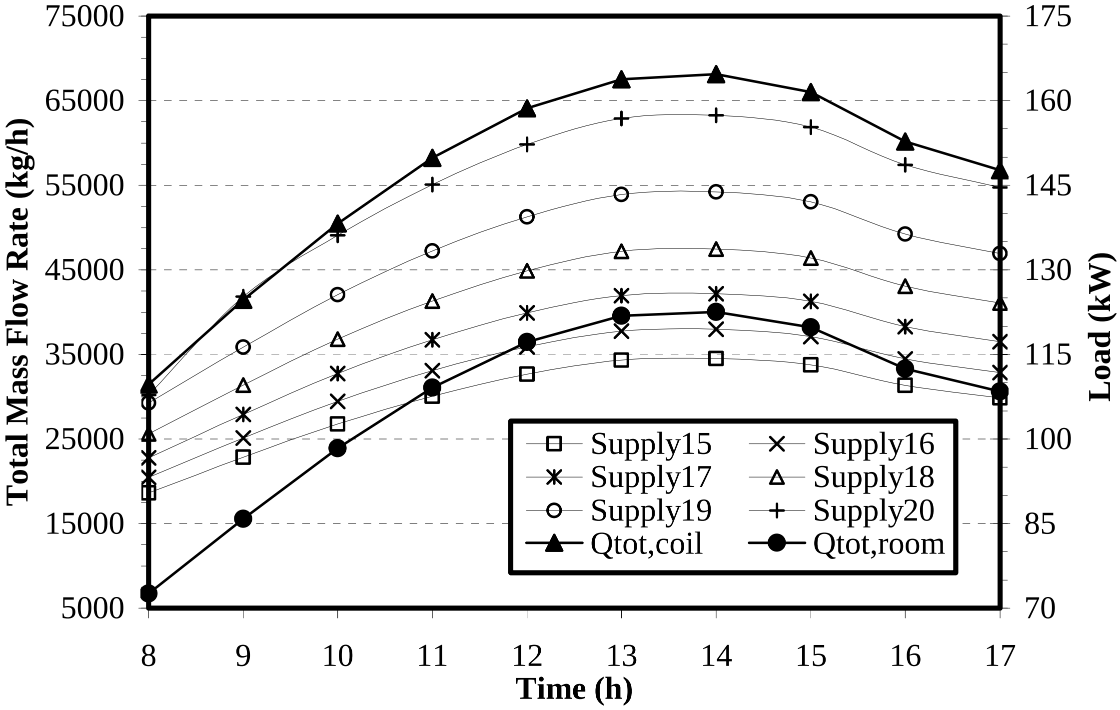

Figure 4.22. Variations of the mass flow rate, cooling load and cooling coil capacity for supply air temperature from 15°C to 20°C

4.4.1.2. Calculation of the Cooling Coil Load for CAV Air Distribution System

Hourly cooling coil load and other psychometric properties were determined using the computer program P_CAV. The cooling coil load was calculated for 6 different total mass flow rates; 34515 kg/h, 37964 kg/h, 42178 kg/h, 47447 kg/h, 54220 kg/h and 63251 kg/h. Total mass flow rate is constant during operating time while the supply air temperature is varied. This air conditioning system is called all-air Constant Air Volume (CAV) system.

Figure 4.23 represents cooling process on the psychometric chart for 10^{00}, 14^{00} and 17^{00} o'clock for July 21.

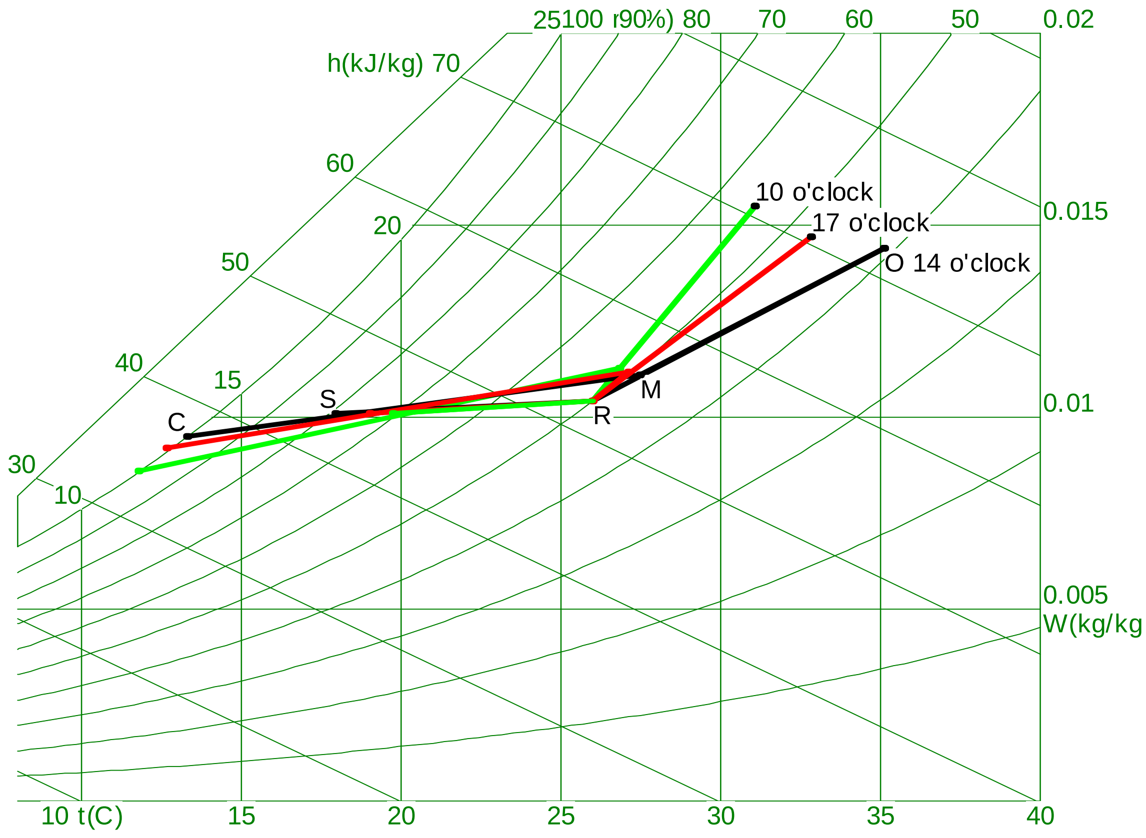

Figure 4.23. Cooling process on the psychometric chart for 10^{00}, 14^{00} and 17^{00} o'clock

As seen from the figure, positions of the apparatus dew point (state C), supply air (state S) and mixed air conditions (state M) in cooling process change on the psychometric chart with time because of varying outdoor conditions. The varying outdoor condition affects other conditions because they are related to each other. The cooling process is a dynamic process again.

Table 4.18 gives psychometric properties (temperature, enthalpy and absolute humidity) for the different total mass flow rates considered. Table 4.19 gives cooling coil capacity, total mass flow rate and some other parameters.

Table 4.18. Some psychometric properties obtained for different total mass flow rates

Time	Suply Air			Outdoor Air			Mixed Air			Apparatus Dew Point			
	T_S [°C]	W_S [kg/kg]	h_S [kJ/kg]	T_O [°C]	W_O [kg/kg]	h_O [kJ/kg]	T_M [°C]	W_M [kg/kg]	h_M [kJ/kg]	T_C [°C]	W_C [kg/kg]	h_C [kJ/kg]	T_W [°C]
	Mass Flow Rate 34515 kg/h												
8^{00}	20.05	0.0099	45.33	27.66	0.0164	69.59	26.38	0.0119	56.77	0.32	0.0039	9.99	2.22
9^{00}	18.71	0.0099	43.95	29.41	0.0160	70.46	26.79	0.0118	56.95	10.94	0.0081	31.50	4.80
10^{00}	17.45	0.0099	42.64	31.10	0.0155	71.00	27.17	0.0117	57.06	12.47	0.0090	35.29	7.73
11^{00}	16.41	0.0099	41.52	32.60	0.0151	71.48	27.51	0.0116	57.15	13.08	0.0094	36.85	9.17
12^{00}	15.59	0.0099	40.68	33.82	0.0148	71.87	27.78	0.0115	57.22	13.43	0.0096	37.77	10.11
13^{00}	15.05	0.0099	40.19	34.69	0.0145	72.14	27.97	0.0114	57.27	13.66	0.0097	38.36	10.71
14^{00}	14.99	0.0099	40.12	35.16	0.0144	72.29	28.08	0.0114	57.30	13.67	0.0098	38.40	10.76
15^{00}	15.23	0.0099	40.40	34.94	0.0144	72.04	28.03	0.0114	57.25	13.64	0.0097	38.31	10.59
16^{00}	16.01	0.0099	41.17	33.98	0.0145	71.34	27.82	0.0114	57.10	13.39	0.0096	37.66	9.83
17^{00}	16.47	0.0099	41.59	32.88	0.0147	70.78	27.57	0.0115	56.99	13.13	0.0094	36.97	9.21
	Mass Flow Rate 37964 kg/h												
9^{00}	19.37	0.0100	44.76	29.41	0.0160	70.46	26.72	0.0117	56.58	10.62	0.0080	30.74	4.00
10^{00}	18.23	0.0100	43.57	31.10	0.0155	71.00	27.06	0.0115	56.68	12.27	0.0089	34.77	7.04
11^{00}	17.28	0.0099	42.55	32.60	0.0151	71.48	27.37	0.0115	56.76	12.92	0.0093	36.44	8.49
12^{00}	16.53	0.0099	41.79	33.82	0.0148	71.87	27.62	0.0114	56.83	13.30	0.0095	37.42	9.43
13^{00}	16.05	0.0100	41.35	34.69	0.0145	72.14	27.8	0.0113	56.88	13.54	0.0097	38.04	10.03
14^{00}	15.99	0.0100	41.28	35.16	0.0144	72.29	27.89	0.0113	56.90	13.56	0.0097	38.10	10.09
15^{00}	16.21	0.0100	41.54	34.94	0.0144	72.04	27.85	0.0113	56.85	13.53	0.0097	38.02	9.94
16^{00}	16.91	0.0100	42.24	33.98	0.0145	71.34	27.65	0.0113	56.72	13.27	0.0095	37.34	9.19
17^{00}	17.34	0.0099	42.61	32.88	0.0147	70.78	27.43	0.0114	56.61	12.99	0.0093	36.61	8.57

Table 4.18. (Continued) Some psychometric properties obtained for different total mass flow rates

Time	Suply Air			Outdoor Air			Mixed Air			Apparatus Dew Point			
	T_S [°C]	W_S [kg/kg]	h_S [kJ/kg]	T_O [°C]	W_O [kg/kg]	h_O [kJ/kg]	T_M [°C]	W_M [kg/kg]	h_M [kJ/kg]	T_C [°C]	W_C [kg/kg]	h_C [kJ/kg]	T_W [°C]
	Mass Flow Rate 42178 kg/h												
9^{00}	20.04	0.0100	45.57	29.41	0.0160	70.46	26.64	0.0115	56.22	10.29	0.0078	29.97	3.17
10^{00}	19.01	0.0100	44.51	31.10	0.0155	71.00	26.96	0.0114	56.30	12.06	0.0088	34.24	6.33
11^{00}	18.15	0.0100	43.59	32.60	0.0151	71.48	27.23	0.0114	56.38	12.76	0.0092	36.02	7.81
12^{00}	17.48	0.0100	42.90	33.82	0.0148	71.87	27.46	0.0113	56.44	13.16	0.0094	37.07	8.76
13^{00}	17.04	0.0100	42.50	34.69	0.0145	72.14	27.62	0.0112	56.48	13.42	0.0096	37.73	9.36
14^{00}	16.99	0.0100	42.44	35.16	0.0144	72.29	27.7	0.0112	56.50	13.45	0.0096	37.80	9.42
15^{00}	17.19	0.0100	42.67	34.94	0.0144	72.04	27.66	0.0112	56.46	13.41	0.0096	37.72	9.28
16^{00}	17.82	0.0100	43.30	33.98	0.0145	71.34	27.49	0.0112	56.34	13.14	0.0094	37.01	8.56
17^{00}	18.20	0.0100	43.64	32.88	0.0147	70.78	27.29	0.0113	56.24	12.85	0.0092	36.24	7.92
	Mass Flow Rate 47447 kg/h												
9^{00}	20.70	0.0101	46.39	29.41	0.0160	70.46	26.57	0.0114	55.85	9.96	0.0076	29.18	2.34
10^{00}	19.78	0.0101	45.44	31.10	0.0155	71.00	26.85	0.0113	55.92	11.84	0.0086	33.71	5.62
11^{00}	19.02	0.0101	44.62	32.60	0.0151	71.48	27.10	0.0113	55.99	12.60	0.0091	35.60	7.13
12^{00}	18.43	0.0101	44.01	33.82	0.0148	71.87	27.30	0.0112	56.04	13.03	0.0094	36.71	8.08
13^{00}	18.04	0.0101	43.66	34.69	0.0145	72.14	27.44	0.0112	56.08	13.30	0.0095	37.41	8.68
14^{00}	17.99	0.0101	43.60	35.16	0.0144	72.29	27.51	0.0111	56.10	13.33	0.0095	37.51	8.75
15^{00}	18.17	0.0101	43.81	34.94	0.0144	72.04	27.48	0.0111	56.06	13.30	0.0095	37.42	8.62
16^{00}	18.73	0.0101	44.37	33.98	0.0145	71.34	27.32	0.0112	55.96	13.02	0.0093	36.69	7.91
17^{00}	19.07	0.0101	44.67	32.88	0.0147	70.78	27.14	0.0112	55.87	12.7	0.0092	35.87	7.27

Table 4.18. (Continued) Some psychometric properties obtained for different total mass flow rates

Time	Supply Air			Outdoor Air			Mixed Air			Apparatus Dew Point			
	T_S [°C]	W_S [kg/kg]	h_S [kJ/kg]	T_O [°C]	W_O [kg/kg]	h_O [kJ/kg]	T_M [°C]	W_M [kg/kg]	h_M [kJ/kg]	T_C [°C]	W_C [kg/kg]	h_C [kJ/kg]	T_W [°C]
	Mass Flow Rate 54220 kg/h												
9^{00}	21.36	0.0101	47.20	29.41	0.0160	70.46	26.50	0.0113	55.48	9.60	0.0074	28.37	1.48
10^{00}	20.56	0.0101	46.37	31.10	0.0155	71.00	26.75	0.0112	55.55	11.63	0.0085	33.17	4.91
11^{00}	19.90	0.0101	45.65	32.60	0.0151	71.48	26.96	0.0112	55.60	12.43	0.0090	35.17	6.44
12^{00}	19.37	0.0101	45.12	33.82	0.0148	71.87	27.13	0.0111	55.65	12.89	0.0093	36.35	7.40
13^{00}	19.03	0.0101	44.81	34.69	0.0145	72.14	27.26	0.0111	55.68	13.17	0.0094	37.09	8.00
14^{00}	18.99	0.0101	44.77	35.16	0.0144	72.29	27.32	0.0111	55.70	13.22	0.0095	37.21	8.08
15^{00}	19.15	0.0101	44.94	34.94	0.0144	72.04	27.29	0.0111	55.67	13.19	0.0094	37.12	7.95
16^{00}	19.64	0.0101	45.43	33.98	0.0145	71.34	27.16	0.0111	55.57	12.89	0.0093	36.36	7.27
17^{00}	19.93	0.0101	45.70	32.88	0.0147	70.78	27.00	0.0111	55.50	12.56	0.0091	35.50	6.62
	Mass Flow Rate 63251 kg/h												
9^{00}	22.02	0.0102	48.01	29.41	0.0160	70.46	26.43	0.0112	55.11	9.24	0.0072	27.53	0.59
10^{00}	21.34	0.0102	47.3	31.10	0.0155	71.00	26.64	0.0111	55.17	11.40	0.0084	32.63	4.19
11^{00}	20.77	0.0102	46.69	32.60	0.0151	71.48	26.82	0.0111	55.22	12.26	0.0089	34.75	5.75
12^{00}	20.32	0.0102	46.23	33.82	0.0148	71.87	26.97	0.0110	55.26	12.75	0.0092	35.99	6.71
13^{00}	20.03	0.0102	45.97	34.69	0.0145	72.14	27.08	0.0110	55.29	13.05	0.0094	36.77	7.31
14^{00}	20.00	0.0102	45.93	35.16	0.0144	72.29	27.13	0.0110	55.30	13.10	0.0094	36.91	7.41
15^{00}	20.13	0.0102	46.08	34.94	0.0144	72.04	27.11	0.0110	55.27	13.07	0.0094	36.82	7.29
16^{00}	20.55	0.0102	46.5	33.98	0.0145	71.34	26.99	0.0110	55.19	12.77	0.0092	36.04	6.63
17^{00}	20.80	0.0102	46.73	32.88	0.0147	70.78	26.86	0.0110	55.13	12.41	0.0090	35.13	5.96

Table 4.19. Some psychometric properties obtained for different total mass flow rates

Time	$Q_{tot.coil}$ [kW]	$Q_{tot.room}$ [kW]	RSHF [%]	M_{out} [kg/h]	ϕ [%]						
					34515 [kg/h]	37964 [kg/h]	42178 [kg/h]	47447 [kg/h]	54220 [kg/h]	63251 [kg/h]	34515 [kg/h]
8^{00}	109.70	72.60	0.80	8005	0.232	-	-	-	-	-	0.232
9^{00}	124.67	85.83	0.83	7963	0.231	0.210	0.189	0.168	0.147	0.126	0.231
10^{00}	138.19	98.34	0.85	7925	0.230	0.209	0.188	0.167	0.146	0.125	0.230
11^{00}	149.86	109.13	0.86	7891	0.229	0.208	0.187	0.166	0.146	0.125	0.229
12^{00}	158.62	117.18	0.87	7864	0.228	0.207	0.186	0.166	0.145	0.124	0.228
13^{00}	163.77	121.84	0.88	7844	0.227	0.207	0.186	0.165	0.145	0.124	0.227
14^{00}	164.71	122.51	0.88	7834	0.227	0.206	0.186	0.165	0.144	0.124	0.227
15^{00}	161.51	119.82	0.88	7840	0.227	0.207	0.186	0.165	0.145	0.124	0.227
16^{00}	152.73	112.46	0.87	7863	0.228	0.207	0.186	0.166	0.145	0.124	0.228
17^{00}	147.64	108.46	0.86	7888	0.229	0.208	0.187	0.166	0.145	0.125	0.229

Variations of hourly supply air temperature and hourly cooling load and cooling coil capacity for different total mass flow rates, which are given in Tables 4.18 and 4.19, are graphically shown in Figure 4.24.

The supply air temperature decreases from 8^{00} to 14^{00} o'clock because of increasing cooling load for all mass flow rates considered. It increases in remaining period parallel to the decrease in the cooling load. The increase of the total mass flow rate increases the supply air temperature.

For example, the supply air temperature is 15.59 °C for mass flow rate of 34515 kg/h, whilst it is 17.48 °C for 42178 kg/h mass flow rate at 12^{00} o'clock (Table 4.18). The cooling coil capacity does not change with mass flow rate.

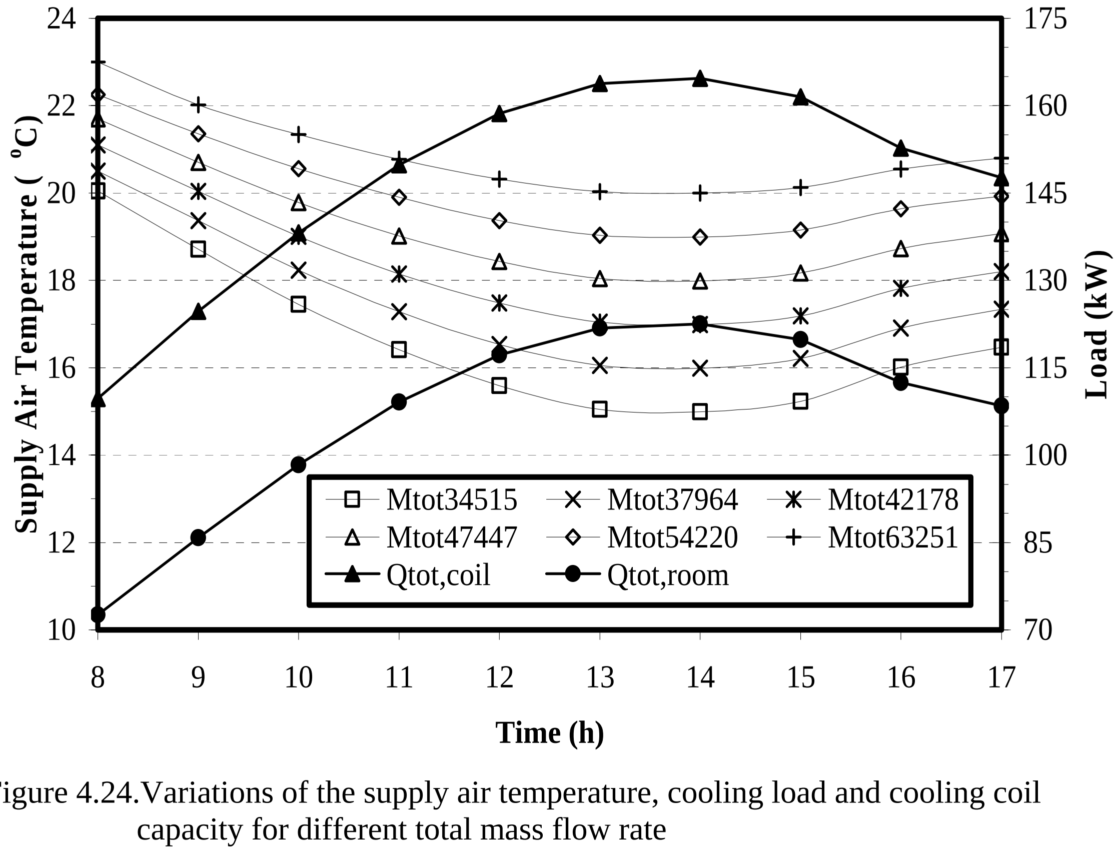

Figure 4.24.Variations of the supply air temperature, cooling load and cooling coil capacity for different total mass flow rate

Distribution of the temperature and enthalpy at different states of the ACS graphically shown in Figures 4.25 and 4.26 respectively for a total mass flow rate of 34515 kg/h (Tables 4.18 and 4.19). Both temperature and enthalpy of the supply air decrease for a fixed mass flow rate, because of increasing hourly outdoor air temperature between 8^{00} and 14^{00} o'clock. They increase from14^{00} to 17^{00} o'clock due to reducing hourly outdoor air temperature. Distribution of the apparatus dew point (T_C) and water (T_W) temperatures obtained for a total mass flow rate of 34515 kg/h have similar trends. Apparatus dew point and water temperatures are approximately 13 °C and 11 °C, respectively.

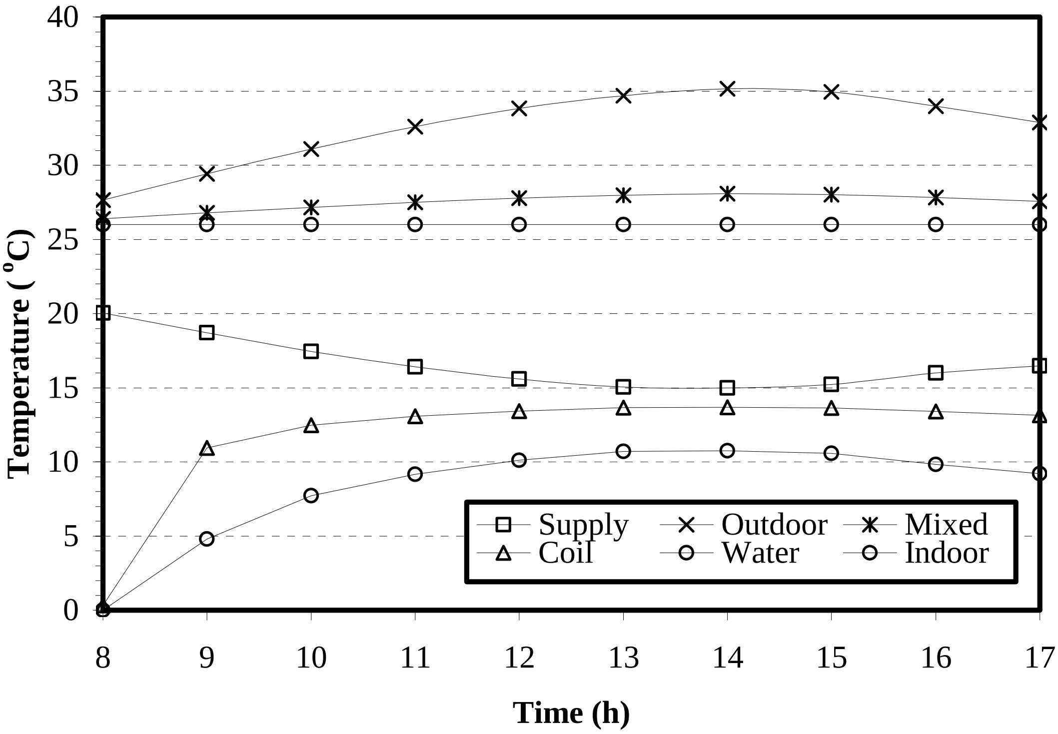

Figure 4.25. Distribution of the temperature at different states for total mass flow rate of 34515 kg/h

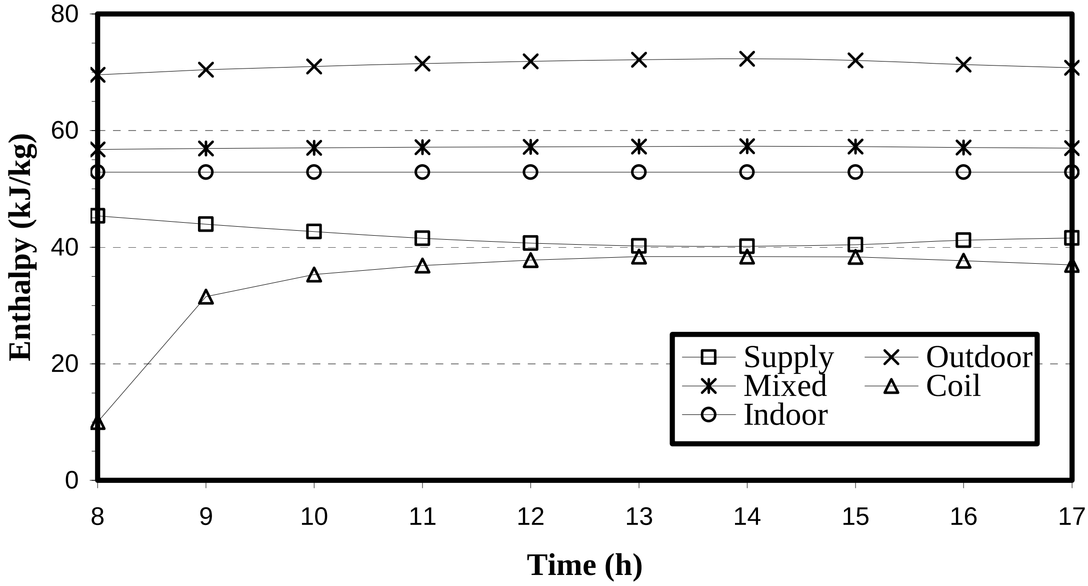

Figure 4.26. Distribution of the enthalpy at different states for total mass flow rate of 34515 kg/h

4.4.2. Operating Capacity of the Cooling Coil during Cooling Season

In this section of the study, firstly hourly total cooling loads of the education building in Adana were calculated during cooling season. Cooling period covers 184 days between April 21 and October 21 for Adana in hot and humid climate. Therefore cooling load was performed for 21^{st} of each month in the cooling season. In calculation of cooling load, daily maximum outdoor dry bulb temperature and daily range for 21^{st} day of the each month considered is taken as outdoor design conditions. Occupation time is assumed between 8^{00} and 24^{00} hours. Hourly total cooling load of the education building was given in Table 4.7. Design cooling load is the maximum load given in this table. The maximum (design) building cooling load for education building is in August (131.1 kW) at 13^{00}. The corresponding sensible heat ratio is 0.89 (Table 4.7).

Secondly, in the calculation of design cooling coil capacity, temperature of the air supplied to the air-conditioned volumes was selected as 15 °C for a VAV system. Using the maximum building cooling load (131.1 kW), sensible heat ratio

(0.89), minimum fresh air ventilation requirement (7001 m^3/h) and fixed supply air temperature (15 °C) as input parameters, the maximum (design) cooling coil capacity and the maximum (design) supply air flow rate were found respectively to be ($Q_{coil,dsg}$) 166.2 kW and (M_{dsg}) 37348 kg/h for the education building. Calculation procedure required an iterative approach; therefore a computer program was used for the calculations. Then, AHU and chiller unit were selected from a local supplier (Alarko-Carrier). The total power of the electric motors of the supply and return fans in AHU that provide air for the CAV or the VAV system is ($P_{fan,dsg}$) 26 kW. Net cooling capacity and electricity consumption of the chiller unit selected are ($Q_{chil,full}$) 185 kW and ($P_{chil,full}$) 80 kW under nominal operating conditions (38°C condenser air inlet temperature, 10°C evaporator inlet and 6°C outlet water temperature), respectively. The compressor in the chiller unit is controlled by a five-stepped proportional control system for part load operations.

For the case of the office center, after similar calculations, the design cooling coil capacity of the CAV or VAV systems and the design mass flow rate of the supply air were found to be ($Q_{coil,dsg}$) 136.1 kW and (M_{dsg}) 36240 kg/h, respectively. The total power of the supply and return fans is ($P_{fan,dsg}$) 26 kW. Net cooling capacity and electricity consumption of the chiller unit are ($Q_{chil,full}$) 146 kW and ($P_{chil,full}$) 66 kW under nominal conditions, respectively.

After selecting HVAC equipments, hourly operating capacity and hourly total mass flow rate for 21st day of each month during the cooling season were computed using computer programs P_VAV and P_CAV according to hourly cooling load of the sample building. In calculations, hourly outdoor air conditions (weather data) for each hour in all days during cooling period were determined using equations (3.42) and (3.49). Therefore, real outdoor air conditions were obtained for each hour in all days during cooling period.

Hourly total mass flow rates requirement of the education building for 21st day of each month during the cooling season are shown in Figure 4.27. It was calculated using P_VAV. Flow rate of the supply air is constant for a CAV system, whilst it is variable for a VAV system. A VAV system operates identically to a CAV system under peak cooling conditions, with AHU operating at maximum supply flow rate. Therefore, the same maximum (design) supply air flow rate obtained for the VAV system (M_{dsg}=37348 kg/h) was selected for the CAV system.

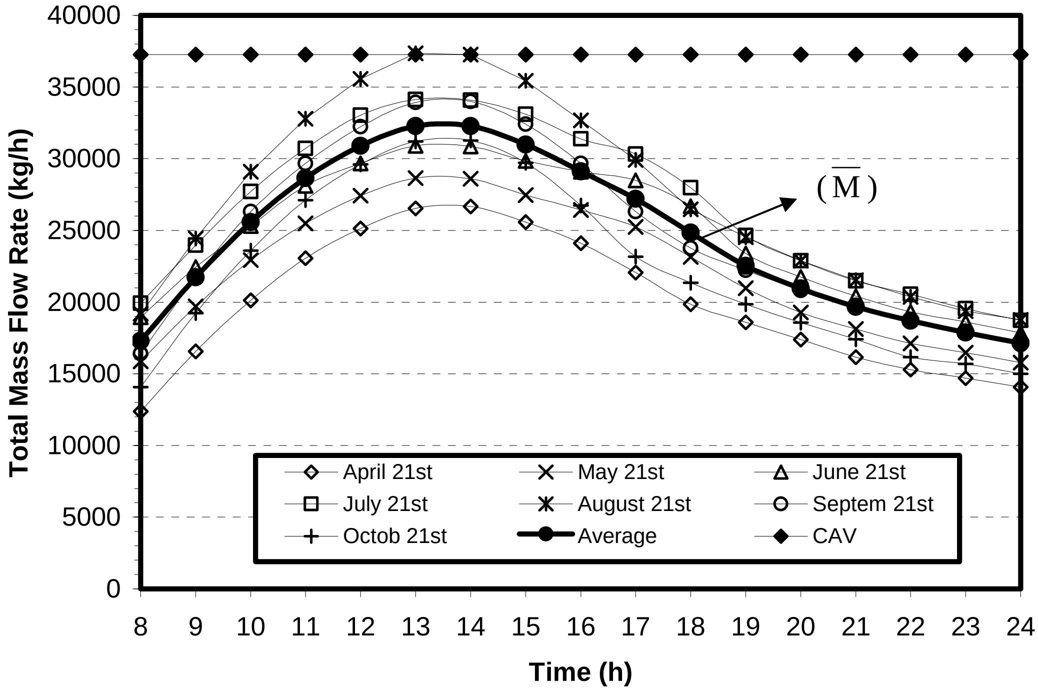

Figure 4.27. Hourly total mass flow rate of the CAV and VAV systems for education building

As can be seen from Figure 4.27, hourly total mass flow rate (load) profile of the CAV system is constant but that of VAV system is not constant and it is varied between 12384 and 37348 kg/h during operation time. Hourly total mass flow rate requirement of education building is observed to be minimum (12384kg/h) at 08^{00} o'clock on April 21 while hourly total mass flow rate requirement at 13^{00} o'clock on August 21 is maximum (37348 kg/h).

The mass flow rates for the days other than 21^{st} of each month were not calculated. Therefore, the results obtained for 21^{st} of each month were integrated for each hour by Simpson Integral Method and seasonal average values of hourly mass flow rate $(\overline{M})$ were obtained. The seasonal average mass flow rate $(\overline{M})$ is also shown in Figures 4.27.

As can be seen from Figure 4.27, maximum (design) mass flow rate is not observed on June 21st which is generally used as design day for cooling system in Turkey. If the cooling system is designed for June 21, in this period (August), total mass flow rate requirement of the building is not provided by the cooling system. For this reason, thermal comfort is not completely achieved.

Similar approach as done for education building was performed for office building. Figure 4.28 shows hourly total mass flow rates requirement of the office building for 21st day of each month during the cooling season and the seasonal average mass flow rate.

Results show that hourly total mass flow rate requirement of the building is greatly changed as function of time. At 8^{00} and 15^{00} on 21 June total mass flow rate requirement of education building are estimated to be 18940 kg/h and 29851 kg/h corresponding to 23.9 °C and 33.6°C outdoor dry bulb temperatures, respectively.

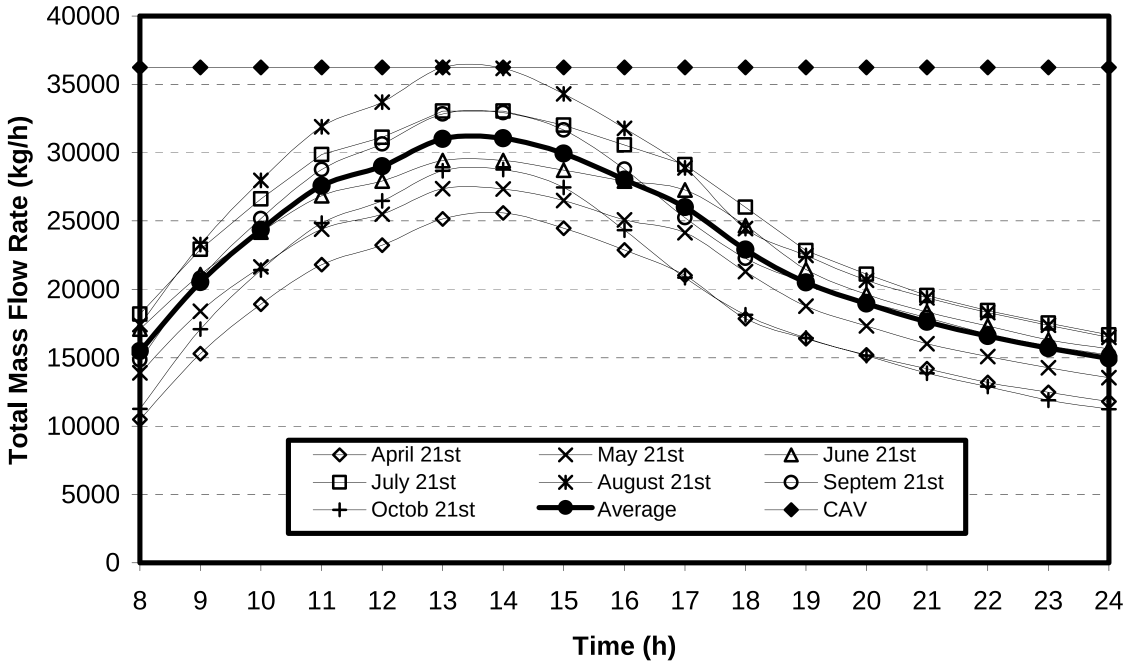

Figure 4.28. Hourly total mass flow rate of the CAV and VAV systems for office center

Distribution of hourly supply air temperature of CAV system for 21st day of each month during the cooling season for education building is shown in Figure 4.29.

It was calculated using P_CAV. As shown in the Figure 4.29, hourly supply air temperature profiles of the CAV system are varied between 15°C and 23°C but that of VAV system is constant at 15 °C during the operation time period. Supply air temperature of the CAV system is minimum corresponding to maximum outdoor temperatures. For example, hourly supply air temperature of the CAV system is maximum (22.53°C) at 08^{00} o'clock on April 21 while it is minimum (15°C) at 13^{00} o'clock on August 21.

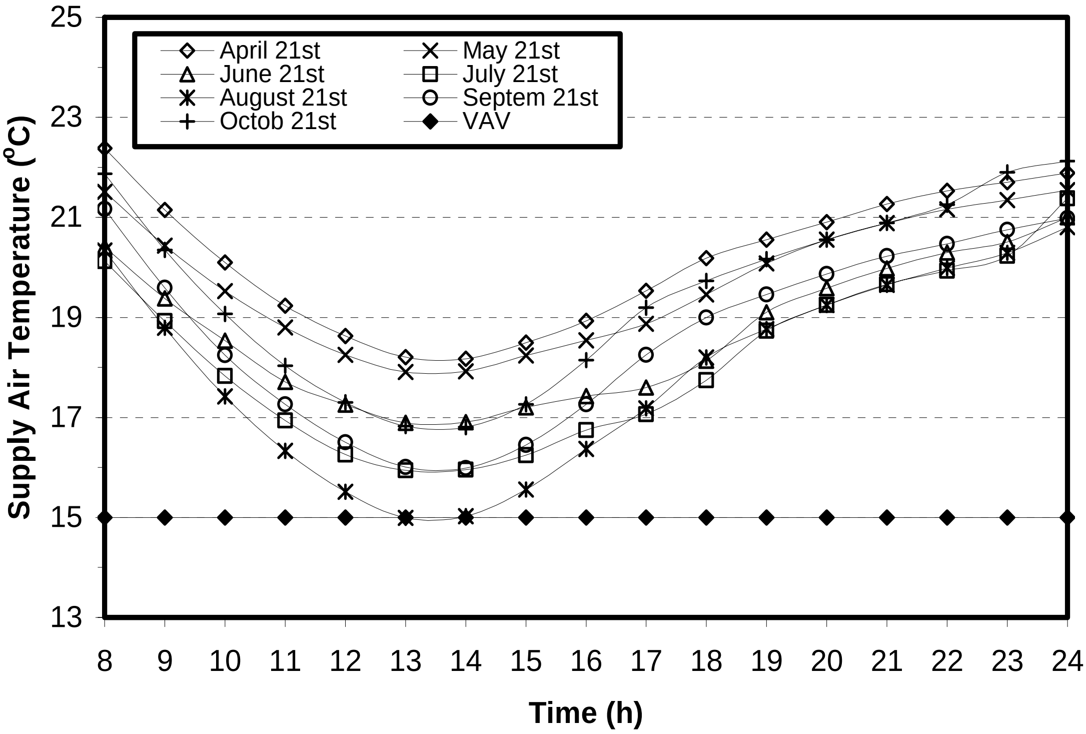

Figure 4.29. Distribution of supply air temperature for the CAV and VAV systems

Hourly cooling coil capacity of the education building for 21^{st} day of each month during the cooling season was calculated using P_VAV. Figure 4.30 shows hourly cooling coil capacity for 21^{st} day of each month during cooling season for the VAV system for the education building. The coil capacity for the days other than 21^{st} of each month was not calculated. Therefore, the results obtained for 21^{st} of each month were integrated for each hour by Simpson Integral Method and seasonal average values of hourly coil capacity ($\overline{Q_{coil}}$) were obtained. The coil capacity is also shown in Figure 4.30.

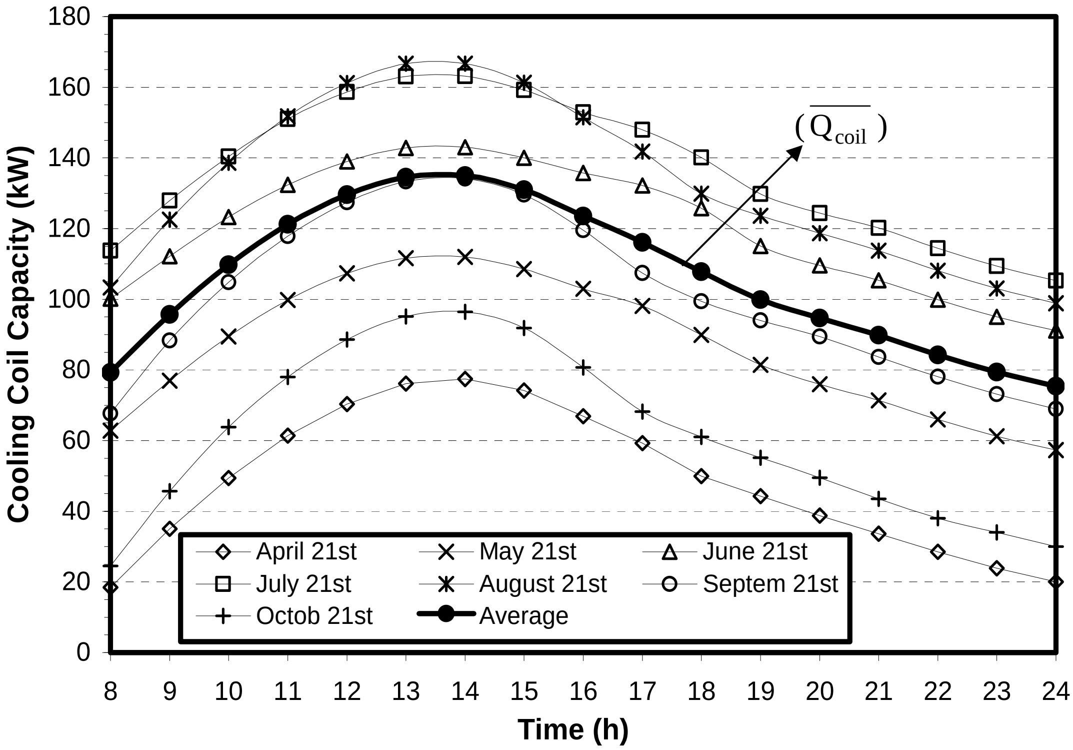

Figure 4.30. Hourly cooling coil capacity for VAV system for the education building

As can be seen in Figure 4.30, the hourly total mass flow rate requirement of the education building under the real operating conditions of the ACS during cooling season is obtained. Hourly cooling coil capacity (load) profile of the ACS is not constant and it is varied between approximately 20 kW and 170 kW during operation. Results show that cooling demand of building is greatly changed as function of time, as similar to mass flow rate required. The least hourly cooling demand of building during cooling season for Adana is observed at 8^{00} on April 21 (18.45 kW) whiles the highest at 13^{00} and 14^{00} o'clock in August (166.70 kW).

Similar approach was performed for office building. Figure 4.31 shows hourly cooling coil capacity of the office building for 21st day of each month during the cooling season and the seasonal average values of hourly coil capacity.

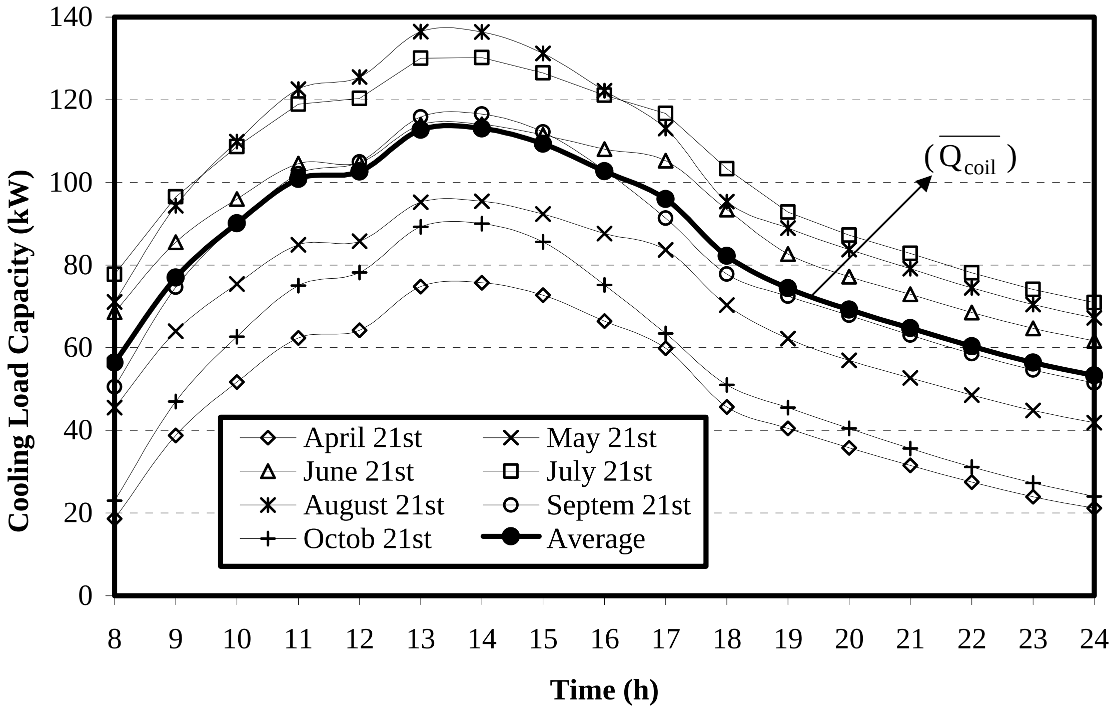

Figure 4.31. Hourly cooling coil capacity for VAV system for the office building

It should be noted that, design cooling coil load using outdoor design condition of 21 July for education building is found to be 186.05 kW. However, as clearly shown from Figure 4.30, the maximum cooling load of this building is observed in August under real conditions. Therefore, if the cooling system is designed for June 21, in real operating time, the cooling demand of the building is not always provided by the cooling system in spite of fact that the design cooling coil load (186.05 kW) obtained for 21 July is 12% higher than the peak operating load at real hourly outdoor conditions (166.70 kW). Because total mass flow rate requirement (35935 kg/h) is lower than design mass flow rate (37348 kg/h). In addition, chiller unit is never operated at the full load during operating time because the capacity of the chiller unit is selected greater for required specification. As a result of this, both initial and operating costs of the cooling system are dramatically increased and not thermal comfort achieved completely.

Ratios of the hourly total mass flow rate for 21st day of each month during the cooling season to the design supply air flow rate (M_{tot}/M_{totmax}) for education building are shown in Figure 4.32. In addition to this, Figure 4.32 contains the seasonal average value of the total mass flow rate ratio. This ratio indicates the percentage of the fan capacity utilization when fan of the ACS is operated (run) under the real operating conditions. For example, if ACS is operated for full load, this ratio is 1. If it is 0.5 (part load), 50 percent of the fan capacity is used by ACS.

As shown in Figure 4.32, the hourly fan capacity ratios (hourly capacity utilization in the fan unit) under the real operating conditions of the ACS during cooling season are obtained. The minimum ratios of the hourly fan capacity are obtained in April. The maximum ratios of the hourly fan capacity are obtained in August. The fan capacity which depends on the outdoor air conditions does not reach to full load. Fan usually operates at a part load under the real operating conditions because of changing the cooling load. Whenever operating loads are less than design loads, total mass flow rate should be reduced with variable air volume for saving energy.

Similar approach was performed for office building. Figure 4.33 shows hourly fan capacity ratio of the air conditioning system for 21st day of each month during the cooling season and the seasonal average values of hourly fan capacity ratio.

Ratios of the hourly cooling coil capacity for 21st day of each month during the cooling season to the design cooling capacity and ratios of the average cooling coil capacity during the cooling season to the design cooling capacity are presented in Figure 4.34.

As shown in Figure 4.34, the minimum ratios of the hourly cooling coil capacity are obtained in April while the maximum ratios of the hourly cooling coil capacity are obtained in August and July.

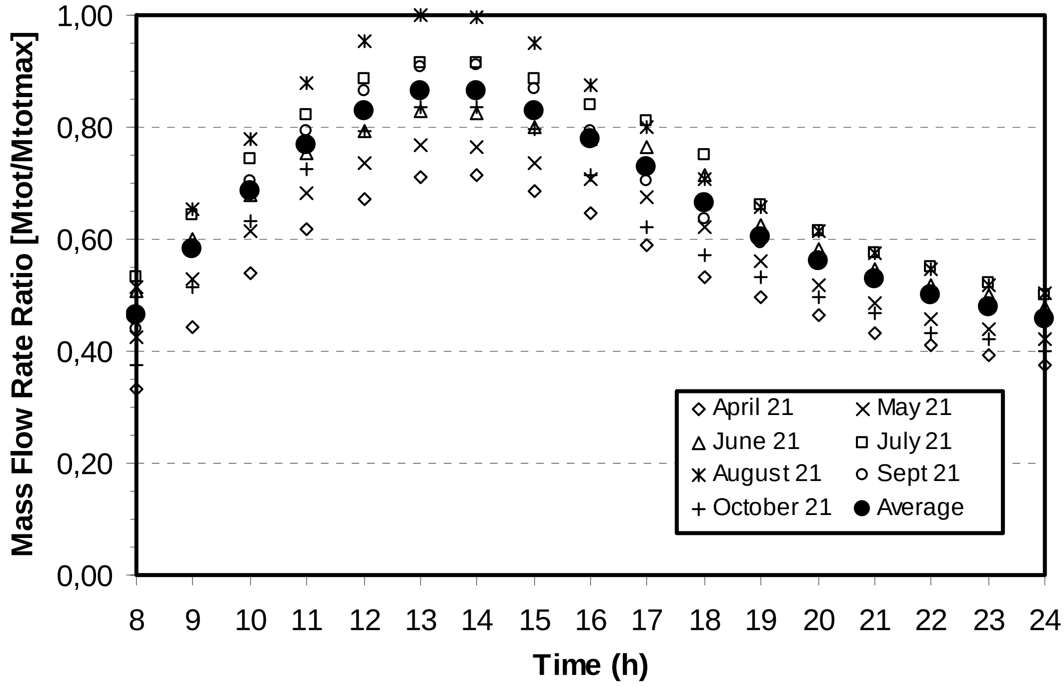

Figure 4.32. Distribution of hourly fan capacity ratio for education building

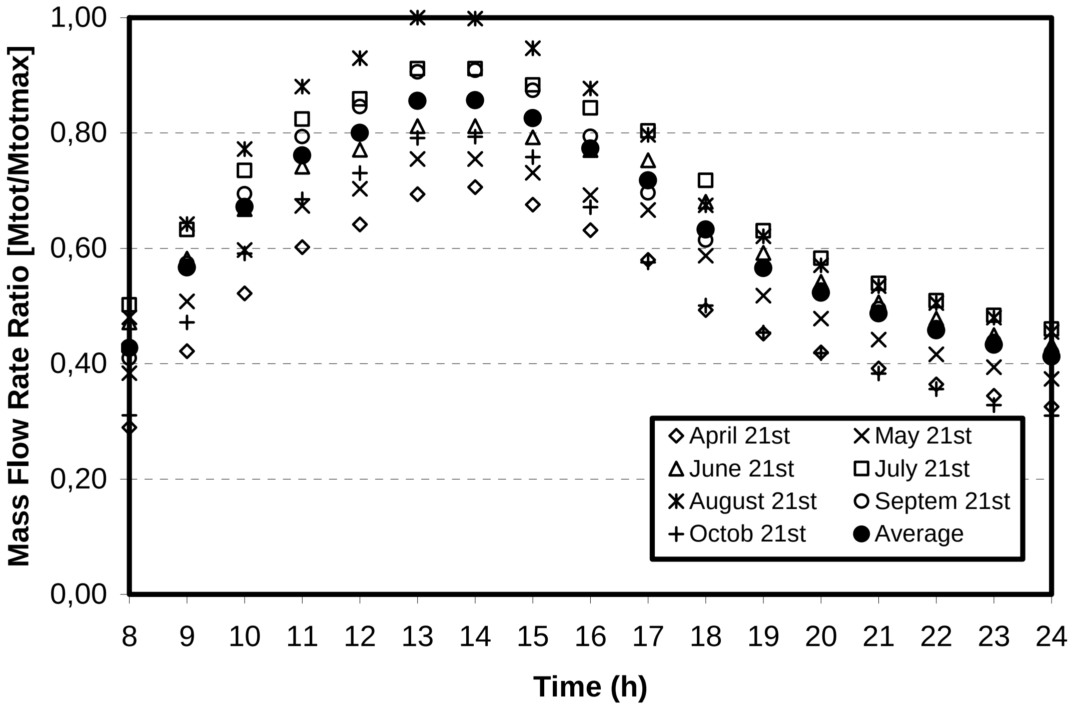

Figure 4.33. Distribution of hourly fan capacity ratio for office center

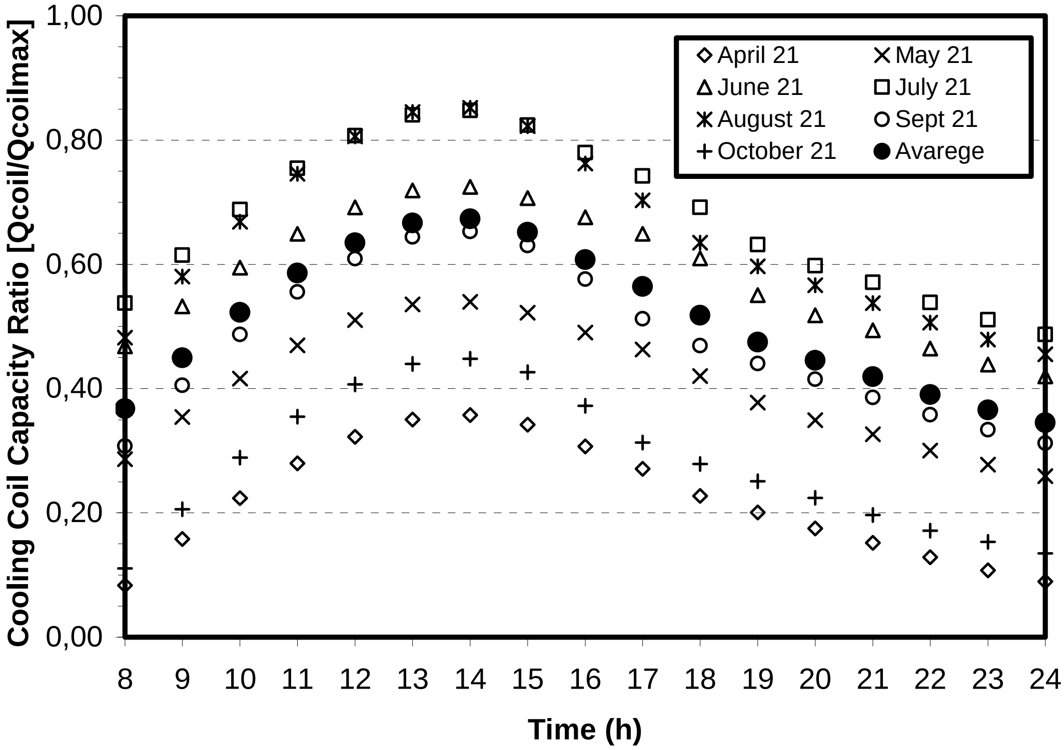

Figure 4.34. Cooling coil capacity ratio for part load of the ACS for education building

Similar calculations were performed for office building. Figure 4.35 shows hourly cooling coil capacity ratio of the air conditioning system for 21st day of each month during the cooling season and the seasonal average values of hourly cooling coil capacity ratio.

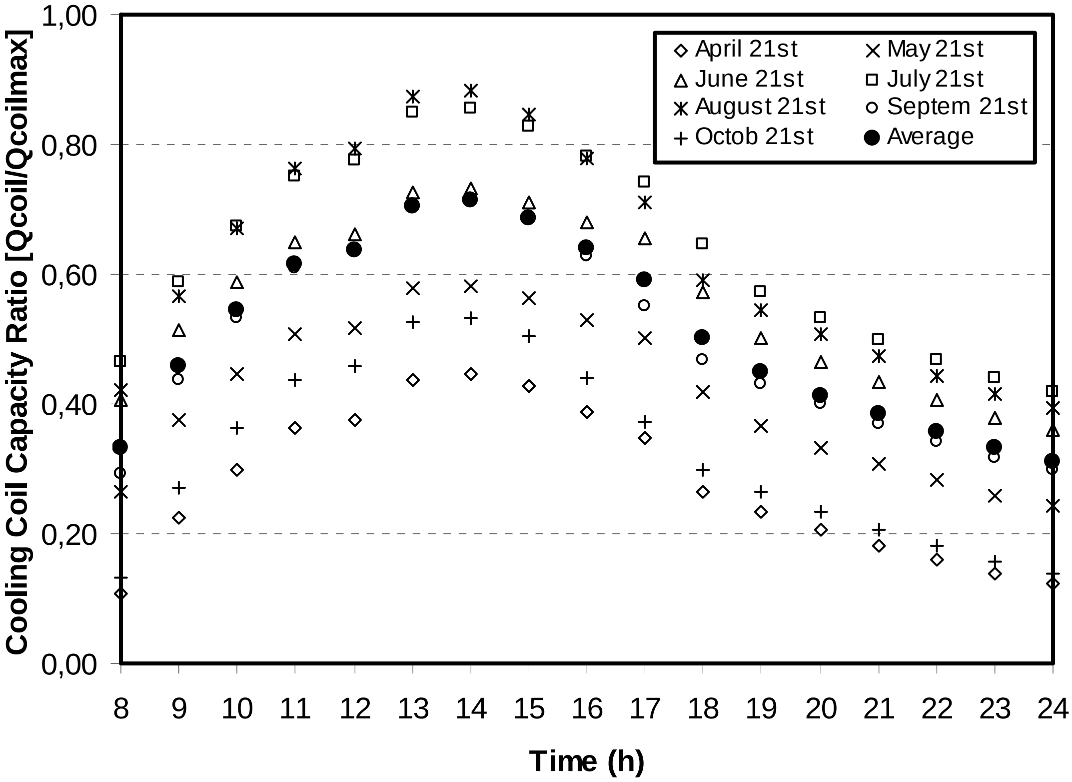

Figure 4.35. Cooling coil capacity ratio for part load of the ACS for office center

4.5. Economic Analyses of CAV and VAV Systems

Purpose of this study is to compare CAV and VAV systems considering different aspects. Figure 4.36 shows schematic of the air conditioning system considered. Since the aim of the study is to compare CAV and VAV systems, both approaches were considered. It can be seen from Figure 4.36, the CAV and the VAV air conditioning systems commonly consist of air handling unit (AHU), air-cooled chiller system, supply and return fans, duct, and control units. The VAV system includes additional two variable speed drive (VSD) units for the supply and return fans and 27 VAV boxes in addition to the other common units. One VAV box is used for each room in the building. Additional units for VAV air conditioning system are shown with dashed line in Figure 4.36.

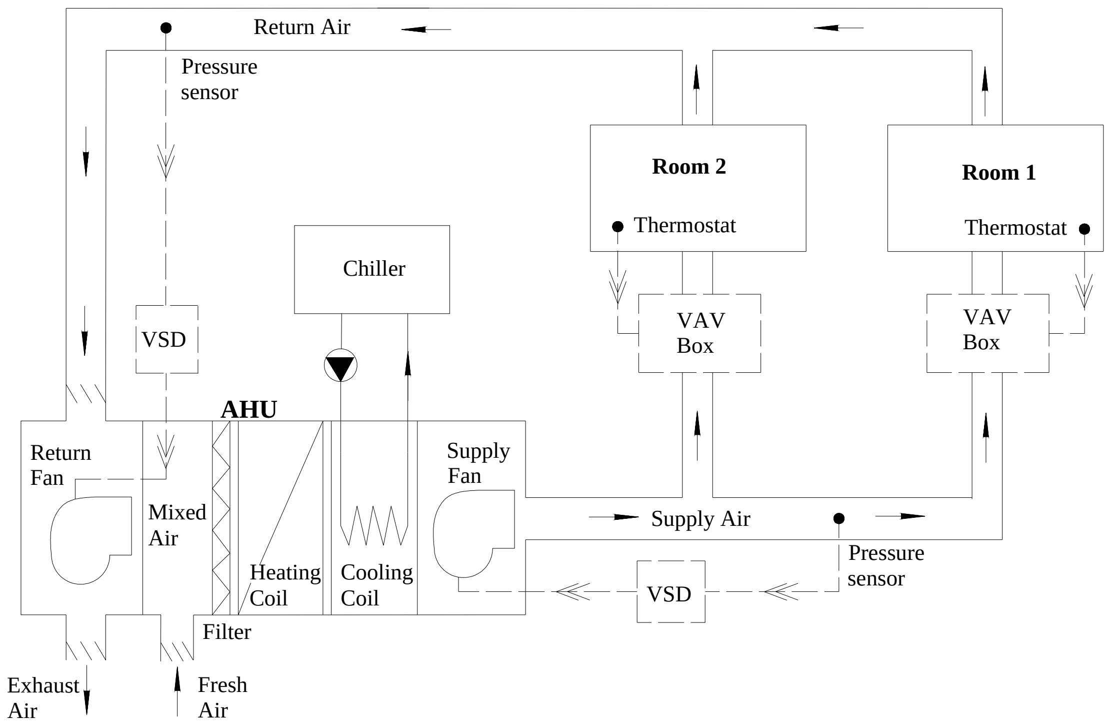

Figure 4.36. Schematic of the CAV and VAV air conditioning system

Air handling unit and chiller were selected from a local supplier (Alarko-Carrier). The AHU contains fans, cooling coil, filters, mixing box and exhaust air section.

For the case of the education building, the total power of the electric motors of the supply and return fans in AHU that provide air for the CAV or the VAV system is ($P_{fan,dsg}$) 26 kW (15 kW and 11 kW). Net cooling capacity and electricity consumption of the chiller unit selected are 185 kW and 80 kW under nominal operating conditions (38°C condenser air inlet temperature, 10°C evaporator inlet and 6°C outlet water temperature), respectively. The compressor in the chiller unit is controlled by a five-stepped proportional control system for part load operations.

For the case of the office center, the total power of the supply and return fans is ($P_{fan,dsg}$) 26 kW. Net cooling capacity and electricity consumption of the chiller unit are 146 kW and 66 kW under nominal conditions, respectively. Compressor in the chiller has four-stepped proportional control for part load. Using the data provided by the manufacturer and the hourly outside air temperature, hourly values of cooling capacity (Q_{chil}) and power consumption (W_{chil}) of the chiller at full load and at part load (for each of the five steps of the chiller) were obtained for 21st day of each month during the cooling season.

As an example to the results, Q_{chil} and P_{chil} are shown in Figures 4.37 and 4.38 for full capacity and compressor step 3, respectively. The trends observed in these figures are due to variation of COP of the chiller system with outdoor air temperature, since the chiller has an air-cooled condenser unit. Q_{chil} decreases and P_{chil} increases with the increase of outdoor air temperature, as expected. Seasonal average hourly values of Q_{chil} and P_{chil} ($\overline{Q_{chil}}$ and $\overline{P_{chil}}$) were then calculated utilizing Simpson Integral Method. Figures 4.37 and 4.38 also show $\overline{Q_{chil}}$ and $\overline{P_{chil}}$.

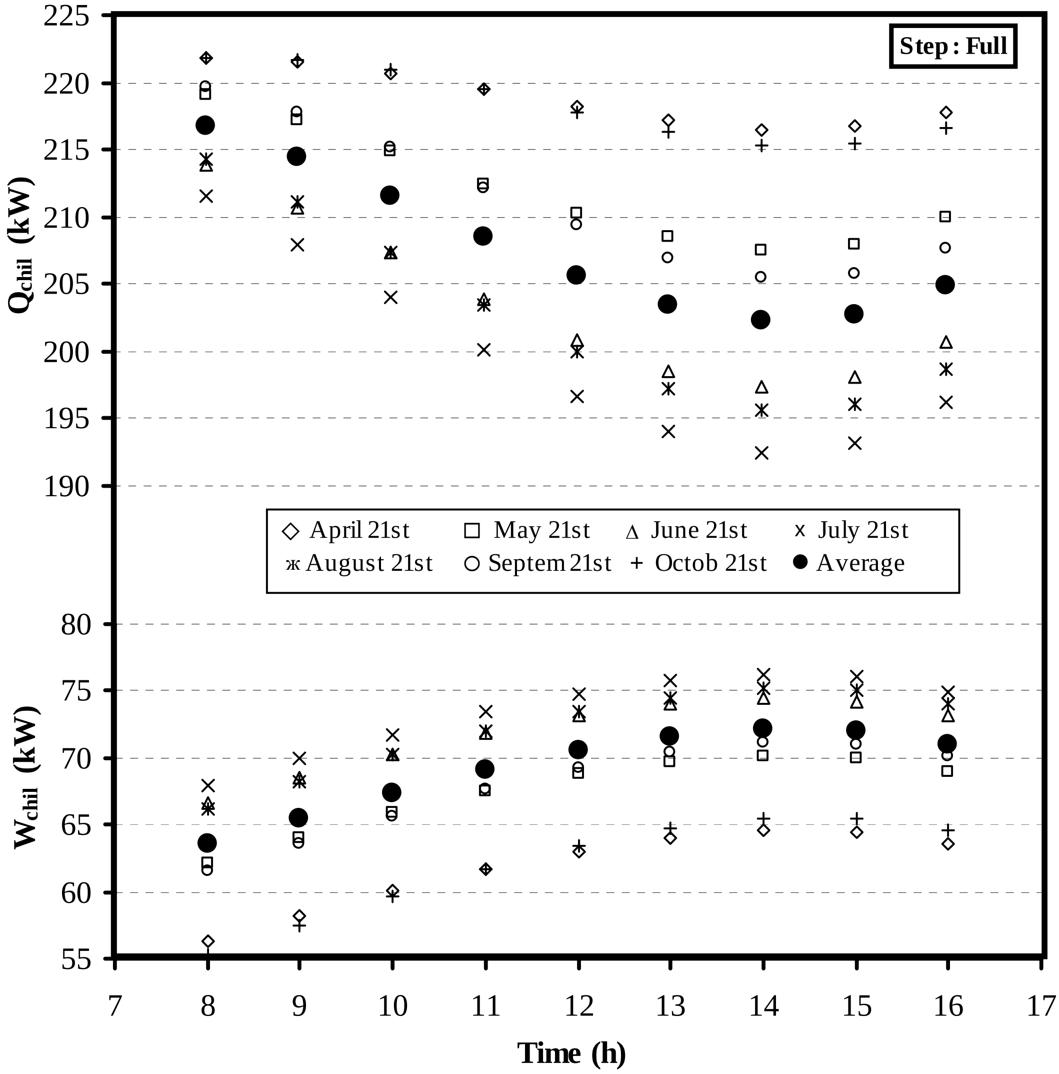

Figure 4.37. The cooling coil load and the power consumption versus time at full step (full load) of the compressor in the chiller

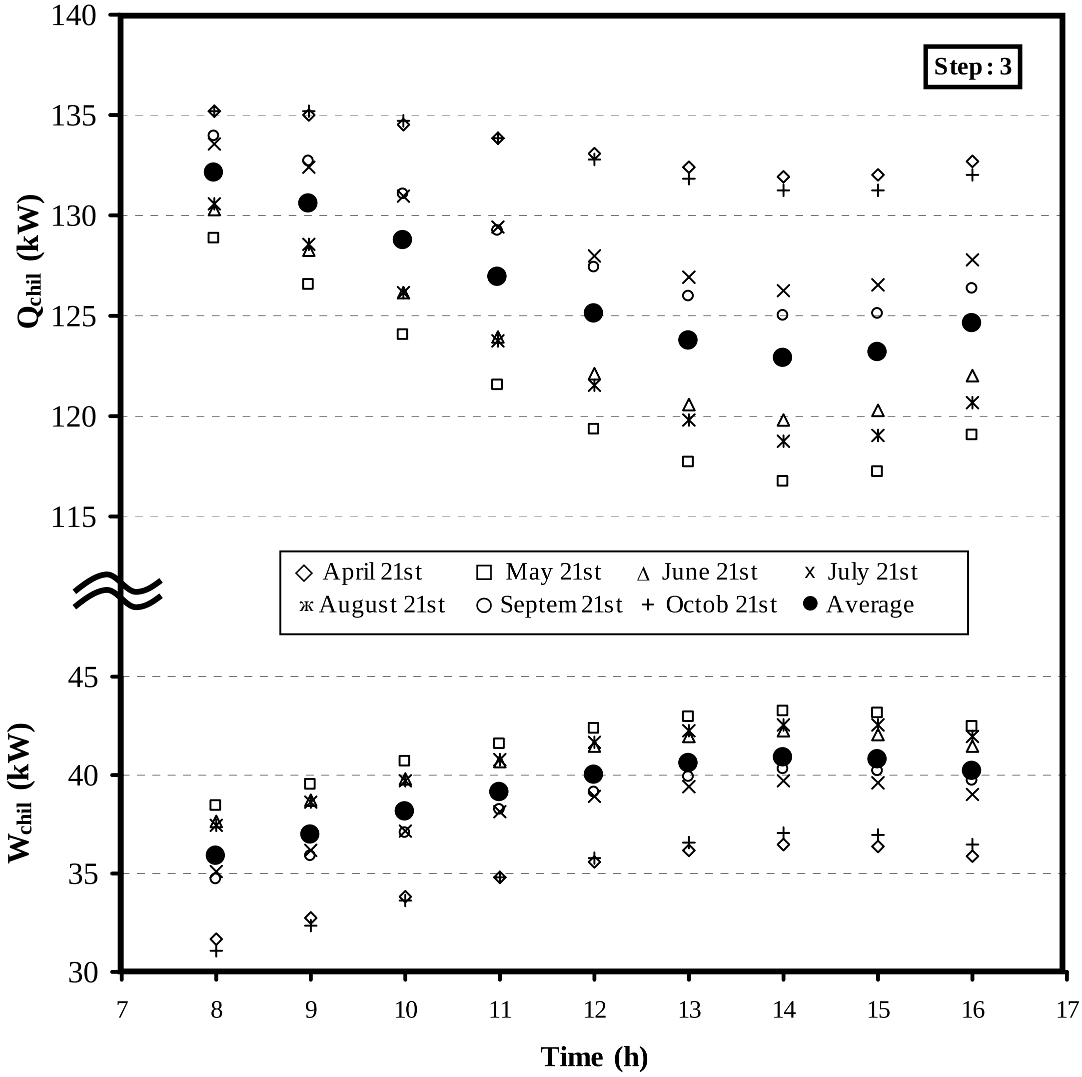

Figure 4.38. The cooling coil load and the power consumption versus time at step 3 of the compressor in the chiller

4.5.1. Costs Analysis of Air Conditioning Systems

4.5.1.1. Initial Costs

Initial costs of the CAV and the VAV systems include AHU, chiller system, ducts, and control units. VAV system includes Variable Speed Drive (VSD) and VAV box in addition to the other common units. Table 4.20 shows the estimated initial costs of the systems considered. As can be seen from Table 4.20, initial cost for the education building is approximately 7% higher than that of the office center. When the initial costs of the CAV and the VAV systems are compared, it is seen that, initial cost of the VAV system is 21% and 23% higher than that of the CAV system for the education building and the office center, respectively.

Table 4.20. Comparison of the initial costs of VAV and CAV systems

	Initial Cost ($)			
	Education Building		Office Center	
Unit	**CAV**	**VAV**	**CAV**	**VAV**
AHU	20355	20355	20355	20355
Duct	20000	20000	20000	20000
Chiller	47495	47495	40710	40710
Automation	6785	11696	6785	11649
VSD	0	4150	0	4150
VAV Box	0	10877	0	10754
Total Initial Cost	94635	114573	87850	107618
Extra investment for the VAV	19938		19768	

4.5.1.2. Operating and Maintenance Costs

Operating costs include the costs of electricity, wages of employees, supplies, water and materials. Electrical operating costs for the systems considered comprise the chiller and AHU including supply and return fans. Electrical costs of the chiller, supply and return fans were calculated separately for the CAV and the VAV systems. Maintenance cost depends on many parameters such as local labor rates, their experience, the age of the system, length of time of operation, and therefore, it is difficult to quantify. Complexity of the air-conditioning system and the relative ease of access to plant play an important role on the maintenance cost [Elsafty and Al-Daini, 2002]. A proper estimation of the maintenance cost requires a detailed analysis, which is beyond the scope of this study. Maintenance cost for the CAV and the VAV systems can be considered approximately to be the same. In the calculations, therefore, maintenance costs and other operating costs such as wages of employees, supplies, etc. were neglected.

Two electricity consuming units in the air-conditioning systems are the fans and the chiller unit. Electric consumption of the other unit such as chilled water pumps will be approximately the same for both systems, and, therefore, they are neglected in the cost analysis. For the CAV system, mass flow rate is constant through the operation of the system, therefore even for the part load conditions the fans consume the maximum power. Under peak cooling conditions, the VAV system operates identically to a CAV system with AHU operating at maximum flow and maximum cooling coil capacity. However, at reduced cooling load, the system airflow is reduced by the combined action of the closing of zonal VAV box dampers and the fan speed controller [Kreider and Rabl, 1994]. Therefore the electricity consumption of the fans may vary greatly through the day or cooling season depending on the cooling load.

4.5.1.3. Calculation of the Operating Costs

For determining the total operating cost of the fans for a cooling season in the VAV system, the power of the fan electric motor under the real operating conditions was calculated using equation (3.58). In equation (3.58), the power required running a fan is proportional to the cube of the air flow rate. In this study, fan power at part load (W) for the education building and the office center was determined hourly during a cooling season using equation (3.58). For this purpose, hourly mass flow rate for the VAV system (M) was calculated using the procedure below:

Total mass flow rate for 21st day of each month during cooling season for the

VAV and the CAV systems and the seasonal average mass flow rate ($\overline{M}$) are given in Figure 4.27 for the education building and Figure 4.28 for the office building, respectively. Figure 4.30 and Figure 4.31 show the seasonal average coil capacity ($\overline{Q_{coil}}$) and hourly cooling coil capacity for 21st day of each month during cooling season for the VAV system for the education building and the office building, respectively.

Inserting the seasonal average mass flow rate ($\overline{M}$) given in Figures 4.27 and 4.28 in Equation (3.58), seasonal average hourly fan power for the VAV system ($\overline{P_{fan}}$) was obtained. Total electric consumption of the fans in a cooling season can be calculated by multiplying average hourly fan power with operating time. Utilizing an electric price of 0.11 $/kWh, annual operating costs for the fans were determined for the CAV and the VAV systems.

In the study, two different operating scenarios, namely scenario 1 and scenario 2, were considered. Operating period of the air-conditioning system is between 8^{00}-17^{00} hours for scenario 1, and between 8^{00}-24^{00} hours for scenario 2.

Table 4.21 shows the estimated annual (for 184 days of operation) operating costs of the fans for the VAV and the CAV systems for the education building according to the scenarios considered. As seen from this table, annual operating cost of the fans in the VAV system is 56% less than that of the CAV system for scenario 1. In the case of scenario 2, the saving is higher (66%), due to longer operating hours.

Table 4.22 shows the estimated annual operating costs of the fans for the VAV and the CAV systems for the office center according to the scenarios considered. As seen from this table, annual operating cost of the fans in the VAV system is 58% less than that of the CAV system for scenario 1. In the case of scenario 2, the saving is higher (69%), due to longer operating hours.

Table 4.21. Annual operating costs of fans for education building

Scenario	System	Operating Time	Power (kW)	Electric Consumption (kWh)	Operating Cost ($)
I	VAV	08^{00}-09^{00}	2.59	475.98	52
		09^{00}-10^{00}	5.12	942.75	104
		10^{00}-11^{00}	8.34	1535.41	169
		11^{00}-12^{00}	11.72	2156.62	237
		12^{00}-13^{00}	14.71	2706.39	298
		13^{00}-14^{00}	16.78	3087.82	340
		14^{00}-15^{00}	16.77	3085.19	339
		15^{00}-16^{00}	14.85	2733.10	301
		16^{00}-17^{00}	12.33	2268.29	250
		Total operating cost of the fans ($) =			2089
	CAV	08^{00}-17^{00}	26	43056	4736
		Total operating cost of the fans ($) =			4736
II	VAV	08^{00}-09^{00}	2.59	475.98	52
		09^{00}-10^{00}	5.12	942.75	104
		10^{00}-11^{00}	8.34	1535.41	169
		11^{00}-12^{00}	11.72	2156.62	237
		12^{00}-13^{00}	14.71	2706.39	298
		13^{00}-14^{00}	16.78	3087.82	340
		14^{00}-15^{00}	16.77	3085.19	339
		15^{00}-16^{00}	14.85	2733.10	301
		16^{00}-17^{00}	12.33	2268.29	250
		17^{00}-18^{00}	10.04	1846.70	203
		18^{00}-19^{00}	7.65	1407.53	155
		19^{00}-20^{00}	5.71	1049.99	115
		20^{00}-21^{00}	4.59	844.48	93
		21^{00}-22^{00}	3.80	699.56	77
		22^{00}-23^{00}	3.26	600.52	66
		23^{00}-24^{00}	2.85	523.66	58
		Total operating cost of the fans ($) =			2856
	CAV	08^{00}-24^{00}	26	76544	8420
		Total operating cost of the fans ($) =			8420

Table 4.22. Annual operating costs of fans for office center

Scenario	System	Operating Time	Power (kW)	Electric Consumption (kWh)	Operating Cost ($)
I	VAV	08^{00}-09^{00}	2.02	372.35	41
		09^{00}-10^{00}	4.73	870.30	96
		10^{00}-11^{00}	7.89	1452.45	160
		11^{00}-12^{00}	11.45	2107.08	232
		12^{00}-13^{00}	13.32	2451.23	270
		13^{00}-14^{00}	16.28	2994.71	329
		14^{00}-15^{00}	16.35	3007.61	331
		15^{00}-16^{00}	14.64	2694.33	296
		16^{00}-17^{00}	12.02	2211.21	243
		Total operating cost of the fans ($) =			1998
	CAV	08^{00}-17^{00}	26	43056	4736
		Total operating cost of the fans ($) =			4736
II	VAV	08^{00}-09^{00}	2.02	372.35	41
		09^{00}-10^{00}	4.73	870.30	96
		10^{00}-11^{00}	7.89	1452.45	160
		11^{00}-12^{00}	11.45	2107.08	232
		12^{00}-13^{00}	13.32	2451.23	270
		13^{00}-14^{00}	16.28	2994.71	329
		14^{00}-15^{00}	16.35	3007.61	331
		15^{00}-16^{00}	14.64	2694.33	296
		16^{00}-17^{00}	12.02	2211.21	243
		17^{00}-18^{00}	9.61	1768.47	195
		18^{00}-19^{00}	6.58	1209.96	133
		19^{00}-20^{00}	4.71	866.72	95
		20^{00}-21^{00}	3.72	684.53	75
		21^{00}-22^{00}	3.00	551.61	61
		22^{00}-23^{00}	2.49	458.32	50
		23^{00}-24^{00}	2.11	388.34	43
		Total operating cost of the fans ($) =			2650
	CAV	08^{00}-24^{00}	26	76544	8420
		Total operating cost of the fans ($) =			8420

A similar approach was followed for the calculation of seasonal operating cost of the chiller unit. In the analysis, variation of Coefficient Of Performance (COP) of the chiller unit with outside air temperature and variation of COP with part load ratio were considered. Part Load Ratio (PLR) was defined as;

$$\mathrm{PLR} = Q_{chil} / Q_{chil,full} \tag{4.3}$$

where, Q_{chil} is the hourly cooling demand on chiller, which is approximately equal to the hourly coil load (Q_{coil}), and $Q_{chil,full}$ is the full cooling capacity of the chiller. Automatic control system of the chiller unit will select a suitable operating step for the compressor depending on the value of PLR. Using the seasonal average hourly values of coil load ($\overline{Q_{coil}}$) obtained previously (Figures 4.30 and 4.31) and chiller capacity at full load ($\overline{Q_{chil,full}}$) given in Figure 4.37, seasonal average hourly part load ratio ($\overline{PLR}$) given in Figure 4.34 and 4.35 and then seasonal average hourly operating step of the compressor ($\overline{ST}$) were determined. From the corresponding part load $\overline{Q_{chil}}$ and $\overline{P_{chil}}$, and operating time it was possible to calculate seasonal work consumption and then the operating cost of the chiller unit.

It should be noted that annual operating cost of the chiller unit is the same both for the CAV and the VAV systems. Table 4.23 shows the annual operating cost of the chiller for the education building. As seen from this table, annual operating cost of the chiller for scenario 2 is 70% higher than that of scenario 1 due to longer operating hours.

Similar calculations were also performed for the office center. Table 4.24 shows the annual operating cost of the chiller for the office center. As seen from this table, annual operating cost of the chiller for scenario 2 is 55% higher than that of scenario 1 due to longer operating hours.

Table 4.23. Annual operating cost of the chiller unit for education building

Scenario	System	Operating Time	Power (kW)	Electric Consumption (kWh)	Operating Cost ($)
I	CAV and VAV	08^{00}-09^{00}	24.58	4522.72	497
		09^{00}-10^{00}	37.00	6808.00	749
		10^{00}-11^{00}	38.12	7014.08	772
		11^{00}-12^{00}	39.13	7199.92	792
		12^{00}-13^{00}	54.59	10044.56	1105
		13^{00}-14^{00}	55.34	10182.56	1120
		14^{00}-15^{00}	55.81	10269.04	1130
		15^{00}-16^{00}	55.65	10239.60	1126
		16^{00}-17^{00}	40.20	7396.80	814
Total operating cost of the chiller ($) =					8105
II	CAV and VAV	08^{00}-09^{00}	24.58	4522.72	497
		09^{00}-10^{00}	37.00	6808.00	749
		10^{00}-11^{00}	38.12	7014.08	772
		11^{00}-12^{00}	39.13	7199.92	792
		12^{00}-13^{00}	54.59	10044.56	1105
		13^{00}-14^{00}	55.34	10182.56	1120
		14^{00}-15^{00}	55.81	10269.04	1130
		15^{00}-16^{00}	55.65	10239.60	1126
		16^{00}-17^{00}	40.20	7396.80	814
		17^{00}-18^{00}	42.13	7751.92	853
		18^{00}-19^{00}	42.73	7862.32	865
		19^{00}-20^{00}	43.32	7970.88	877
		20^{00}-21^{00}	43.91	8079.44	889
		21^{00}-22^{00}	44.51	8189.84	901
		22^{00}-23^{00}	30.62	5634.08	620
		23^{00}-24^{00}	31.01	5705.84	628
Total operating cost of the chiller ($) =					13736

Table 4.24. Annual operating costs of the chiller for office center

Scenario	System	Operating Time	Power (kW)	Electric Consumption (kWh)	Operating Cost ($)
I	CAV and VAV	08^{00}-09^{00}	23.46	4316.64	475
		09^{00}-10^{00}	24.25	4462.00	491
		10^{00}-11^{00}	39.33	7236.72	796
		11^{00}-12^{00}	40.45	7442.80	819
		12^{00}-13^{00}	41.36	7610.24	837
		13^{00}-14^{00}	42.02	7731.68	850
		14^{00}-15^{00}	42.38	7797.92	858
		15^{00}-16^{00}	42.25	7774.00	855
		16^{00}-17^{00}	41.63	7659.92	843
Total operating cost of the chiller ($) =					6824
II	CAV and VAV	08^{00}-09^{00}	23.46	4316.64	475
		09^{00}-10^{00}	24.25	4462.00	491
		10^{00}-11^{00}	39.33	7236.72	796
		11^{00}-12^{00}	40.45	7442.80	819
		12^{00}-13^{00}	41.36	7610.24	837
		13^{00}-14^{00}	42.02	7731.68	850
		14^{00}-15^{00}	42.38	7797.92	858
		15^{00}-16^{00}	42.25	7774.00	855
		16^{00}-17^{00}	41.63	7659.92	843
		17^{00}-18^{00}	40.88	7521.92	827
		18^{00}-19^{00}	25.50	4692.00	516
		19^{00}-20^{00}	25.00	4600.00	506
		20^{00}-21^{00}	24.52	4511.68	496
		21^{00}-22^{00}	24.04	4423.36	487
		22^{00}-23^{00}	23.59	4340.56	477
		23^{00}-24^{00}	23.19	4266.96	469
Total operating cost of the chiller ($) =					10603

Summary of the results obtained for the operating cost analysis is given in Table 4.25. In the table, also shown is annual operating cost savings due to use of VAV system. For the education building, annual total saving of the VAV system is 21% and 25% for scenarios 1 and 2, respectively. In the case of office center, slightly higher savings were obtained (24% for scenario 1 and 30% for scenario 2).

Table 4.25. Summary of the results obtained from the operating cost analysis

<table>
<tr><th rowspan="2">Building</th><th rowspan="2">Scenario</th><th rowspan="2" colspan="2">System</th><th colspan="3">Operating Cost ($)</th></tr>
<tr><th>Chiller</th><th>Fans</th><th>Total</th></tr>
<tr><td rowspan="8">Education Building</td><td rowspan="4">I</td><td colspan="2">CAV</td><td rowspan="2">8105</td><td>4736</td><td>12841</td></tr>
<tr><td colspan="2">VAV</td><td>2089</td><td>10194</td></tr>
<tr><td rowspan="2">Saving</td><td>$</td><td rowspan="2">0</td><td>2647</td><td>2647</td></tr>
<tr><td>%</td><td>56</td><td>21</td></tr>
<tr><td rowspan="4">II</td><td colspan="2">CAV</td><td rowspan="2">13736</td><td>8420</td><td>22156</td></tr>
<tr><td colspan="2">VAV</td><td>2856</td><td>16592</td></tr>
<tr><td rowspan="2">Saving</td><td>$</td><td rowspan="2">0</td><td>5564</td><td>5564</td></tr>
<tr><td>%</td><td>66</td><td>25</td></tr>
<tr><td rowspan="8">Office Center</td><td rowspan="4">I</td><td colspan="2">CAV</td><td rowspan="2">6824</td><td>4736</td><td>11560</td></tr>
<tr><td colspan="2">VAV</td><td>1998</td><td>8821</td></tr>
<tr><td rowspan="2">Saving</td><td>$</td><td rowspan="2">0</td><td>2738</td><td>2738</td></tr>
<tr><td>%</td><td>58</td><td>24</td></tr>
<tr><td rowspan="4">II</td><td colspan="2">CAV</td><td rowspan="2">10603</td><td>8420</td><td>19023</td></tr>
<tr><td colspan="2">VAV</td><td>2650</td><td>13253</td></tr>
<tr><td rowspan="2">Saving</td><td>$</td><td rowspan="2">0</td><td>5770</td><td>5770</td></tr>
<tr><td>%</td><td>69</td><td>30</td></tr>
</table>

4.5.2. Results of Economic Analysis

Analyses of overall initial and operating costs for two air-conditioning systems were developed in this study. LCC analysis was carried out to compare the VAV and the CAV systems. In the analysis, two economic techniques described above were used for evaluating the systems. Those techniques have been used to examine all of the costs of the two alternative systems (CAV and VAV) and operating scenario over the analysis period, in terms of their present worth value and their uniform equivalent annual value. System life of the VAV and the CAV system is expected to be the same, and it was taken 15 years. The present worth cost technique was used to examine total (initial and operating) costs of the two alternative systems (CAV and VAV) and two operating scenarios (scenario 1 and scenario 2) over the analysis period. Results of the LCC analysis are directly affected by the economic measures. In analysis, annual interest and annual inflation rate were taken respectively 6% and 0%.

For the education building, it was found above that by paying an extra investment of $19938 (Table 4.20) for the VAV system, it is possible to save $2647 for scenario 1 and $5564 for scenario 2 each year from the operating costs (Table 4.25).

Comparison of the results obtained under operating conditions during cooling season for education building, presented in Figures 4.39 to 4.42, shows operating costs of the VAV system is (21%-25%) less than that of the CAV system for keeping the space at a desired level of comfort. However investment is also higher (21%). VAV system has advantage under the operating condition for scenario 1. The total cost of the VAV system at the end of the lifetime (15 year) is 3% lower than that of the CAV system using the present worth cost and equivalent annual cost methods (Figure 4.39). Although VAV system saves $2647 per year (%21), payback period shown in Figure 4.41 is 10.32 years.

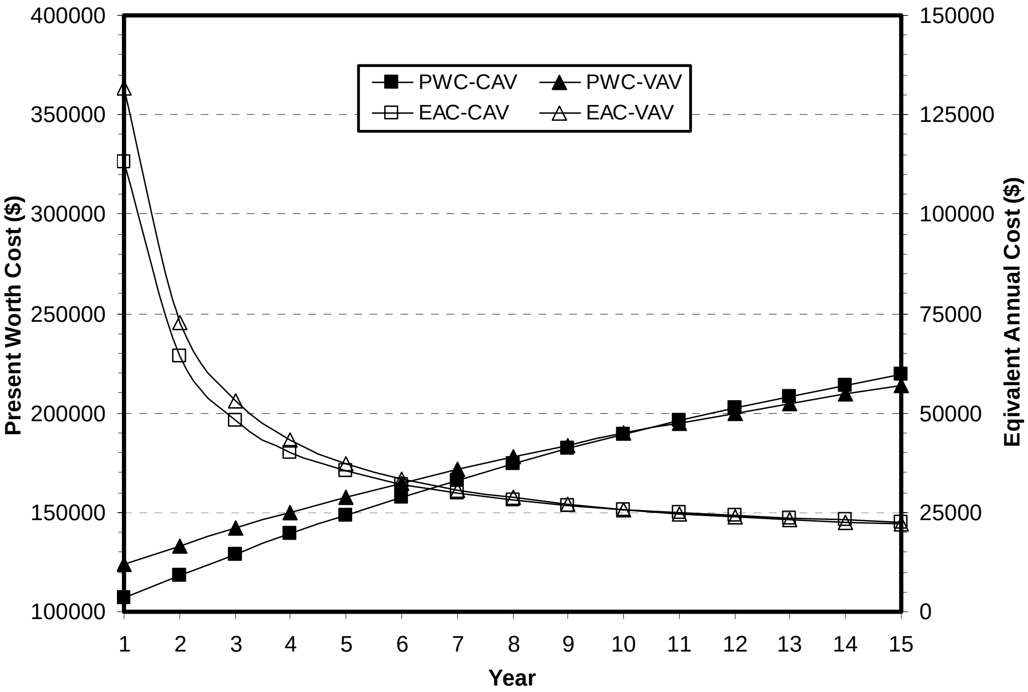

Figure 4.39. Comparison of results obtained using PWC and EAC methods for scenario 1 for education building

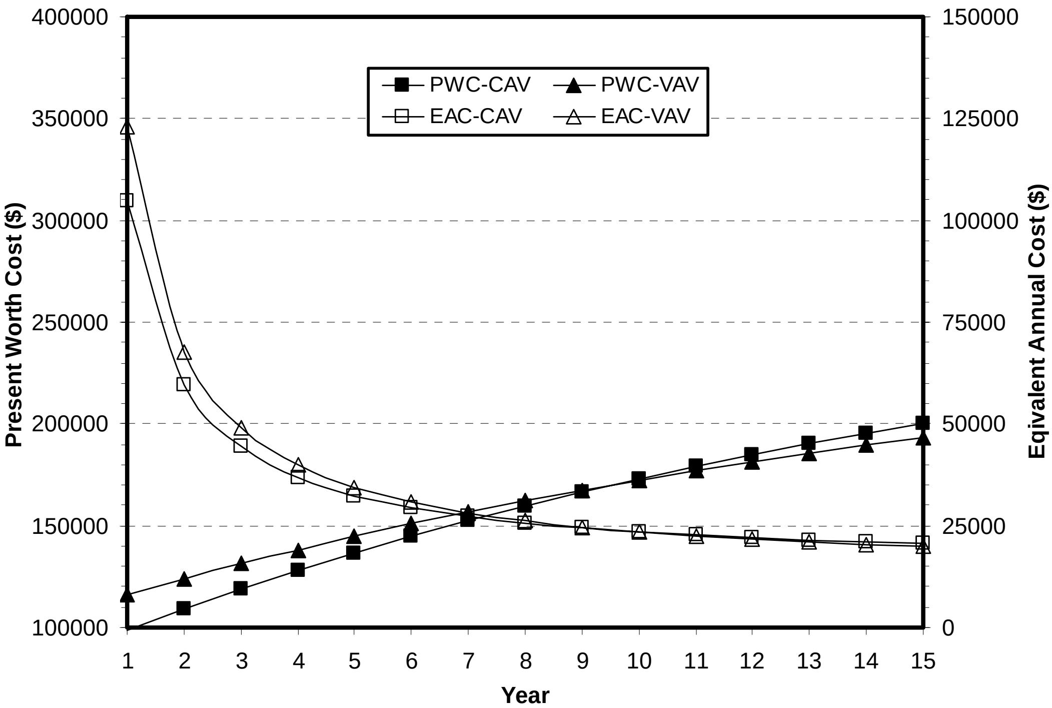

Figure 4.40. Comparison of results obtained using PWC and EAC methods for scenario 2 for education building

In case of scenario 2, VAV system has following advantages due to long operating time. The total cost of the VAV system at the end of the lifetime is found to be 11% lower than that of the CAV system using the two LCC methods used in this study (Figure 4.40). VAV system saves $5565 per year (%25) and payback period that shown in Figure 4.41 is 4.15 years.

The results obtained under operating conditions of the two scenarios at the end of the lifetime for the education building are represented in Figure 4.42.

In case of the use of this building as officer center, it was found above that by paying an extra investment of $19768 (Table 4.20) for the VAV system, it is possible to save $2738 for scenario 1 and $5770 for scenario 2 each year from the operating costs (Table 4.25) respectively.

Comparison of the results obtained under operating conditions during cooling season for office center, are given in Figures 4.43 to 4.46. VAV system has advantage under the operating condition for scenario 1. The total cost of the VAV system is found to be approximately 4% lower than that of the CAV system using the present worth cost method and equivalent annual comparison method (Figures 4.43). Although VAV system saves $2738 per year (%24), payback period is found to be 9.74 years (Figures 4.45).

In case of scenario 2, VAV system has following advantages because operating time of the systems is longer than the other scenario. The VAV system costs 14% less than the CAV system using the two methods considered in this analysis (Figures 4.44) at the end of the lifetime. VAV system saves $5770 per year (%30) and payback period that shown in Figure 4.45 is 3.95 years.

The results obtained in the office center season under operating conditions of the two scenarios for economical analysis is presented in Figure 4.46.

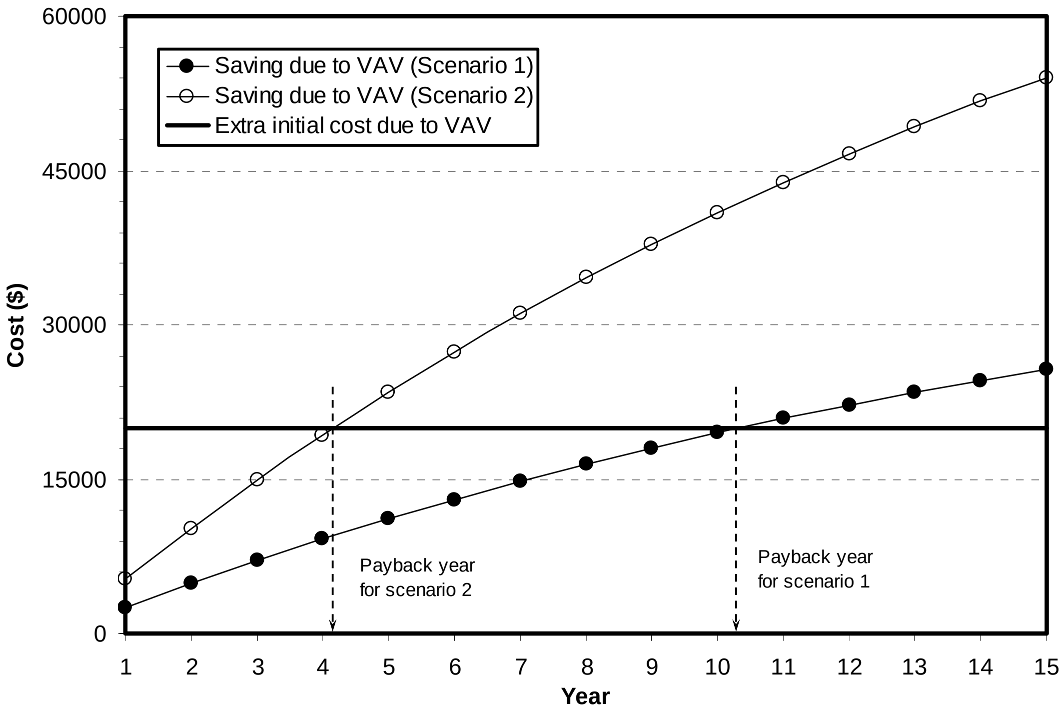

Figure 4.41. The payback period of the VAV system used in the education building

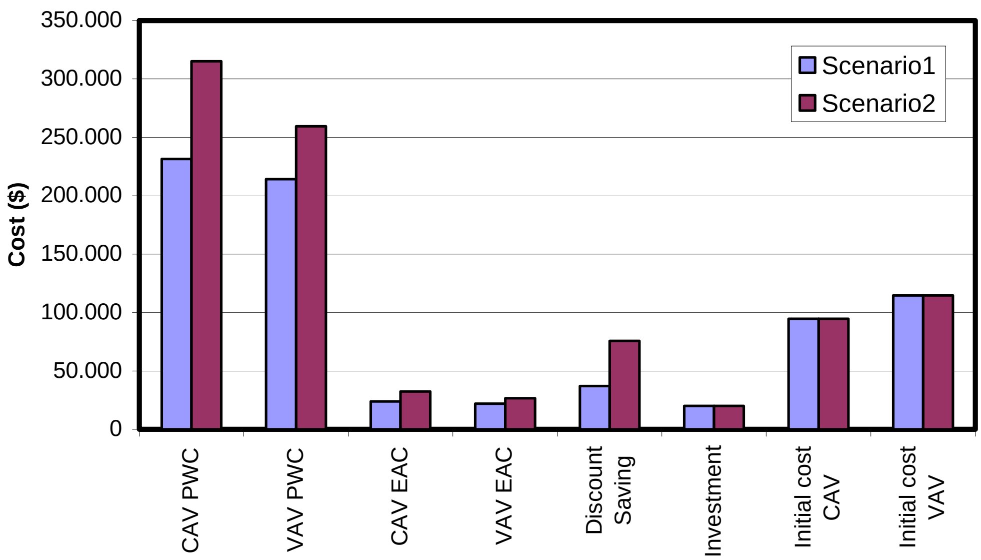

Figure 4.42. The results for the education building at the end of lifetime

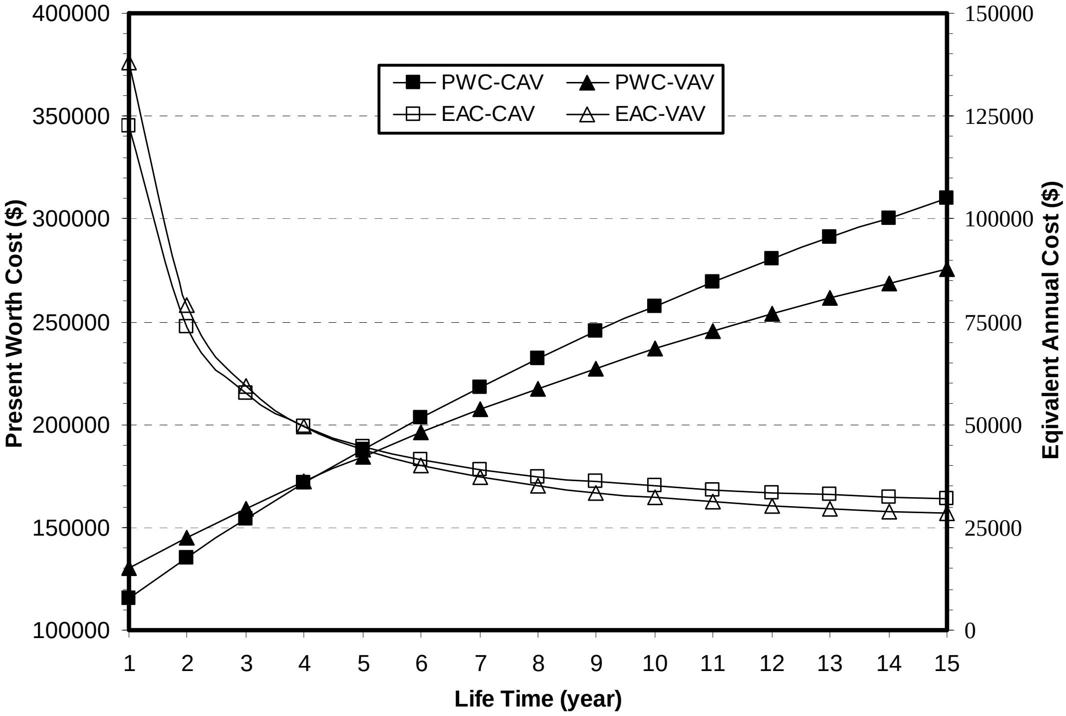

Figure 4.43. Comparison of results obtained using PWC and EAC methods for scenario 1 for office building

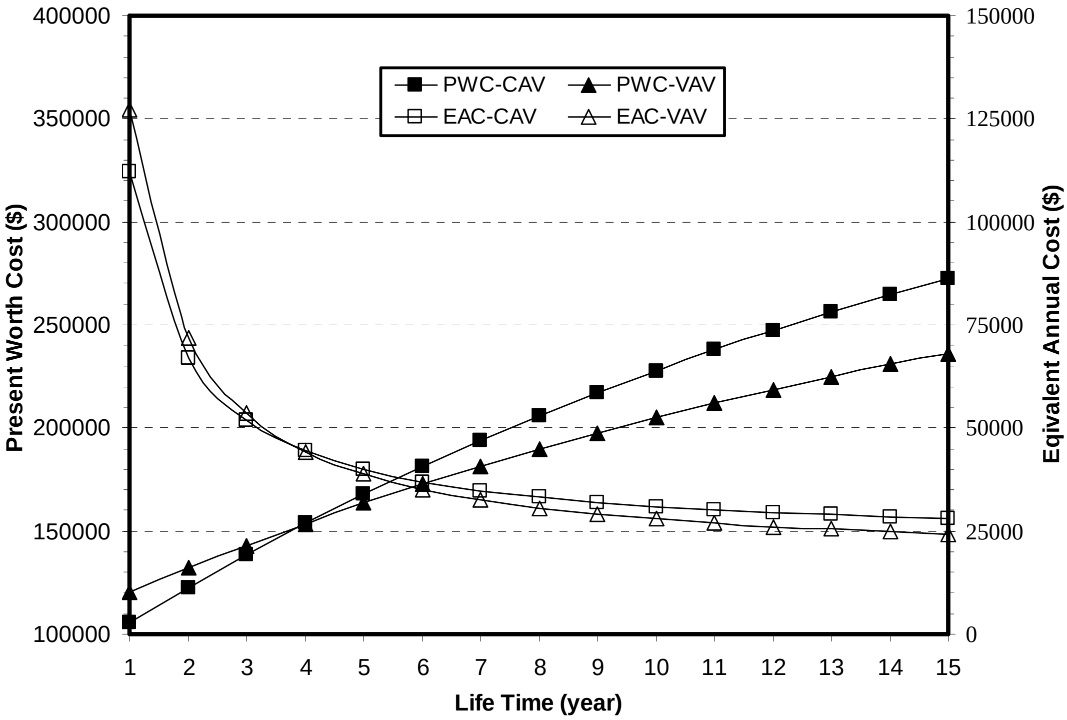

Figure 4.44. Comparison of results obtained using PWC and EAC methods for scenario 2 for office building

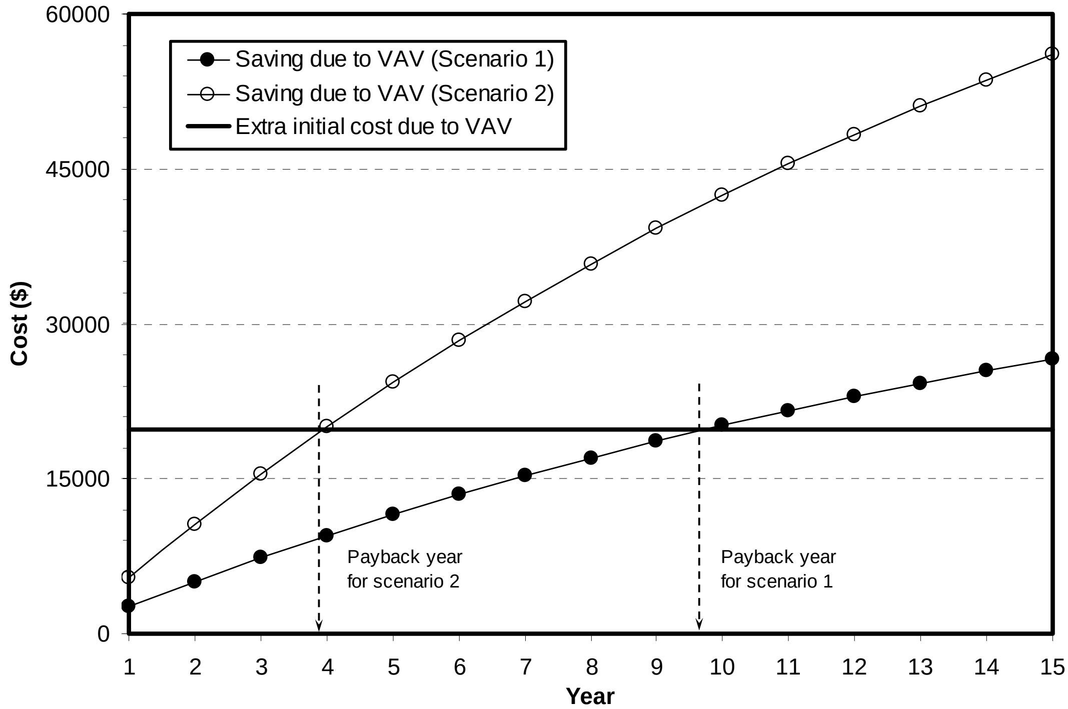

Figure 4.45. The payback period of the VAV system used in office center

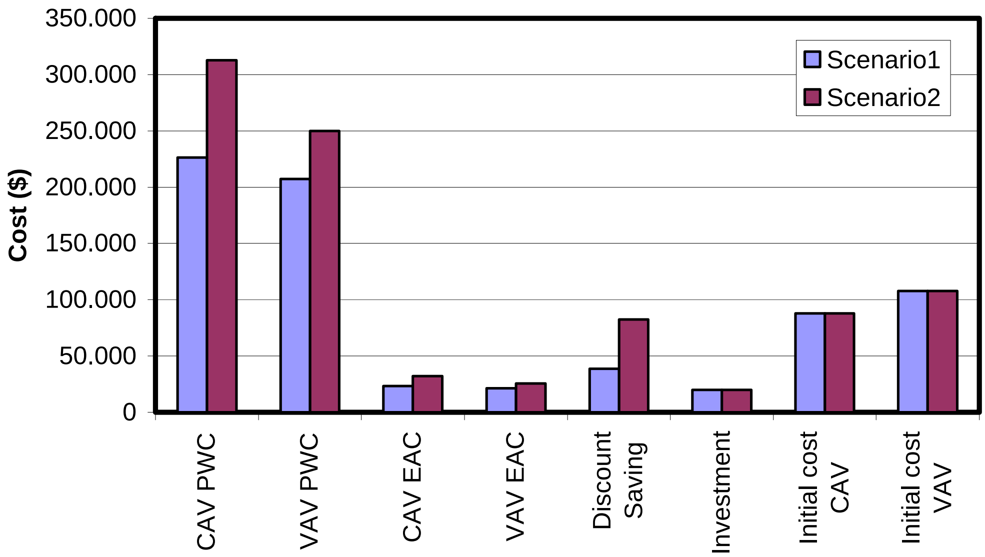

Figure 4.46. Results of the economic analysis for office center

Maximum cooling load of the building occurs only limited hours each year. The maximum cooling load on one side of the building occurs at a different time of the day and often in a different month of the year, than on the another side of the building. At the same time, required total mass flow rates in all zones of the building occur at a different time of the day and in a different month of the year. This situation is the advantage of VAV system.

On the other hand, recently, CAV terminal unit are used in the air conditioning applications in which constant mass flow rate is necessary, for examples for clean rooms; building of theatres and laboratories. Filters, cooling coil and heating coil units in the AHU are polluted gradually under the continuous operation of ACS. Therefore, total mass flow rate requirement is not provided by AHU. For preventing this situation CAV box should be used in the ACS. Initial cost is increased if CAV terminal unit is used in the ACS.

In this study, initial costs of the VAV system for both education building and office center are (21%-23%) higher than initial costs of the CAV system, because the VAV system includes VSDs and VAV box units in addition to CAV system. However, the annual operating cost of the fans in the VAV system for scenario 1 and scenario 2 are (least 56% and 69%) lower than CAV system respectively.

Payback time for VAV system in different scenarios varied between approximately 4 and 10 years (Table 4.26). It can be concluded that, the VAV system is recommended for the applications similar to scenario 2.

Although a shorter payback time is better for an investment, it is difficult to quantify the feasible maximum payback time. An investment is considered roughly to be “excellent” if payback time is less than one-third of the lifetime of the investment. It is “good” if the payback time is less than one-half of the lifetime [Kreider and Rabl, 1997]. A high performance building can be designed at little or no cost premium with annual energy savings of 20%-50% compared to an average building. Paybacks of only one to five years are common [Kolderup et all, 2003].

If one follows this rule of thumb, a VAV based air-conditioning system for both buildings (school and office) is “excellent” for scenario 2. With the economic conditions, the VAV system is not economically alternative for scenario 1 for both buildings. If a long period of operating hours present (scenario 2), the VAV system becomes very attractive, and the investment can be described “excellent”.

Table 4.26. Life-cycle cost analysis results for scenarios 1 and 2

Building	Scenario	System	PWC at the end of Lifetime	Payback year of VAV system	Comment
Education Building	I	VAV	$213576	10.32	Normal
		CAV	$219347		
	II	VAV	$275718	4.15	Excellent
		CAV	$309817		
Office Center	I	VAV	$193292	9.74	Normal
		CAV	$200120		
	II	VAV	$236330	3.95	Excellent
		CAV	$272602		

5. CONCLUSION

Energy consumption in Turkey has risen dramatically over the past 20 years due to the combined demands of industrialization and urbanization. Domestic energy production has not exceeded half of energy demand. Turkey imports over 65% of energy consumption because of its limited energy resources. Recently, HVAC systems have commonly been used in a space to provide conditions for thermal comfort and indoor air quality (IAQ) in a building. Consequently, there is an increasing trend in energy consumption in Turkey like world energy consumption.

The performance of HVAC equipment changes with outdoor climatic conditions. The better the design heating and cooling applications in buildings, the more energy efficiently comfortable buildings can be obtained. Outdoor design conditions are weather data information for design purposes, which show the characteristic features of the climate at a particular location. They affect building loads and economical design. The effect of incorrect selection of outdoor conditions can be dramatic. In Turkey, HVAC systems are designed using the peak outdoor design conditions. The peak load occurs only a few hours each year and the peak load on one side of the building occurs at a different time of day and often in a different month of the year, than on another side of the building. This may lead to an uneconomic design and oversizing may result in HVAC applications. Actually, the space requires only part of the designed capacity of the conditioning equipment most of the time.

In this study, influence of outdoor air conditions on air conditioning system for a sample building was investigated and analyzed.

5.1. Building Cooling load

Hourly total cooling load of a sample building was calculated by a computer program called CoolingLoadRTS which was developed in this study according to RTS method. This is latest load calculation method suggested by ASHRAE. Detailed hourly profile of the building cooling load for design day and cooling season was determined and analyzed for Adana and some provinces of Turkey in this study. In addition, the results of the building cooling load obtained using RTS and CLTD/SCL/CLF cooling load calculation methods were compared. It was found that the maximum total cooling load calculated using the RTS is 10% higher at 13^{00} o'clock than that is obtained using the CLTD/SCL/CLF method. The difference between the total building cooling loads which were computed using two methods is explained by the difference between the cooling loads due to windows and equipments. A general agreement between the results of the total cooling load obtained using the RTS and the CLTD/SCL/CLF methods was observed.

RTS method is suggested for calculation of hourly cooling load in detail, because it is simple and more accurate than current simplified methods.

5.2. Cooling Coil Load

In this study, three computer programs were developed in order to simulate hourly operating of the air conditioning systems and determine the coiling coil load. They were written in FORTRAN programming language. The first computer program given in Appendix A2 (P_CCWT) was written to determine the condition of the supply air (the air conditions leaving the coil) under the condition of constant coil wall temperature. The second program given Appendix A3 (P_VAV) can be used to calculate the apparatus dew-point temperature (coil wall temperature) and amount of variable air volume under the condition of constant supply air temperature. The third computer program given Appendix A4 (P_CAV) was written to determine the condition of the supply air (the air conditions leaving the coil) under the conditions of constant air volume.

Cooling coil operating capacity for the design day and real operating conditions during cooling season was analyzed by the programs developed for different air distribution systems (constant and variable volume air systems). Influence of outdoor air conditions on operating capacity of air conditioning systems was investigated and discussed. Hourly psychometric properties, hourly cooling coil load, hourly total and mass flow rate were calculated by computer programs. It was found that they are significantly affected by changing outside conditions. Results show that the hourly mass flow rate and cooling demand of building is greatly changed as function of time during operating time period.

In addition, design cooling coil load and the parameter considered were calculated for the currently used in Turkey and different outdoor design conditions suggested by ASHRAE for Adana in order to compare equipment capacities of HVAC. Results show that the design cooling coil capacity obtained with current design conditions used in Turkey is higher than that obtained with alternative outdoor design conditions sets considered in this study. For a set of design conditions, it is seen that the risk level has almost an influence on the design cooling coil capacity.

5.3. Economic Analysis

In this study, constant-air-volume (CAV) and variable-air-volume (VAV) air-conditioning systems were compared calculating initial and operating costs for a sample building located in Adana-Turkey. For comparison, life-cycle cost analysis was used with the present worth cost (PWC) and annual equivalent cost (EAC) methods and comparison was made for different cases. It was found that present worth cost (PWC) and annual equivalent cost (EAC) of the VAV system is always lower than that of the CAV system at the end of the lifetime for all the cases considered. The extra investment of the VAV system with respect to the CAV system pays itself back after approximately 10 years for scenario 1 and 4 years for scenario 2. Results of the economic analyses show that VAV air conditioning system is more economical than conventional air-conditioning system for nonresidential building such as education building and office center in special.

REFERENCES

AL-HOMOUD, M.S., 1997. Optimum Thermal Design of Office Buildings. International Journal of Energy Research, 21:941-957.

AL-RABGHI, O.M., and AL-JOHANI, K.M., 1997. Utilizing Transfer Function Method for Hourly Cooling Load Calculations. Energy Conversion and Management 38(4):319-332.

AL-RABGHI, O.M., AL-BEIRUTTY, M.H., and FATHALAH, K.A., 1999. Estimation and Measurement of Electric Energy Consumption Due To Air Conditioning Cooling Load. Energy Conversion & Management, 40:1527-1542.

ARCH, 2005. Air Conditioning System, Department of Architecture, The University of Hong Kong, http://www.arch.hku.hk/~kpcheung/new2001/ac/

ARONOFF, S., and KAPLAN, A., 1997. Total Workplace Performance, WDL Publication, Canada, ISBN 0-921804-95-4.

ASHRAE, 1993. ASHRAE Handbook-1993 Fundamentals, American Society of Heating, Refrigerating and Air-Conditioning Engineers, Atlanta.

ASHRAE, 1997. ASHRAE Handbook-1997 Fundamentals, American Society of Heating, Refrigerating and Air-Conditioning Engineers, Atlanta.

ASHRAE, 2001. ASHRAE Handbook-2001 Fundamentals, American Society of Heating, Refrigerating and Air-Conditioning Engineers, Atlanta.

ATMACA, H., 2003. Binalarda Soğutma Yükü Hesabı Yapan Bir Bilgisayar Programı. Mühendislik Bilimleri Genç Araştırmacılar 1. Kongresi, 17-20 Şubat 2003, İstanbul.

BALARAS, C.A., 1996. The Role of Thermal Mass on the Cooling Load of Buildings. An Overview of Computational Methods. Energy and Buildings 24:1-10.

BAUMGARTH, S., HÖRNER, B., and REEKER, J., 2000. Handbuch Der Klimatechnik, 4. Auflage, Band 1, Grundlagen, Verlag, C.F.Müler, Heidelberg.

BELLIA, L., MAZZEI, P., MINICHIELLO, F. and PALOMBO, A., 2000. Outdoor-Air Design Conditions Relating To the Capacity of Air-Conditioning Systems. International Journal of Energy Research 24:121-135.

BULUT, H., 2001. Determination of Weather Data for Turkey for Heating and Cooling Systems. PhD Thesis, Çukurova University, Adana.

BULUT, H., BÜYÜKALACA O., ve YILMAZ, T., 1999. Türkiye'nin 15 ili için Bazı İklim Verilerinin Eşitliklerle İfadesi, TMMOB Makina Mühendisleri Odası, Tesisat Mühendisliği Dergisi, 51: 48-56.

BULUT, H., BÜYÜKALACA O., and YILMAZ, T., 2002. New Outdoor Cooling Design Data for Turkey, Energy 27:923-946.

CHECKET, B., 2002. HVAC Load Calculations, Old and New, Air Conditioning, Heating/ Refrigeration the News Agust 5.

CSE, 2005, "Variable Air Volume System with VSD Fan Control", CSE Industrial Electrical Distributors, http://www.cse-distributors.co.uk/abbdrives/ abb_case_studies/VSD_fan _control .htm

DAĞSÖZ, A.K., ve YÜKSEL, H.M., 2000. Yapılarda Isı Yalıtımının Bireylere ve Ülkemiz Ekonomisine Katkıları. Enerji 2000-Ulusal Enerji Verimliliği Kongresi Bildiriler Kitabı, Ankara, 97-107.

DANIEL, C., WOOD, F.S., and GORMAN,J.W., 1971. Fitting Equations to Data. John Wiley&Sons, Inc. USA.

DAVIES, M.G., 1999. Current Methods to Handle Wall Conduction and Room Internal Heat. ASHRAE Transactions 105(1):142-153.

Devlet Meteoroloji İşleri Genel Müdürlüğü, Meteorolojik verileri (DMİ), 1981-1998, Ankara.

DRAGAN, A., 2000. HVAC Design Approach and Design Criteria for Health Care Facilities. ASHRAE Transaction: Annual Meeting, 637-645.

EALIWA, M.A., TAKI, A.H., HOWARTH, A.T. and SEDEN, M.R., 2001. An Investigation into Thermal Comfort in the Summer Season of Ghadames, Libya. Building and Environment 36:231-237.

Economic Analysis Handbook, 1993. Naval Publications (SN 0525-LP-543-5200), Philadelphia, NAVFAC P-442.

ELOVITZ, D.M., 2002. Selecting the Right HVAC System. ASHRAE Journal January 2002 24-30.

ELSAFTY, A., and AL-DAINI, A.J., 2002. Economical Comparison Between A Solar Powered Vapor Absorption Air-Conditioning System And A Vapor Compression System In The Middle East, Renewable Energy 25:569–583.

Energy Information Administration (EIA), International Energy Outlook 2003, Washington, DC, February 2003 USA.

ESKİN, N., ve TÜRKMEN, H.İ., 2003. Konutdışı Binaların Soğutma Yüklerinin Transfer Fonksiyonu Yöntemi ile Hesaplanması. VI. Ulusal Tesisat Mühendisliği Kongresi ve Sergisi (TESKON 2003), 8-11 Ekim 2003, İzmir.

HARRISON, B., 2004. Diversity Design Provides Safety and Lower Costs for Allelix Biopharmaceuticals, Phoneix Control Corporation, Acton Massachusetts USA.(http:/www.phoenixcontrols.com/solutions/allelix.pdf)

HASAN, A., 1999. Optimizing Insulation Thickness for Buildings Using Life Cycle Cost, Applied Energy 63:115-124.

HASSID, S., SANTAMOURIS, M., PAPANIKOLAOU, N., LINARDI, N., KLITSIKAS, N., GEORGAKIS, C., and ASSIMAKOPOULOS, D.N., 2000. The Effect of the Athens Heat Island on Air Conditioning Load. Energy and Buildings, 32:131-141.

HOSNI, M.H., JONES, B.W., and HANMING, X., 1999. Experimental Results for Heat Gain and Radiant/Convective Split from Equipment in Buildings. ASHRAE Transactions 105(1):527-539.

HOSNI, M.H., JONES, B.W., SIPES, J.M., and YUE, X., 1998. Total Heat Gain and Split between Radiant and Convective Heat Gain from Office and Laboratory Equipment in Buildings. ASHRAE Transactions 104(1):356-365.

HUI, S.C.M., 1999. Web-based information system for energy efficient technologies in HVAC and the built environment, In Proc. Of the 1999 Asia-Pacific Conference on Built Environment, 29 November-2 December 1999, Taipei, Taiwan.

JOHNSON, R.A., and BHATTACHARYYA, G.K., 1996.Statistics:Principles and Methods, John Wiley&Sons, Inc. Canada.

JOUDI, K.A., and DHAIDAN, N.S., 2001. Application of Solar Assisted Heating and Desiccant Cooling System for a Domestic Building. Energy Conversion and Management 42:995-1022.

JOUDI, K.A., and SALAH, M.M., 2000. Application of Indirect Evaporative Cooling To Variable Domestic Cooling Load. Energy Conversion and Management 42:995-1022.

KILKIŞ, B., 1991. Binaların Isıtılmasında Doğal Gaz Kullanımı: Tasarruf Olanakları ve Yeni Seçenekler. Ankara Sanayi Odası Yayını:7-11.

KOLDRUP, E., HONG, T., TAYLOR, S. and STEIN, J., 2003. Advanced VAV System Design Guide, California Energy Commission.

KOSSECKA, E., and KOSNY, J., 2002. Influence of Insulation Configuration on Heating and Cooling Loads in a Continuously Used Building. Energy and Buildings 34:321-331.

KREIDER, J.F., and RABL, A., 1994. Heating and Cooling of Buildings, McGraw-Hill Inc., America, ISBN 0-07-834776-9.

KÜÇÜKÇALI, R., 2003. Klima Sistemlerinde Enerji Ekonomisi ve Uygulama Önerileri, VI.Ulusal Tesisat Mühendisliği Kongresi ve Sergisi, (TESKON) İzmir .

LEE, W.L.A., YIK, F.W.H., and JONES, P., 2003. A Strategy for Prioritizing Interactive Measures for Enhancing Energy Efficiency of Air-Conditioned Buildings, Energy 28:877–893.

LI, D.H.W., and LAM, J. C., 2001. Analysis of Solar Heat Gain Factors Using Sky Clearness Index and Energy Implications. Energy Conversion and Management 42:555-571.

LI, D.H.W., WONG, S.L., and LAM, J. C., 2003. Climatic Effect on Cooling Load Determination in Subtropical Regions. Energy Conversion and Management 44:1831-1843.

LIESEN, R.J., and PEDERSEN, C.O., 1997. An Evaluation of Inside Surface Heat Balance Models for Cooling Load Calculations. ASHRAE Transactions 103(2):485-502.

LIESEN, R.J., STRAND R.K., and PEDERSEN, C.O., 1998. The Effect of Varying the Radiative/Convective Split for Internal Gains on Cooling Load Calculations: A Case Study for the Pentagon. ASHRAE Transactions 104(2):1790-1802.

MATHEWS, E.H., ARNDT, D., and GEYSERB, M.F., 2002. Reducing the Energy Consumption Of A Conference Centre—A Case Study Using Software. Building and Environment 37:437-444.

MCCLELLAN, T.M., and PEDERSEN, C.O., 1997. Investigation of Outside Heat Balance Models for Use in a Heat Balance Cooling Load Calculation Procedure. ASHRAE Transactions 103(2):469-484.

MCQUISTON, F.C., and SPITLER J.D., 1992. Cooling and Heating Load Calculation Manuel ASHRAE, Inc.

MOUJAES, S.F., and BRICKMAN, R.A., 1998. Effect of a Radiant Barrier on the Cooling Load of a Residential Application in a Hot and Arid Region: Attic Duct Effect. International Journal of HVAC&R RESEARCH 4(3):231-244.

MUMMA, S.A., and BOLIN, R.J., 1997. Energy Optimized-Ventilation Constrained VAV System Control, Automation in Construction 6:463-470.

OEE, 2004. Use of Variable Frequency Drives for Fan and Pump Control, Office of Energy Efficiency, Natural Resources Canada, ISBN-0-662-315-1. (http://oee.nrcan.gc.ca/eii/)

Office of Energy Efficiency and Renewable Energy (EERE):2004. Sizing Residential Heating and Air Conditioning Systems. Department of Energy, USA.

OĞULATA, R.T., ve YILMAZ, T., 1989. Çevre Sıcaklığının Zamansal Değişiminin Eşitliklerle Hesaplanması, Ç. Ü. Müh. Mim. Fak., Dergisi, 4(1):85-95.

ÖNEN, E., 1985. Havalandırma ve Klima Tesisatı, Bayındırlık ve İskan Bakanlığı, Teknik Yayınlar:9, Başbakanlık Basımevi, Ankara.

ÖZKUL, N., 1985. Uygulamalı Soğutma Tekniği, Makine Mühendisleri Odası Yayın No:115, Ankara.

PAN, Y., ZHOU, H., HUANG, Z., ZENG, Y., and LONG, W., 2003. Measurement and Simulation of Indoor Air Quality and Energy Consumption in Two Shanghai Office Buildings with Variable Air Volume Systems, Energy and Buildings 35:877–891.

PAPADOPOULOS M.A., 2001. The Influence of Street Canyons on the Cooling Loads of Buildings and the Performance Air Conditioning Systems. Energy and Buildings 33:601-607.

PEDERSEN, C.O., FISHER, D. E., and LIESEN, R.J., 1997. A Heat Balance Based Cooling Load Calculation Procedure. ASHRAE Trans. 103(2):459-468.

POWELL, F.L., 2002. Calculating the Saving for Reducing Fan Volume Using the Fan Laws, TABB Talk: The Newsletter of The Professional's Choice, Winter 2002, Issue No.2.

REDDY, T.A., LIU, M., and CLARIDGE D.E., 1998. A Study of Energy Use and Satisfactory Zone Ventilation of Different Outdoor Air Ventilation Strategies for Terminal Reheat Variable Air Volume Systems, Energy and Buildings 29:65-75.

REES, S.J., SPITLER, J.D., and HAVES P., 1998. Quantitative comparison of North American and U.K. Cooling Load Calculation Procedures- Results. . ASHRAE Transactions 104(2):36-46.

REES, S.J., and SPITLER, J.D., 1999. Proposals for a building Loads Diagnostic Test Procedure. ASHRAE Transactions 105(1):514-519.

SAWHNEY, R.L., BUDDHI, D., and THANU, N.M., 1999. An Experimental Study of Summer Performance of a Recirculation Type Underground Airpipe Air Conditioning System. Building and Environment 34:189-196.

SHARIAH, A., TASHTOUSH B., and ROUSAN, A., 1997. Cooling and Heating Loads in Residential Buildings in Jordan. Energy and Buildings 26:137-143.

SPITLER, J.D., and FISHER, D.E., 1999. On The Relationship between the Radiant Time Series and Transfer Function Methods for Design cooling load Calculations. HVAC&RESEARCH 5(2):125-138.

SPITLER, J.D., and REES, S.J., 1998. Quantitative comparison of North American and U.K. Cooling Load Calculation Procedures- Methodology. ASHRAE Transactions 104(2):47-61.

SPITLER, J.D., FISHER, D.E., and PEDERSEN, C.O., 1997. The Radiant Time Series Cooling Load Calculation Procedure. ASHRAE Transactions 103(2):503-515.

Thermal Insulation Regulation in Buildings. Ankara: Official gazette (24043), 8 May 2000.

TIANZHEN, H., CHOU, S.K., and BONG, T.Y., 1999. A Design Day for Building Load and Energy Estimation. Building and Environment, 34:469-477.

Turkish Standard 825. Thermal insulation in buildings. Ankara: Official gazette (23725), 14 June 1999.

U.S. Energy Protection Agency (EPA), 1991. Indoor Air Facts No:4 Sick Building Syndrome. http://www.epa.gov/iaq/pubs/sbs.html

WIEL, S., MARTIN, N., LEVINE, M., PRICE, L., and SATHAYE, J., 1998. The role of building energy efficiency in managing atmospheric carbon dioxide, Environmental Science&Policy, vol.1, no.1:27-38.

World Energy Council Turkish National Committee (WECTNC). Energy report 1999. Ankara: WECTNC, 2000.

World Energy Council Turkish National Committee (WECTNC). Energy balances 2002. Ankara: WECTNC, 2003.

YIK, F.W.H., BURNETT, J., and PRESCOTT, I., 2001. Predicting Air-Conditioning Energy Consumption of a Group of Buildings Using Different Heat Rejection Methods. Energy and Buildings. 33:151-166.

YILMAZ, T., ÖZGÖREN, M., ve GÜRÇINAR, Y., 1995. Mutlak Nemin Günlük ve Yıllık Değişimi, 10. Ulusal Isı Bilimi ve Tekniği Kongresi Bildiriler Kitabı, Ankara, Sayfa 593-602.

YILMAZ, T., ve BULUT, H., 1996. Şanlıurfa İli İçin Meteorolojik Değerlerin Günlük, Yıllık Değişiminin Sürekli Fonksiyonlarla İfadesi, 4. Ulusal Soğutma ve İklimlendirme Tekniği Kongresi Bildiriler Kitabı, Adana, Sayfa 188-198.

CURRICULUM VITAE

Mehmet Azmi AKTACİR was born on November 29, 1973 in Şanlıurfa. After being graduated from premier and high School in Şanlıurfa, he enrolled in Mechanical Engineering Department of Fırat University. He graduated from Fırat University as a Mechanical Engineer in June 1993. He started his Master of Science education in the Department of Mechanical Engineering, Harran University in 1993. He graduated from Harran University in 1995. He worked as a research assistant in the Department of Mechanical Engineering of Harran University between 1993 and 2000. He has been working as a research assistant in the Department of Mechanical Engineering Çukurova University since 2000. He is married and has a son.

APPENDIX A1

In this thesis, a program named CoolingLoadRTS was developed in order to calculate the building cooling load. The program was written on MS-EXCEL according to RTS method procedure. CoolingLoadRTS consists of 7 spreadsheets shown in Figure A1.1 to A1.7. Hourly outdoor air temperatures using outdoor design temperature and daily range are given in Figure A1.1. Hourly solar-air temperatures calculated from Equation (3.26.) are given in Figure A1.2. Figures A1.3 and A1.4 present hourly fenestration total cooling load and hourly total cooling load of the external surfaces (Wall and Roof) respectively. Figure A1.5 shows hourly total cooling loads due to internal heat gain (people, lighting and equipment). Figure A1.6 shows hourly total cooling load from interior surface (interior wall, ceiling and floor). Parts of building total cooling load each component and building total cooling load are shown at Figure A1.7. For full details, chapter 3 of this thesis should be consulted. Coefficients (RTS, CTS, A, B, C, etc.) used in CoolingLoadRTS was taken from ASHRAE Fundamental Handbook 2001.

Tdesign
38
Daily Range
12,4

TIME	Tout_air
1	27,2
2	26,6
3	26,1
4	25,7
5	25,6
6	25,8
7	26,5
8	27,6
9	29,2
10	31,1
11	33,2
12	35,1
13	36,6
14	37,6
15	38,0
16	37,6
17	36,8
18	35,4
19	33,8
20	32,2
21	30,8
22	29,6
23	28,6
24	27,8

Figure A1.1. Spreadsheet based on MS-Excel according to RTS procedure to determine outdoor air temperature

Latitude	Declination
36,59	20,6

ET	-6,2
LON	35,18
LSM	30
A	1085
B	0,207
C	0,136
ρg	0,2
α/ho	0,052

Vertical	Ψ
Norht	180
Sorth	0
East	-90
West	90

Σ	90

Horizantal	
Ψ	0
Σ	0

SOLAR-AIR TEMPERATURE					
TIME	North	East	Sorth	West	Horizantal
1	27,2	27,2	27,2	27,2	23,5
2	26,6	26,6	26,6	26,6	22,9
3	26,1	26,1	26,1	26,1	22,4
4	25,7	25,7	25,7	25,7	22,0
5	26,6	27,8	25,8	25,8	22,3
6	35,4	54,6	28,4	28,4	32,1
7	35,2	65,9	30,7	30,7	43,6
8	33,2	68,2	34,8	33,2	54,8
9	35,8	65,4	42,6	35,8	64,8
10	38,3	56,9	48,0	38,3	72,8
11	40,8	50,4	54,3	40,8	78,5
12	42,9	42,9	56,9	46,4	81,3
13	44,2	44,2	56,7	59,2	80,6
14	44,6	44,6	53,8	69,9	76,7
15	44,1	44,1	48,6	76,9	69,8
16	44,5	42,6	42,6	78,5	60,1
17	46,5	40,3	40,3	72,6	48,7
18	42,4	36,8	36,8	53,2	36,4
19	33,8	33,8	33,8	33,8	30,1
20	32,2	32,2	32,2	32,2	28,5
21	30,8	30,8	30,8	30,8	27,1
22	29,6	29,6	29,6	29,6	25,9
23	28,6	28,6	28,6	28,6	24,9
24	27,8	27,8	27,8	27,8	24,1

Figure A1.2. Spreadsheet based on MS-Excel according to RTS procedure to determine sol-air temperature

Troom
26

North	
Area	12
U	2,4
Sorth	
Area	0
U	2,4
East	
Area	0
U	2,4
West	
Area	0
U	2,4

latitude	Declination
36,59	20,6

θ	SGHC
0	0,86
40	0,84
50	0,82
60	0,78
70	0,67
80	0,42
90	0
Σ	90
$(SGHC)_D$	0,78
ET	-6,2
LON	35,18
LSM	30
A	1085
B	0,207
C	0,136
ρg	0,2

Glass Split Ratio	
Radiant	Convection
1	0

WINDOW Solar RTS
0,54
0,16
0,08
0,04
0,03
0,02
0,01
0,01
0,01
0,01
0,01
0,01
0,01
0,01
0,01
0,01
0,01
0,01
0,01
0,00
0,00
0,00
0,00
0,00

WINDOWS COOLING LOAD					
TIME	North	Sorth	East	West	TOTAL
1	162	0	0	0	162
2	140	0	0	0	140
3	120	0	0	0	120
4	103	0	0	0	103
5	187	0	0	0	187
6	924	0	0	0	924
7	1009	0	0	0	1009
8	1011	0	0	0	1011
9	1156	0	0	0	1156
10	1305	0	0	0	1305
11	1425	0	0	0	1425
12	1496	0	0	0	1496
13	1514	0	0	0	1514
14	1484	0	0	0	1484
15	1395	0	0	0	1395
16	1329	0	0	0	1329
17	1417	0	0	0	1417
18	1275	0	0	0	1275
19	617	0	0	0	617
20	434	0	0	0	434
21	332	0	0	0	332
22	271	0	0	0	271
23	224	0	0	0	224
24	190	0	0	0	190

Figure A1.3. Spreadsheet based on MS-Excel according to RTS procedure to determine window cooling load z01

WALL				ROOF
North	Sorth	East	West	Horizonta
U	U	U	U	U
0,61	0,61	0,61	0,61	0,42
Area	Area	Area	Area	Area
16,5	0	0	12	0
Troom	Troom	Troom	Troom	Troom
26	26	26	26	26

Wall Split Ratio	
Radiant	Conv.
0,63	0,37

Roof Split Ratio	
Radiant	Conv.
0,84	0,16

WALL		ROOF	
CTS	Nonsolar RTS	CTS	Nonsolar RTS
0,01	0,41	0,02	0,41
0,01	0,20	0,02	0,20
0,03	0,12	0,05	0,12
0,06	0,08	0,06	0,08
0,07	0,05	0,07	0,05
0,08	0,04	0,07	0,04
0,08	0,03	0,06	0,03
0,08	0,02	0,06	0,02
0,08	0,01	0,06	0,01
0,07	0,01	0,05	0,01
0,06	0,01	0,05	0,01
0,06	0,01	0,05	0,01
0,05	0,01	0,04	0,01
0,04	0,00	0,04	0,00
0,04	0,00	0,04	0,00
0,03	0,00	0,04	0,00
0,03	0,00	0,03	0,00
0,03	0,00	0,03	0,00
0,02	0,00	0,03	0,00
0,02	0,00	0,03	0,00
0,02	0,00	0,03	0,00
0,01	0,00	0,03	0,00
0,01	0,00	0,02	0,00
0,01	0,00	0,02	0,00

WALL &ROOF COOLING LOAD	
TIME	TOTAL
1	199
2	190
3	178
4	166
5	152
6	139
7	125
8	113
9	103
10	95
11	89
12	86
13	86
14	90
15	98
16	110
17	126
18	145
19	164
20	182
21	195
22	203
23	206
24	204

Figure A1.4. Spreadsheet based on MS-Excel according to RTS procedure to calculate wall and roof cooling load

z01

People Load	
Sensible	75
Latent	55
People	5
Split ratio	
Radiant	Conv.
0,58	0,42

Lighting	
Heatgain	480
Split ratio	
Radiant	Conv.
0,59	0,41

Equipment	
Sensible	2000
Latent	0
Split ratio	
Radiant	Conv.
0,7	0,3

PEOPLE			
		TOTAL CL	
TIME	Occup	Sensible	Latent
1	0	8	0
2	0	6	0
3	0	5	0
4	0	3	0
5	0	2	0
6	0	0	0
7	0	0	0
8	1	223	275
9	1	255	275
10	1	274	275
11	1	287	275
12	1	295	275
13	1	301	275
14	1	306	275
15	1	309	275
16	1	311	275
17	1	312	275
18	0	91	0
19	0	61	0
20	0	43	0
21	0	30	0
22	0	22	0
23	0	16	0
24	0	11	0

LIGHTING				
TIME	Ful	Fsa	Occup	TOTAL CL
1	1	0,3	0	4
2	1	0,3	0	3
3	1	0,3	0	3
4	1	0,3	0	2
5	1	0,3	0	1
6	1	0,3	0	0
7	1	0,3	0	0
8	1	0,3	1	94
9	1	0,3	1	111
10	1	0,3	1	121
11	1	0,3	1	128
12	1	0,3	1	132
13	1	0,3	1	136
14	1	0,3	1	138
15	1	0,3	1	140
16	1	0,3	1	141
17	1	0,3	1	141
18	1	0,3	0	48
19	1	0,3	0	32
20	1	0,3	0	23
21	1	0,3	0	16
22	1	0,3	0	12
23	1	0,3	0	8
24	1	0,3	0	6

EQUIPMENT				
			TOTAL CL	
TIME	Ful	Occup	Sensibl	Latent
1	1	0	70	0
2	1	0	56	0
3	1	0	42	0
4	1	0	28	0
5	1	0	14	0
6	1	0	0	0
7	1	0	0	0
8	1	1	1174	0
9	1	1	1454	0
10	1	1	1622	0
11	1	1	1734	0
12	1	1	1804	0
13	1	1	1860	0
14	1	1	1902	0
15	1	1	1930	0
16	1	1	1944	0
17	1	1	1958	0
18	1	0	798	0
19	1	0	532	0
20	1	0	378	0
21	1	0	266	0
22	1	0	196	0
23	1	0	140	0
24	1	0	98	0

Figure A1.5. Spreadsheet based on MS-Excel according to RTS procedure to calculate cooling load due to internal heat gains z01

INTERIOR SURFACES				
Wall1	Wall2	Wall3	Ceiling	Floor
U	U	U	U	U
1,75	1,75	1,75	1,6	1,6
Area	Area	Area	Area	Area
10	10	10	45	45
Troom	Troom	Troom	Troom	Troom
26	26	26	26	26

Wall Split Ratio	
Radiant	Conv.
0,63	0,37

Roof Split Ratio	
Radiant	Conv.
0,84	0,16

INTERIOR SURFACES			
Wall CTS	Floor&Ceiling CTS	Wall RTS	Floor&Ceiling RTS
0,01	0,02	0,41	0,41
0,01	0,02	0,20	0,20
0,03	0,05	0,12	0,12
0,06	0,06	0,08	0,08
0,07	0,07	0,05	0,05
0,08	0,07	0,04	0,04
0,08	0,06	0,03	0,03
0,08	0,06	0,02	0,02
0,08	0,06	0,01	0,01
0,07	0,05	0,01	0,01
0,06	0,05	0,01	0,01
0,06	0,05	0,01	0,01
0,05	0,04	0,01	0,01
0,04	0,04	0,00	0,00
0,04	0,04	0,00	0,00
0,03	0,04	0,00	0,00
0,03	0,03	0,00	0,00
0,03	0,03	0,00	0,00
0,02	0,03	0,00	0,00
0,02	0,03	0,00	0,00
0,02	0,03	0,00	0,00
0,01	0,03	0,00	0,00
0,01	0,02	0,00	0,00
0,01	0,02	0,00	0,00

	INTERIOR SURFACES COOLING LOAD
TIME	TOTAL
1	648
2	622
3	584
4	536
5	482
6	422
7	359
8	296
9	237
10	185
11	145
12	121
13	118
14	136
15	176
16	234
17	306
18	384
19	462
20	533
21	591
22	632
23	655
24	660

Figure A1.6. Spreadsheet based on MS-Excel according to RTS procedure to determine interior surface cooling load

z01	PARTS of COOLING LOAD										TOTAL COOLING LOAD			
	Wall		Interior	Infiltration			People		Equipment					
TIME	Roof	Window	Surfaces	Latent	Sens.	Lighting	Latent	Sens.	Latent	Sens.	Sensib.	Latent	Total	SHR
1	199	197	648	0	0	4	0	8	0	70	1126	0	1126	1,00
2	190	137	622	0	0	3	0	6	0	56	1014	0	1014	1,00
3	178	92	584	0	0	3	0	5	0	42	904	0	904	1,00
4	166	55	536	0	0	2	0	3	0	28	790	0	790	1,00
5	152	113	482	0	0	1	0	2	0	14	764	0	764	1,00
6	139	763	422	0	0	0	0	0	0	0	1323	0	1323	1,00
7	125	930	359	0	0	0	0	0	0	0	1414	0	1414	1,00
8	113	993	296	0	0	94	275	223	0	1174	2894	275	3169	0,91
9	103	1191	237	0	0	111	275	255	0	1454	3350	275	3625	0,92
10	95	1396	185	0	0	121	275	274	0	1622	3693	275	3968	0,93
11	89	1585	145	0	0	128	275	287	0	1734	3968	275	4243	0,94
12	86	1745	121	0	0	132	275	295	0	1804	4183	275	4458	0,94
13	86	1835	118	0	0	136	275	301	0	1860	4336	275	4611	0,94
14	90	1852	136	0	0	138	275	306	0	1902	4424	275	4699	0,94
15	98	1798	176	0	0	140	275	309	0	1930	4451	275	4726	0,94
16	110	1741	234	0	0	141	275	311	0	1944	4481	275	4756	0,94
17	126	1781	306	0	0	141	275	312	0	1958	4624	275	4899	0,94
18	145	1623	384	0	0	48	0	91	0	798	3089	0	3089	1,00
19	164	1023	462	0	0	32	0	61	0	532	2274	0	2274	1,00
20	182	765	533	0	0	23	0	43	0	378	1924	0	1924	1,00
21	195	590	591	0	0	16	0	30	0	266	1689	0	1689	1,00
22	203	454	632	0	0	12	0	22	0	196	1520	0	1520	1,00
23	206	349	655	0	0	8	0	16	0	140	1375	0	1375	1,00
24	204	270	660	0	0	6	0	11	0	98	1249	0	1249	1,00

Figure A1.7. Spreadsheet based on MS-Excel according to RTS procedure to determine building total cooling load separately

APPENDIX A2

****

This program is called P_CCWT. It is calculated design conditions of the Air-conditioning system under the condition of constant coil wall temperature (T_C). The program uses the outdoor design conditions (T_O, W_O), amount of fresh air ($M_{outdoor}$), apparatus dew-point (coil wall) temperature (T_C), sensible heat load of the conditioned space ($Q_{sen,room}$) and RSHF as input data.

****

```
      DOUBLE PRECISION PW,PWS,C8,C9,C11,C12,C13,C10,PAT,PWSY,W1,W2,W3,PWC
      OPEN(5,FILE='----.TXT',STATUS='new')
C*******Outdoor design condition DBT and W ***********************************************************
      WRITE(*,*)' Outdoor Design Temperature and Absolute Humidity '
      READ(*,*) TK1,W
      WRITE(5,80)TK1,W
80    FORMAT('Room DBT =',F6.2,'  ROOM RH =',F4.2)
C*******Read indoor design condition DBT and RH'****************************************************
      WRITE(*,*)'Room DBT and RH'
      READ(*,*,END=70)TK3,BN3
      WRITE(5,82)TK3,BN3
82    FORMAT('Room DBT =',F6.2,'  ROOM RH =',F4.2)
C*******Read quantity of fresh air (m3/h)' ***************************************************************
      WRITE(*,*)' Write quantity of fresh Air (m3/h)'
      READ(*,*,END=70)ATH
      WRITE(5,85)ATH
85    FORMAT('Fresh air (m3/h)=',F10.2)
C*******Read DBT of coil wall ******************************************************************************
      WRITE(*,*)'Write temperature of coil wall'
      READ(*,*,END=70)TCh
      WRITE(5,86)TCh
86    FORMAT('Temperature coil wall',F6.2)
      PAT=101.325
      C8=-5800.2206
….
…..
      C13=6.5459673
C*******Read building total sensible heat gain and Sensible Heat Ratio (RSHF)*****************
      READ(,*)DI,DIO
```

```
C*******Condition of (O) is calculated*******************************************************************
      TB=273.15+tk1
      H1=1.006*TK1+W*(2501+1.805*TK1)
      V1=8.31441*TB*(1+1.6078*W)/(28.9645*PAT)
C     *********Condition of (C) is calculated**************************************************************
      TY2=TCH
      TK2=TY2
      TE=273.15+TCH
      PWSS2=EXP((C8/TE)+(C9+C10*TE)+(C11*TE**2)+(C12*TE**3)+(C13*LOG(TE)))
      WSS2=(0.62198*PWSS2)/(PAT-PWSS2)
      W2=((2501-2.381*TY2)*WSS2)/(2501+1.805*TK2-4.186*TY2)
      H2=1.006*TK2+W2*(2501+1.805*TK2)
C***********Condition of (R) is calculated**************************************************************
      TL=273.15+TK3
      PWS3=EXP((C8/TL)+(C9+C10*TL)+(C11*TL**2)+(C12*TL**3)+(C13*LOG(TL)))
….
….
….
C**********Condition of (M) is calculated***************************************************************
51    OK=1
 5    WK=OK*W+(1-OK)*W3
      HK=OK*H1+(1-OK)*H3
      TK=OK*TK1+(1-OK)*TK3
…..
…..
…..

20    IF(TK1.LT.TK.OR.TK.LT.TK3)THEN
            WRITE(5,72) ww,wv,tk1,w
            GOTO 65
      ELSE
            GOTO 30
      ENDIF
C*********Condition of (S) is calculated****************************************************************
30    CONTINUE
      EM1=(WK-W2)/(TK-TK2)
      EM3=(1/DIO-1)*(1.007/2544)
…
….
```

```
101 HKU=1.006*TK+WU*(2501+1.805*TK)
    QCK=AMTOP*(HKU-HU)/3600.0
    QCtop=AMTOP*(HK-HU)/3600.0
    IF(AMTOP.LT.AMDIS)THEN
            GOTO 51
    ELSE
            GOTO 88
            ENDIF
88  CONTINUE
    IF(TU.LT.TCH.OR.TU.GT.TK)THEN
            WRITE(5,74) ww,wv,tk1,w
74          FORMAT(2f5.1,2x,'DBTsupply is not found under the conditions',2x,f5.2,F7.4)
    ELSE
            WRITE(5,11)WW,WV,TK1,W
            WRITE(5,12)AMTOP,AMDIS,OK,Tk,WK,TU,WU,QCtop,TI,DIO
11          FORMAT(2f5.1,2X,F7.2,F8.4)
12          FORMAT(2f9.2,f7.3,f7.2,F8.4,F7.2,F8.4,f7.2,f7.2,2x,f4.2)
    ENDIF
 65 CONTINUE
    STOP
    END
```

APPENDIX A3

****

The computer program called P_VAV was developed in order to simulate hourly operating of the variable air volume (VAV) air conditioning system and to determine the design cooling coil load and total mass flow rate. The outdoor air conditions (T_O, W_O) which can be calculated using equations (3.42) and (3.49), indoor design conditions (T_R, RH_R), amount of the fresh air ($M_{outdoor}$), dry bulb temperature of the supply air (T_S), simulation time (operating date) or design day, sensible cooling load of the conditioned space ($Q_{sen,room}$) and RSHF can be used as input data in the program.

****

```
      DOUBLE PRECISION PW,PWS,C8,C9,C11,C12,C13,C10,PAT,PWSY,W2,W3,PWC
      OPEN (5,FILE='adana.TXT')
C*******************************Read days for analyses**************************************************
      WRITE(*,*)'Write number between start and finish days of the year for analyses '
      READ(*,*,END=70)MH1,MH2
      WRITE(5,81)MH1,MH2
81    FORMAT('DAYS =',I3,2X,I3)
C*******************************Read indoor design condition DBT and RH'***************************
      WRITE(*,*)'Room DBT and RH'
      READ(*,*,END=70)TK3,BN3
      WRITE(5,82)TK3,BN3
82    FORMAT('Room DBTI =',F6.2,' Room RH =',F4.2)
C********************************Read quantity of fresh air (m3/h)' ************************************
      WRITE(*,*)' Write quantity of fresh air (m3/h)'
      READ(*,*,END=70)ATH
      WRITE(5,85)ATH
85    FORMAT('Fresh air (m3/h)=',F10.2)
C********************************Read DBT supply air temperature ************************************
      WRITE(*,*)' Write DBT supply air temperature'
      READ(*,*,END=70)TU
      WRITE(5,86)TU
86    FORMAT('supply air temperature',F7.2)
….
…..
…..
```

```
      C13=6.5459673
      DO 61 WW=MH1,MH2
      OPEN(4,FILE='DIO.TXT',STATUS='OLD')
      DO 62 WV=1,24
      READ(4,*,END=70)DI,DIO
      CALL TEMP (WW,WV,TK1)
      CALL HEM (WW,WV,W)
      TB=273.15+TK1
      H1=1.006*TK1+W*(2501+1.805*TK1)
      V1=8.31441*TB*(1+1.6078*W)/(28.9645*PAT)
C     *********************************Conditions of (R) are calculated***********************************
      TL=273.15+TK3
      PWS3=EXP((C8/TL)+(C9+C10*TL)+(C11*TL**2)+(C12*TL**3)+(C13*LOG(TL)))
      PW3=BN3*PWS3
      W3=(0.62198*PW3)/(PAT-PW3)
      H3=1.006*TK3+W3*(2501+1.805*TK3)
      V3=8.31441*TL*(1+1.6078*W3)/(28.9645*PAT)
C     ***********************************Conditions of (S) are calculated*********************************
      WU=W3-((1.006/2537)*(TK3-TU)*(1/DIO-1))
      HU=1.006*TU+WU*(2501+1.805*TU)
C     *********************************Conditions of (M) are calculated***********************************
      TI=(DI*3600)/DIO
      AMTOP=TI/(H3-HU)
….
….
….
      ENDIF
18    IF(TK1.LT.TK3)GOTO 10
      GOTO 20
10    IF(TK1.GT.TK.OR.TK.GT.TK3)THEN
            WRITE(5,72) WW,WV,TK1,W
72          FORMAT(2f5.1,2x,' DBTmixing is not found under the conditions ',2x,f5.2,F7.4)
            GOTO 65
      ELSE
            GOTO 30
      ENDIF
….
….
….
```

```
C     ************************************Conditions of (C) are calculated********************************
30    EM1=(WK-WU)/(TK-TU)
      Tz=273.15
 51   Ti=Tz-273.15
      PWSC=EXP((C8/Tz)+(C9+C10*Tz)+(C11*Tz**2)+(C12*Tz**3)+(C13*LOG(Tz)))
      WSC=(0.62198*PWSC)/(PAT-PWSC)
      WC=WK-EM1*(TK-Ti)
      DC=ABS(1-WC/WSC)
      IF(DC.LT.0.0001)THEN
              T2=Ti
              W2=WC
              H2=1.006*T2+W2*(2501+1.805*T2)
              V2=8.31441*(T2+273.15)*(1+1.6078*W2)/(28.9645*PAT)
….
….
….
      QCtop=AMTOP*(HK-HU)/3600.0
      IF(T2.GT.TU)THEN
              WRITE(5,74) WW,WV,TK1,W
74            FORMAT(2f5.1,2x,' DBTcoil is not found under the conditions',2x,f5.2,F7.4)
      ELSE
              WRITE(5,11) WW,WV,TK1,W,AMTOP,AMDIS,OK,Tk,WK,T2,W2,QCTOP,DI,DIO
11            FORMAT(2f5.1,2X,F5.2,F7.3,2f12.2,f7.3,f7.2,F8.4,F7.2,F8.4,2X,f10.2,f9.3,2x,f4.2)
      ENDIF
65    CONTINUE
62    CONTINUE
      CLOSE(4)
61    CONTINUE
70    STOP
      END
```

APPENDIX A4

****

A computer program called P_CAV was written to calculate psychometric properties of all-air constant air volume (CAV) air conditioning system. The outdoor air conditions, which can be calculated using Equations (3.42) and (3.49), indoor design conditions (dry bulb temperature (T_R) and relative humidity RH_R), amount of the fresh air ($M_{outdoor}$) and total mass flow rate (M_{tot}), simulation time (operating time) or design day, sensible cooling load of conditioned space ($Q_{sen,room}$) and RSHR are used as input data in the program.

****

```
      DOUBLE PRECISION PW,PWS,C8,C9,C11,C12,C13,C10,PAT,PWSY,W2,W3,PWC
      OPEN (5,FILE='adana.TXT')
C*******************************Read days for analyses**************************************************
      WRITE(*,*)'Write number between start and finish days of the year for analyses '
      READ(*,*,END=70)MH1,MH2
      WRITE(5,81)MH1,MH2
83    FORMAT('DAYS =',I3,2X,I3)
C*******************************Read indoor design condition DBT and RH'**************************
      WRITE(*,*)'Room DBT and RH'
      READ(*,*,END=70)TK3,BN3
      WRITE(5,82)TK3,BN3
84    FORMAT('Room DBTI =',F6.2,' Room RH =',F4.2)
C********************************Read quantity of fresh air (m3/h)' *************************************
      WRITE(*,*)' Write quantity of fresh air (m3/h)'
      READ(*,*,END=70)ATH
      WRITE(5,85)ATH
86    FORMAT('Fresh air (m3/h)=',F10.2)
C*******************************Read quantity of total mass flow rate (kg/h)*************************
      WRITE(*,*)' Write quantity of C'
      READ(*,*,END=70)AMTOP
      WRITE(5,86)AMTOP
86    FORMAT('total mass flow rate (kg/h)=',F10.2)
      PAT=101.325
….
….
….
```

```
      OPEN(4,FILE='DIO.TXT',STATUS='OLD')
      DO 62 WV=1,24
      READ(4,*,END=70)DI,DIO
      CALL TEMP (WW,WV,TK1)
      CALL HEM (WW,WV,W)
C     **********************************Conditions of (O) are calculated************************************
      TB=273.15+TK1
      H1=1.006*TK1+W*(2501+1.805*TK1)
      V1=8.31441*TB*(1+1.6078*W)/(28.9645*PAT)
C     **********************************Conditions of (R) are calculated************************************
      TL=273.15+TK3
      PWS3=EXP((C8/TL)+(C9+C10*TL)+(C11*TL**2)+(C12*TL**3)+(C13*LOG(TL)))
      PW3=BN3*PWS3
….
….
….
      DHDI=(ATH/V1)*(HGD-H3)/3600
      DHGI=(ATH/V1)*(H1-HGD)/3600
      GI=QI-DI
      CDIO=(DI+DHDI)/(DI+GI+DHDI+DHGI)
      EM=(1/CDIO-1)*(1.006/2537)
      HU=H3-(QI*3600)/(AMTOP)
      TUF=TK
200   WUF=WK-EM*TK+EM*TUF
      WUF2=(HU-(1.006*TUF))/(2501+1.805*TUF)
      BC=ABS(1-WUF/WUF2)
….
….
….
 75            FORMAT(2f5.1,2x,' DBTcoil is not found under the conditions',2x,f5.2,F7.4)
               GOTO 65
      ELSE
               GOTO 30
      ENDIF
      IF(TK1.LT.TK.OR.TK.LT.TK3)THEN
               write(5,75 WW,WV,TK1,W
               GOTO 65
      ELSE
               GOTO 30
```

```
      ENDIF
C     ************************************Conditions of (C) are calculated********************************
30    CONTINUE
      EM1=(WK-WU)/(TK-TU)
      Tz=273.15
 51   TI=Tz-273.15
      PWSC=EXP((C8/Tz)+(C9+C10*Tz)+(C11*Tz**2)+(C12*Tz**3)+(C13*LOG(Tz)))
      WSC=(0.62198*PWSC)/(PAT-PWSC)
      WC=WK-EM1*(TK-TI)
      DC=ABS(1-WC/WSC)
….
….
….
      HKU=1.006*TK+WU*(2501+1.805*TK)
      QCduy=AMTOP*(HKU-HU)/3600
      QCtop=AMTOP*(HK-HU)/3600.0
      IF(T2.GT.TU)THEN
              WRITE(5,75) WW,WV,TK1,W
      ELSE
              TSU=(3*T2-4.5-TU)/2
              WRITE(5,11) WW,WV,TK1,W,AMTOP,AMDIS,OK,Tk,WK,T2,W2,TSU,QCTOP
11            FORMAT(2f5.1,2X,F5.2,F7.32f12.2,f7.3,f7.2,F8.4,F7.2,F8.4, F7.2,2X,f10.2)
      ENDIF
65    CONTINUE
62    CONTINUE
      CLOSE(4)
61    CONTINUE
70    STOP
      END
```